MICROCOPY RESOLUTION TEST CHART

NATIONAL BUREAU OF STANDARDS 1963 A

AFWAL - TR - 81 - 2117

PROTECTION OF ADVANCED ELECTRICAL POWER SYSTEMS FROM ATMOSPHERIC ELECTROMAGNETIC HAZARDS

BOEING MILITARY AIRPLANE COMPANY
SEATTLE, WASHINGTON 98124

DECEMBER 1981

FINAL REPORT FOR PERIOD JUNE 1979 TO OCTOBER 1981

AERO PROPULSION LABORATORY
AIR FORCE WRIGHT AERONAUTICAL LABORATORIES
AIR FORCE SYSTEMS COMMAND
WRIGHT-PATTERSON AIR FORCE BASE, OHIO 45433

DTIC
ELECTE
MAR 3 0 1982
A

82   05   29   059

REPORT DOCUMENTATION PAGE		READ INSTRUCTIONS BEFORE COMPLETING FORM
1. REPORT NUMBER AFWAL-TR-81-2117	2. GOVT ACCESSION NO. AD-A117612	3. RECIPIENT'S CATALOG NUMBER
4. TITLE *(and Subtitle)* Protection of Advanced Electrical Power Systems From Atmospheric Electromagnetic Hazards		5. TYPE OF REPORT & PERIOD COVERED Final Report -
		6. PERFORMING ORG. REPORT NUMBER D180-26154-2
7. AUTHOR(s) D. L. Sommer		8. CONTRACT OR GRANT NUMBER(s) F33615-79-C-2006
9. PERFORMING ORGANIZATION NAME AND ADDRESS Boeing Military Airplane Company Mechanical/Electrical Systems Technology MS 47-03, P.O. Box 3707, Seattle, WA 98124		10. PROGRAM ELEMENT, PROJECT, TASK AREA & WORK UNIT NUMBERS 3145 29 58
11. CONTROLLING OFFICE NAME AND ADDRESS Aero Propulsion Laboratory (AFWAL/POO) Air Force Wright Aeronautical Laboratories, AFSC Wright-Patterson Air Force Base, Ohio 45433		12. REPORT DATE December 1981
		13. NUMBER OF PAGES 231
14. MONITORING AGENCY NAME & ADDRESS(*If different from Controlling Office*)		15. SECURITY CLASS. *(of this report)* Unclassified
		15a. DECLASSIFICATION/DOWNGRADING SCHEDULE

16. DISTRIBUTION STATEMENT *(of this Report)*

Approved for public release; distribution unlimited

17. DISTRIBUTION STATEMENT *(of the abstract entered in Block 20, if different from Report)*

18. SUPPLEMENTARY NOTES

19. KEY WORDS *(Continue on reverse side if necessary and identify by block number)*

Aircraft	Induced Voltages	Filters
Composite Structures	Lightning Transients	Shielding
Computer Models	Lightning Protection	Hand Calculation
Electrical Systems	Attenuation	Computer Analysis

20. ABSTRACT *(Continue on reverse side if necessary and identify by block number)*

This report contains results of a two-phase study program investigating the effects of lightning strikes on aircraft and the resulting transients coupled onto the electrical systems. The final report also includes a summary of the design guide which also contains results of the Study Program.

The historical background and overall scope of the study are contained in Section I of the final report. Section II of this report defines (continued)

DD FORM 1473 EDITION OF 1 NOV 65 IS OBSOLETE

20. ABSTRACT (continued)

the lightning threat and develops electrical system math models.
Section III evaluates the normal design of aircraft for inherent
hardness. Included in this assessment are wire routing, equipment
location, fiber optics, threat level comparisons and the
evaluation of specific electrical circuits (e.g., generators,
converters, beacon lights, etc.). Section IV of the report
analyzes the effects of using add-on protection to suppress induced
transients on the electrical system. Protection schemes analyzed
include cable shielding, linear protection devices, non-linear
protection devices and conductive coatings applied to the
aircraft skin.

Section V of the final report contains a summary of the design guide
which provides the electrical systems engineer with a means of
selecting the most appropriate lightning hardening techniques for
his design. Section VI discusses reliability/maintainability,
system safety and design to cost considerations. Section VII of
the report contains the conclusions and recommendations of the
study which include protection criteria to develop a lightning
tolerant electrical system.

PREFACE

This Final Report presents the results of work performed by the Boeing
Military Airplane Company, Seattle, Washington, under Air Force Contract
F33615-79-C-2006, during the period June 15, 1979 to October 15, 1981. The
work was sponsored by the Aero Propulsion Laboratory, Air Force Wright
Aeronautical Laboratories, Wright-Patterson Air Force Base, Ohio, under
Project 3145, Task 31459, Work Unit 3142958, with Mr. Duane Fox, AFWAL/POOS-2,
as the project engineer.

This document fulfills the requirement of CDRL item numbers 7, Final Technical
Report and CDRL item number 10, Drawings, Engineering and Associated Lists.

The technical work was done by Mr. David L. Sommer, Mr. D. K. Heier and
Dr. W. P. Geren, and the report was prepared by Mr. Sommer under the direction
of Mr. I. S. Mehdi, Boeing Program Manager.

iii

TABLE OF CONTENTS

CONTENTS (Cont.)

CONTENTS (Cont.)

CONTENTS (Cont.)

LIST OF ILLUSTRATIONS

LIST OF ILLUSTRATIONS (CONT.)

LIST OF ILLUSTRATIONS (Cont.)

LIST OF ILLUSTRATIONS (Cont.)

LIST OF TABLES

LIST OF TABLES (Cont.)

LIST OF ABBREVIATIONS, ACRONYMS, AND SYMBOLS

SYMBOL	DEFINTION
A	Amperes
BL MOD	Beacon Light Moderate Threat
BL SEV	Beacon Light Severe Threat
CCTC	Common Mode Wire Self Capacitance
CCTR	Common Mode Wire Mutual Capacitance
IBUSLOAD	Current at the Bus Input Terminals
ICON	Current at the Converter Output Terminals
IGEN	Current at the Generator Output Terminals
IGENNEU	Current at the Generator Neutral Terminals
ILOAD	Current at the Load Input Terminals
ISC	Short Circuit Current
Kv	Kilovolts
LSELF	Wire Self Inductance
mS	Milliseconds
Mutual	Wire Bundle Mutual Inductance
RCNDAC	Wire AC Resistance
RCNDDC	Wire DC Resistance
S.E.	Shielding Effectiveness
TEM	Transverse Electromagnetic
T1,T2	Test Points 1 and 2
V	Voltage
VBUSLOAD	Voltage at the Bus Load
VCON	Voltage at the Converter Output Terminals
V_d	Reverse Biased Device Voltage
VGEN	Voltage at the Generator Output Terminals

VGENNEU	Voltage at the Generator Neutral Terminals
VLOAD	Voltage at the Load Input Terminals
VOC	Voltage Open Circuit
V_r	Reverse Stand Off Voltage
VSCF	Variable Speed Constant Frequency
S	Microseconds
WH MOD	Window Heater Moderate Threat
WH SEV	Window Heater Severe Threat
6MF	Six Meter Wire Behind Fiberglass
12GE35	Twelve Meter Wire 2 Feet Behind 35 Plies of Graphite/Epoxy
12GE45	Twelve Meter Wire 2 Feet Behind 45 Plies of Graphite/Epoxy
12GE50	Twelve Meter Wire 2 Feet Behind 50 Plies of Graphite/Epoxy
12GE51	Twelve Meter Wire 1 Foot Behind 50 Plies of Graphite/Epoxy
12GE52	Twelve Meter Wire 0.5 Foot behind 50 Plies of Graphite/Epoxy
12MF	Twelve Meter Wire Behind Fiberglass
12M3MF	Twelve Meter Wire Behind Three Mil Foil on Fiberglass
18MF	Eighteen Meter Wire Behind Fiberglass

SUMMARY

This final report contains results of the work conducted under the program
titled "Protection of Advanced Electrical Power System from Atmospheric
Electromagnetic Hazards." The program was conducted in three tasks in Phase I
and a fourth task in Phase II. The objective of this program is to define the
electromagnetic threat imposed on advanced aircraft electrical system in
metallic and non-metallic aircraft due to lightning strikes and to develop
cost effective techniques for protection of the electrical systems from these
threats.

The approach to assess the threats due to lightning strikes consisted of
utilizing computer programs and analysis methods to calculate the threat
levels for typical aircraft electrical system circuits. Several circuits were
evaluated for three types of aircraft; cargo, fighter and fighter-bomber. For
each type of aircraft an engineering survey was performed to obtain
geometrical data. The survey included visual examination of various aircraft
in the Air Force inventory to determine the important electromagnetic energy
coupling paths. Open circuit voltages, short circuit currents, and energy
coupled on to nine of the circuits were determined.

After the threats for the various circuits were determined, several key
circuits were selected for further evaluation in Task 2. In this task the
circuits were terminated in the appropriate impedances that would normally be
expected and again the voltages and currents at key points in the circuits
were determined. This data was used to examine some of the equipment that
would be exposed to these transients and their impact on the equipment was
evaluated. In addition, the various specificaitons and standards were also
examined to determine the level of hardness that present day equipment are
required to meet. The impact of wire routing to reduce the electromagnetic
flux coupling onto conductors was also examined.

In the third task, the circuits selected in the previous task were reevaluated
to determine the impact of added protection such as linear filters and
non-linear protective devices along with various methods of shielding. An

alternative to signal transmission via the use of fiber optics was also examined.

In phase II, the definition of lightning hardness criteria was developed, and the evaluation of various hardening methods to meet these criteria was accomplished. A trade-off of the alternatives was conducted on the basis of cost, weight, reliability and maintainability. Based on this analysis, data for selection of optimum protection has been developed and included in the design guide and summarized in this final report.

The results of the study did indicate that lightning strike would impose transients on the electrical systems of aircraft with metal or composite structures. These transients will be higher than the equipment inherent hardness. Present specifications do not cover the level of the threats expected due to lightning strikes. However, there are various alternatives available to provide protection from these transients or harden the equipment. The design guide and final report contain all the alternatives that were examined and sufficient data to allow the electrical systems designer to make an appropriate selection for his application. A summary of the design guide is included in this report.

SECTION I

INTRODUCTION

1. BACKGROUND

The interaction of lightning with an aircraft, either by direct strike or near-miss, induces electrical transients into the aircraft circuitry. The next generation of military aircraft may contain large amounts of poorly conducting composite material in skin and structure. In addition, the advanced electrical power systems used in these aircraft will contain solid state components. The combination of the two; i.e., reduced inherent shielding effectiveness of nonmetallic materials coupled with circuit components that have lower tolerance to electrical transients, presents a serious problem for aircraft designers. To trade-off the penalties/benefits of advanced structure and electrical power systems against conventional structures and systems, an in-depth analysis of the lightning problem is required, as is an evaluation of the effectiveness of various protection methods.

Lightning-induced transients present a hazard to electrical power systems which must be met by the provision of an adequate protection system (i.e., the occurrence of several direct strikes to a given aircraft during the service life of the aircraft is a certainty). For a direct strike to an electrical cirucit; e.g., a power feeder, considerable physical damage is done to the wiring, as well as circuit components attached to the wires. When the typical twenty-kiloamp lightning current is injected into wires, magnetic forces and resistive heating will break or vaporize even heavy-gauge wiring. At the very least, dielectric breakdown of wire insulation will occur, which may disable the circuit. If the circuit is not struck directly, it will still have potentially damaging transient levels induced by magnetic coupling to the lightning currents flowing through aircraft structure. These indirectly induced transients will have sufficient energy to damage or upset solid state components. Therefore, lightning protection of aircraft electrical systems is a design requirement.

1

The mechanism whereby lightning currents induce voltages in aircraft electrical circuits is as follows. As lightning current flows through an aircraft, strong magnetic fields which surround the conducting aircraft and change rapidly in accordance with the fast-changing lightning-stroke currents are produced. Some of this magnetic flux may leak inside the aircraft through apertures such as windows, radomes, canopies, seams, and joints. Other fields may arise inside the aircraft when lightning current diffuses to the inside surfaces of skins. In either case these internal fields pass through aircraft electrical circuits and induce voltages in them proportional to the rate of change of the magnetic field. These magnetically induced voltages may appear between both wires of a two-wire circuit, or between either wire and the airframe. The former are often referred to as line-to-line voltages and the latter as common-mode voltages.

In addition to these induced voltages, there may be resistive voltage drops along the airframe as lightning current flows through it. If any part of an aircraft circuit is connected anywhere to the airframe, these voltage drops may appear between circuit wires and the airframe. For metallic aircraft made of highly conductive aluminum, these voltages are seldom significant except when the lightning current must flow through resistive joints or hinges. However, the resistance of titanium is 10 times that of aluminum, so the resistive voltages in future aircraft employing this material may be much higher.

Upset or damage of electrical equipment by these induced voltages is defined as an indirect effect. It is apparent that indirect effects must be considered along with direct effects in assessing the vulnerability of aircraft electrical and electronics systems. Most aircraft electrical systems are well protected against direct effects but not so well against indirect effects.

Until the advent of solid state electronics in aircraft, indirect effects from external environments, such as lightning and precipitation static, were not much of a problem and received relatively little attention. No airworthiness criteria are available for this environment. There is increasing evidence, however, of troublesome indirect effects. Incidents of upset or damage to

avionic or electrical systems, for example, without evidence of any direct
attachment of the lightning flash to an electrical component are showing up in
lightning-strike reports.

While the indirect effects are not presently a major safety hazard, there are
trends in aircraft design and operations which could increase the potential
problem. These include the following:

o Increasing use of plastic or composite skin
o Further miniaturization of solid state electronics
o Greater dependence on electronics to perform flight-critical functions

Design of protective measures against indirect effects is treated in the
design guide.

A major difficulty in aircraft design is to provide the designer with
sufficient information about design options and trade-offs to make intelligent
choices for the aircraft under consideration. For lightning protection, which
is a relatively new and rapidly-changing technology, this is particularly
true. The addition of lightning protection hardware to an aircraft carries
with it various cost/weight/volume penalties, and, in some cases, will
compromise the performance of the protected systems (e.g., surge arrestors may
degrade with age and fail, shorting out the system they were intended to
protect). This can result in an over-designed protection system that may be
almost as bad as one that is inadequate. An accurate assessment of the
lightning threat is required as is an accurate evaluation of the effectiveness
of protection hardware.

2. PROGRAM OBJECTIVE

The objective of this program is to define the electromagnetic threat imposed
on advanced aircraft electrical systems in metallic and non-metallic aircraft
due to lightning strikes and to develop cost effective techniques for
protection of the electrical systems from these threats.

3. APPROACH

This program is divided into two phases. The first phase was divided into the following three tasks as shown in Figure 1.

Task 1. Threat Assessment
Task 2. Evaluation of Normal Design for Inherent Hardness
Task 3. Add-on Protection Device Evaluation

The approach to assess the threats due to lightning strikes consisted of utilizing computer programs and analysis methods to calculate the threat levels for typical aircraft electrical system circuits. Several circuits were evaluated for three types of aircraft; cargo, fighter and fighter-bomber. For each type of aircraft an engineering survey was performed to obtain geometrical data. The survey included visual examination of various aircraft in the Air Force inventory to determine the important electromagnetic energy coupling paths. Open circuit voltage, short circuit current, and energy coupled on to nine of the circuits was determined.

After the threats for the various circuits were determined, several key circuits were selected for further evaluation in Task 2. In this task the circuits were terminated in the appropriate impedances that would normally be expected and again the voltages and currents at key points in the circuits were determined. This data was used to examine some of the equipment that would be exposed to these transients and their impact on the equipment was evaluated. In addition, the various specifications and standards were also examined to determine the level of hardness that present day equipment are required to meet. The impact of wire routing to reduce the electromagnetic flux coupling onto conductors was also examined.

In the third task, the circuits selected in the previous task were reevaluated to determine the impact of added protection such as linear filters and non-linear protective devices along with various methods of shielding. An Alternative to signal transmission via the use of fiber optics was also examined.

4

PHASE I—
TECHNICAL
EFFORT

LIGHTNING THREAT

AIRCRAFT AND WIRING PARAMETERS

MATH MODELS

THREAT LEVELS

TASK 1—
THREAT ASSESSMENT

NORMAL DESIGN PRACTICES

ALTERNATE DESIGNS

ADVANCED ELECTRICAL SYSTEMS

TEST DATA (IF REQUIRED)

EVALUATION

IMPACT OF CHANGING SPECIFICATIONS

TRADE STUDY DESIGN DATA

TASK 2—
EVALUATION OF NORMAL DESIGN FOR INHERENT HARDNESS

PROTECTION SYSTEM DESIGN DATA

TEST DATA (IF REQUIRED)

EVALUATION

TRADE STUDY DESIGN DATA

INTERIM REPORT

TASK 3—
ADD-ON PROTECTION DEVICE EVALUATION

PHASE II, TASK 4—
TRADE STUDY
AND HANDBOOK
PREPARATION

OPTIMUM SYSTEM TRADE STUDY

HARDENED SYSTEM DESIGN

HANDBOOK PREPARATION

HANDBOOK

FINAL REPORT
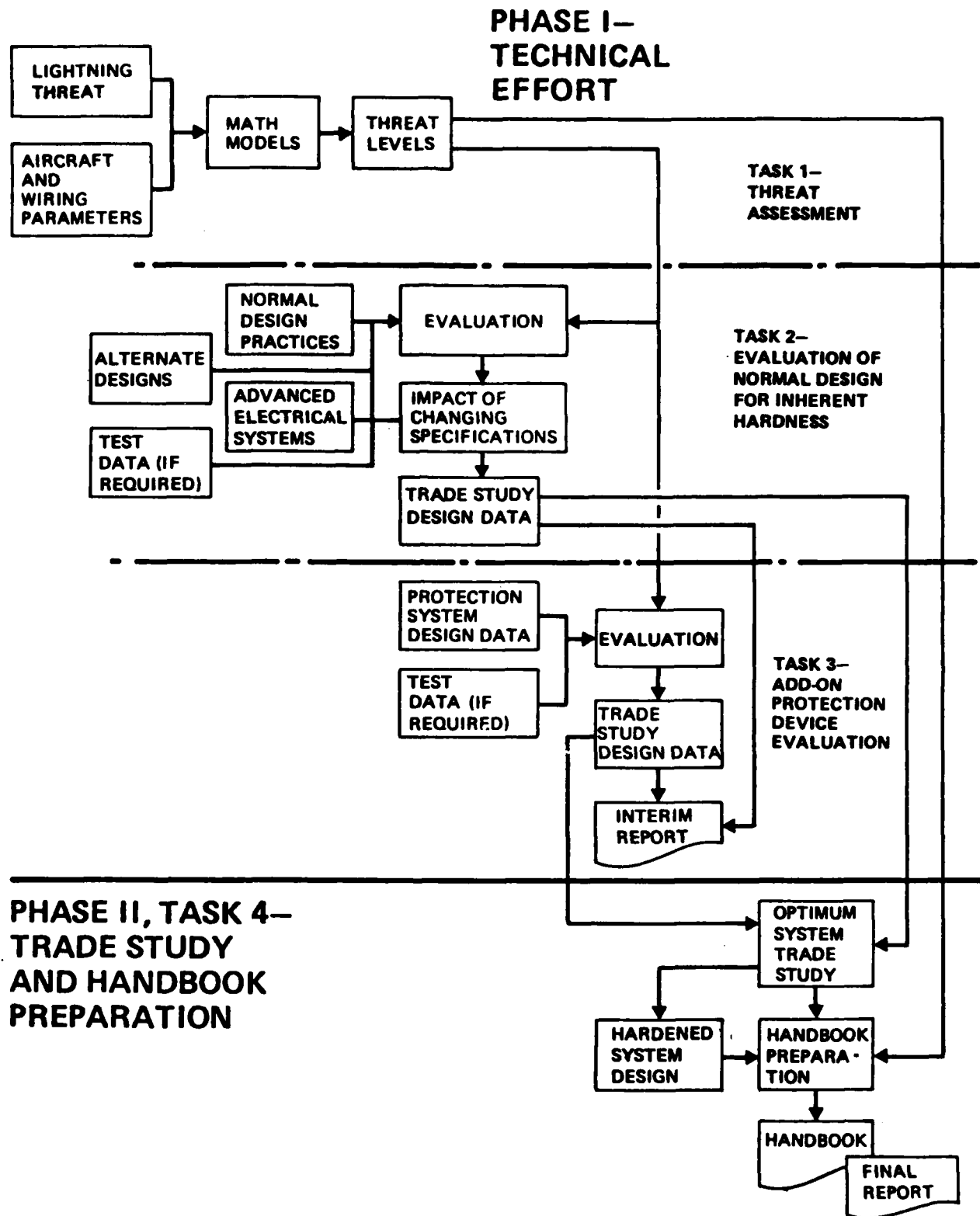
Figure 1   Program Approach

5

In phase II, task 4, Trade Study and Handbook Preparation, a trade study of the various hardening concepts with respect to cost, weight, reliability and maintainability was conducted. The trade study data is incorporated in the design guide, along with examples of how this data can be used in the design of future airplane electrical systems.

4. RESULTS

a. PHASE I THREAT ASSESSMENT AND HARDNESS EVALUATION

Engineering surveys were performed upon the C-14, FB-111, and F-15 to identify power-related circuits for threat assessment. Based upon this data, twenty-three circuits were evaluated, to varying levels of detail, as indicated below:

1. Obtained Detailed circuit models   nine circuits
   and threat waveforms

2. Desired Equations required for   seven circuits
   threat calculation

3. Found to present a   three circuits
   negligible threat

4. Similar to circuits under   three circuits
   1 or 2.

5. Direct strike threat   one circuit

The waveforms obtained from the detailed circuit models consisted, in general, of a low frequency component plus a resonant response. The transients for peak open circuit voltage and peak short circuit current are shown in Table 1.

The following seven circuits were analyzed for electrical transients induced due to severe lightning strikes.

o VSCF Circuit with generator and converter on wing

o VSCF Circuit with generator on wing, converter in fuselage

o Generator on Wing Circuit

o F15 Generator Circuit

o Beacon Light Circuit

o Window Heater Circuit

o Upper Surface Blowing Actuator Circuit

In each case, the circuits were terminated with appropriate impedances at both
ends and at intermediate points of the circuits to represent typical aircraft
systems. The induced transients at various points were computed using the
TRAFFIC computer program. Considerable data was developed with various
configurations and this data is reported in the body of this report. A
summary of the results for the VSCF circuit with generator and converter on
the wing and anticipated transient data at the bus located in the fuselage is
shown in Table 2.a. As can be seen, the most severe transient coupling occurs
with the generator feeders routed in the fiberglass leading edge of the wing.

Addition of shielding does reduce the induced voltage by two orders of
magnitude with shielded feeders terminated using pigtails. An additional
order of magnitude reduction can be achieved if the shielding is
circumferentially terminated. This is due to the fact that the pigtail
inductance produces a voltage drop which drives the feeders. Essentially the
same amount of attenuation as the feeder shielded and circumferentailly
terminated is a achieved when TRANSZORB devices are used to limit the
transient. Addition of 3 mil foil to the fiberglass pratically elminates the
transient induced in the generator feeders, provided that the foil makes good
electrical contact with underlying structure.

A second set of evaluations was conducted with the same circuit but with the
leading edge of the wing being a graphite epoxy composite material with
varying number of plies. Again the induced transients are reduced by two
orders of magnitude by virtue of the fact that the graphite epoxy has some
conductivity even though it is about 1000 times less than aluminum.

7

TABLE 1   TASK 1 PEAK TRANSIENTS

CIRCUIT	MODERATE THREAT Peak V_{oc}	Peak I_{sc}	SEVERE THREAT Peak V_{oc}	Peak I_{sc}
C-14 USE ACTUATOR				
AT ACTUATOR	7.6 KV[2]	36 A[3]	30 KV[2]	305 A[3]
AT INTERFACE UNIT	Negligible*	37 A[3]	Negligible*	305 A[3]
C-14 WING TIP BEACON				
AT TRANSFORMER	11 KV[1]	30 A[4]	52 KV[1]	320 A[4]
AT POWER BUSS	1.1 KV[1]	30 A[4]	4.4 KV[1]	320 A[4]
C-14 WINDSHIELD HEATER				
AT POWER BUSS	30 KV[3]	18 A[1]	300 KV[3]	90 A[1]
C-14 VERTICAL STABILIZER	21 V[1]	0.06 A[3]	80 V[1]	0.6 A[3]
F-111 PITOT HEATER				
AT FORWARD BULKHEAD	27 KV[2]	280 A[2]	105 KV[2]	1100 A[2]
F-111 COCKPIT MAP READING LIGHT AT POWER BUSS	220 V[2]	94 A[4]	860 V[2]	940 A[4]
F-15 PITOT HEATER				
AT ESSENTIAL POWER BUSS	136 V[3]	5.4 A[3]	1360 V[3]	54 A[3]
F-15 EXTERNAL FUEL TANK QUANTITY INDICATOR**	16 KV[1]	Not Available**	62 KV[1]	Not Available**
F-15 GENERATOR FEEDERS AT CIRCUIT BREAKER	37 V[2]	1.4 A[4]	140 A[1]	15 A[4]

1. Waveform dominated by circuit resonance.

2. Waveform follows time derivative of lightning current.

3. Waveform follows lightning current.

4. Other low frequency waveform (none of the above).

Note: Arcing through wire insulation will limit voltages to 20-50 KV maximum for most circuits.

* Negligible voltage because of loading effects (both ends of wire bundle were open circuit).

** Levels are for transient voltage appearing across gap between fuel tank and fuselage. This voltage will appear as a source in wiring crossing the gap.

TABLE 2a Severe Lightning Strike Transients at the Power Bus
for the VSCF Generator and Converter Located 12 Meters from Fuselage

TEST CONDITIONS	VOLTAGE PEAK	TRANSIENT DURATION	CURRENT PEAK	TRANSIENT DURATION
An all aluminum wing with fiberglass leading edge, 22 meters from the power bus				
Bus Open Circuit	75 KV	7 mS		
Bus Short Circuit			2.65 KA	0.7 mS
50% Loaded Bus	65 KV	8 mS	289 A	0.15 mS
100% Loaded Bus	58 KV	8 uS	550 A	0.6 mS
Feeder Shielding with Pigtail Terminations and 50% Loaded Bus	5.4 KV	0.5 mS	132 A	1 mS
Feeder Shielding with Circumferential Terminations and 50% Loaded Bus	295 V	0.4 mS	104 A	1 mS
Transzorb Protection at 50% Loaded Bus	285 V	0.5 mS	82 A	0.6 mS
An all aluminum wing with 3-Mil foil behind the fiberglass leading edge, 22 meters from the power bus				
50% Loaded Bus	11.2 V	1 mS	8.5 A	1 mS
An all aluminum wing with a graphite epoxy leading edge, 22 meters from the power bus				
50% Loaded Bus, 35 Plies	410 V	1 mS	305 A	1 mS
50% Loaded Bus, 45 Plies	320 V	1 mS	235 A	1 mS
50% Loaded Bus, 50 Plies, L.E. is 2 ft ahead of feeder	285 V	1 mS	215 A	1 mS
50% Loaded Bus, 50 Plies, L.E. is 1 ft ahead of feeder	570 V	1 mS	420 A	1 mS
50% Loaded Bus, 50 Plies, L.E. is 1/2 ft ahead of feeder	1.14 KV	1 mS	840 A	1 mS

Only two military specifications require equipment to be designed to with stand short duration electrical transients or spikes. These are MIL-STD-704 and MIL-E-6051. The most severe of these is a 600 volt 10 microsecond spike requirement in the Rev A & B of MIL-STD-704. However, this was deleted for Rev C of this specification. Most of the transients coupled due to lightning strike exceed these limits both in magnitude and duration. Examination of electrical equipment showed that most of the components in them would be damaged if exposed to transients that exceed the 600 volts design requirements.

Routing the wiring close to metallic structure reduces the amount of electromagnetic energy that can be coupled on to the wiring. The induced voltage levels are approximately proportional to the height of the wire above the metallic structure.

Fiber optics does offer a signal transmission capability that is essentially immune to lightning induced transients, however, considerable development in areas of termination and signal division equipment is required.

b. PHASE II TRADE STUDY AND DESIGN GUIDE PREPARATION

In Phase II, criteria were developed to best protect the electrical system from EM hazards. These criteria were incorporated in the Design Guide (Reference 14) and summarized in Section V. The protection alternatives developed in Phase I were assessed and protection techniques are recommended for system design. Table 2b is a summary of lightning threats and protection techniques.

5. CONCLUSIONS

From the detailed examination of power circuits, protection is required from the severe lightning threat for several cases. The transient levels coupled onto the power bus exceed MIL-STD-704B and MIL-E-6051D requirements. The transients can be reduced to values below the military specifications by various methods (i.e., shielding cables, add on protection, changing skin material composition and thickness, re-routing wiring, etc.).

TABLE 2.5 TRADE STUDY SUMMARY OF LIGHTNING PROTECTION TECHNIQUES

TYPE CIRCUIT (LOCATION)	SEVERE THREAT LEVEL	TYPE THREAT	INHERENT HARDENING TECHNIQUE	TRANSIENT LEVEL	TYPE OF ADDITIONAL PROTECTION REQUIRED AND TRANSIENT LEVEL			COMMENTS
					1	2	3	
METALLIC WING FIBER-GLASS LEAD-ING EDGE								
1. GENERATORS (ON WINGS)	200 KA	MAGNETIC COUPLING ON FEEDER	FEEDER ROUTED 2 INCHES ABOVE METALLIC SPAR	30 V	-	-	-	PROTECT FOR DIRECT ATTACHMENT ONLY
2. POWER BUS (FUSELAGE)	200 KA	MAGNETIC COUPLING ON FEEDER	FEEDER ROUTED 2 INCHES ABOVE METALLIC SPAR	65 KV	FEEDER SHIELD: 5.4 KV; 295 V	TRANSZORB: 285 V	3 MIL FOIL ON*	SHIELDING COMPARES PIGTAIL & CIRCUMFERENTIAL GROUNDING RESPECTIVELY.
3. WING TIP BEACON LIGHTS	200 KA	MAGNETIC COUPLING ON 20 GAUGE WIRES	ROUTE WIRES NEAR STRUCTURE	2.2 KV AT POWER BUS	WIRE SHIELD: 190 V	TRANSZORB: 285 V	3 MIL FOIL ON* WING: 10.V	TRANSZORBS MUST BE PARALLELED BACK TO BACK IN EACH CASE.
4. WINDSHIELD HEATERS	200 KA	CAPACITIVELY COUPLED ONTO HEATER ELEMENTS	LOCATION OF HEATER ELEMENTS	920 V AT POWER BUS	-	TRANSZORB: 285 V	-	OTHER SIMILAR PROTECTION DEVICES
COMPOSITE WING AND FUSELAGE								
1. GENERATORS (FUSELAGE)	200 KA	DIFFUSION COUPLING ON FEEDERS	MINIMIZED EXPOSED FEEDER	5.8 KV	CIRCUMFERENTIAL* GROUNDED FEEDER SHIELD: 320 V	TRANSZORB: 285 V		
2. POWER BUS	200 KA	DIFFUSION COUPLING ON FEEDERS	MINIMIZED EXPOSED FEEDER	2.5 KV	CIRCUMFERENTIAL* GROUNDED FEEDER SHIELD: 130 V	TRANSZORB: 285 V		

* PREFERRED, DUE TO: 1. GREATEST PROTECTION
                       2. WEIGHT
                       3. RELIABILITY AND COST

11

Based upon our investigation of graphite epoxy structure, we conclude that electrical power systems in composite structure aircraft may be adequately protected by a combination of structural shielding, wire shielding, and voltage suppression devices.

6. RECOMMENDATIONS

The study has shown that lightning protection must be considered in the initial design of all new generator aircraft. The impact of lightning on advanced composite materials and advanced electrical power systems must be assessed early in the design phases. To assure that the lightning problem is assessed accurately, hardware testing of prototype systems should be accomplished. These tests would provide valuable data to the design engineer.

SECTION II

THREAT ASSESSMENT

1. LIGHTNING THREAT DEFINITION

The cloud-to-ground lightning strike begins with the leader process. i.e., the formation of a plasma channel of ionized air. This is followed by a current surge, the return stroke. During the leader process, the average currents are on the order of 100 amps. Return stroke currents have peak values of tens of kiloamps. A positive strike consists of a single return stroke; a negative strike will have from 3 or 4 to as many as 26 consecutive return strokes and has a duration on the order of tenths of a second.

There are two types of lightning threat - direct attachment to the aircraft and a nearby strike. Previous work on a Navy contract (Reference 1) indicates that the direct attachment case is much more severe than the nearby strike. Hence protection requirements will be determined by the direct attachment threat, and the threat assessment is accordingly limited to the direct attachment case. For the directly attached case, there are two separate processes: initial leader attachment and return stroke (or strokes). The latter has much larger associated surface currents and is considered to be the dominant threat of the two. Task 1 considered only the return stroke threat.

The starting point in threat definition is the lightning current waveform at the aircraft altitude. The most important lightning current parameters for induced effects analysis are peak amplitude, peak rate-of-rise, and total change transfer for a single stroke.

The lightning current waveform was represented as a double exponential, with rise time, fall time, and peak determined by the anticipated threat parameters (i.e., peak amplitude, peak rate-of-rise, and total change transfer). The transients calculated in Task 1 were based on two double exponential waveforms, which corresponded to the following threat parameters:

13

Severe:

        Peak current = 200 kA

        Peak rate-of-rise = 2.1×10^{11} A/sec

        Total Charge = 41 Coulombs

Moderate:

        Peak current = 20 kA

        Peak rate-of-rise = 5.4×10^{10} A/sec

        Total Charge = 1.6 Coulombs

These two threats are composites based on statistics for cloud-to-ground positive strokes, negative first strokes and negative subsequent strokes. Since all three categories of strokes are possible, the statistical data were treated independently.

The double exponential is intended to simulate only the so-called "current peak" of the stroke. The current peak has a duration of a few hunderd microseconds and is followed by a slowly-varying continuing current (also referred to as intermediate current) which lasts for several milliseconds. This low-frequency continuing current does not excite appreciable induced transients. However, this low frequency continuing current could add an additional voltage of up to 20 volts (see Appendix F) to equipment that use the metallic airframe structure for circuit return. Present practices require that all equipment sensitive to a voltage change in the return path will have a dedicated wire for circuit return. Equipment insensitive to a quartersecond variation in voltage which use the structure for the return path will most likely not be affected by the additional voltage developed by the low frequency continuing current as is the case with present day metallic aircraft. The dominant threat is the current peak component which does induce transients on the wiring.

The severe stroke parameters chosen above fall in the upper 1% to 10% of the statistical distribution; the moderate stroke parameters are around the median. For example, the severe and moderate peak rate-of-rise values correspond to the upper 1% and upper 30%, respectively, for negative subsequent strokes (Reference 2).

a. LIGHTNING CHARACTERISTICS

All aircraft flying inside or in the vicinity of a thundercloud or cloud cover are potential victims of a lightning strike. When struck, the aircraft becomes a part of the discharge circuit of the lightning. The source of lightning strikes which may hit the the aircraft are categorized into three types: the cloud-to-ground strokes, the intra-cloud discharges, and the cloud-to-cloud discharges.

According to Pierce, et. al., (Reference 3) the outstanding differences between the intra-cloud discharges the cloud-to-cloud discharges, and the cloud-to-ground strokes are as follows:

1) Global lightning strike statistics compiled the ratio between the frequency of occurrence of intra-cloud discharges and the cloud-to-ground strokes as well as that between the cloud-to-cloud discharges and cloud-to-ground to be approximately 3:1.

2) The return stroke phenomena are often observed in the case of the cloud-to-ground, however, none has been noted through observation concerning the intra-cloud discharges or cloud-to-cloud discharges. The peak value and the rise rate of the lightning current caused by the intra-cloud discharges or cloud-to-cloud discharges are both smaller than those caused by the cloud-to-ground strokes. The effects of the intra-cloud discharges or the cloud-to-cloud discharges on aircraft are generally less serious than the effects of the cloud-to-ground strokes.

3) The danger of receiving the cloud-to-ground strokes is always present within a range of altitude from 0 to about 3000 meters; however, the danger suddenly diminishes from 3,000 meters upwards.

4) The danger of the intra-cloud discharges strikes is present from an altitude of about 1,000 meters upwards and the danger increases along with the altitude. At an altitude of 3,000 meters and higher, the danger of the intra-cloud discharges and the cloud-to-ground strokes strikes are about equal. The upper limit of the intra-cloud discharges is normally 6,000 meters.

5) Approximately 95% of all the strikes take place within an altitude range from 0 to 16,000 feet. Over the 20,000 foot altitude, the incidence of strokes is about 1%.

6) Lightning strikes occur most frequently at about 0°C. About 65% of all the strikes take place within a temperature range from -5°C to +5°C. About 90% occurs between -10°C and +10°C. These facts indicate that strikes to aircraft take place most frequently in a relatively low layer of a thundercloud.

b. LIGHTNING STROKE ZONES FOR AIRCRAFT

Generally, aircraft are zoned according to the probable magnitude of lightning strike. The zones help the designer and lightning test engineer to determine the extent and type of protection required for any specific aircraft component. Test techniques that make use of these zones are discussed in References 3 and 10.

Lightning strike zones are illustrated in Figure 2 and are defined below. The zones are shown to illustrate the concept. Zones are normally developed for specific aircraft by long arc tests on scale-model aircraft or by comparison to zones established for an aircraft similar in size and configuration.

Zone 1--Direct-Stroke Attachment Zone. As the name implies, this zone is subject to initial attachment by a lightning strike. It is possible for lightning to attach to this area and remain attached for the entire duration of a stroke. Discharge times can approach, and in rare instances exceed, 1 sec. This zone includes--

a. All surfaces of the wingtips located within 18 inches of the tip, measured parallel to the lateral axis of the aircraft, and surfaces within 18 inches of the leading-edge on wings having leading-edge sweep angles of more than 45 deg

b. Projections such as engine nacelles, external fuel tanks, propeller disks, and fuselage nose

c. Tail group within 18 inches of the tips of the horizontal and vertical stabilizers, trailing edge of the horizontal stabilizer, tail cone, and any other protuberances

16

Zone 1   Zone 2   Zone 3

ZONE 2B

B C D

ZONE 1A

A B

ZONE 2A

B C D

ZONE 3

A C

ZONE 1B

A B C D
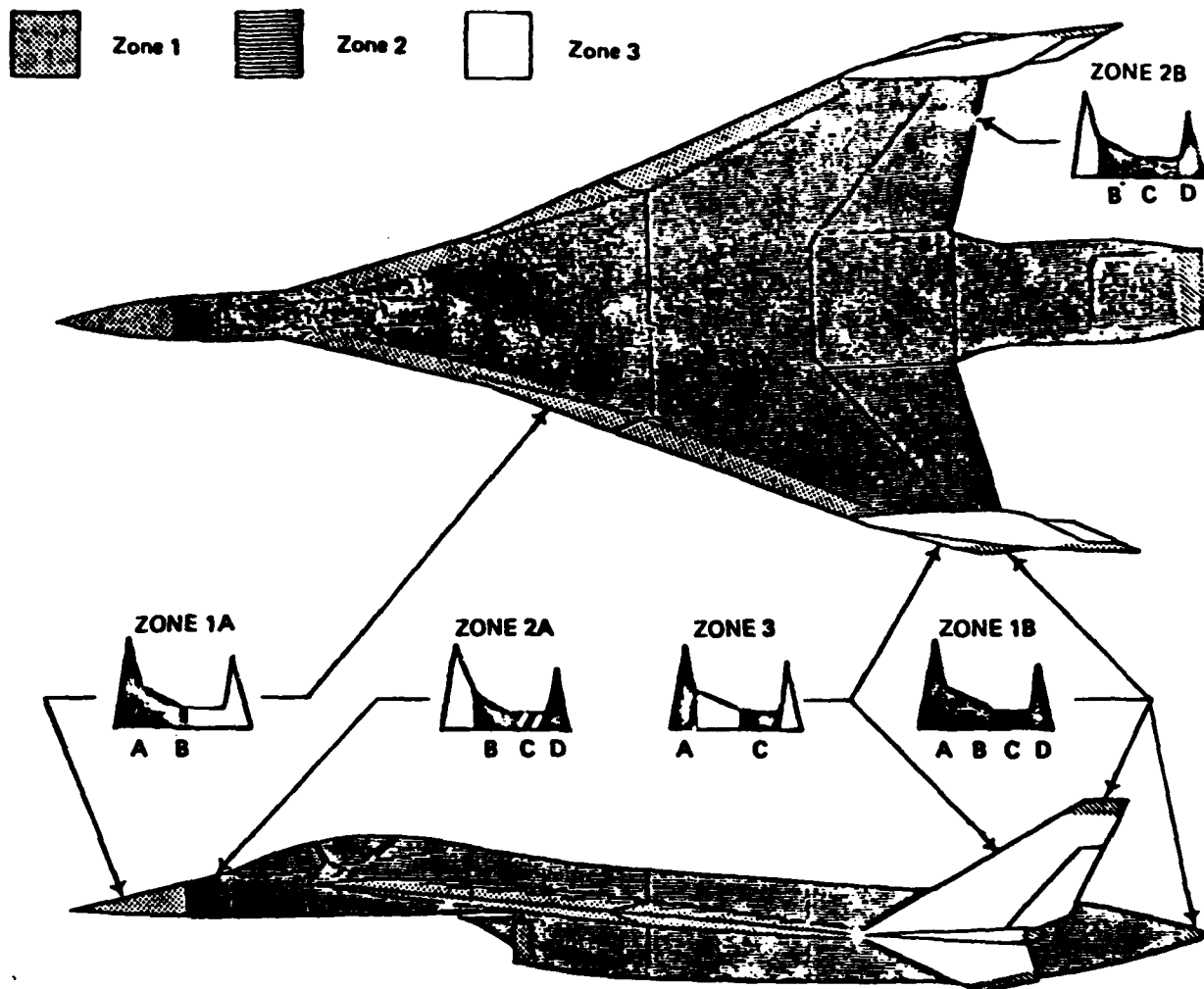
FIGURE 2   AIRCRAFT LIGHTNING STRIKE ZONES

d. Any other projecting part that might constitute a point of direct strike attachment

Zone 2--Swept-Stroke Attachment Zone. Swept-stroke surfaces are surfaces for which there is a possibility of strikes being swept rearward from a zone 1 point of direct strike attachment. This zone includes--

a. Surfaces that extend 18 inches laterally to each side of fore and aft lines passing through the zone 1 forward projection points of strike attachment

b. All fuselage and nacelle surfaces, including 18 inches of adjacent surfaces, not defined as zone 1

Zone 3. Zone 3 includes all of the vehicle areas other than those covered by zones 1 and 2. In zone 3, there is a low probability of any attachment of the direct lightning flash arc.

Zone 3 areas may carry substantial amounts of electrical current, but only by direct connection between some pair of direct or swept-stroke attachment points.

Zones 1 and 2 can be further divided into A- and B- regions, depending on the probability that the flash will hang on for any protracted period of time. An A-region is one in which there is low probability that the arc will remain attached and a B-region is one in which there is high probability that the arc will remain attached. Some examples of zone subdivisions follow.

a. Zone 1A: Initial attachment point with low probability of flash hang-on, such as a nose

b. Zone 1B: Initial attachment point with high probability of flash hang-on, such as a tail cone

c. Zone 2A: A swept-stroke zone with low probability of flash hang-on, such as a wing midspan

d. Zone 2E: A swept-stroke zone with high probability of flash hang-on, such as a wing trailing edge

2. COUPLING MECHANISMS

Four basic coupling mechanisms were considered in Task 1, as listed below:

      o EXPOSED CONDUCTORS - conductors directly exposed
        to the lightning fields (e.g., windshield heater,
        front and rear spar wiring).

      o APERTURES - non-conductive portions of airplane
        exterior. Some examples are the cockpit canopy,
        windows, and fiberglass access doors.

      o JOINTS - electrical discontinuities in aircraft
        exterior; e.g., the narrow gap between a metallic
        access door and underlaying airframe or the interface
        between two graphite epoxy panels.

      o DIFFUSION - low-frequency penetration of fields into
        the interior of metallic or graphite-epoxy fuselage,
        wings; etc.

a. COUPLING ANALYSIS METHODS

The analysis methods employed for the various coupling mechanisms are as follows:

1) Exposed wires - using the method described in Section II.3.a, one obtains the fields directly. For more complicated structure, such as landing gear, it is necessary to do further analysis to obtain the fields on structural members protruding from the basic airframe.

2) Apertures - when a conducting surface is interrupted by openings (e.g., cockpit canopy), the exterior surface fields penetrate into the interior.

At low frequencies, this coupling mechanism may be decomposed into
magnetic and electric coupling or, equivalently, stray inductance and
capacitance between conductors in the interior of the body and
the exterior surface. The magnetically and electrically-coupled interior
fields are proportional to the surface current and charge density which
would appear on a shorted aperture. With certain restrictions, the
interior fields due to magnetic coupling may be modeled as those due to a
magnetic dipole. With similar restrictions, the electrically-coupled
fields may be approximated as those of an electric dipole. In the general
case, one may solve for the interior fields by calculating the fields in
the aperture and using the equivalent sources, distributed over the
aperture, to solve the interior problem. The process is simplified by the
fact that, for the lightning frequency spectrum, the apertures of interest
are electrically small, reducing the problem to a quasistatic one.

An aperture of particular interest is the narrow slot. On equipment bay
doors, for example, the hinge and latch side make good electrical contact
with structure, while the two other sides form narrow slot apertures. The
fields of the gap may be modeled as those of a magnetic dipole. For wires
lying across the gap, however, the voltage induced in the wire is simply
the gap voltage at the wire location.

3) Joints - Well-formed joints (those of uniform construction without cracks
   or large openings) can be described in terms of a distributed
   admittance/unit length. The joints are similar to the narrow slot, except
   that the voltage along the joint is approximately constant. For either
   joint or slot, the interior fields may be obtained by using the fields in
   the opening to obtain the equivalent sources for solving the interior
   problem.

4) Diffusion - In the low frequency limit, this mechanism is equivalent to
   what has been referred to in lightning studies as the so-called "IR drop".
   For all-aluminum aircraft, this mechanism is important only for the low
   frequency continuing current and is a threat only to circuits using
   structural return. For a graphite epoxy aircraft, however, the
   electromagnetic fields associated with the high frequency peak current can
   diffuse entirely through the structure, inducing considerable voltage in
   interior wiring.

20

b. EQUATIONS FOR THREAT ESTIMATION

As indicated in Section VII, the complex circuit models developed under Task 1
are not appropriate for preliminary lightning protection design requirements.
A more cost-effective approach is to estimate the common mode threat seen on
the circuit and determine circuit survivability by analysis or a threat
simulation test. The threat simulation test is described in Section II.2.c.

For simplicity, the threat waveforms are categorized according to four types
of coupling, i.e., exposed wire, inductive slot, resistive joint, and
diffusion. For each type of coupling, the open circuit voltage and short
circuit current are computed for two cases, $Z_T = 0$ (the terminating common
mode load at the far end is small compared to the common mode characteristic
impedance of the wire bundle) and $Z_T = \infty$ (the terminating load is large
compared to the common mode characteristic impedance). In obtaining the
equations shown in Tables 3 to 6, it was assumed that airframe resonances may
be neglected for the direct strike case. Analysis of airframe resonances
using the transmission line model of Section II.3.a, together with limited
in-flight data show that this is the case.

The rationale for limiting the threat definition to a common mode transient is
as follows. For a common mode excitation (i.e., the incident electromagnetic
field is the same at all wires in the bundle), the differential mode
transients are determined by the terminating loads. If the computed common
mode threat is injected into the interconnecting wire bundle with the
terminating equipment loads attached, then the differential mode transients
(as well as common mode) obtained in the test will be an adequate simulation
of the true threat. For determination f survivability by analysis, the
application of the common mode threat is more complicated. A worst case
approximation to the threat may be obtained on a case-by-case basis, by
identifying the circuit component most likely to suffer voltage breakdown, and
assuming that it draws the full short circuit current taking into account the
circuit loads at the far end of the cable.

c. THREAT SIMULATION FOR EQUIPMENT TESTS

In order to define a test which adequately simulates an induced transients
threat, the following is required:

TABLE 3 EQUATIONS FOR THREAT ESTIMATION FOR EXPOSED WIRE

	Low Frequency Component	Damped Cosine Amplitude	Damped Sine Amplitude	Resonance
V_{OC} ($Z_T=0$)	$F(\dot{I}_L)$	$(4F)\dot{I}_{PK}/\pi$	$(4F\dfrac{\dot{I}_{PK}}{\pi})(Z_L/\beta Z_A)$	$\lambda/4$
I_{SC} ($Z_T=0$)	$\dfrac{F}{L_W}(I_L)$	$(2F\dot{I}_{PK}/\pi Z_C)(Z_L/\beta Z_A)$	$(2F)\dot{I}_{PK}/\pi Z_C$	$\lambda/2$
I_{SC} ($Z_T=\infty$)	$\dfrac{F}{Z_C}(\dot{I}_L)$	$(4F\dot{I}_{PK}/\pi Z_C)(Z_L/\beta Z_A)$	$(4F)\dot{I}_{PK}/\pi Z_C$	$\lambda/4$
V_{OC} ($Z_T=\infty$)	$\dfrac{Z_C F}{L_W}(I_L)$	$(2F)\dot{I}_{PK}/\pi$	$(2F\dot{I}_{PK}/\pi)(Z_L/\beta Z_A)$	$\lambda/2$

$F = \mu\displaystyle\int_{exposure} hdx/C(x)$ $\mu = 4\pi \times 10^{-7}$ henries/meter

h = height of wire above ground plane

$C(x)$ = effective circumference of airframe

Z_C = common mode characteristic impedance of wire bundle

Z_L = characteristic impedance of lightning channel

Z_A = characteristic impedance of airframe

β = common mode relative velocity of wire bundle

I_L = lightning current waveform

$\dot{I}_{PK}$ = peak rate-of-rise of lightning current

L_W = common mode total inductance of wire bundle

TABLE 4   EQUATIONS FOR THREAT ESTIMATION FOR INDUCTIVE SLOT

	Low Frequency Component	Damped Cosine Amplitude	Damped Sine Amplitude	Resonance
V_{OC} ($Z_T=0$)	$K\,L_S\,\dot{I}_L$	$4\,K\,L_S\,\dot{I}_{PK}/\pi$	0	$\lambda/4$
I_{SC} ($Z_T=0$)	$K\,L_S\,I_L/L_W$	0	$2KL_S\,\dot{I}_{PK}/\pi Z_C$	$\lambda/2$
I_{SC} ($Z_T=\infty$)	*$K\,L_S\,C_W\,(1-X/1)\ddot{I}_L$	0	$4\,KL_S\,\dot{I}_{PK}/\pi Z_C$	$\lambda/4$
V_{OC} ($Z_T=\infty$)	$K\,L_S(1-X/1)\,\dot{I}_L$	$2\,KL_S\,\dot{I}_{PK}/\pi$	0	$\lambda/2$

K, L_S defined in Appendix C; ($V_{wire} = K\,V_{slot}$)

X = distance from end of wire bundle to slot

1 = length of wire bundle

All other parameters described under Table 2-1

* There is insufficient data to determine $\ddot{I}_L$.

TABLE 5   EQUATIONS FOR THREAT ESTIMATION FOR RESISTIVE JOINT

	Low Frequency Component	Damped Cosine Amplitude	Damped Sine Amplitude	Resonance
V_{OC} ($Z_T=0$)	$KR_J\,I_L$	0	$4\,KR_J\,\dot{I}_{PK}/\pi W_0$	$\lambda/4$
I_{SC} ($Z_T=0$)	$\dfrac{KR_J\,Q_L}{L_W}$	$2\,KR_J\,\dot{I}_{PK}/\pi W_0 Z_C$	0	$\lambda/2$
I_{SC} ($Z_T=\infty$)	$KR_J C_W(1-X/1)\dot{I}_L$	$4\,KR_J\,\dot{I}_{PK}/\pi W_0 Z_C$	0	$\lambda/4$
V_{OC} ($Z_T=\infty$)	$KR_J(1-X/1)\,I_L$	0	$2\,KR_J\,\dot{I}_{PK}/\pi W_0$	$\lambda/2$

K defined in Appendix C; ($V_{wire}=K\,V_{slot}$)

$R_J = 1/(Y_J C)$

Y_J = joint admittance/length

C = effective circumference of airframe at joint

C_W = total common mode capacitance of wire bundle

$W_0 = 2\pi f_o$, fo = resonant frequency

$Q_L(t) = \int^t I_L(\bar{t})d\bar{t}$

23

TABLE 6 EQUATIONS FOR THREAT ESTIMATION FOR DIFFUSION

	Low Frequency Component	Damped Cosine Amplitude	Damped Sine Amplitude	Resonance
$V_{OC}(Z_T=0)$	$Z_M(0)\, K\, I_L$	$4K\, B(W_0)\dot{I}_{PK}/\pi W_0$	$4\, K_A(W_0)\dot{I}_{PK}/\pi W_0$	$\lambda/4$
$I_{SC}(Z_T=0)$	$\dfrac{Z_M(0)\, K\, Q_L}{L_W}$	$2K\, A(W_0)\dot{I}_{PK}/\pi W_0 Z_C$	$2\, KB(W_0)\dot{I}_{PK}/\pi W_0 Z_C$	$\lambda/2$
$I_{SC}(Z_T=\infty)$	$Z_M(0)K_1 C_W \dot{I}_L$	$4K\, A(W_0)\dot{I}_{PK}/\pi W_0 Z_C$	$4\, KB(W_0)\dot{I}_{PK}/\pi W_0 Z_C$	$\lambda/4$
$V_{OC}(Z_T=\infty)$	$Z_M(0)K_1\, I_L$	$2K\, B(W_0)\dot{I}_{PK}/\pi W_0$	$2\, KA(W_0)\dot{I}_{PK}/\pi W_0$	$\lambda/2$

$$K = \int_{exposure} dx/C(x)$$

$C(x)$ = effective circumference of airplane at x

$Z_M(W)$ = transfer impedance for diffusive surface

$Z_M(W) = A(W) + jB(W)$

$Z_M(0) = 1/(\sigma t)$

  σ = conductivity of material

  t = thickness of material

  $$K_1 = \int_{exposure} (1-X/1)\, dx/C(x)$$

$W_0 = 2\pi f_0$, f_0 = resonant frequency

  1 = length of wire bundle

24

1. An accurate representation of the threat waveform seen at the circuits, i.e., the spectral content and energy.
2. An accurate source impedance for the pulser.
3. Representative hardware, which includes:
   a. Terminating loads
   b. Interconnecting wire bundles
4. A well-defined pass-fail criterion
   A detailed test procedure is beyond the scope of this section. It is intended, to instead, to give an overview of test methods. A forthcoming document being drafted by the SAE committee AF4L (Reference 12) will give general guidelines for test definition.

There are three test methods for simulating an induced transient threat:

1. Direct injection into interface circuits.
2. Transformer coupling to interconnecting wiring.
3. Exposure of equipment and interconnecting wiring to TEM fields in a parallel-plate simulator.

In the following disucssion, only a common-mode threat simulator will be considered.

(1) DIRECT INJECTION METHOD

In order to illustrate this method, consider a pair of LRU's connected by an unbranched wire bundle which is exposed to lightning-induced fields. Designate the LRU to be tested as "Box A" and the other as "Box B". Given the common mode termination of the wire bundle at Box B, one can compare this to the characteristic impedance of the wire bundle and determine whether to use $Z_T=0$ or $Z_T=\infty$ in Tables 3 thru 6. The appropriate source impedances are:

Table 7   Source Impedances for Direct Low Frequency Injection Tests

	Low Frequency Component	Damped Sine or Cosine
$Z_T=0$	jwL_w	$2\,Z_c$
$Z_T=\infty$	$1/jwC_w$	$Z_c/2$

Where the parameters are defined in Tables 3 thru 6. For a pulser with the appropriate source impedance, the threat waveform may be established by comparing the pulser output to the desired V_{oc} or I_{sc}.

(2) TRANSFORMER COUPLING TO INTERCONNECTING WIRING

Again consider a pair of LRU's connected by a wire bundle. The test will consist of coupling an induced transient on the interconnecting wire bundle with Box A at one end and Box B, or a simulation thereof, at the other. If the test bundle is the same length as that which will be used in the aircraft, the simulator need only produce the low frequency component, as the resonances will be produced by the wire bundle. If the test bundle is appreciably shorter than the actual installation, then both the low frequency and resonant waveforms must be simulated.

(3) PARALLEL-PLATE SIMULATOR

For a system consisting of several LRU's, it may be appropriate to excite the interconnecting wiring simulataneously. For this test, the wiring and equipment for the entire system should be representative of that to be used on the aircraft. The threat waveform for the TEM fields produced in the simulator should approximate the lightning current waveform. The lay of the wire bundles, which determines the characteristic impedance, should be the same as the aircraft installation.

Ideally, the simulator should be sufficiently large to enable one to lay out the wiring in straight runs between equipment boxes. The termination of the parallel plates enables one to test for TEM (matched), H-field only, (short circuit), or E-field only (open circuit).

3. LIGHTNING MATH MODEL DEVELOPMENT

The threat assessment performed under Task 1 consisted of developing computer models of selected circuits, using survey data, and calculating lightning-induced transients for the moderate and severe threats. In developing the circuit models, it became apparent that certain design

modifications can significantly reduce the lightning induced transients. These modifications are noted in the text describing the circuit models.

The direct attachment of the lightning column to aircraft wiring was not analyzed. Rather, it was decided to protect against this threat by controlling the wire routing and adding protective coatings to non-conductive structure to prevent this occurence. This protection will be more reliable and cost-effective than incorporating protective devices in the wiring and circuitry adequate for the full lightning current. (See Section IV.2)

a.   LIGHTNING-AIRFRAME INTERACTION MODEL

The lightning channel-airframe interaction was modeled as a mismatched transmission line. The lightning channel impedance was chosen to be 500 ohms. The airframe impedance was obtained by approximating the fuselage wing as an ellipsoid of revolution.

This simple model gives the total current and charge in the airframe at any point along the current path. The surface current and charge were then obtained by calculating the effective circumference at the point of interest. The current density on the leading edge of a wing of rectangular cross section, for example, is give by the equation:

$$J_S = I/C_{eff}$$
$$C_{eff} = C\sqrt{\frac{\pi b}{a}}$$

Where C = circumference of wing, a = wing chord, and b = wing thickness. The current and charge density along the leading and trailing edges of the wing (approximated as an ellipse) will be enhanced 2 or 3-fold above that for a cylinder of the same circumference.

The end result of the analysis of the lightning-airframe interaction is the charge and surface current densities over the conducting exterior surfaces of the airframe. These quantities are then used to obtain the fields at the location of wire bundles as described in the following section.

b. WIRE MODELING

The geometry of aircraft wiring lends itself naturally to transmission line analysis. In Task 1, the transmission line parameters were obtained from computing self and mutual inductances and capacitances for the individual wires, along with wire and ground return resistances. These parameters were obtained from wire radius, wire-to-wire separation, height above ground plane, and dielectric constant of insulation, using textbook formulas. These line parameters were then entered, along with the sources, into the Boeing TRAFFIC code for computation of transients.

(1) DESCRIPTION OF MAGNETIC COUPLING

Figure 3 depicts magnetic coupling of lightning surface currents to a wire. The voltage, e, is the open cicuit voltage seen at the end of a wire which is grounded at the other end.

If only common-mode voltages without transmission effects are considered, the coupled transient voltage will be as shown in equation 1. This voltage will appear between the end of the wire bundle and nearby airplane structure. For a wire which is terminated in circuit loads, this voltage will divide between the loads at the ends of the bundle inversely as the impedance of the loads.

$$e = \frac{d\phi}{dt} = (\mu_o)(A)\left(\frac{dH}{dt}\right), \tag{1}$$

where A = area of loop: meters squared

μ_o = permeability of free space, $4\pi \times 10^{-7}$: henries per meter

ϕ = total flux linked: webers

H = magnetic field intensity: amperes per meter

t = time: seconds

e = voltage: volts

Expressed in inch units:

$$e = 8.11 \times 10^{-10} (1)(h)\left(\frac{dH}{dt}\right), \tag{2}$$

28

$$e = \frac{d\phi}{dt}$$
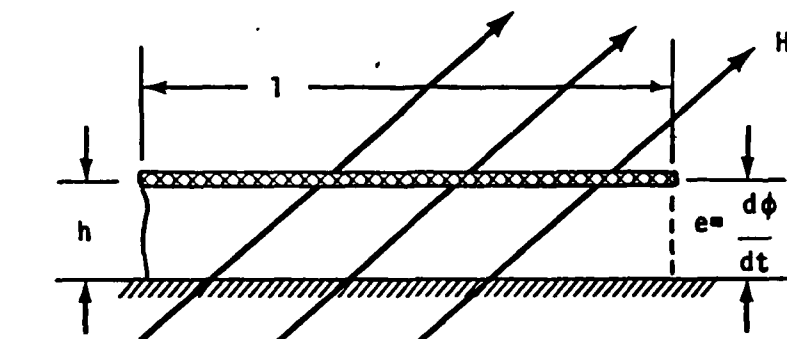
(a)
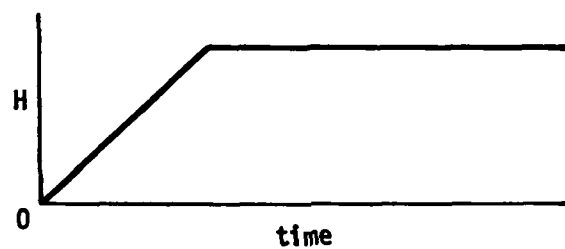
(b)
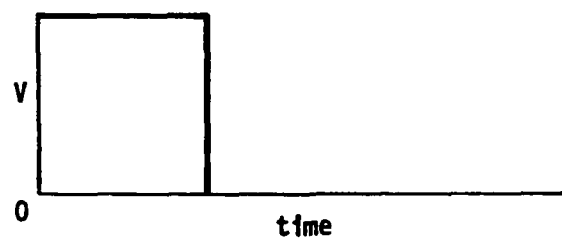
(c)

(a) Physical circuit schematic

(b) Magnetic field waveshape

(c) Voltage waveshape

Figure 3   Open Circuit Voltage/Magnetic Field Dramatization

29

where l = length of cable bundle: inches

h = height above ground plane: inches

H = magnetic field intensity: amperes per meter

t = time: seconds

In the development of the models, the effects associated with the resonant response of the transmission line were included. Figure 4 shows the open circuit voltage and the open end of a magnetically excited, resonant line. In general airplane wiring is grouped into bundles consisting of both short and long conductors, so when exposed to a magnetic field the resultant transient responses in the voltage waveshapes are more complex.

c. DESCRIPTION OF CIRCUIT MODELS

The starting point in Task 1 was to obtain engineering survey data from existing aircraft. The aircraft types considered were cargo, fighter-bomber, and fighter. The aircraft models surveyed were C-14, F-111, and F-15. The C-14 surveyed was located at the Boeing Company Developmental Center. For the F-111 and F-15, trips were made to McClellan AFB, California, and Warner-Robbins AFB, Georgia.

The visual engineering survey is an indispensable element of the lightning threat assessment. Wiring schematics and line drawings are insufficient for determining likely penetration points. In addition, critical geometric details (e.g., wire heights above the ground plane), are available only from visual inspection.

During the engineering surveys, circuits which would be exposed to the lightning threat were determined by visual inspection. Each survey began with a general walk-around of the aircraft, with particular attention to wiring in the following areas:

  o Exposed leading and trailing edges of the wings.
  o Wiring on landing gear struts.
  o Wiring in the vicinity of large slots or apertures (e.g., cargo doors, passenger windows, cockpit canopy cabin, windshields, equipment bay doors).

30
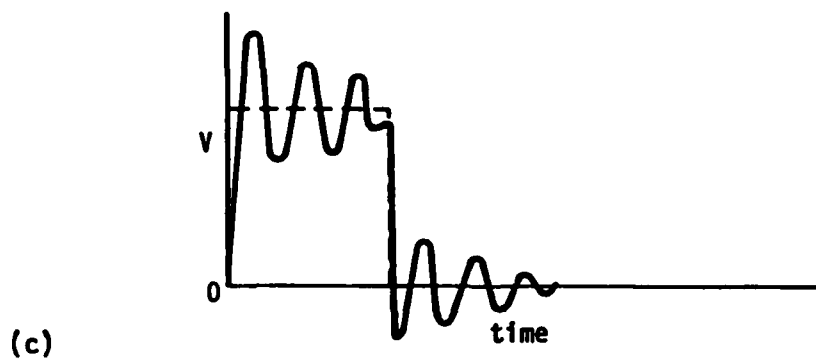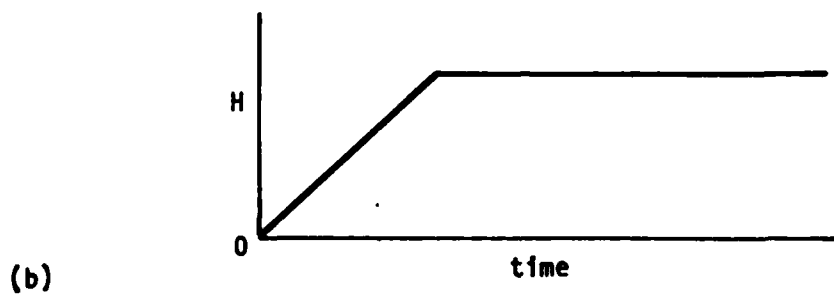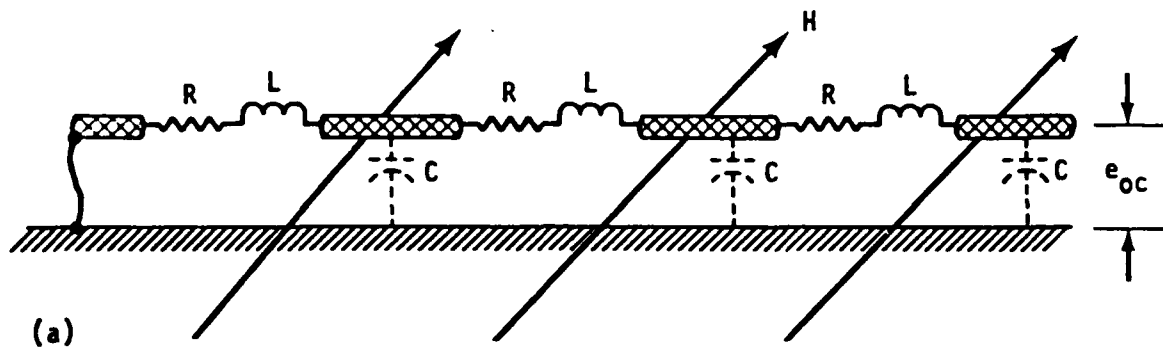
(a) Physical R,L,C circuit schematic

(b) Magnetic field waveshape

(c) Voltage waveshape

Figure 4   Open Circuit Voltage Response Caused by a Changing Magnetic Field

o Wiring underneath fiberglass or graphite-epoxy structure.

o Wiring in the radome area, especially near the forward pitot tube ground wire.

o Wiring along the leading and trailing edge of the vertical stabilizer.

o Wiring to externally-attached payload (e.g., external fuel tank, releasable bombs).

o Wiring to critical or sensitive circuit (e.g., flight controls, computers).

o Wiring to systems which have recorded damage from lightning strike.

o Extremities with non-conductive external structure (e.g., fiberglass wiring tips).

Based upon these criteria, the following circuits and components were surveyed. (The asterisk indicates cirucits for which the impact of substituting composite structure for metal was examined):

C-14   1) Upper Surface Blowing Actuator
       2) Wing Tip Beacon Light
       3) Windshield Heater
       4) *Vertical Stabilizer Actuator

F-111   5) Pitot Heater
       6) Radar
       7) Map Reading Light
       8) Head-Up Display (HUD) Wiring
       9) Trailing Edge Flap Actuator
      10) Fiberglass Wing Tip
      11) Forward Landing Gear Steering Unit and Main Landing Gear Position Indicator Switch.
      12) *Vertical Stabilizer Light
      13) Weapons Release Actuators
      14) Generator and Generator Control Unit
      15) Wing Root Area

F-15   16) Right Outboard Pylon Power
      17) *Pitot Heater
      18) External Fuel Tank Quantity Indicator
      19) Generator Feeders and Generator Control Unit

20) Forward Landing Gear Taxi Lights
    Main Gear Down and Lock Switch
21) Wing Tip Formation Light
22) Radar
23) Essential Power Buss Feeders
24) Power Wires to Roll/Yaw and Pitch Computers
25) Vertical Stabilizer Lights

(1)   C-14 UPPER SURFACE BLOWING ACTUATOR

The circuit consists of a 12-wire bundle which runs from the actuator mounted
on the trailing edge of the wing, along the rear spar, into the cargo bay, to
the interface unit in the electrical equipment rack. The wire bundle includes
power wires which continue on to the power panel in the forward cargo area.
The modeled circuit consisted of the wire run from the actuator to interface
unit, and included the magnetically-induced lightning voltage source along the
rear spar.

The dominant source in the circuit is the magnetic coupling to lightning
surface currents due to the large (.9 square meters) loop between the wire
bundle and rear spar. Figure 5 is a block diagram of the circuit model. Open
circuit, short circuit, and matched circuit conditions were imposed at both
the actuator and interface unit for moderate and severe strokes.

The design modification for reducing the transient is to reduce the loop area
between the wire bundle and the rear spar. The voltage source is proportional
to the area.

(2) C-14 WING TIP BEACON LIGHT

The beacon light located on the wing tip is powered by a single wire which
runs from the main power bus in the forward cargo area to the power supply at
the wing tip and back to a ground point in the fuselage, near the wing root.

The dominant source in the circuit is magnetic coupling to lightning surface
currents on the leading edge of the wing. Figure 6 is a block diagram of the

33

circuit model. Figures 7 to 10 depict the transients at the transformer and
at the power bus for moderate and severe strokes. The open circuit, short
circuit, and matched circuit conditions were imposed at both the transformer
and power bus for each case.

The wire height above the front spar was assumed to be 3 inches along the full
length of the exposed run. Reducing this height would reduce the induced
transient levels proportionally.

(3) C-14 WINDSHIELD HEATER

The C-14 windshields are heated by thin resistive layers imbedded in the
windshield. The element is powered by a 115 V AC line from the power bus.
Wiring details vary according to window, so a 30 meter run of 2 #12 AWC wires
was assumed.

The dominant source is capacitive coupling between the heater element and the
external lightning-induced electric field. The derivation of the coupling
model is described in Appendix A. The windshield heater source consists of a
current source in parallel with the capacitance of the heater element. Figure
11 depicts the circuit model. The transients at the power bus are indicated
in Figures 12 and 13. A design modification which would reduce the induced
transients at the power bus is to use structure for return by grounding the
power return a short distance from the windshield. This will short out the
large voltage between the heater element and nearby airframe, and shunt the
lightning induced current into the airframe.

(4) C-14 VERTICAL STABILIZER ACTUATOR

This circuit model is applicable to a C-14 with a non-metallic composite toe
ramp. For a metal toe ramp, the induced transients will be negligible. The
vertical stabilizer actuator circuit is powered by 115 V AC from the main
power bus in the forward cargo area. This circuit was analyzed to scope the
effect of lightning induced fields fringing through the gap (or slot) between
the cargo doors. The gap is 130 inches long with an insulated gap of
.85 inches wide. The gap is transverse to the main lightning current flow for
a nose-to-tail strike. The lightning current flowing around the gap will
induce magnetic fields inside the cargo area. Appendix B describes the
derivation of the coupling model.

ACTUATOR LOADS

SRC1
SRC2
SRC3
SRC4
SRC5
SRC6

* WING BUNDLE

L = 1.36
M = .876

C = 2.12
CM = 3.53
RDC = .017

RAC = .15

length=3.66 Meters

* FUSELAGE BUNDLE

L = 1.12
M = .636

C = 2.92
CM = 3.43
RDC = .017

RAC = .15

length=13.72 Meters

INTERFACE
UNIT
LOADS

*All units as follows:

L,M - microhenries/m
C,CM - picofarads/m
RDC - ohms/m
RAC - ohms/m at 1 MHz

$V_s = (j)(w)(\mu)$ (AREA) $(I_w) \cdot K_{conc}/CIRC$

$K_{conc} = 2$
CIRC = wing circumference
AREA = .91 m^2.
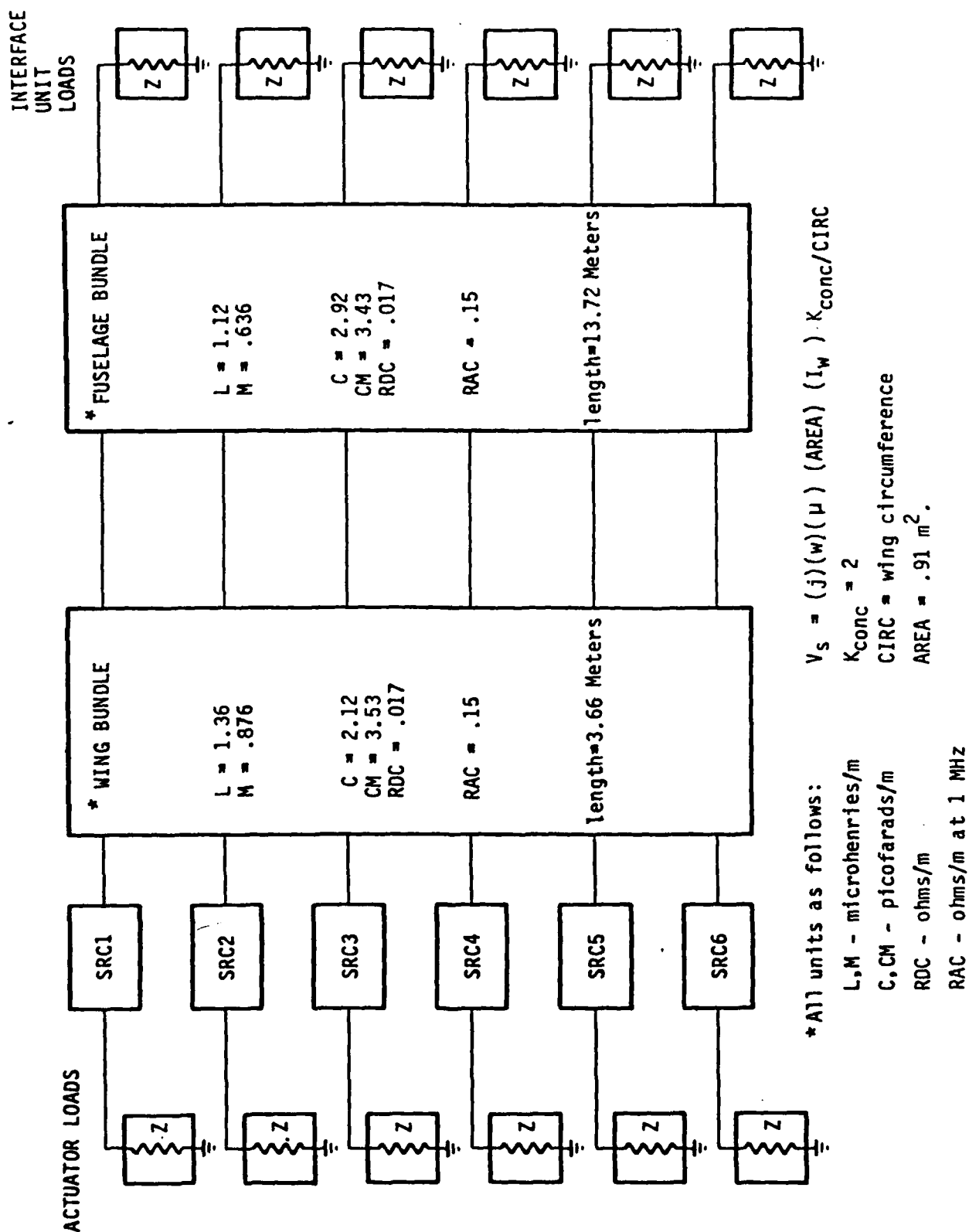
FIGURE 5   Block Diagram for Upper Surface Blowing Actuator Circuit

35

POWER
BUS LOADS

Z_2

* FUSELAGE

L=1.1
C=5.1
RDC=.017
RAC=.15

Length =
20.2m

* WING 3

SAME AS
WING 1

Length =
7.71m

S5

S6

* WING 2

SAME AS
WING 1

Length =
4.66 m

S3

S4

* WING 1

L= .819
M= .750
C= 7.42
CM= 77.4
RDC= .017
RAC= .15

Length =
4.66m

S1

S2

Z_1

Z_1
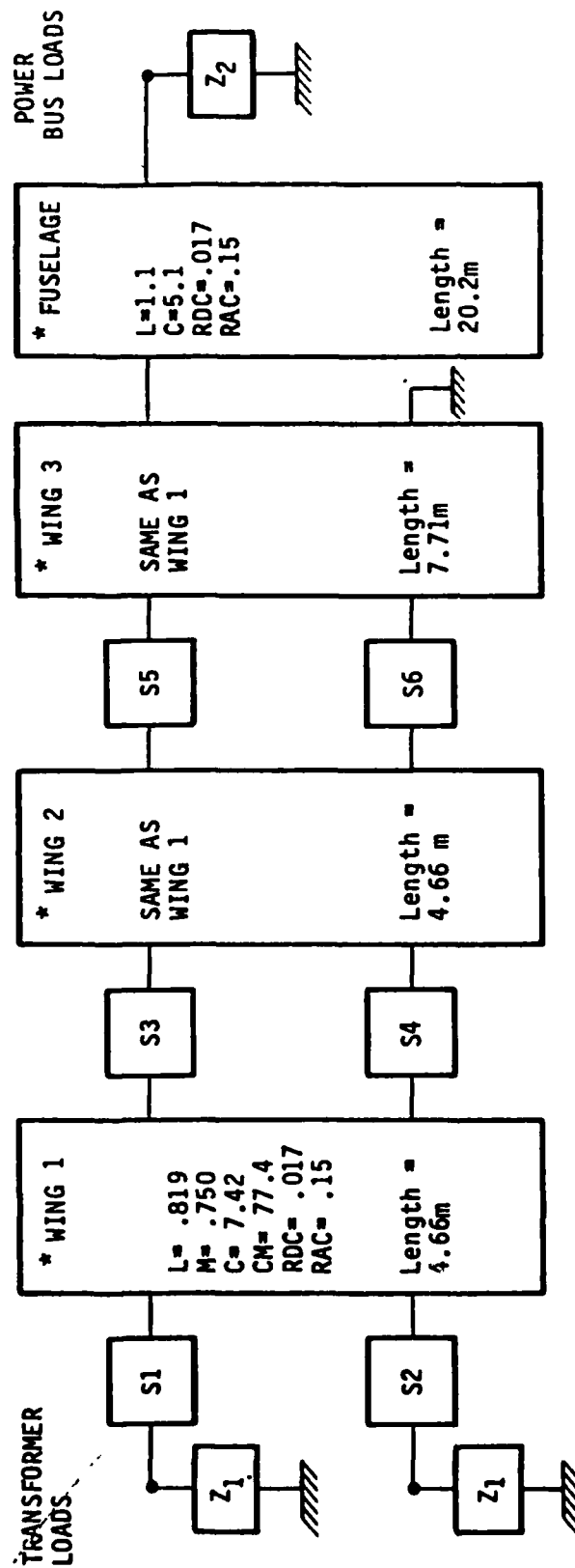
TRANSFORMER
LOADS

* All units as follows:

L,M – microhenries/m

C,CM – picofarads/m

RDC – ohms/m

RAC – ohms/m @ 1 MHz

FIGURE 6   Block Diagram for C-14 Wing Tip Beacon Light Circuit

36
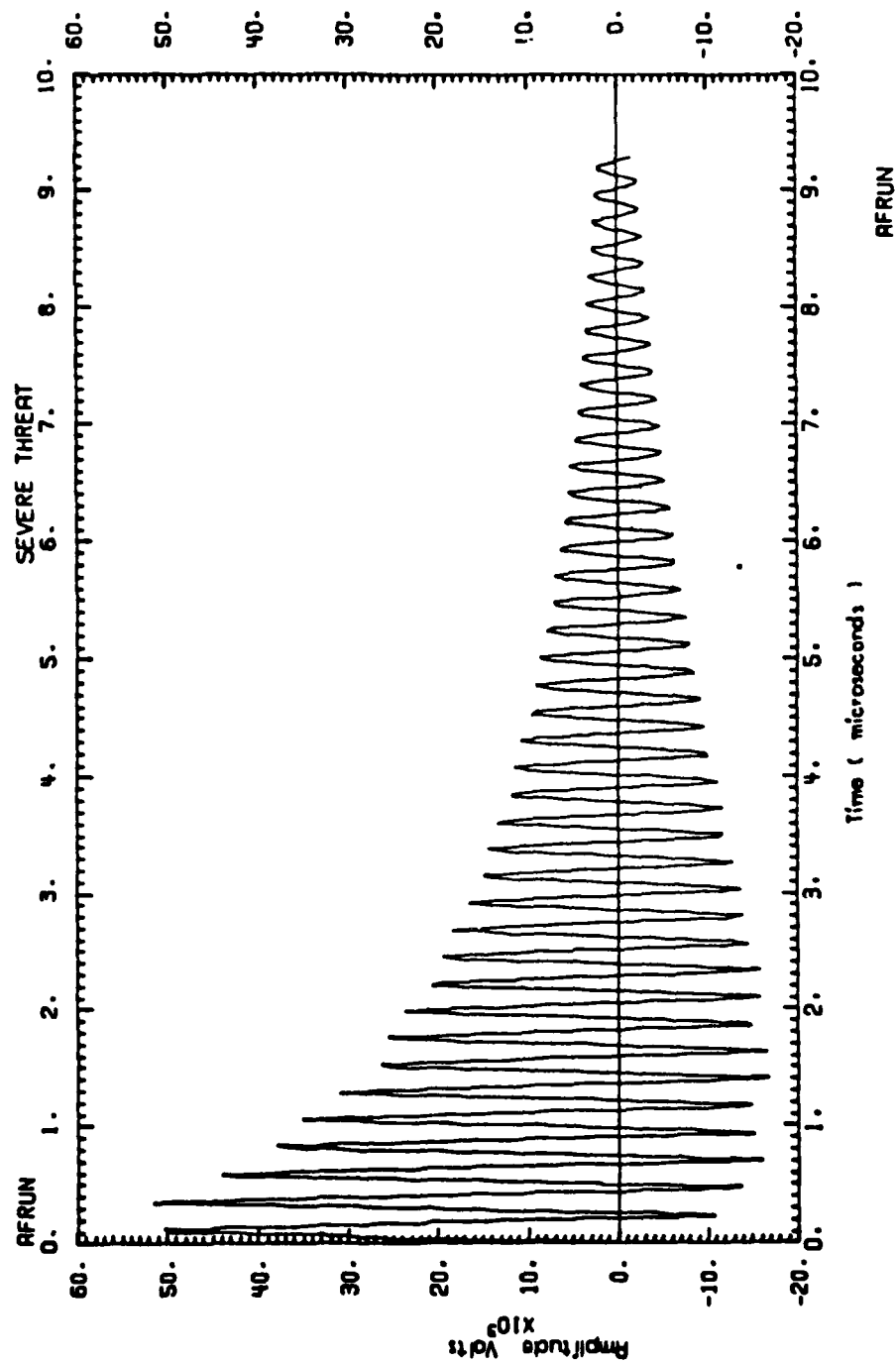
FIGURE 7 V_{OC} AT THE TRANSFORMER

37
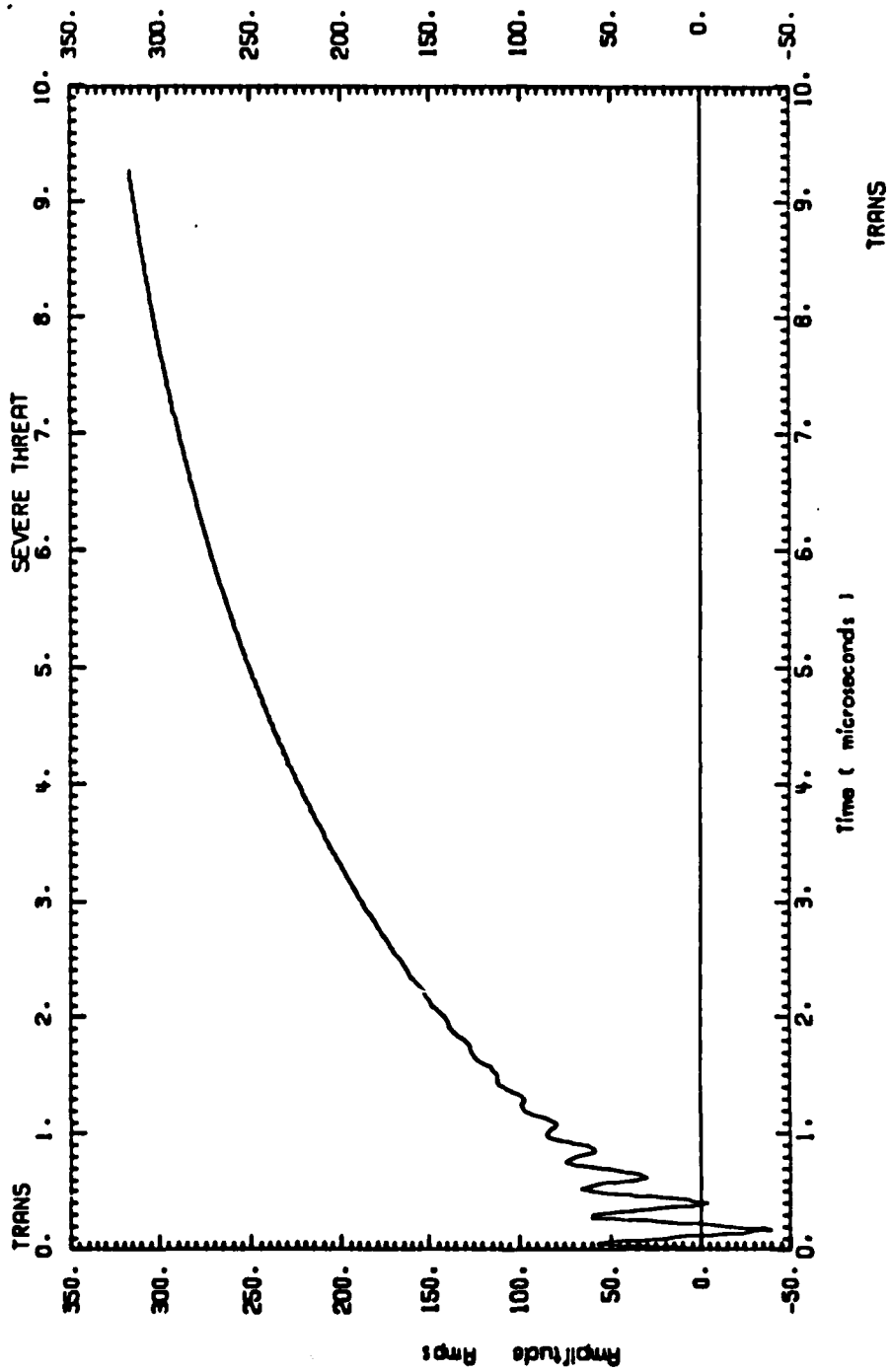
FIGURE 8 I_{SC} AT THE TRANSFORMER

SEVERE THREAT

Time (microseconds)

Amplitude   Amps

TRANS

MEMBER = TRANS   DATA SET= ISMFCFI

16.39.01. 79/08/30 BLYACHK

SEVERE THREAT

AFRUN

AFRUN

Time (microseconds)

Amplitude Volts
x10³
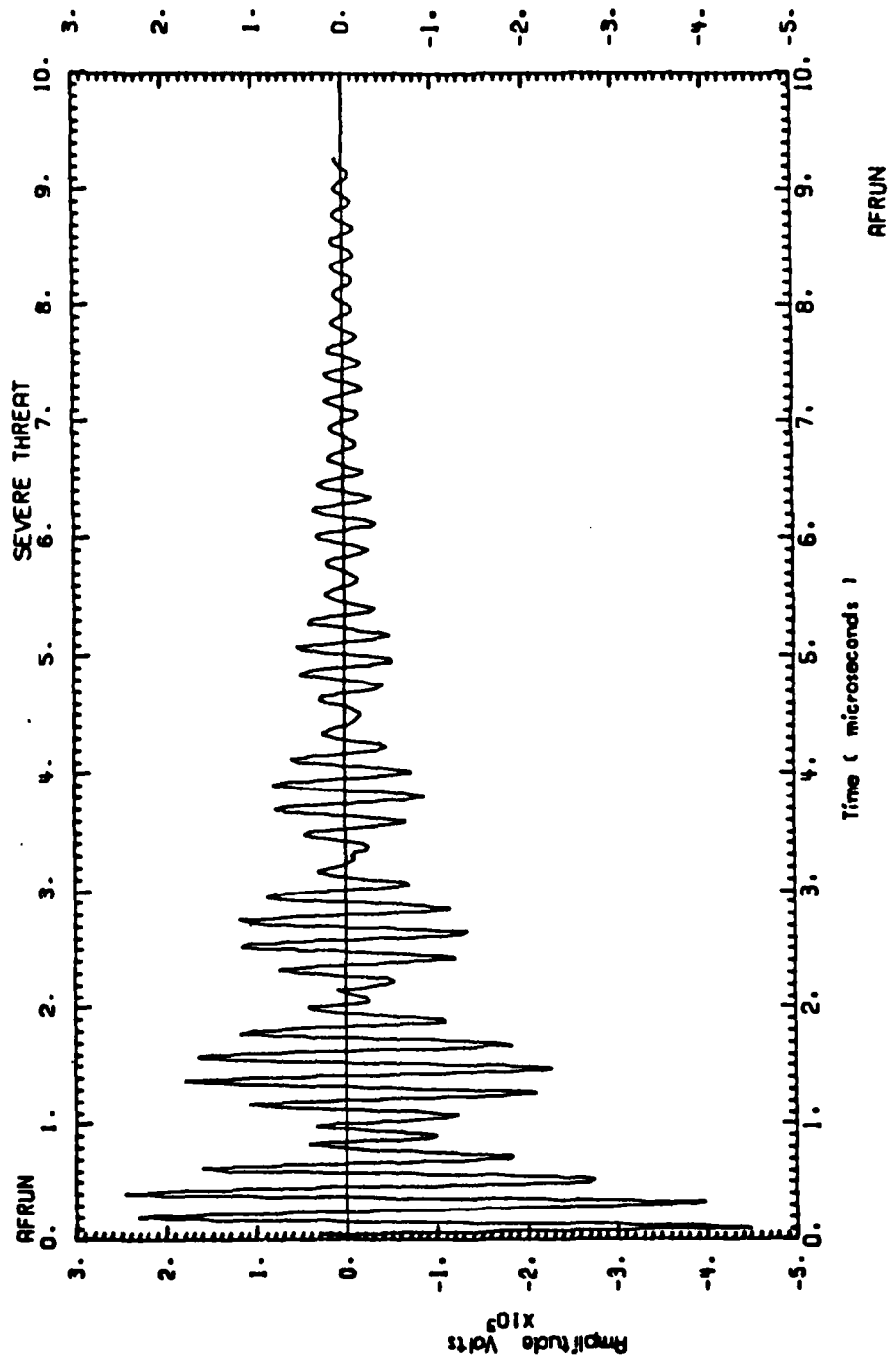
MEMBER : AFRUN   DATA SET: VOPMC12   FIGURE 9   V_OC AT THE POWER BUS

16.40.06. 79/08/30 BLYACHK

SEVERE THREAT

TRANS

Time (microseconds)

Amplitude Amps
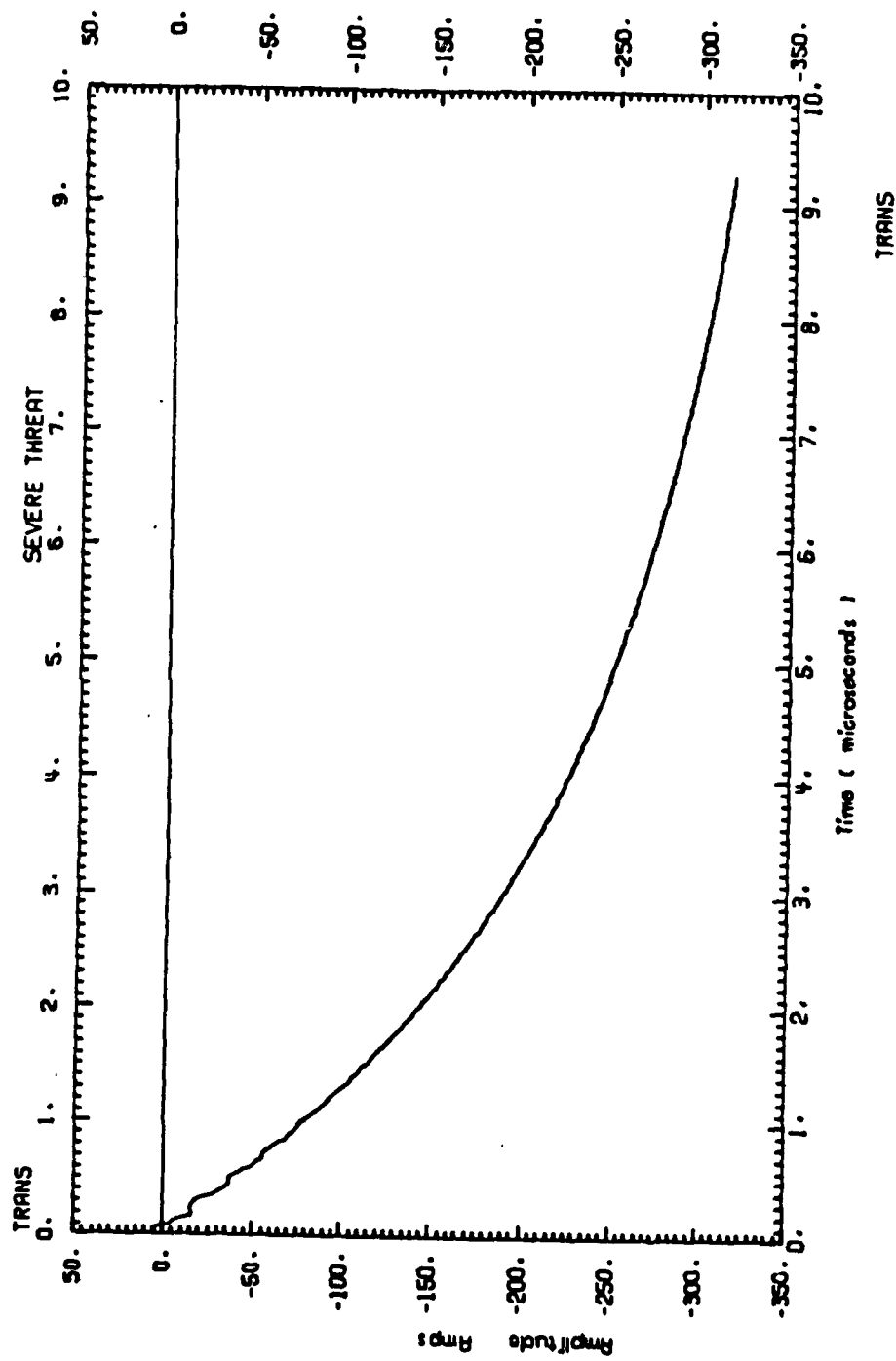
MEMBER : TRANS   DATA SET: ISKREF2   FIGURE 10 I_{SC} AT THE POWER BUS

POWER BUS
LOADS

* HEATER WIRES

L = .876   RDC = .017

M = .807   RAC = .15

C = 6.89

CM = 77.7

LENGTH = 30 M.
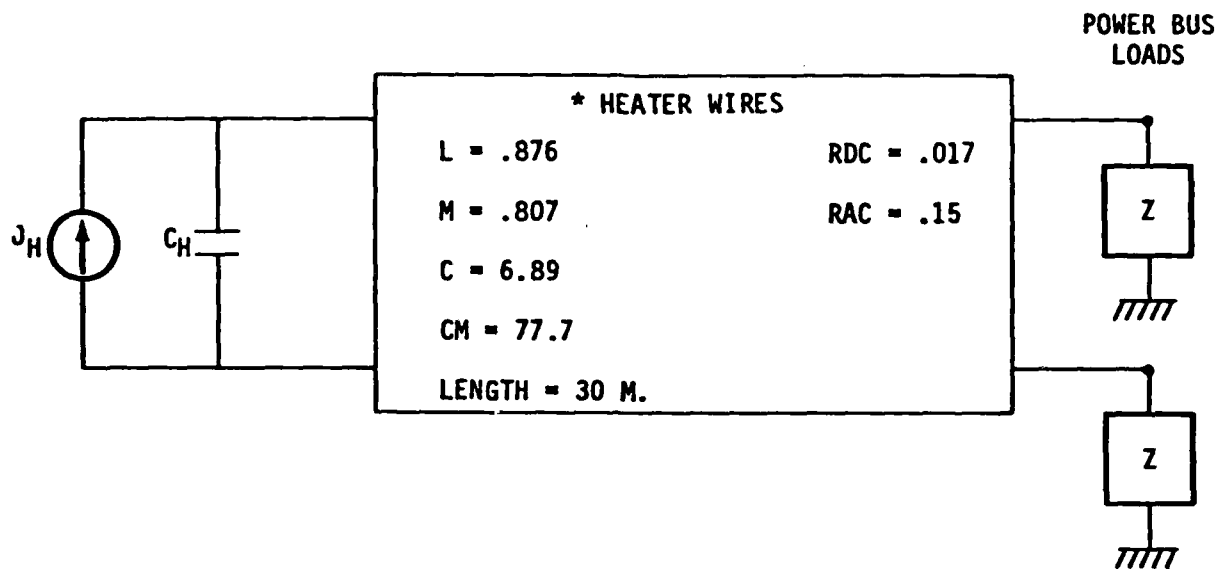
C_H = 41 PICOFARADS

J_H = jw ϵ_o x AREA * EN

EN = NORMAL LIGHTNING-INDUCED ELECTRIC FIELD ON AIRCRAFT EXTERIOR

AREA = .627 m^2 = HEATER AREA

*UNITS AS FOLLOWS:

L,M - MIRCROHENRIES/M

C,CM - PICOFARADS/M

RDC - OHM/M

RAC - OHM/M AT 1 MHz

FIGURE 11 Block Diagram for C-14 Windshield Heater Circuit

41

20.52.25. 79/10/16 BLYABRE

AFRUN   TYPE = 3 C14 WINDSHIELD HEATER CIRCUIT-SEVERE THREAT

Amplitude Volts
x10³

Time (microseconds)
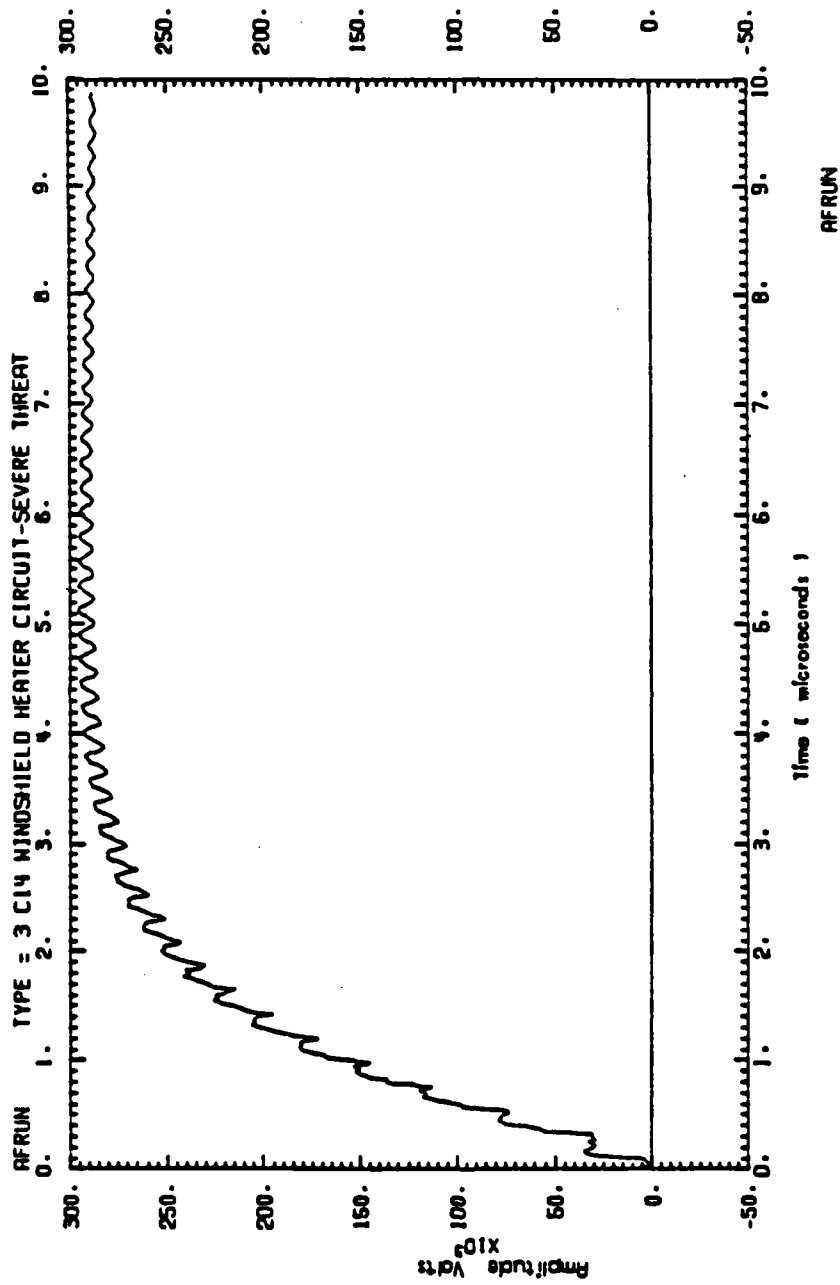
AFRUN

MEMBER = AFRUN   DATA SET: VOC

FIGURE 12 V_{OC} AT THE POWER BUS

20.52.50. 79/10/16 BLYABRE

TRANS   TYPE = 3 C14 WINDSHIELD HEATER CIRCUIT-SEVERE THREAT
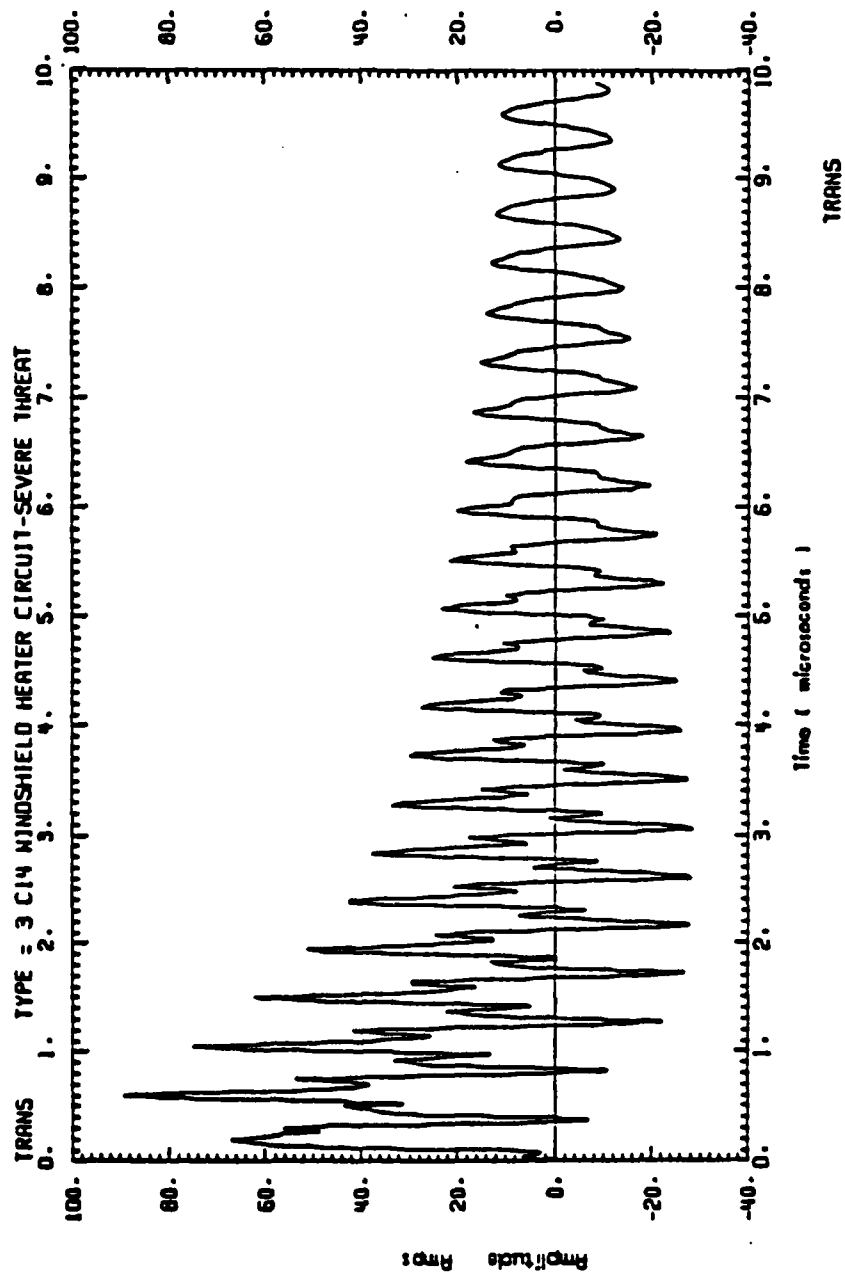
FIGURE 13 I_{SC} AT THE POWER BUS

MEMBER : IMAG   DATA SET: ISC

Figure 14 depicts the circuit model. Only the severe stroke was considered, as the transients were relatively low. The wire was assumed to lie a distance of 6 inches above the side of the cargo area wall in the exposed area and was 2.5 feet from the side of the slot.

The cargo door slot in the C-14 surveyed was shorted by a metal toe ramp. This would reduce the induced transient to a negligible value. However, if this metallic ramp is replaced by a non-conductive composite material, the circuit model is applicable. For such a case, the transients induced in the circuit may be reduced by decreasing the height of the wire from the wall and increasing the distance from the wire to the edge of the slot. See Appendix C for equations.

(5) F-111 PITOT HEATER CIRCUIT

In the F-111, the metal pitot boom is attached to the forward part of the radome. When the aircraft is struck by lightning, this metal rod is a highly probable attachment point. The pitot boom is grounded to the forward bulkhead by a heavy gauge wire. The pitot heater wires are strung alongside the ground strap and will pick up induced transients when the pitot boom is struck by lightning. Appendix D describes the circuit model in detail.

The heater wires form a narrow loop as is shown in Figure 15. The magnetic coupling to the pitot heater wires may be reduced by laying them symmetrically alongside the ground strap as shown in Figure 16. The electric coupling may be reduced by laying the wires tightly against the ground strap. The equations for coupling are explained in Appendix D. The pitot heater wires couple capacitively and inductively to the electromagnetic fields induced by lightning currents flowing through the ground strap. Figure 17 depicts the block diagram for the circuit. The open circuit voltage, short circuit current, and matched voltage and current (into a 300 ohm load) seen on the heater wire at the forward bulkhead were calculated for the moderate strike. The severe strike waveforms may be obtained by scaling the moderate strike units by the factor;

$$I_{pk}^{severe}/I_{pk}^{moderate} = 2.1 \times 10^{11}/5.4 \times 10^{10} = 4X.$$

44

LOADS AT ACTUATOR

* WIRE BUNDLE AFT OF SLOT (SAME AS FOWARD BUNDLE)

Length=22m

S1 S2 S3 S4 S5 S6

* WIRE BUNDLE FORWARD OF SLOT

L=1.12
M=.636
C=2.92
CM=3.43
RDC=.017
RAC=.15
Length=9.4m

* TWO-WIRE BUNDLE

L=.819
M=.750
C=7.4
CM=77.4
RDC=.017
RAC=.15
Length=16m

LOADS AT POWER BUS

Z_l Z_l
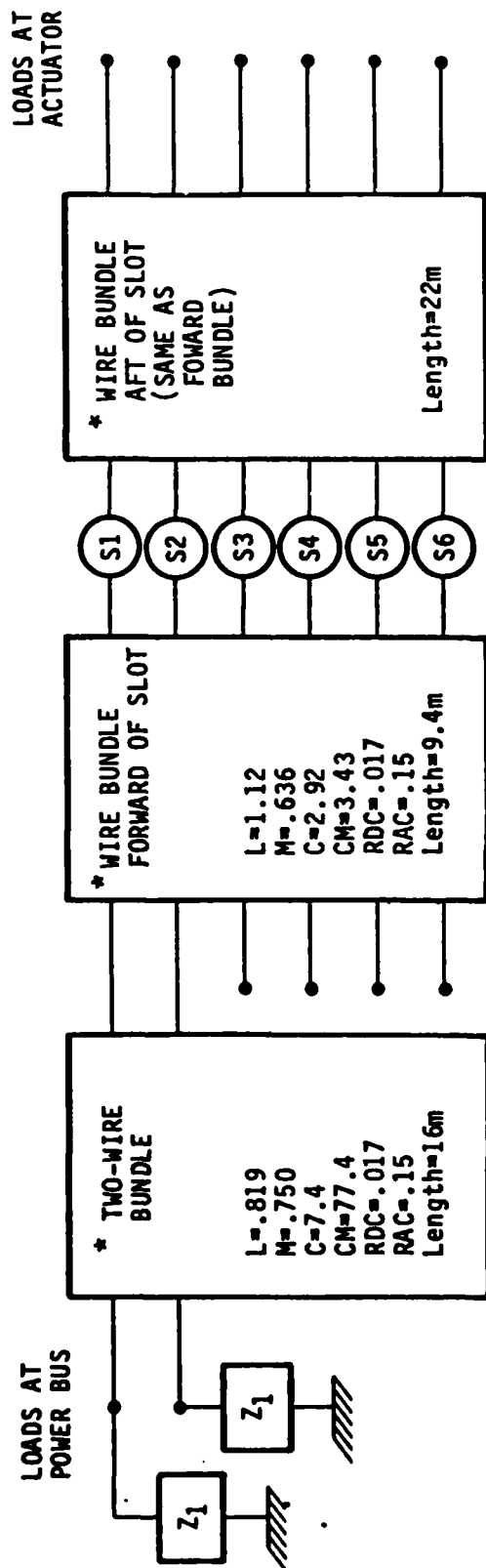
$S1, S2 \ldots S6 = Jw(\mu_0)\,(K)\,(h)\,I/circ$

K = coupling factor (see appendix B)

h = height of wire above wall

I = lightning current in airframe at cargo door

circ = circumference of fuselage at cargo door

* units as follows:

L,M - microhenries/m

C,CM - picofarads/m

RDC - ohms/m

RAC - ohms/m at 1 MHz

FIGURE 14   Block Diagram for C-14 Vertical Stabilizer Actuator Circuit
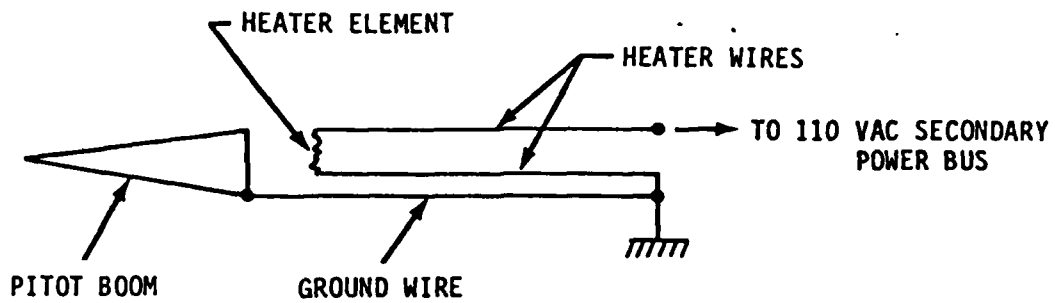
FIGURE 15 Pitot Heater Wire Configuration
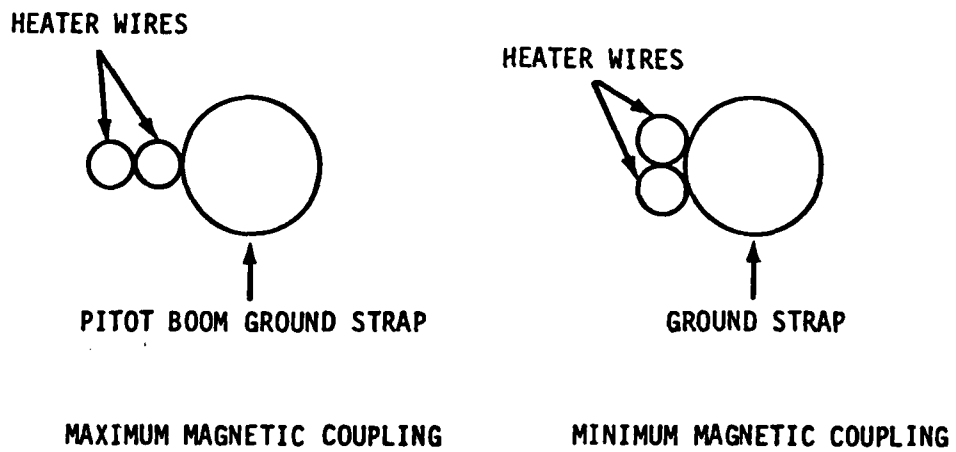
FIGURE 16 Magnetic Coupling on Pitot Heater Wires

46

TO 110 V AC
SECONDARY
BUS

TERMINATING
LOADS AT FORWARD
BULKHEAD

V_{oc}

L_W

C_W

I_{sc}

L_H

R_H

$I_{sc} = jw \, (K_m) \, (F_s)$
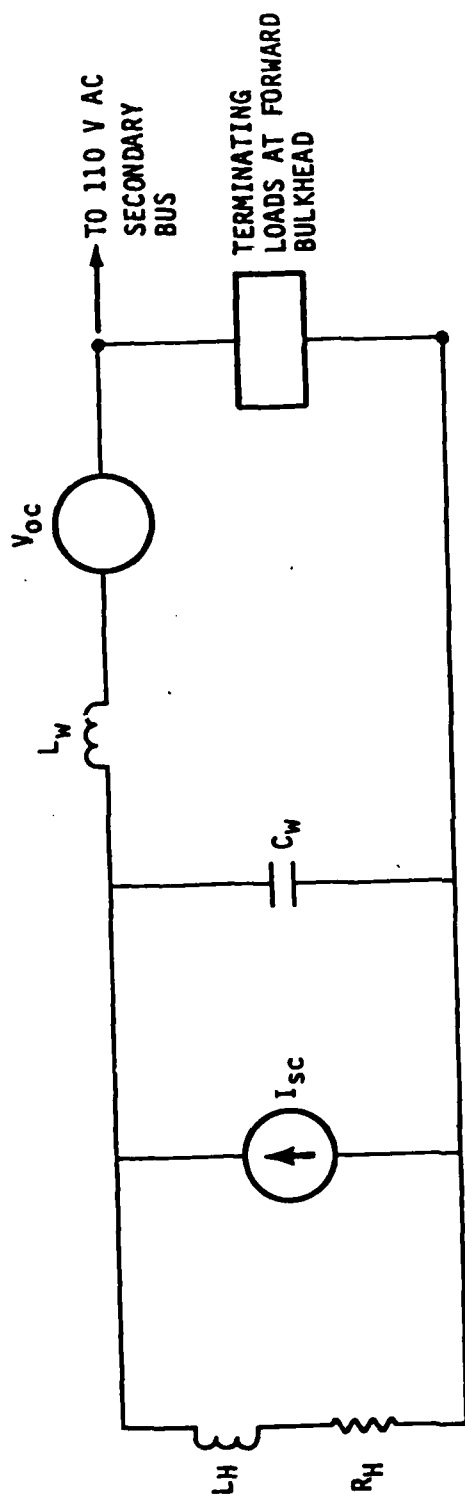
$V_{oc} = jw \, (\mu_0) \, (K_E) \, (J_s)$

$L_H = 100 \text{ nH}$

$R_H = 115 \text{ ohms}$

$C_W = 66 \text{ pF}$

$L_W = 420 \text{ nH}$

FIGURE 17 Block Diagram for F-111 Pilot Heater Wire Circuit
(see Appendix D for equations and explanation)

47

(6) F-111 RADAR DRIVE MOTORS FOR FORWARD-LOOKING ATTACK RADAR AND ATTACK
RADAR

The power wires to the radar drive motors will be exposed to the magnetic
fields in the radome area due to lightning currents flowing in the pitot boom
ground strap. The open circuit voltage induced in these small loops may be
well approximated by the expression:

$$V_{oc} = 2(\mu_0)(A) \cos\theta(\dot{I}/2\pi d)$$

where: $\mu o = 4\pi \times 10^{-7}$ H/m
         A = loop area in square meters
         d = distance from loop to ground strap (in
             meters)
         θ = angle between loop normal and radial vector
             from ground strap to loop
         $\dot{I}$ = time derivative of lightning current

The lightning induced transients in these power circuits are proportional to
loop area. Hence, the transients may be substantially reduced by routing the
wires flush against metallic structure and locating the ground strap the
maximum possible distance from the exposed loops.

(7) F-111 COCKPIT MAP READING LIGHT

The power wires to the cockpit map reading light are routed along the center
part of the cockpit canopy. For a nose-tail strike, lightning currents
flowing through the canopy post will couple magnetically to the light wires.

The current through the post is approximately $I_{post} = I_L \times S/C$, where I_L is
the total current through the airframe at the post location, S is the arc
length of the canopy (in cross-section), and C the total circumference of the
airframe including the canopy. The lightning-induced magnetic field alongside
the canopy post is

48

$H_t = I_{post} / 2(t+w)$. The voltage source is then
$V_{oc} = (\mu_0)(A)(\dot{H}_t)$, A = h x 1, 1 = wire length,
t = width of canopy post, h = height of wire above post,
w = depth of canopy post

The circuit model is indicated in Figure 18. The open circuit voltage and
short circuit current on the power wires at the aft end of the canopy were
produced for the moderate strike.

(8) F-111 COCKPIT INSTRUMENT PANEL WIRING - HEAD UP DISPLAY

The wiring behind the instrument panel lays underneath a fiberglass dashboard
and is exposed to magnetic fields due to lightning currents flowing through
the canopy post.

The open circuit voltage induced in a wire bundle is given by:

V_{oc} = (μ_0) (A)$(\dot{H})$, where
A = loop area between wire bundle and instrument panel metal frame
H = $\dot{I}_{post}$ / πR (2x factor due to proximity of interior conducting surface)
$\dot{I}_{post}$ = $(S/_C)$ $\dot{I}_L$
R = perpendicular distance from wire bundle to canopy post
I_L = time derivative of lightning current in airframe at cockpit location
S = arc length of canopy (in transverse section)
C = circumference of airplane including cockpit

(9) F-111 TRAILING EDGE FLAP ACTUATION

The flap actuator on the trailing edge of the F-111 wings is powered by 28 V
DC wiring routed along the exposed trailing edge at a height of approximately
1" above the trailing edge. The open circuit voltage induced in the wiring by
a strike to the wing is given by:

V_{oc} = $(\mu_0)(h)(1)(K_{conc})$ $(\dot{I}_L)$ x <1/c>, where
h = height of wire above loading edge
1 = length of wire (actuator to fuselage)
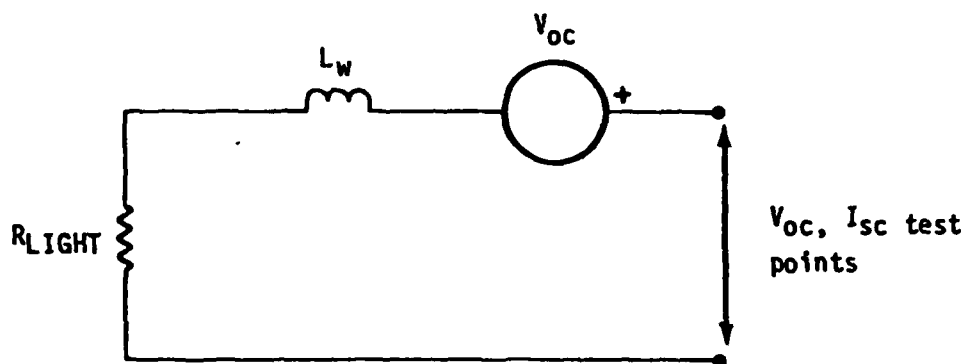
$V_{oc} = jw \ (\mu_o) \ (H_t) = jw \ (\mu_o) \ (h) \ (1) \ (H_t)$

$H_t = I_{post} \ / \ 2 \ (t+w)$

$I_{post} = (S/C) \ I_H = I_L/3$

$t = 2.5 \ cm$

$w = 10 \ cm$

$h = .6 \ cm$

$1 = .6 \ m$

$L_{wire} = 300 \ nH$

$R_{Light} = 1 \ ohm$

FIGURE 18   Block Diagram for F-111 Cockpit Map Reading Light

K_{conc} = concentration factor (see Section II.3.c(4) F-111 Vertical Stabilizer Light)

$\dot{I}_L$ = time derivative of total lightning current in wing at wire location

$\langle 1/c \rangle$ = average of inverse wing circumference along length of exposed wire

(10) F-111 FIBERGLASS WING TIP

The wing tip of the F-111 has a fiberglass cap of approximately 4 inches depth which extends the width of the wing tip fore and aft. Since the wing tip is a probable area for lightning attachment, any circuits underneath the fiberglass may be directly struck by lightning. This threat may be met by adding protective coatings to the fiberglass or relocating underlying circuits. (See Section IV)

(11) F-111 FORWARD LANDING GEAR STEERING UNIT AND MAIN LANDING GEAR POSITION INDICATOR.

When the landing gear are extended, the circuits along the struts are exposed to lightning fields. The F-111 and F-15 are sufficiently similar that only the F-15 landing gear circuits were analyzed. (See Section II.3.c). The model for the F-15 main gear down and lock switch is applicable to the F-111 Steering Unit and Position Indicator circuits.

(12) F-111 VERTICAL STABILIZER LIGHT

Power to the vertical stabilizer lights is provided by wires routed along the leading edge of the vertical stabilizer. For a nose/vertical stabilizer strike, the wire bundles will be exposed to lightning surface currents, if the leading edge is non-metallic. There are two non-metal candidates for the leading edge:

1. Composite structure of low conductivity
2. Non-conducting structure (e.g., fiberglass)

The open circuit lightning voltage sources for the wire bundles in the two cases are:

51

1. Composite structure of conductivity σ and thickness t:

$V_{oc} = (Z_T)(J_S)(1)$

$Z_T = 1/\sigma t$ 1 = wire length

$J_S = (I_L)(K_{conc}) \times (<1/C>)$

I_L = total lightning current in tail

K_{conc} = concentration factor

$<1/c>$ = average of inverse of circumference along wire run

Values of K_{conc} for various width-to-thickness   ratios are:

Width/Thickness	K_{conc}
1	1
2	1.54
5	3.34
10	6.47

A general expression for K_{conc} is:

$$K_{conc} = (\tfrac{W}{T}) \times \frac{2E(k)}{\pi} \text{ , where}$$

E=Complete elliptic intergral of first kind

$$k = \sqrt{1 - \left(\frac{T}{W}\right)^2}$$

T = thickness of wing or tail

W = width of wing or tail

2. Non - conducting structure:

$V_{oc} = (\mu_0)(h)(1)(J_S)$

h = height of wire bundle above leading edge

1 = length of wire

$\dot{J}_S = (\dot{I}_L)(K_{conc}) <1/c>$

$\dot{I}_L$ = time derivative of lightning current waveform

(13) F-111 WEAPONS RELEASE ACTUATORS AND NAVIGATION LIGHT

Some of the wire bundles to weapons-carrying pylons are routed along the
leading edge of the wing, along with the power wires to the navigation light
transformer. For a metallic leading edge, these wires are well shielded from
lightning transients. If the leading edge is replaced by non-metallic
structure, the same considerations apply as for the F-111 vertical stabilizer
light. The same expressions for open circuit induced voltage due to a
nose-wing tip strike are applicable. (See Section II.3.c(12)).

(14) F-111 GENERATOR FEEDERS AND GENERATOR CONTROL UNIT (GCU)

On the F-111, the generators are mounted on the engines inside the fuselage.
Hence the generator feeders and GCU wires are routed inside the fuselage
between the engines and the forward equipment bays. The only apparent source
for lightning - induced transients is magnetic coupling through engine and
equipment bay access door slots. In addition, some magnetic coupling will be
induced in the generator feeders routed through the main landing gear wheel
well, when the landing gear is down.

The results for magnetic coupling through access door slots is described in
the F-15 circuit model for generator feeders and GCU wires. (See Section
II.3.c(19)).

(15) F-111 WING ROOT AREA

The movable wing on the F-111 presents an additional problem for lightning
induced transients due to the concentration of lightning currents in the wing
pivot, for a lightning strike to the wing. Inspection of the aircraft
revealed that a large bundle of wing wires is routed around the pivot, and
will be exposed to the concentrated lightning currents flowing through the
pivot (8 inches in diameter). This coupling problem does not lend itself to
a simple analysis, since the current distribution in the wing root area is
complicated and dependent on the electrical contact between the pivot pin and
adjacent structure. A detailed analysis and experimental data for the
electrical contact between the pivot pin and adjacent structure is required to
develop a coupling model for this exposure.

(16) F-15 RIGHT OUTBOARD PYLON POWER

The power wires to the pylons are exposed to the lightning-induced voltage appearing between the pylons structure and adjacent wing surface. For a direct strike to the pylon, this open circuit voltage is given by the expression:

$$V_{oc} = (\mu o) (L_{pylon}) (\dot{I}_L), \text{ where}$$
$$\dot{I}_L = \text{time derivative of lightning current}$$
$$L_{pylon} = \text{inductance of pylon supports}$$

An approximate expression for L_{pylon} is:

$$L_{pylon} = \frac{\mu o}{2\pi} \ln(\lambda /2\pi a)(1/N)$$

a   = radius of pylon support in meters

N   = number of supports

λ = wave length representative of rise time of lightning strike = 1.8×10^3m

l   = length of pylon support

For a strike to the wing tip, the method for calculating the induced voltage is described in Section II.3.c.18, F-15 External Fuel Tank Circuit.

(17) F-15 PITOT HEATER CIRCUIT

This model assumes that metal structure is replaced with composite material. For conventional metal structure, the induced transients would be negligible. The pitot tubes on the F-15 are mounted aside the fuselage on the forward equipment bay access doors. The wiring is well shielded by airframe, for metallic access doors. In the circuit model, composite doors were assumed of thickness .1" and conductivity 10^4 mho/m (representative of Graphite Epoxy). The circuit model is shown in Figure 19.

The lightning induced transients are due to diffusion of electromagnetic fields through the (assumed) low-conductivity graphite-epoxy access doors. Induced transients at the essential power bus and standard power bus for open

ESSENTIAL POWER
BUS
LOADS

TWO WIR *

L=1100
M=500
C=7.2
CM=6.5
RDC=.03
RAC=.09
Length = 1.8m

LWIR *
(SAME AS
TWO WIRE)

Length = 8.8m

L_H R_H

VL

L_H R_H

VL

STANDARD
POWER BUS
LOAD

ONE WIR *
L = 1100
C = 11
RDC = .03
RAC = .09
Length = 3m

RWIR *
(SAME AS
TWO WIR)

Length = 4.4m

L_H R_H

VR

L_H R_H

VR
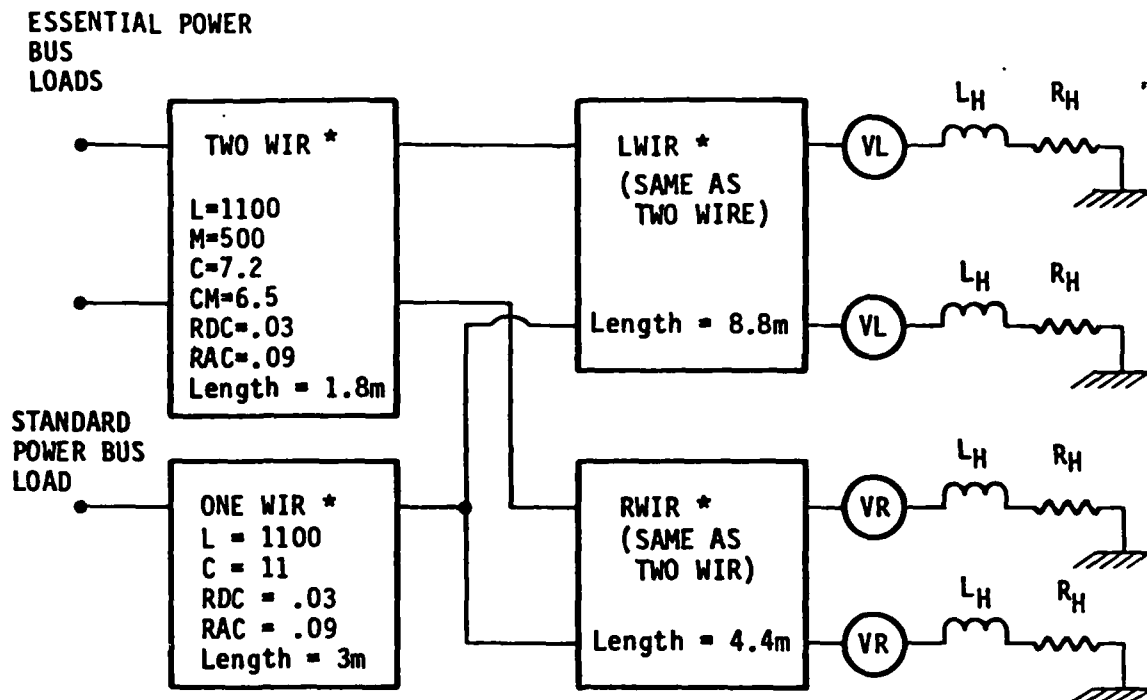
$L_H = 10^{-6}$ H

$R_H = 25$ ohms

* ALL UNITS ARE

L = M = nH/m

C = CM = pF/m

RDC = ohm/m

RAC = ohm/m (at 1 MHz)

VL, VR = Z_T x I_L / CIRC

Z_T = transfer impedance for graphite epoxy

CIRC = 4.4 meters

I_L = lightning current in airframe at pitot heater

FIGURE 19 Block Diagram for F-15 Pitot Heater Circuit

circuit, short circuit, and the matched terminations were computed for the moderate stroke threat.

(18) F-15 EXTERNAL FUEL TANK QUANTITY INDICATOR

The external fuel tanks on the F-15 are supported by pylons connected to the airplane by two support ports. Wiring routed from the fuel tank into the aircraft is exposed to the lightning-induced voltage appearing across the gap between the pylon and fuselage. This voltage source was modelled for the center fuel tank for a nose-tail strike. Figure 20 depicts the assumed fuel tank geometry and circuit model. The coupling mechanism is capacitive coupling of lightning-induced normal electric fields to the external fuel tank.

The capacitance, C_{TANK}, is the total capacitance between the fuel tank and fuselage, which is the sum of two terms: 1) capacitance of gap at the top of the pylon and 2) capacitance between the fuel tank and fuselage. The inductance, L_{POST}, is the parallel combination of the two pylon support inductances.

The open circuit voltage uced in wiring crossing the pylon gap (see Figure 20) is shown in Figure 21. ihe high frequency ringing (24MHZ) is due to the resonance of the L-C circuit for the fuel tank and pylon support ports. Wiring routed across the gap may be protected by wire shields. If shields are used to protect the wiring, they should be grounded to structure at the pylon and fuselage. The voltage appearing across the gap may be reduced by bonding straps.

(19) F-15 GENERATOR FEEDERS AND GENERATOR CONTROL UNIT

The F-15 generators are mounted near the forward end of the engines. The generator feeders and generator control unit wires are routed within the fuselage from the generators to the forward equipment bays. The primary source of coupling is magnetic coupling through access door gaps (the two access doors forward of the engine). The feeder wires were routed directly across two gaps of length 22 inches and 14.5 inches. A nominal gap width of .1 inches was assumed for each. the generator feeder wires were combined in

56
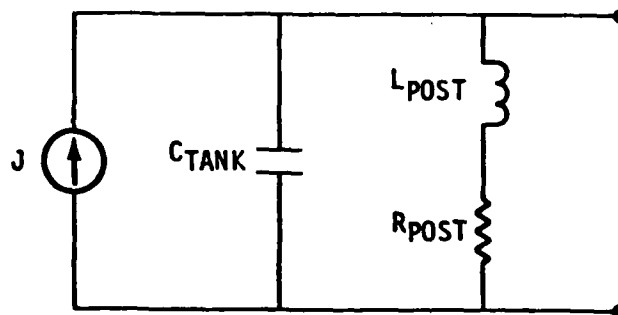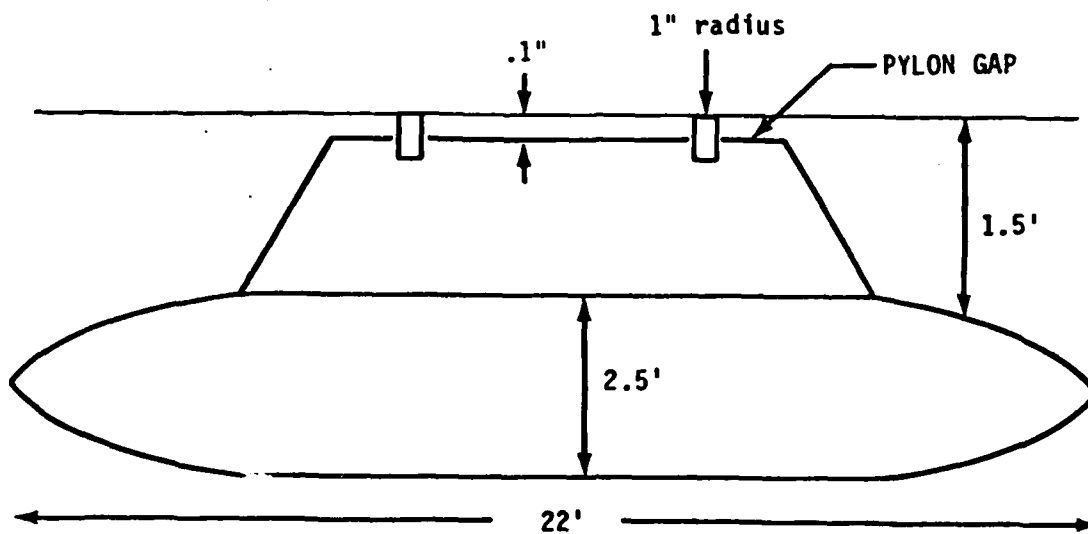
$J = jw\left(C_{TANK}\right)\left(h\right)E_n$

C_{TANK} = 612 pF

L_{POST} = 70 nH

R_{POST} = .04 ohms

h = .1"

E_n = normal electric field on airframe at external fuel tank

FIGURE 20   Geometry and Circuit Model
for External Fuel Tank Quantity Indicator

57

AFRUN   TYPE = 3 FIGHTER EXTERNAL FUEL TANK CIRCUIT-MODERATE THREAT

Amplitude Volts x10^5

Time (microseconds)
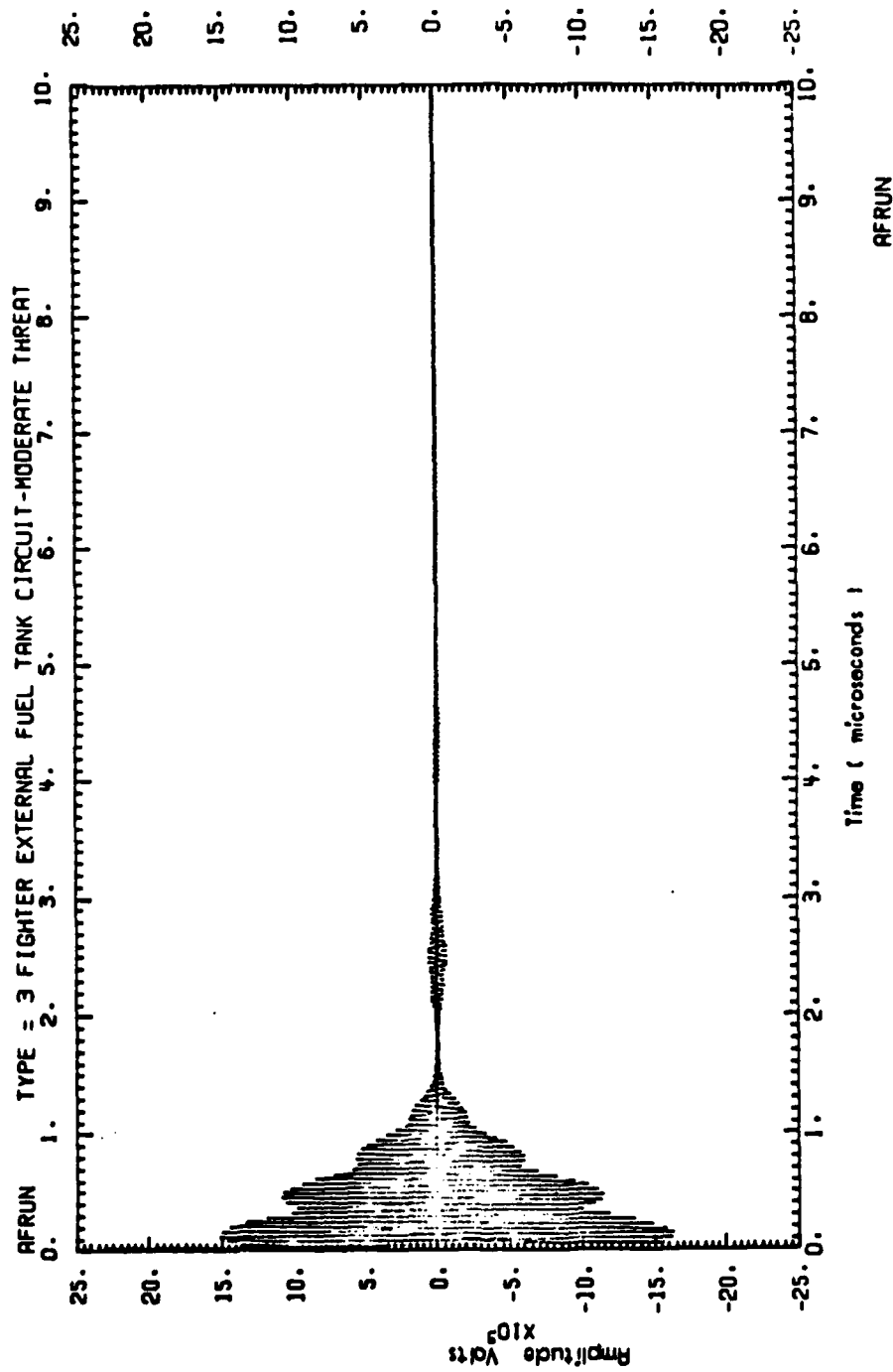
AFRUN

MEMBER = AFRUN   DATA SET= VOC   FIGURE   21   V$_{OC}$ INDUCED ON F-15 EXTERNAL FUEL TANK QUANTITY INDICATOR

common mode for each phase and neutral (3 wires each). The circuit model is shown in Figure 22. Only the generator feeders were modelled, as the lightning threat for the GCU wires is similar. The induced transients may be considerably reduced by routing the wires away from the access door gaps, i.e., off to the side or back against the airframe structure. Alternatively, conductive gasket material may be used around the perimeter of the access door to electrically short out the gap.

(20) F-15 FORWARD LANDING GEAR TAXI LIGHTS AND MAIN GEAR DOWN AND LOCK SWITCH.

When the landing gear are extended, wiring strung alongside the gear is exposed to lightning-induced fields. The taxi lights wiring is routed a distance of .9 meter along the exposed part of the forward strut. The main gear down and lock switch is routed alongside the exposed main gear a distance of approximately 1 meter. Both circuits are exposed to appreciable lightning-induced fields on the strut. A preliminary analysis of the electromagnetic coupling problem is presented in Appendix E.

The induced transients may be reduced by routing the wires flush against the gear struts and by shielding the wiring with overbraid.

(21) F-15 WING TIP FORMATION LIGHT

A visual survey of the F-15 revealed that the large wing tip formation lights may be exposed both to a direct strike and induced transients threat. The light cover attaches to the wing as part of the tip and is U-shaped in cross-section, with a length of about 30 inches and depth (in the "U") of 6 inches. Protection against direct strike hazard requires a protective coating on the light cover. (See Section IV.2).

The light element has appreciable area and will couple capacitively to lightning-induced surface fields on the wing tip. The circuit model for the light element is similar to that for the C-14 windshield heater. Further details of the internal construction of the light are needed before a model can be obtained.

59

CONTACTOR LOADS - 1

VOLTAGE SOURCES

GENERATOR LOADS - 2

BWIR *
L = 690
M = 580
C = 9.1
CM = 89
RDC = .03
RAC = .09
LENGTH = 10m

V1 +
V2 +
V3 +
V4 +

B GEN *
L = 673
M = 550
C = 7.3
CM = 61
RDC = .03
RAC = .09
LENGTH = 1m

NEUTRAL GROUND POINT
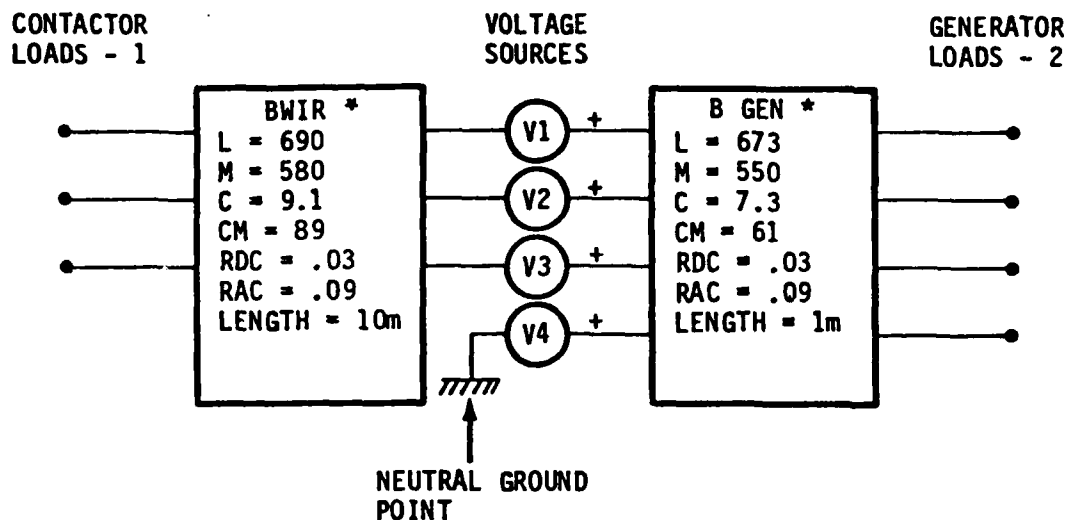
* All units as follows:

$L = M = nH/m$

$C = CM = pF/m$

$RDC = ohm/m$

$RAC = ohm/m$ at 1 MHz

VOLTAGE SOURCE:

$V = (jwL) \ (w) \ (J_s)$

$L = (\mu_o) \ (\pi) \ (w) \ /16 \left\{ \ln (4w/t) -1 \right\}$

J_s = surface current density at slot

w = slot length

t = slot width

FIGURE 22 Circuit Model for F-15 Feeder Generator Wires

60

(22) F-15 RADAR

The F-15 has no metal structure extending from the nose of the radome. Hence,
a likely attachment point for lightning is to the metal frame of the radar.
Consider a wire attached to the pedestal and routed a height, h, above the
forward bulkhead. The magnetic field threading the loop between the wire and
metal structure will induce the open circuit voltage:

$$V_{oc} = (\mu_0) (\dot{I}_L) (A_{eff}/C_{eff})$$

If the loop extends radially outward from the pedestal a distance l, and h<<l,
the induced voltage is:

$$V_{oc} = - \frac{(\mu_0) (h) \dot{I}_L}{2\pi} \ln (\frac{l + rp}{rp})$$

rp = radius of pedestal

h = height of wire above bulkhead

l = length of wire

$\dot{I}_L$ = time derivative of lightning current

(23) F-15 ESSENTIAL POWER BUSS FEEDERS

The wire bundle from the essential power bus to the essential AC contactor may
be exposed to magnetic field coupling through access doors, since the two
components are in adjacent equipment bays. If the wires are routed directly
across access door gaps, the induced voltage may be approximated as described
in the F-15 generator feeder model. However, line drawings for the F-15
indicate that these feeders are routed well to the side of the door gaps and
should not see appreciable transients.

(24) F-15 POWER WIRES TO ROLL/YAW AND PITCH COMPUTERS

The roll/yaw and pitch computers are located in the upper middle of the

right-hand forward equipment bay. The power wires to the computers tie to the
No. 2 miscellaneous relay panel in the right rear of the cockpit. This bundle
will not be exposed to appreciable magnetic fields unless routed across the
access door gaps at the aft end of the forward equipment bay, or if the wire
is exposed to magnetic fields in the cockpit area at the miscellaneous relay
panel.

(25) F-15 VERTICAL STABILIZER LIGHTS

The threat to these circuits are similar to that for the F-111 vertical
stabilize lights. On the F-15 surveyed, the leading edge covering the wiring
was metal. If this is replaced by a non-conductor or low-conductivity
composite, the analysis is the same as for the F-111 vertical stabilizer.
(See Section II.3.c(12)).

4. COMPUTER MODEL DEVELOPMENT

The computer routine used in the evaluation of the circuits examined was
developed for the Defense Nuclear Agency in 1978. The TRAFFIC modeling
library is used with the PRESTO applications code (Reference 11) for the
frequency-domain modeling and analysis of cables, antennas and other
distributed conducting structures. Contained in the library are the modeling
subroutines CABLE for multiconductor transmission lines, THRBRD for signal
leakage through braided shields, LOOP for pickup on small closed loops, PROBE
for examination of the fields due to the electromagnetic environment, and the
modeling program WIRANT for conducting structures described as a collection of
thin wires. Available electromagnetic environments include linearly polarized
plane waves, horizontal or vertical monopole and dipole radiators, and
user-defined arbitrary non-plane waves.

The modeling programs and subroutines model the pickup and propagation of
signals on electrical systems and conducting structures. The pickup and
propagation characteristics are analyzed using models of transmission lines
and antennas. This includes intentional signal paths such as communication
and control cables, and unintentional signal paths such as power systems and
other conducting structures.

The succeeding pages describe the various subroutines used in the detailed examination of circuits in Section III. The output of the listed subroutines is in the form of an N-node Norton equivalent circuit, i.e., a short circuit current, $C(I)$, and source admittance $Y(I,J)$ where I,J range from 1 to N. Since all subroutines correspond to ideal voltage sources, the source admittance was that for a micro-ohm resistor. The micro-ohm resistor is the origin of the factor of 10^6 appearing in $Y(I,J)$ and $C(I)$.

a. MAGNETICALLY COUPLED EXPOSED CONDUCTOR SUBROUTINE EQUATIONS

The equations listed below were used to calculate the amount of magnetically coupled voltage on the leading edge wire bundle for an all aluminum wing with a figerglass leading edge. Magnetically coupled exposed conductor subroutine definitions are described in Table 8.

```
W=2.*PI*FM*1.E6
IL=PEAKI*(1./(ALPHA+J*W)-1./(BETA+J*W))
VEL=3.E8
RHO=(RL-ZC)/(RL+ZC)
GAML=CEXP(J*W*L/VEL)
GAMLX=CEXP(J*W*(L-X)/VEL)
ZIN=ZC*(GAML+RHO/GAML)/(GAML-RHO/GAML)
TX=(GAMLX-RHO/GAMLX)/(GAML-RHO/GAML)
I=((2.*RL)/(RL+ZIN))*TX*IL
V=J*W*U*I*PI*PRAM(1)*PRAM(2)*PRAM(4)/PRAM(3)
Y(1,1)=(1.E6,0.)
Y(2,2)=Y(1.1)
Y(1,2)=(-1E6,0.)
Y(2,1)=Y(1,2)
C(1)=1E6*V
C(2)=-1E6*V
```

Table 8 MAGNETICALLY COUPLED EXPOSED CONDUCTOR SUBROUTINE DEFINITIONS

INPUT PARAMETERS

Physical Quantity Name	Description	Units
ALPHA	Fall Time Constant For Lightning Current	Seconds -1
BETA	Rise Time Constant For Lightning Current	Seconds -1
C	Output Current Vector	Amps
FM	Frequency	Megahertz
J	Imaginary Operator Of Complex Number	
L	Length Of Lightning Path Through Airframe	Meters
PEAKI	Peak Current Amplitude Constant For Lightning	Amps
PI		3.14159
PRAM 1	Wire Route Length	Meters
PRAM 2	Wire Height Above Ground Plane	Meters
PRAM 3	Wing Circumference	Meters
PRAM 4	Concentration Factor	
RL	Lightning Channel Characteristic Impedance	Ohms
U	Permeability of Free Space	Henries/Meter
VEL	Velocity Of Light	Meters/Second
X	Distance From Attachment Point To Source	Meters
Y	Output Admittance Matrix	Mhos
ZC	Airframe Characteristic Impedance	Ohms

OUTPUT PARAMETERS

CAML	Phase Shift Parameter	
GAMLX	Phase Shift Parameter	
I	Lightning Current In Airframe At X	Amps/Rad
IL	Lightning Current Spectrum	Amps/Rad
RHO	Reflection Coefficient For Airplane/ Lightning Column Mismatch	
TX	Transfer Function Ratio Of Input Current To Current At X	
V	Output Voltage	Volts
W	Frequency	Rad/Sec
ZIN	Input Impedance For Aircraft Transmission Line	Ohms

b. ELECTRIC FIELD DIFFUSION COUPLING SUBROUTINE EQUATIONS

The equations listed below were used to calculate the amount of electric field induced voltage on the leading edge wire bundle for an all aluminum wing with 3 mil foil inside a fiberglass leading edge. This same subroutine was used in the graphite/epoxy case. Electric field diffusion coupling subroutine definitions are described in Table 9.

```
W=2.*PI*FM*1.E6
IL=PEAKI*(1./(ALPHA+J*W)-1./(BETA+J*W))
VEL=3.E8
RHO=(RL-ZC)/(RL+ZC)
GAML=CEXP(J*W*L/VEL)
GAMLX=CEXP(J*W*(L-X)/VEL)
ZIN=ZC*(GAML+RHO/GAML)/(GAML-RHO/GAML)
TX=(GAMLX-RHO/GAMLX)/(GAML-RHO/GAML)
I=((2.*RL)/(RL+ZIN))*TX*IL
SIG=3.54E7
T=7.62E-5
DEL=.503/SQRT(FM*SIG)
TD=T/DEL
D=SINH(TD)*COS(TD)+J*COSH(TD)*SIN(TD)
ZT=(1.+J)/(SIG*DEL*D)
VHF=ZT*(I/PRAM(3))*PRAM(1)*PRAM(4)*(PRAM(2)/PRAM(5))
VLF=RW*I*PRAM(1)*(PRAM(2)/PRAM(5))
V=(J*W*TAU)/(1.+J*W*TAU)*VHF+1./(1.+J*W*TAU)*VLF
Y(1,1)=(1.E6,0.)
Y(2,2)=Y(1,1)
Y(1,2)=(-1.E6,0.)
Y(2,1)=Y(1,2)
C(1)=1.E6*V
C(2)=-1.E6*V
```

Table 9 ELECTRIC FIELD DIFFUSION COUPLING SUBROUTINE DEFINITIONS

INPUT PARAMETERS

Physical Quantity Name	Description	Units
ALPHA	Fall Time Constant For Lightning Current	Seconds -1
BETA	Rise Time Constant For Lightning Current	Seconds -1
C	Output Current Vector	Amps
FM	Frequency	Megahertz
J	Imaginary Operator Of Complex Number	
L	Length Of Lightning Path Through Airframe	Meters
PEAKI	Peak Current Amplitude Constant For Lightning	Amps
PI		3.14159
PRAM 1	Wire Route Length	Meters
PRAM 2	Wire Height Above Ground Plane	Meters
PRAM 3	Wing Circumference	Meters
PRAM 4	Concentration Factor	
PRAM 5	Distance Between Leading Edge And Wire	Meters
RL	Lightning Channel Characteristic Impedance	Ohms
SIG	Conductivity Of 3 Mil Foil	Mhos/Meter
T	Thickness Of 3 Mil Foil	Meters
TAU	Break Frequency	Hertz
VEL	Velocity Of Light	Meters/Second
X	Distance From Attachment Point To Source	Meters
Y	Output Admittance Matrix	Mhos
ZC	Airframe Characteristic Impedance	Ohms

OUTPUT PARAMETERS

D	Intermediate Variable	
DEL	Skin Depth	Meters
GAML	Phase Shift Parameter	
GAMLX	Phase Shift Parameter	
I	Lightning Current In Airframe At X	Amps/Rad
IL	Lightning Current Spectrum	Amps/Rad
RHO	Reflection Coefficient For Airplane/ Lightning Column Mismatch	
TD	Intermediate Variable	
TX	Transfer Function Ratio Of Input Current To Current At X	
V	Output Voltage	Volts
VHF	Voltage-Function Of High Frequencies	Volts
VLF	Voltage-Function Of Low Frequencies	Volts
W	Frequency	Rad/Sec
ZIN	Input Impedance For Aircraft Transmission Line	Ohms
ZT	Transfer Impedance	Ohms

c. MAGNETIC FIELD APERTURE COUPLING SUBROUTINE EQUATIONS

The equations listed below were used to calculate the amount of magnetically coupled voltage on a fuselage wire bundle of the F15 from aperture coupling at the access doors. Magnetic field aperture coupling subroutine definitions are described in Table 10.

```
W=2.*PI*FM*1.E6
IL=PEAKI*(1./(ALPHA+J*W)-1./(BETA+J*W))
VEL=3.E8
RHO=(RL-ZC)/(RL+ZC)
GAML=CEXP(J*W*L/VEL)
GAMLX=CEXP(J*W*(L-X)/VEL)
ZIN=ZC*(GAML+RHO/GAML)/(GAML-RHO/GAML)
TX=(GAMLX-RHO/GAMLX)/(GAML-RHO/GAML)
I=((2.*RL)/(RL+ZIN))*TX*IL
L1=24.E-9
L2=17.E-9
W1=.56
W2=.37
V=J*W*(L1*W1+L2*W2)*(I/CIRC)
Y(1,1)=(1.E6,0.)
Y(2,2)=Y(1.1)
Y(1,2)=(-1E6,0.)
Y(2,1)=Y(1,2)
C(1)=1.E6*V
C(2)=-1.E6*V
```

Table 10   MAGNETIC FIELD APERTURE COUPLING SUBROUTINE DEFINITIONS

INPUT PARAMETERS

Physical Quantity Name	Description	Units
ALPHA	Fall Time Constant For Lightning Current	Seconds -1
BETA	Rise Time Constant For Lightning Current	Seconds -1
C	Output Current Vector	Amps
CIRC	Fuselage Circumference	
FM	Frequency	Megahertz
J	Imaginary Operator Of Complex Number	
L	Length Of Lightning Path Through Airframe	Meters
L1	Inductance across Aperture One	Henries
L2	Inductance across Aperture Two	Henries
PEAKI	Peak Current Amplitude Constant For Lightning	Amps
PI		3.14159
RL	Lightning Channel Characteristic Impedance	Ohms
VEL	Velocity Of Light	Meters/Second
W1	Length of Aperture One	Meters
W2	Length of Aperture Two	Meters
X	Distance From Attachment Point To Source	Meters
Y	Output Admittance Matrix	Mhos
ZC	Airframe Characteristic Impedance	Ohms

OUTPUT PARAMETERS

GAML	Phase Shift Parameter	
GAMLX	Phase Shift Parameter	
I	Lightning Current In Airframe At X	Amps/Rad
IL	Lightning Current Spectrum	Amps/Rad
RHO	Reflection Coefficient For Airplane/ Lightning Column Mismatch	
TX	Transfer Function Ratio Of Input Current To Current At X	
V	Output Voltage	Volts
W	Frequency	Rad/Sec
ZIN	Input Impedance For Aircraft Transmission Line	Ohms

d. MAGNETIC FIELD DIFFUSION COUPLING SUBROUTINE EQUATIONS

The equations listed below were used to calculate the amount of magnetically coupled voltage on a fuselage wire bundle of the F15 assuming diffusion coupling through a graphite epoxy skin. Magnetic field diffusion coupling subroutine definitions are described in Table 11.

```
W=2.*PI*FM*1.E6
IL=PEAKI*(1./(ALPHA+J*W)-1./(BETA+J*W))
VEL=3.E8
RHO=(RL-ZC)/(RL+ZC)
GAML=CEXP(J*W*L/VEL)
GAMLX=CEXP(J*W*(L-X)/VEL)
ZIN=ZC*(GAML+RHO/GAML)/(GAML-RHO/GAML)
TX=(GAMLX-RHO/GAMLX)/(GAML-RHO/GAML)
I=((2.*RL)/(RL+ZIN))*TX*IL)
SIG=16666.67
T=6.89E-3
DEL=.503/SQRT(FM*SIG)
TD=T/DEL
D=COS(TD)*SINH(TD)+J*SIN(TD)*COSH(TD)
ZT=(1.+J)/(SIG*DEL*D)
V=ZT*(I/CIRC)*WIREL
Y(1,1)=(1.E6,0)
Y(2,2)=Y(1,1)
Y(1,2)=(-1.E6,0)
Y(2,1)=Y(1,2)
Y(2,1)=Y(1,2)
C(1)=1.E6*V
C(2)=-1.E6*V
```

Table 11 MAGNETIC FIELD DIFFUSION COUPLING SUBROUTINE DEFINITONS

INPUT PARAMETERS

Physical Quantity Name	Description	Units
ALPHA	Fall Time Constant For Lightning Current	Seconds -1
BETA	Rise Time Constant For Lightning Current	Seconds -1
C	Output Current Vector	Amps
CIRC	Fuselage Circumference	
FM	Frequency	Megahertz
J	Imaginary Operator Of Complex Number	
L	Length Of Lightning Path Through Airframe	Meters
PEAKI	Peak Current Amplitude Constant For Lightning	Amps
PI		3.14159
RL	Lightning Channel Characteristic Impedance	Ohms
SIG	Conductivity Of Graphite Epoxy	Mhos/Meter
T	Thickness Of Graphite Epoxy	Meters
TAU	Break Frequency	Hertz
VEL	Velocity Of Light	Meters/Second
WIREL	Length of excited wire	Meters
X	Distance From Attachment Point To Source	Meters
Y	Output Admittance Matrix	Mhos
ZC	Airframe Characteristic Impedance	Ohms

OUTPUT PARAMETERS

D	Intermediate Variable	
DEL	Skin Depth	Meters
GAML	Phase Shift Parameter	
GAMLX	Phase Shift Parameter	
I	Lightning Current In Airframe At X	Amps/Rad
IL	Lightning Current Spectrum	Amps/Rad
RHO	Reflection Coefficient For Airplane/ Lightning Column Mismatch	
TD	Intermediate Variable	
TX	Transfer Function Ratio Of Input Current To Current At X	
V	Output Voltage	Volts
W	Frequency	Rad/Sec
ZIN	Input Impedance For Aircraft Transmission Line	Ohms
ZT	Transfer Impedance	Ohms

71

e. MAGNETICALLY COUPLED PIGTAIL SHIELDED CONDUCTOR SUBROUTINE EQUATIONS

The equations listed below were used to calculate the amount of magnetically coupled voltage on the leading edge pigtail shielded wire bundle for an all aluminum wing with a figerglass leading edge. This same subroutine was used with the circumferential ground wire bundle, with minor parameter substitutions. Magnetically coupled shield conductor subroutine definitions are described in Table 12.

```
W=2.*PI*FM*1.E6
IL=PEAKI*(1./(ALPHA+J*W)-1./(BETA+J*W))
VEL=3.E8
RHO=(RL-ZC)/(RL+ZC)
GAML=CEXP(J*W*L/VEL)
GAMLX=CEXP(J*W*(L-X)/VEL)
ZIN=ZC*(GAML+RHO/GAML)/(GAML-RHO/GAML)
TX=(GAMLX-RHO/GAMLX)/(GAML-RHO/GAML)
I=((2.*RL)/(RL+ZIN))*TX*IL
ISCS=((J*W*U*PRAM(2))/(RS+J*W(LL+LP/(2*PRAM(1)))))*(I*PRAM(4)/PRAM(3))
V=((RS+J*W*LS)*PRAM(1)+RP+J*W*LP)*ISCS
Y(1,1)=(1.E6,0.)
Y(2,2)=Y(1.1)
Y(1,2)=(-1.E6,0.)
Y(2,1)=Y(1,2)
C(1)=1.E6*V
C(2)=-1.E6*V
```

Table 12 MAGNETICALLY COUPLED SHIELD CONDUCTOR SUBROUTINE DEFINITIONS

INPUT PARAMETERS

Physical Quantity Name	Description	Units
ALPHA	Fall Time Constant For Lightning Current	Seconds -1
BETA	Rise Time Constant For Lightning Current	Seconds -1
C	Output Current Vector	Amps
FM	Frequency	Megahertz
J	Imaginary Operator Of Complex Number	
L	Length Of Lightning Path Through Airframe	Meters
LL	Shield Inductance	Henries/Meter
LP	Pig Tail Inductance	Henries
LS	Transfer Inductance Throught Shield	Henries/Meter
PEAKI	Peak Current Amplitude Constant For Lightning	Amps
PI		3.14159
PRAM 1	Wire Route Length	Meters
PRAM 2	Wire Height Above Ground Plane	Meters
PRAM 3	Wing Circumference	Meters
PRAM 4	Concentration Factor	
RL	Lightning Channel Characteristic Impedance	Ohms
RP	Pig Tail Resistance	Ohms/Meter
RS	Transfer Resistance Through Shield	Ohms/Meter
U	Permeability of Free Space	Henries/Meter
VEL	Velocity Of Light	Meters/Second
X	Distance From Attachment Point To Source	Meters
Y	Output Admittance Matrix	Mhos
ZC	Airframe Characteristic Impedance	Ohms

OUTPUT PARAMETERS

GAML	Phase Shift Parameter	
GAMLX	Phase Shift Parameter	
I	Lightning Current In Airframe At X	Amps/Rad
IL	Lightning Current Spectrum	Amps/Rad
ISCS	Current in Shield	Amps
RHO	Reflection Coefficient For Airplane/ Lightning Column Mismatch	
TX	Transfer Function Ratio Of Input Current To Current At X	
V	Output Voltage	Volts
W	Frequency	Rad/Sec
ZIN	Input Impedance For Aircraft Transmission Line	Ohms

EVALUATION OF NORMAL DESIGN FOR INHERENT HARDNESS

1. EVALUATION OF TYPICAL CONVENTIONAL ELECTRICAL SYSTEMS

The availability of information about the various circuit impedances determined which of the electrical circuits developed in Task I were to be examined in detail and evaluated in Task II. The following circuits were analyzed to various levels:

a. VSCF Circuit with Generator and Converter on Wing
b. VSCF Circuit with Generator on Wing, Converter in Fuselage
c. Generator on Wing Circuit
d. F15 Generator Circuit
e. Beacon Light Circuit
f. Window Heater Circuit
g. Upper Surface Blowing Actuator Circuit

a. VSCF GENERATOR AND CONVERTER CIRCUIT

The VSCF electrical power schematic shown in Figure 23 and examined in this study was originally designed for the F-18 aircraft. The generator is a wound rotor salient pole brushless machine rated 55KVA, 165 volts, and delivers six phase, 1660 Hz to 3500 Hz power to three identical legs of the cycloconverter that convert the variable frequency power to a constant 400 Hz, three phase power. There are 12 thyristors in each cycloconverter leg that are gated by modulators to form the 400 Hz output (Reference 4). Each cycloconverter leg is followed by a filter (the interphase transformer and capacitor) to remove the cycloconverter ripple frequency. The system was examined in three different configurations, a. Both the generator and converter located out on the wing, b. The generator located out on the wing with the converter in the fuselage, and c. The generator located out on the wing without the converter.
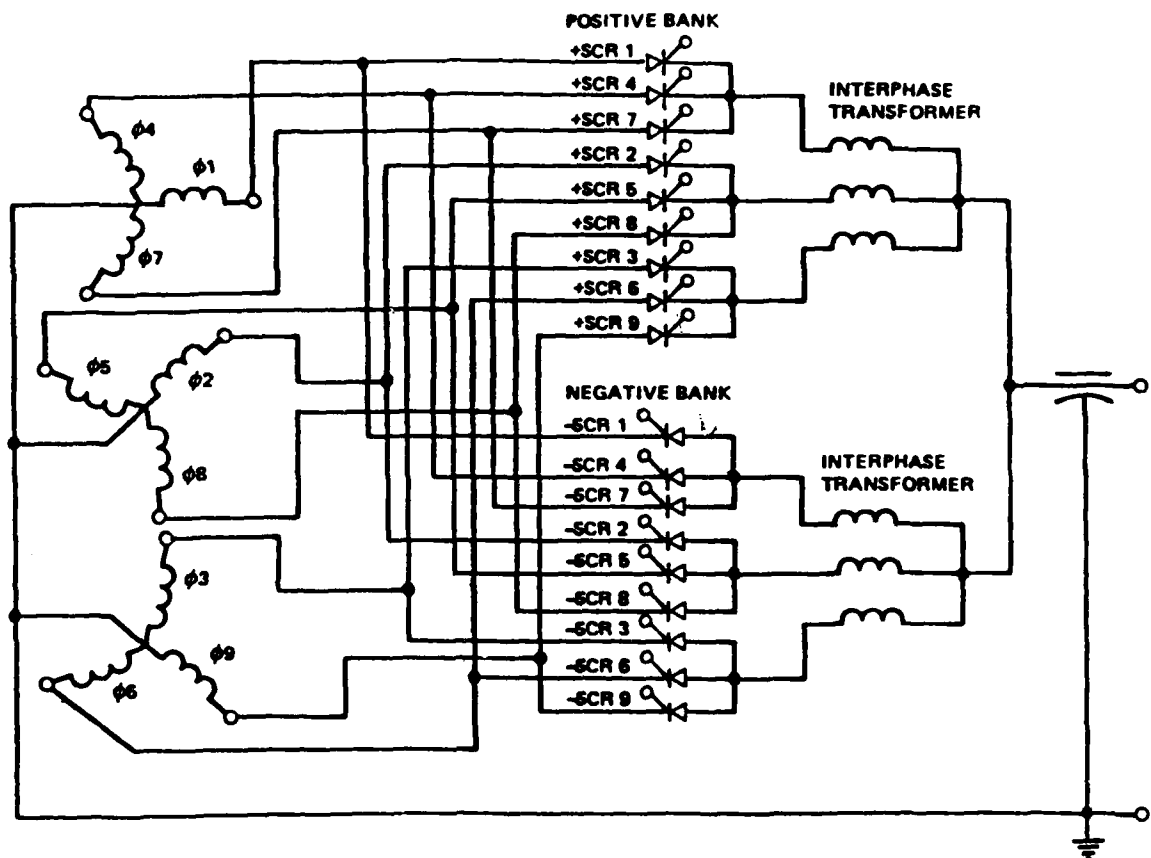
Figure 23 VSCF Power Circuit

(1) VSCF GENERATOR AND CONVERTER ON WING

The baseline VSCF generator and converter circuit consisted of the generator and converter package located 12 meters out on the wing connected via feeders to the bus located in the fuselage. Figures 24 is the one line diagram and Figure 25 is the modelled equivalent circuit. The one line diagram displays the VSCF system as the circuit was broken down into blocks and modelled in the computer simulation. Test points were taken at the generator/converter output and the bus input for severe lightning threats. Figure 25, the modelled equivalent circuit, shows the various component parameters used within the simulation blocks. The generator neutral wire is grounded to the nearest spar 3 meters from the generator. Using the common mode configuration, which assumes balanced loading, simplified the analysis by allowing the phases to be paralleled into equivalent impedances. The lightning strike attaches to the wing tip and travels toward the fuselage. The threat is magnetically coupled to the wing feeder, between the generator located out on the wing and the converter located inside the fuselage, at nodes SRC1 and SRC2 in Figure 25. Inside the fuselage, the feeder model connecting the converter to the bus is not directly exposed to the lightning current.

FIBERGLASS WING LEADING EDGE

A bundle of six number four gauge feeder wires were excited via magnetic coupling of the lightning transient as they feed a half loaded bus and then a full load. The bundle was located two inches above the leading edge spar of an all aluminum wing and behind a fiberglass leading edge. The lightning source Fortran subroutine equations and definitions are given in Section II.4.a and Table 8, respectively. The length of the excited feeder was varied from the baseline 12 meters to 6 and 18 meters. Table 13, VSCF/1 PEAK TRANSIENTS FIBERGLASS LEADING EDGE, lists the severe threat transients first for the half load and then full load case transients monitored at the two test points (T1, T2) shown on Figures 24 and 25. The test case labels in Table 13, 6MF, 12MF, and 18MF correspond with the length of excited feeder. Figures 26 and 27, plot the positive amplitude voltage and current peaks versus feeder length for the two cases.
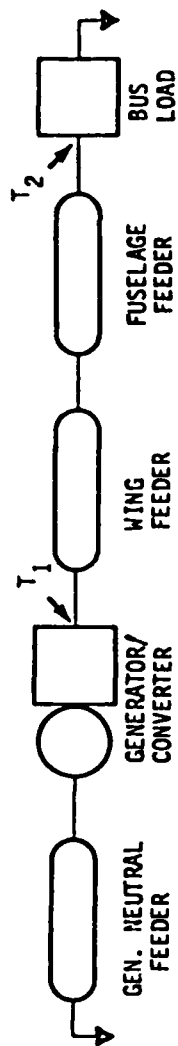
Figure 24 VSCF Generator/Converter on Wing to Bus in Fuselage Block Diagram
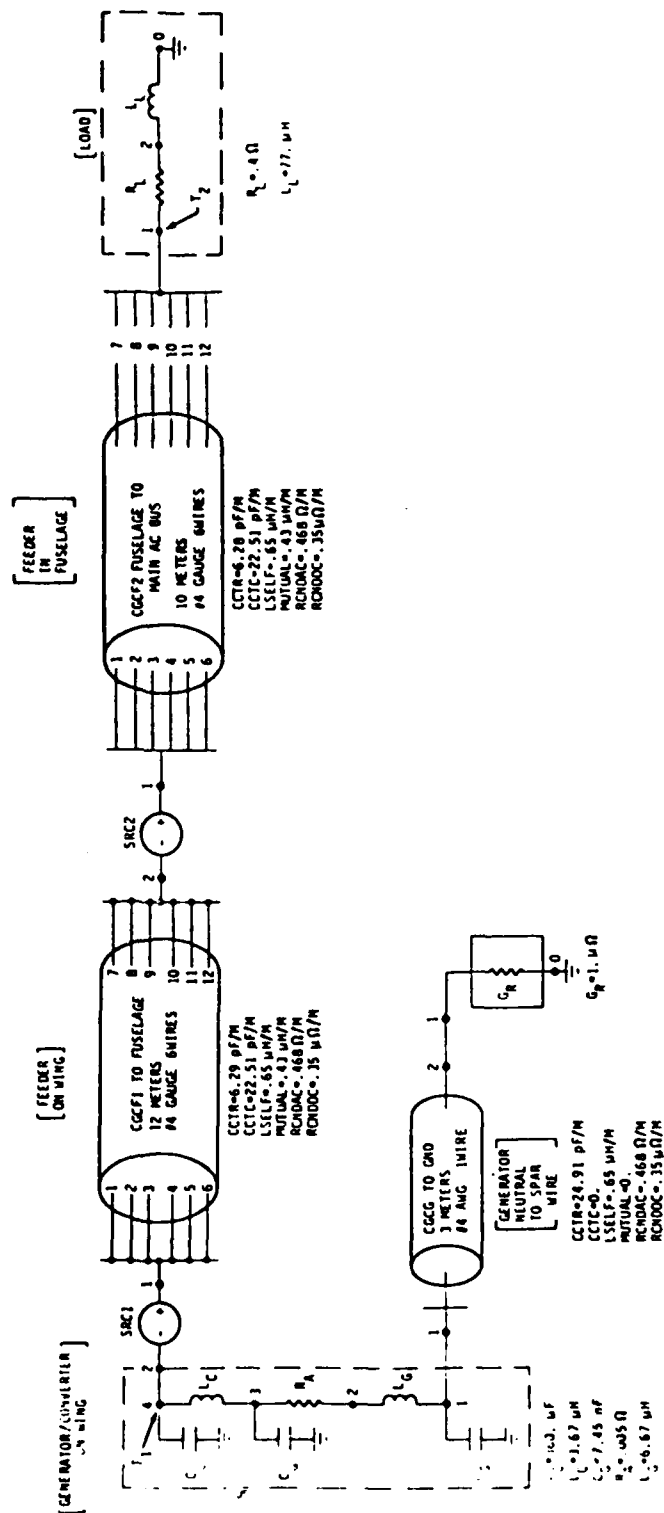
Figure 25 VSCF Generator/Converter on Wing to Bus in Fuselage Equivalent Circuit

77
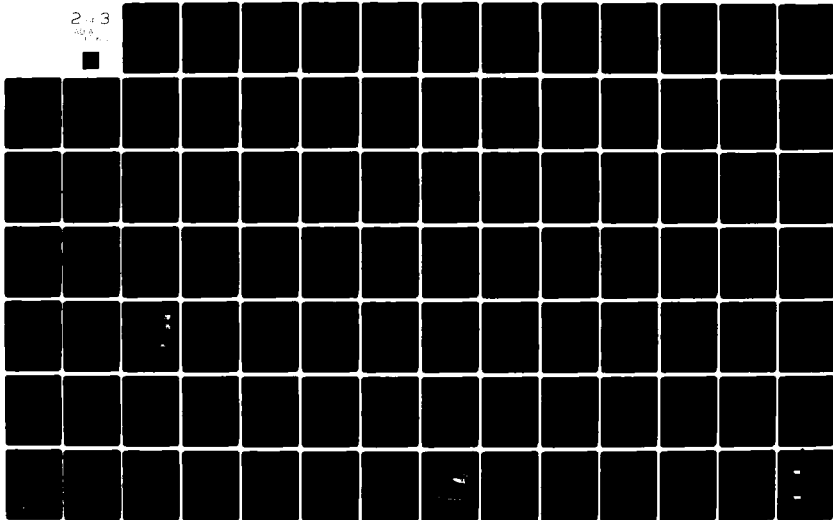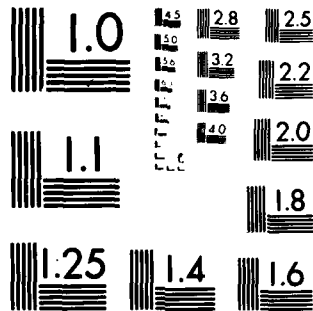
MICROCOPY RESOLUTION TEST CHART

TABLE 13 VSCF/1 PEAK TRANSIENTS FIBERGLASS LEADING EDGE

TEST CASE	TEST POINT/ NAME	TRANSIENT DURATION	POSITIVE AMPLITUDE	NEGATIVE AMPLITUDE	DC OFFSET
			(50% LOAD)		
6MF	T1/VCON	1.0 mS	13.5 V	-15.5 V	+0.2 V
6MF	T1/ICON	1.0 mS	92.0 A	-62.0 A	+1.8 A
6MF	T2/VLOAD	5.0 uS	42.0 KV	-36.0 KV	-8.0 KV
6MF	T2/ILOAD	.15 mS	148.0 A	-16.0 A	+6.0 A
12MF	T1/VCON	1.0 mS	27.0 V	-30.0 V	+0.5 V
12MF	T1/ICON	1.0 mS	180.0 A	-120.0 A	+4.0 A
12MF	T2/VLOAD	8.0 uS	65.0 KV	-40.0 KV	0.0 V
12MF	T2/ILOAD	.15 mS	289.0 A	0.0 A	0.0 A
18MF	T1/VCON	1.0 mS	38.0 V	-44.0 V	+0.4 V
18MF	T1/ICON	1.0 mS	260.0 A	-175.0 A	+6.4 A
18MF	T2/VLOAD	8.0 uS	99.0 KV	-68.0 KV	-14.0 KV
18MF	T2/ILOAD	.15 mS	425.0 A	-45.0 A	+15.0 A
			(100% LOAD)		
6MF	T1/VCON	1.0 ms	24.0 V	-28.0 V	0.0 V
6MF	T1/ICON	1.0 ms	160.0 A	-100.0 A	+5.0 A
6MF	T2/VLOAD	6.0 us	38.0 KV	-19.0 KV	-8.0 KV
6MF	T2/ILOAD	0.6 ms	280.0 A	-35.0 A	+10.0 A
12MF	T1/VCON	1.0 ms	46.0 V	-52.0 V	0.0 V
12MF	T1/ICON	1.0 ms	300.0 A	-200.0 A	+12.7 A
12MF	T2/VLOAD	8.0 us	58.0 KV	-36.0 KV	+16.0 KV
12MF	T2/ILOAD	0.6 ms	550.0 A	-60.0 A	+30.0 A
18MF	T1/VCON	1.0 ms	64.0 V	-74.0 V	0.0 V
18MF	T1/ICON	1.0 ms	440.0 A	-280.0 A	+10.0 A
18MF	T2/VLOAD	10.0 us	78.0 KV	-50.0 KV	+19.0 KV
18MF	T2/ILOAD	0.7 ms	750.0 A	-90.0 A	+50.0 A
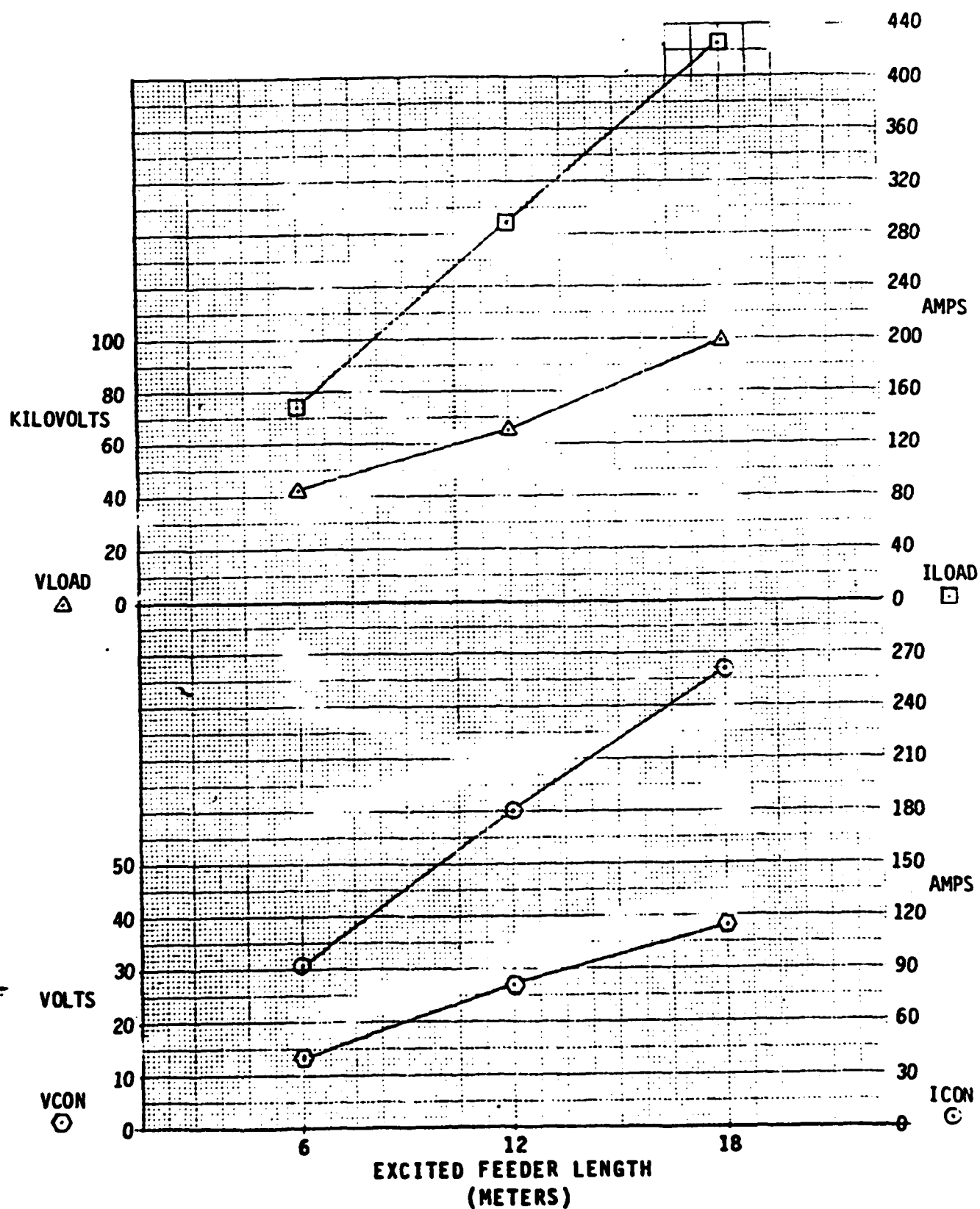
FIGURE 26   Fiberglass Leading Edge 50% Loaded Bus

79
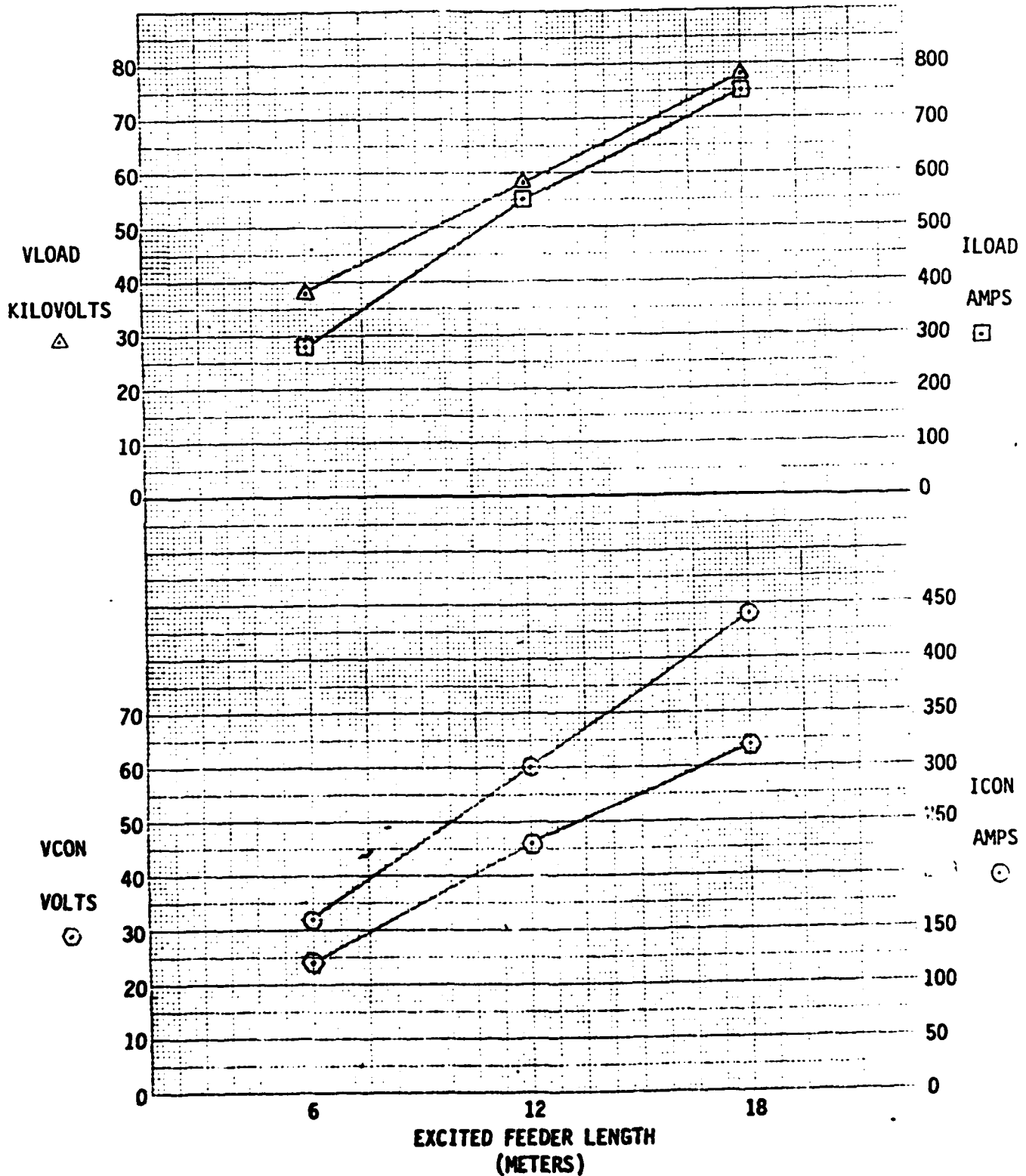
FIGURE 27   Fiberglass Leading Edge 100% Loaded Bus

80

FIBERGLASS WING LEADING EDGE WITH 3 MIL FOIL

Additional development of the circuit includes the effect of adding a layer of
three mil foil to the fiberglass leading edge as shown in the lightning source
Fortran subroutine equations and definitions given in Section II.4.b and Table
9, respectively. The twelve meter length of excited feeder was connected to
the 50% loaded bus. The Table 14, VSCF/1 PEAK TRANSIENTS 3 MIL FOIL
FIBERGLASS LEADING EDGE, lists the severe threat transients monitored at the
generator/converter output terminals and bus input terminal, T1 and T2,
respectively.

GRAPHITE/EPOXY WING LEADING EDGE

In the development of the graphite epoxy leading edge, an extremely low
frequency response in the VSCF circuit, primarily caused by the generator,
resulting in the domination of the low frequency spectral content of the
threat waveform was found. The lightning source Fortran subroutine equations
and definitions are given in Section II.4.b and Table 9, respectively. In
comparison of the subroutine equations for the graphite epoxy and three mil
foil on fiberglass leading edge cases, a change in the conductivity and
thickness of the leading material was the difference.

The test points, (T1 and T2), were the same as in the previous cases. The
first three blocks of data in Table 15, VSCF/1 PEAK TRANSIENTS GRAPHITE EPOXY
LEADING EDGE, namely test cases 12GE35, 12GE45, and 12GE50 compare the results
of varying the thickness of the graphite epoxy material on the leading edge.
The thickness, a function of the number of .005 inch plies, was varied from
0.175 to 0.225 to 0.25 inches for each respective case. Figure 28 plots the
positive amplitude voltage and current peaks with respect to the change in
leading edge thickness.

Test cases 12GE50, 12GE51, and 12GE52 compare the results of varying the
distance between the graphite composite leading edge and the excited wire
bundle. The wire bundle was positioned two inches above the ground plane.
Distances used for each respective case were 2.0, 1.0 and 0.5 feet. Figure
29 plots the positive amplitude voltage and current peaks with respect to the
change in the distance between the leading edge and the bundle.

TABLE 14 VSCF/1 PEAK TRANSIENTS 3 MIL FOIL FIBERGLASS LEADING EDGE

TEST CASE	TEST POINT/ NAME	TRANSIENT DURATION	POSITIVE AMPLITUDE	NEGATIVE AMPLITUE	DC OFFSET
12M3MF	T1/VCON	1.0 mSec	0.6 V	-1.3 V	0.0
12M3MF	T1/ICON	1.0 mSec	12.0 A	-2.0 A	0.0
12M3MF	T2/VLOAD	1.0 mSec	11.2 V	-1.0 V	+2.4
12M3MF	T2/ILOAD	1.0 mSec	8.5 A	-2.0 A	0.0

TABLE 15 VSCF/1 PEAK TRANSIENTS GRAPHITE EPOXY LEADING EDGE

TEST CASE	TEST POINT/ NAME	TRANSIENT DURATION	POSITIVE AMPLITUDE	NEGATIVE AMPLITUDE	DC OFFSET
12GE35	T1/VCON	1.0 mSec	24.0 V	-47.0 V	+2.0
12GE35	T1/ICON	1.0 mSec	435.0 A	-70.0 A	+12.0
12GE35	T2/VLOAD	1.0 mSec	410.0 V	-35.0 V	+85.0
12GE35	T2/ILOAD	1.0 mSec	305.0 A	-62.0 A	+5.0
12GE45	T1/VCON	1.0 mSec	18.0 V	-37.0 V	+1.5
12GE45	T1/ICON	1.0 mSec	340.0 A	-60.0 A	+10.0
12GE45	T2/VLOAD	1.0 mSec	320.0 V	-25.0 V	+60.0
12GE45	T2/ILOAD	1.0 mSec	235.0 A	-50.0 A	+5.0
12GE50	T1/VCON	1.0 mSec	16.0 V	-33.0 V	+1.3
12GE50	T1/ICON	1.0 mSec	305.0 A	-50.0 A	+10.0
12GE50	T2/VLOAD	1.0 mSec	285.0 V	-25.0 V	+50.0
12GE50	T2/ILOAD	1.0 mSec	215.0 A	-45.0 A	+5.0
12GE51	T1/VCON	1.0 mSec	32.0 V	-68.0 V	+2.0
12GE51	T1/ICON	1.0 mSec	610.0 A	-100.0 A	+10.0
12GE51	T2/VLOAD	1.0 mSec	570.0 V	-50.0 V	+100.0
12GE51	T2/VLOAD	1.0 mSec	420.0 A	-90.0 A	+10.0
12GE52	T1/VCON	1.0 mSec	65.0 V	-135.0 V	+5.0
12GE52	T1/ICON	1.0 mSec	1.22 KA	-200.0 A	+20.0
12GE52	T2/VLOAD	1.0 mSec	1.14 KV	-100.0 V	+200.0
12GE52	T2/VLOAD	1.0 mSec	840.0 A	-180.0 A	+20.0
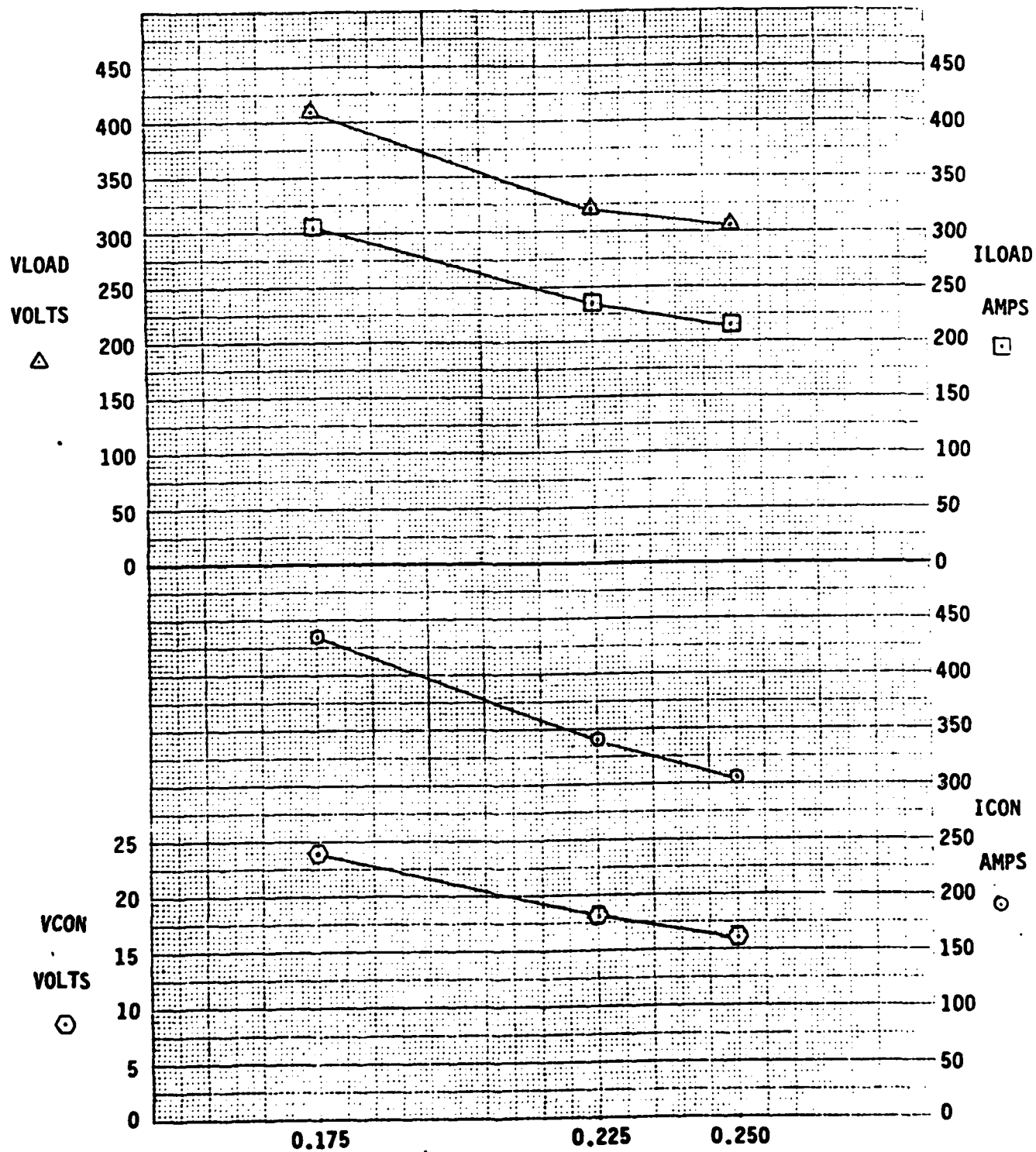
FIGURE 28 Graphite/Epoxy Leading Edge Thickness
(Inches)

83
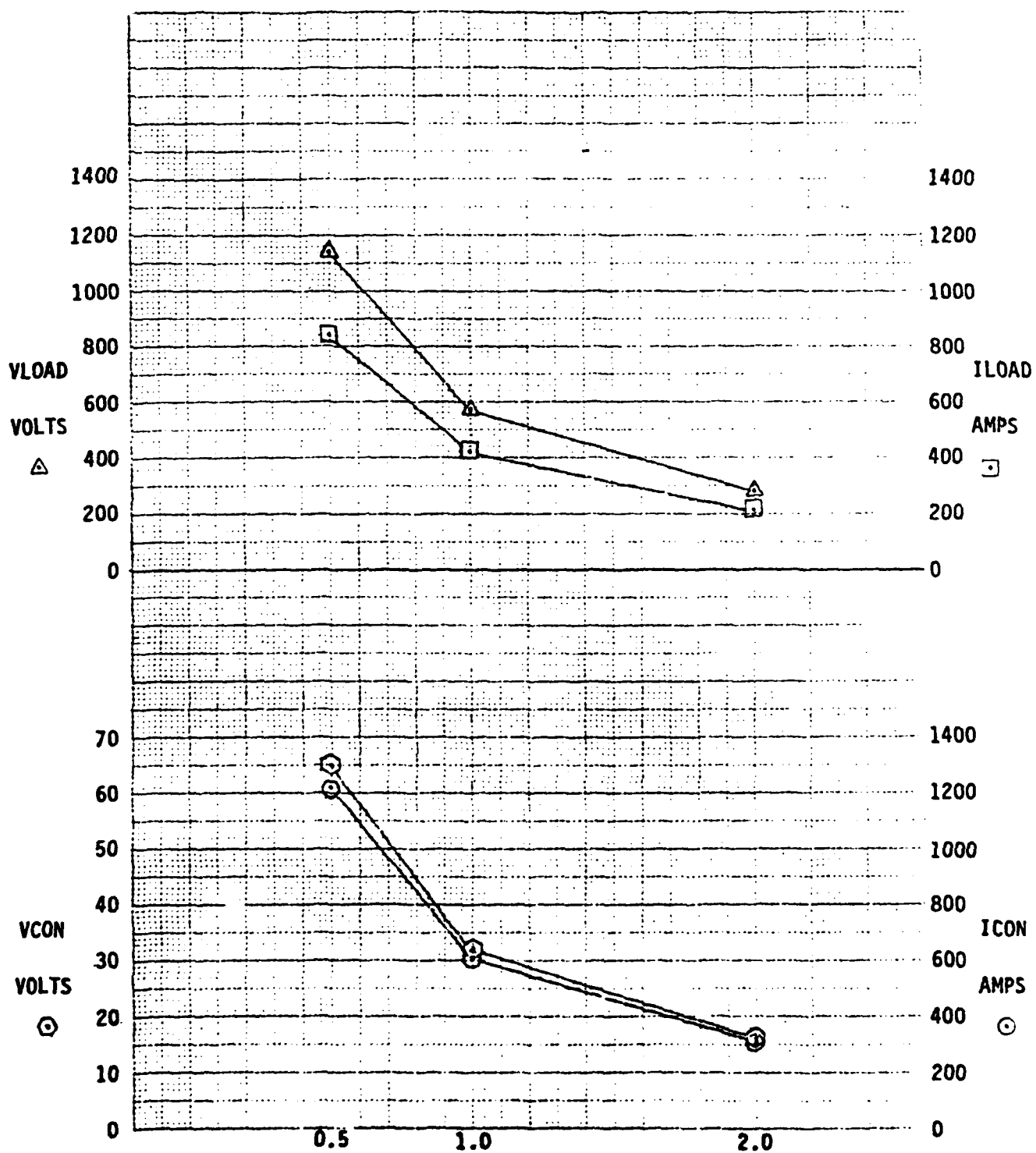
FIGURE 29 Distance Separating Graphite Epoxy Leading Edge and Wire Bundle
(Feet)

84

(2) VSCF GENERATOR ON WING, CONVERTER IN FUSELAGE

The VSCF circuit examined in this case consisted of the 55KVA synchronous
generator, described in Section III.1.a, positioned on the wing twelve meters
from the fuselage and VSCF converter. The unshielded feeder model included a
return neutral wire from the generator to the converter ground. The system
one line diagram and equivalent circuit modelled are shown in Figures 30 and
31, respectively. Impedance values for the generator, feeders, converter, and
a 50% bus load tied in a common mode configuration were put into the TRAFFIC
analysis routine format for computation on the CDC 175.

FIBERGLASS WING LEADING EDGE

Using the circuit described in Section III.1.a(2), a bundle of seven number
ten gauge wires twelve meters long were excited by the magnetic field of first
a moderate and then a severe lightning transient. The feeder bundle located
two inches above the leading edge spar of an all aluminum wing and behind a
fiberglass leading edge was connected to a 50% loaded bus. An unexcited
feeder bundle of six number four gauge wires twelve meters long tied the
converter to the power bus. The lightning source Fortran subroutine equations
and definitions used are given in Section II.4.a and Table 8, respectively.
Table 16, VSCF/2 PEAK TRANSIENTS FIBERGLASS LEADING EDGE, lists the moderate
and severe threat transients as monitored at the three test points, T1, the
generator output terminals, T2, the converter input terminals, and T3, the bus
input terminals, shown in Figures 30 and 31.

(3) GENERATOR ON WING, BUS IN FUSELAGE

This case consisted of removing the converter from the circuit described in
Section III.1.a(1) and shown in the one line diagram and equivalent circuit of
Figures 24 and 25, respectively. Test points were taken at the generator
output terminals, T1, and bus input terminals, T2, for a severe lightning
strike.
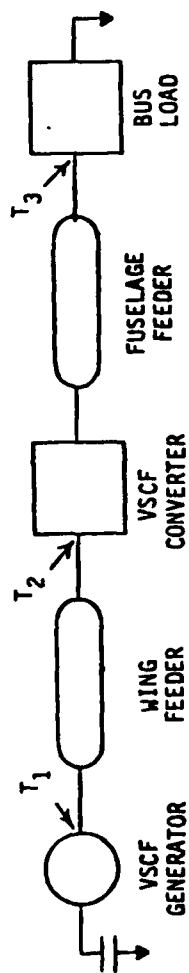
Figure 30   VSCF Generator on Wing to Converter and Bus in Fuselage Block Diagram
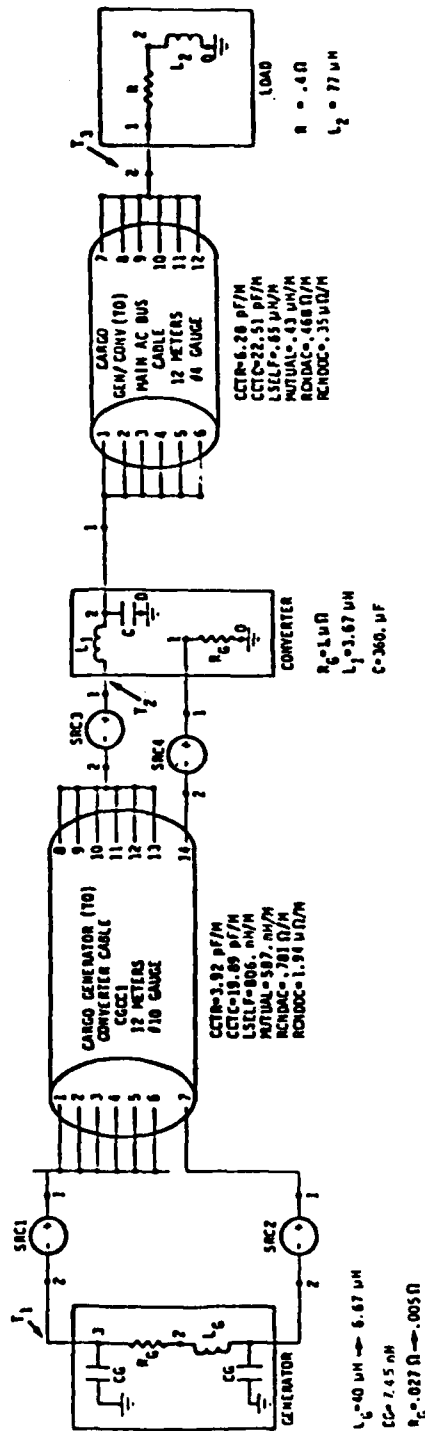
Figure 31   VSCF Generator on Wing to Converter and Bus in Fuselage Equivalent Circuit

TABLE 16 VSCF/2 PEAK TRANSIENTS FIBERGLASS LEADING EDGE

TEST CASE	TEST POINT/ NAME	TRANSIENT DURATION	POSITIVE AMPLITUDE	NEGATIVE AMPLITUDE	DC OFFSET
			(MODERATE)		
12MF	T1/VGEN	5 uSec	2.2 KV	12.3 KV	+200.0 V
12MF	T1/IGEN	5 uSec	16.5 A	11.0 A	+1.0 A
12MF	T2/VCON	5 uSec	1.05 KV	1.18 KV	-50.0 V
12MF	T2/ICON	5 uSec	20.0 A	18.0 A	-3.0 A
12MF	T3/VLOAD	5 uSec	6.5 mV	4.5 mV	-0.8 mV
12MF	T3/ILOAD	>10 uSec	110.0 uA	14.0 uA	0.0 A
			(SEVERE)		
12MF	T1/VGEN	3u Sec.	2.0 KV	53.0 KV	+1.0 KV
12MF	T1/IGEN	5u Sec.	65.0 A	45.0 A	+4.0 A
12MF	T2/VCON	5u Sec.	4.2 KV	4.5 KV	-200.0 V
12MF	T2/ICON	5u Sec.	76.0 A	68.0 A	-12.0 A
12MF	T3/VLOAD	5u Sec.	27.0 mV	16.0 mV	-3.0 mV
12MF	T3/ILOAD	>10u Sec.	94.0 uA	10.0 uA	0.0 A

TABLE 17 VSCF/GEN PEAK TRANSIENTS FIBERGLASS LEADING EDGE

TEST CASE	TEST POINT/ NAME	TRANSIENT DURATION	POSITIVE AMPLITUDE	NEGATIVE AMPLITUDE	DC OFFSET
12MFG	T1/VGEN	20.0 us	2.8 KV	-4.8 KV	-800.0 V
12MFG	T1/IGEN	150.0 us	600.0 A	-340.0 A	+20.0 A
12MFG	T2/VLOAD	8.0 us	58.0 KV	-40.0 KV	+12.0 KV
12MFG	T2/ILOAD	150.0 us	280.0 A	-35.0 A	+5.0 A

TABLE 18 F15 GENERATOR FEEDER PEAK TRANSIENTS

SEVERE THREAT ALUMINUM - APERTURE COUPLING					
TEST POINT	TEST POINT NAME	POSITIVE AMPLITUDE	NEGATIVE AMPLITUDE	DC OFFSET	TRANSIENT DURATION
T1	VGEN	560. V	-700. V	20. V	40 msec
T1	TGEN	36. A	-37. A	-33. A	9 msec
T2	VGENNEU	3400. V	-4000. V	600. V	10 msec
T2	IGENNEU	290. A	-300. A	-280. A	10 msec
T3	VBUSLOAD	3200. V	-3200. V	-600. V	6 msec
T3	IBUSLOAD	7 A	-7. A	-7.4 A	30 msec

FIBERGLASS WING LEADING EDGE

Using the circuit described in Section III.1.a(3), a bundle of six number four
gauge feeder wires twelve meters long were excited by the magnetic field of a
lightning strike transient traveling from the wingtip attachment point toward
the fuselage as they feed a half loaded bus. The bundle was located two
inches above the leading edge spar of the all aluminum wing and behind a
fiberglass leading edge. The lightning source Fortran subroutine equations
and definitions are given in Section II.4.a and Table 8, respectively. Table
17, VSCF/GEN PEAK TRANSIENTS FIBERGLASS LEADING EDGE, lists the severe threat
transients monitored at the two test points, T1 and T2.

b. FI5 GENERATOR CIRCUIT

The F15 generator system is typical of most fighters with a 40/50 KVA the
generator and feeders located inside the fuselage. The main generator feeder
bundle is 2 meters long and is made up of 24 #12 AWG wires, 6 wires per phase
and 6 wires for the neutral. The neutral is grounded at the end of the 2
meter run. Routed forward from the generator to the engine firewall (2 meters
in length) are the feeders and the neutral. The feeders penetrate the
firewall, where the neutral is grounded, and are routed to the main bus 10
meters from the firewall. This segment was considered to be unexposed to the
lightning threat. This is a valid assumption since much of the run is at
right ar 'es to the lightning path (assuming a tail-to-nose strike) and
because the feeder, once past the firewall, is fairly well shielded by the
aircraft structure. The transients induced on the generator system are
assumed to originate on the 2 meter feeder segment (24 #12 AWG bundle) in the
engine compartment. In the case of the graphite/epoxy fuselage, this run is
varied in length from 2 to 15 meters. Figures 32 and 33 show the F15 circuit
block diagram and modelled equivalent circuit, respectively. The lightning
source used in the F15 analyses was the "severe threat" (200 KA strike).

(1) ALUMINUM FUSELAGE

An aluminum fuselage provides a good shield for the generator feeders;
however, any openings in the aluminum will allow electric fields to penetrate
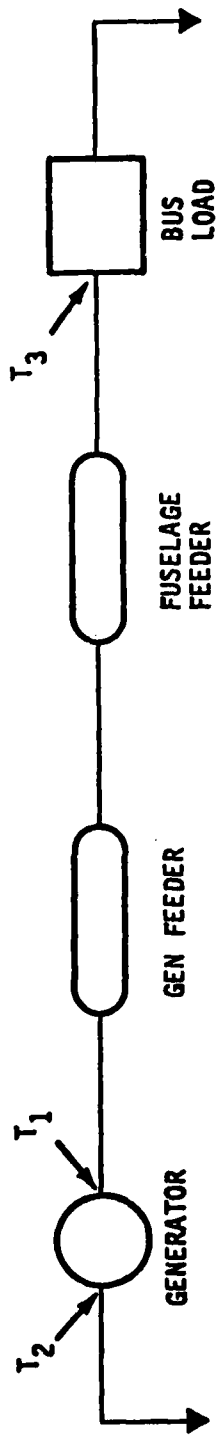
FIGURE 32 · F15 Model Block Diagram
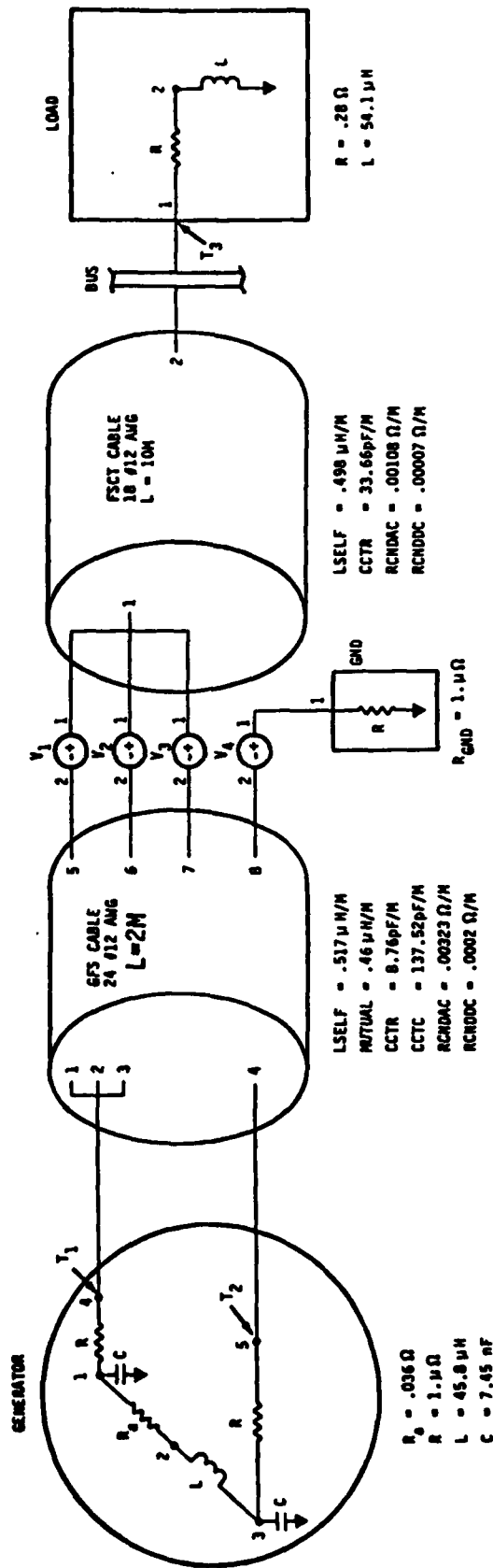
FIGURE 33 F15 Model Circuit Diagram

89

into the fuselage and couple onto the feeders. These openings exist in the
engine compartment area in the form of gaps in the access door seals. The
model used to simulate the F15 is shown in Figure 34. Two slots,
perpendicular to the lightning path and running across the feeders, provide
the source of the lightning induced transients on the feeders. These slots
represent gaps in the access door seals. Results of the computer simulation
run shown in Table 18, F15 GENERATOR FEEDER PEAK TRANSIENTS ALUMINUM, were
made with a full load on the bus. The maximum voltage transient seen at the
bus was 3200 volts and decayed to 10 percent of the maximum within 6
microseconds. The maximum voltage transient at the generator output terminal
was -700 volts. The subroutine/equations used to calculate the transient
voltage are recorded in Section II.4.c.

(2) GRAPHITE/EPOXY FUSELAGE

To investigate the effects of a graphite/epoxy composite fuselage on lightning
induced transients, the F15 model was modified to represent a fuselage made of
graphite/epoxy. Only the feeder section in the engine compartment (from
generator to firewall) was assumed to be exposed to the lightning threat.
Since graphite/epoxy is not as good a conductor as aluminum, magnetic fields
produced by the lightning current flowing on the fuselage will penetrate into
the interior of the aircraft. The penetrating magnetic field couples onto the
feeder (diffusion coupling) producing voltage and current transients on the
feeders. In the analysis of the graphite/epoxy fuselage model, the exposed
feeder length was varied from 2 to 15 meters. The induced voltage is related
to the length of the feeder since the magnetic field is penetrating the
fuselage wherever the lightning current is flowing.

Computer simulations of a lightning strike were made for four lengths of
exposed feeder, 2,5,10 and 15 meters. The configuration of the model is shown
in Figure 35. As the length was increased, the voltage and current transients
increased. The results of the computer analysis are summarized in Table 19,
F15 GENERATOR FEEDER PEAK TRANSIENTS, GRAPHITE EPOXY. The relation between
the induced transient and the length of the exposed feeder is shown in Figure
36, at the generator terminals, and in Figure 37, at the main bus. The
induced transients, as was expected, increased as the length of the exposed

90

LIGHTNING PATH

ALUMINUM FUSELAGE

TAIL END

GEN

EXPOSED FEEDER

NONEXPOSED FEEDER

42.7 KVA
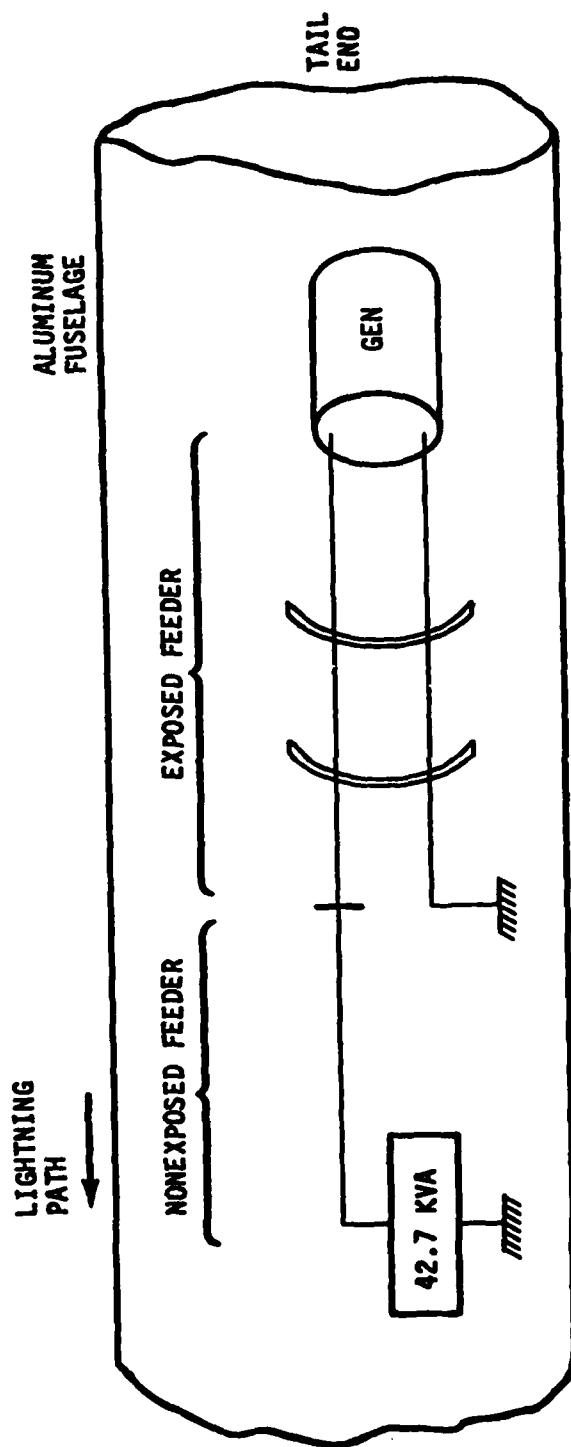
NONEXPOSED FEEDER - 10 METERS

EXPOSED FEEDER - 2 METERS

WIDTH OF APERTURES - .1 INCH

LENGTH OF APERTURES - .56 METERS, .37 METERS

FIGURE 34   F15 Aluminum - Generator Feeder Configuration

91
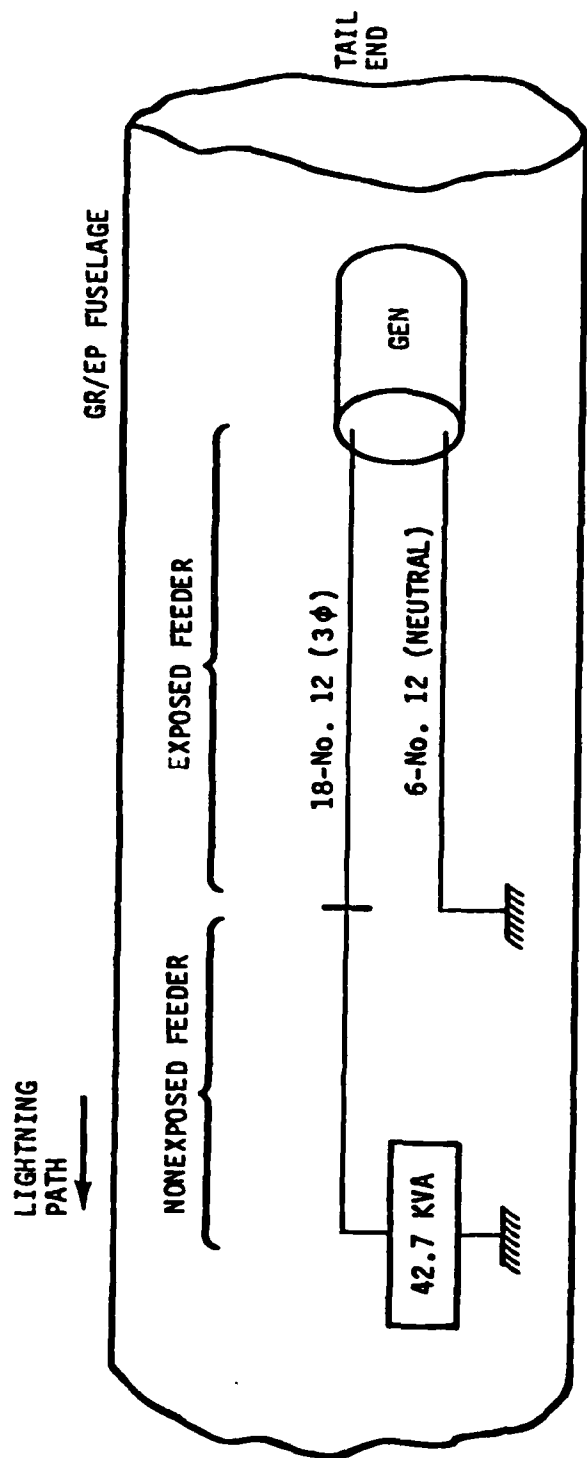
NONEXPOSED FEEDER - 10 METERS
EXPOSED FEEDER - 2,5,10,15 METERS

FIGURE 35   F15 Graphite/Epoxy - Generator Feeder Configuration

TABLE 19 F15 GENERATOR FEEDER PEAK TRANSIENTS

SEVERE THREAT - GRAPHITE/EPOXY - DIFFUSION COUPLING				
2 METERS				
TEST POINT	TEST POINT NAME	POSITIVE AMPLITUDE	NEGATIVE AMPLITUDE	DC OFFSET
T1	VGEN	20. V	-670. V	-170. V
T1	IGEN	1.75 A	-1.75 A	.25 A
T2	VGENNEU	-15. V	-435. V	-15. V
T2	IGENNEU	5. A	-4.5 A	-1.0 A
T3	VBUSLOAD	260. V	-270. V	-150. V
T3	IBUSLOAD	2.35 A	-2.25 A	-.8 A
5 METERS				
T1	VGEN	-180. V	-1280. V	-180. V
T1	IGEN	2.3 A	-2.9 A	.2 A
T2	VGENNEU	40. V	-1120. V	20. V
T2	IGENNEU	8.5 A	-11. A	1.25 A
T3	VBUSLOAD	310. V	-340. V	-200. A
T3	IBUSLOAD	3. A	-2.6 A	.8 A
10 METERS				
T1	VGEN	1100. V	-3500. V	1100. V
T1	IGEN	5. A	-7.8 A	-2.2 A
T2	VGENNEU	50. V	-2300. V	50. V
T2	IGENNEU	26. A	-34. A	5. A
T3	VBUSLOAD	1400. V	-1450. V	950. V
T3	IBUSLOAD	15. A	-14. A	-2. A
15 METERS				
T1	VGEN	1700. V	-5800. V	1500. V
T1	IGEN	12. A	-17.5 A	4. A
T2	VGENNEU	900. V	-4300. V	800. V
T2	IGENNEU	54. A	-56. A	18. A
T3	VBUSLOAD	2500. V	-2500. V	700. V
T3	IBUSLOAD	27. A	-26. A	-7. A

F15 GEN FEEDER - GR/EP

GEN TERMINALS
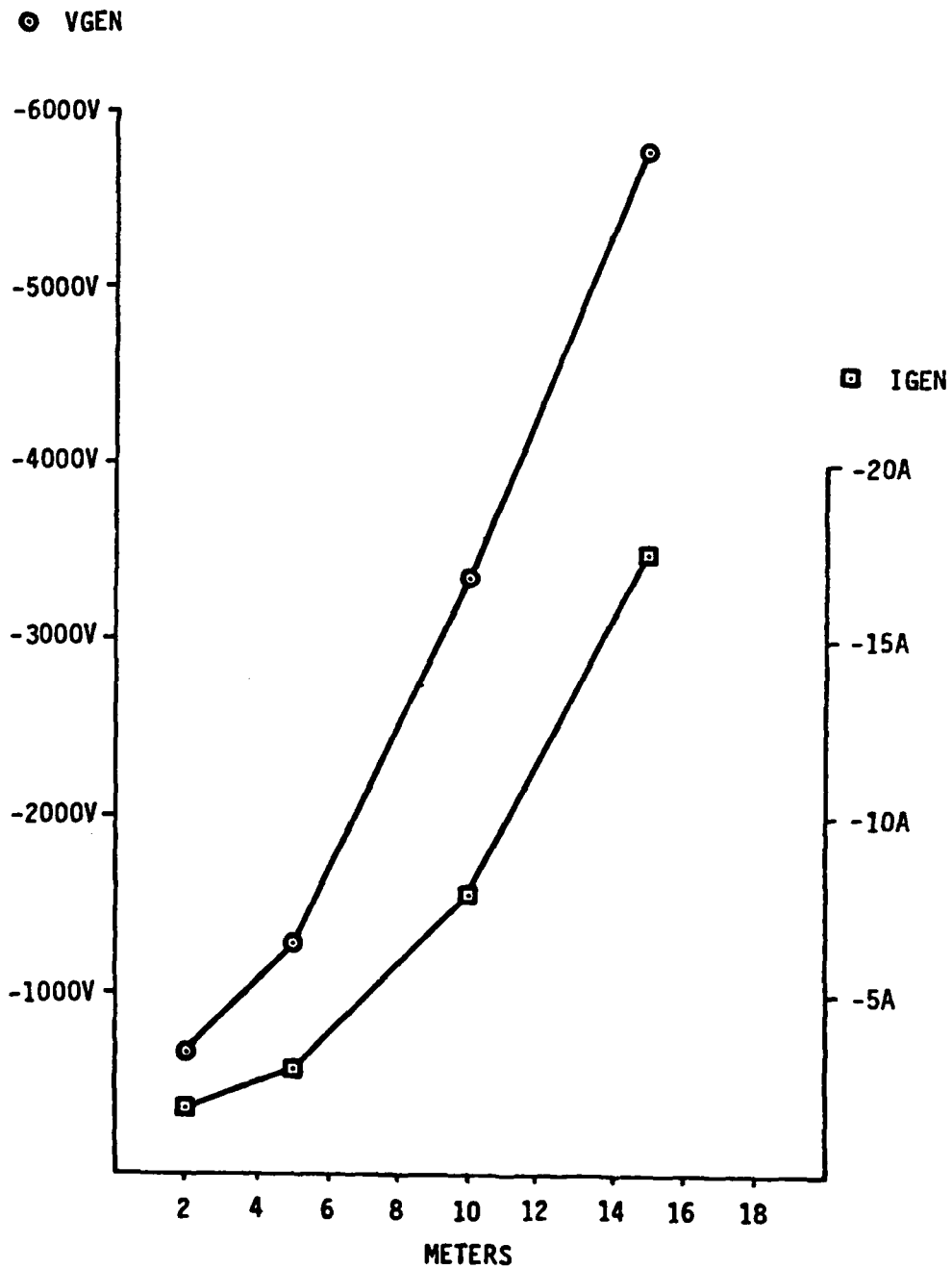
FIGURE   36   F15 Graphite/Epoxy - Voltage Vs Current Curves

94

F15 GEN FEEDER - GR/EP
MAIN BUS
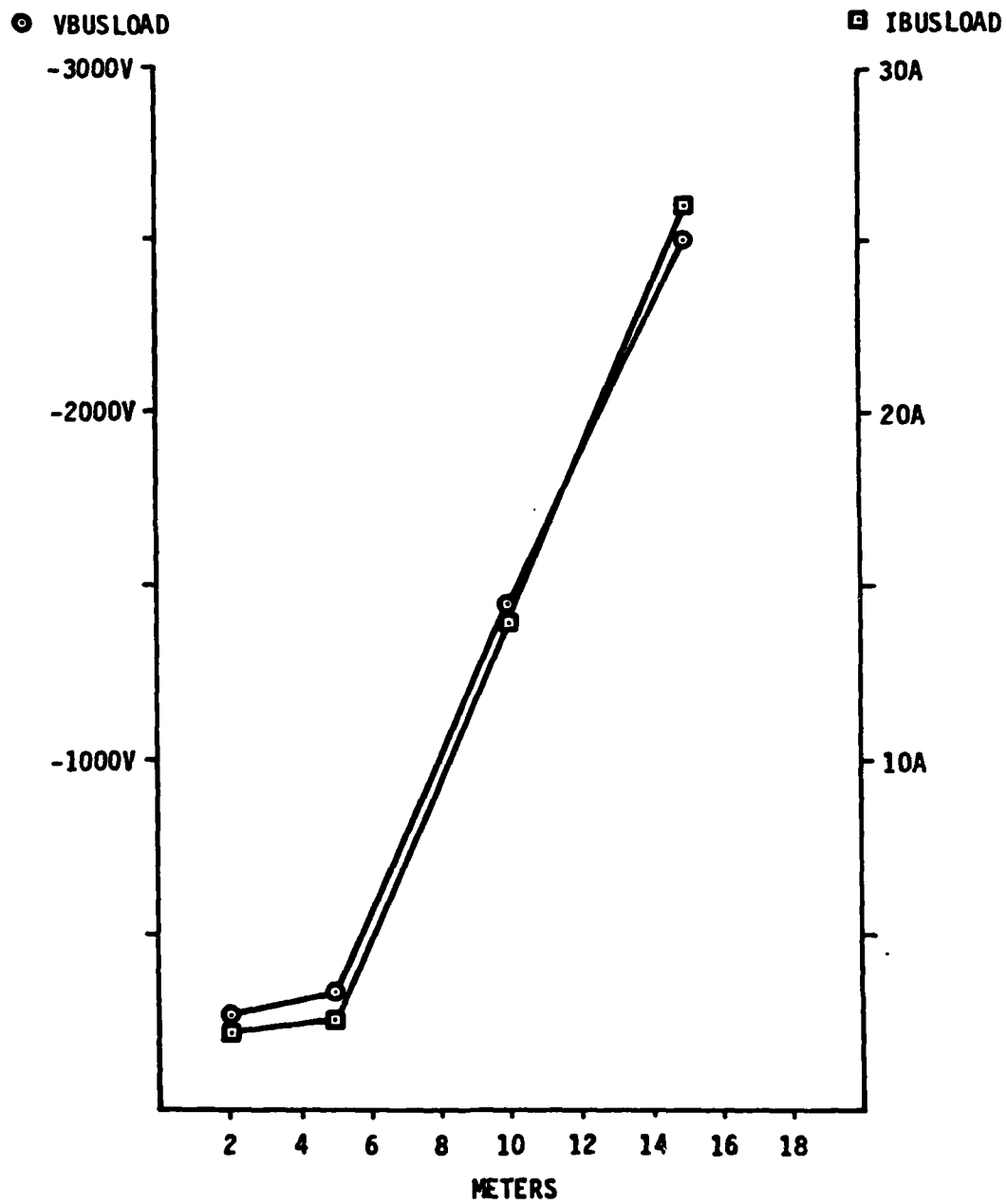
FIGURE 37   F15 Graphite/Epoxy - Voltage Vs Current Curves

95

feeder increased. Section II.4.d lists the subroutine equations used to calculated the transeint voltage.

c. BEACON LIGHT CIRCUIT

The cargo beacon light was modelled as shown in the one line diagram of Figure 38 and the equivalent circuit in Figure 39. This circuit consisted of a pair of 20 gauge wires running along the front spar connecting the bus circuit breaker to the beacon light transformer at the wing tip. Resistance, inductance, and capacitance values for each block including a 50% loaded bus are recorded on Figure 39, the modelled equivalent circuit. Peak transient voltage to ground and line current test points were taken at the beacon light transformer primary (T1) and at the input side of the bus (T2).

(1) FIBERGLASS WING LEADING EDGE

Using the circuit described in Section III.1.c, the pair of 20 gauge wires were excited by the magnetic field of a lightning transient traveling from the wing tip attachment point toward the fuselage. As is shown in Figure 39, the excited wing section of the circuit was broken into three sections, each 4.66 meters in length. The wire pair was located behind a fiberglass leading edge two inches above the ground plane or front spar of an all aluminum wing. Listed in Section II.4.a and Table 8 are the lightning source fortran subroutine equations and definitions used in the TRAFFIC computer analysis routine. Table 20, PEAK TRANSIENTS BEACON LIGHT, lists the moderate and severe transients monitored at the two test points, T1 and T2.

d. WINDOW HEATER CIRCUIT

The windshield heater circuit was modelled with the aircraft nose being the lightning attachment point. Surface charge on the airframe exterior from the lightning strike capacitively coupled onto the heater element. A pair of number 12 gauge power wires connected the heater element through a controller to the bus. Shown in Figure 40 is the circuit one line diagram. Figure 41, displays the modelled equivalent circuit of the interconnection of the feeders with the windshield to the controller and bus. Impedance values in terms of
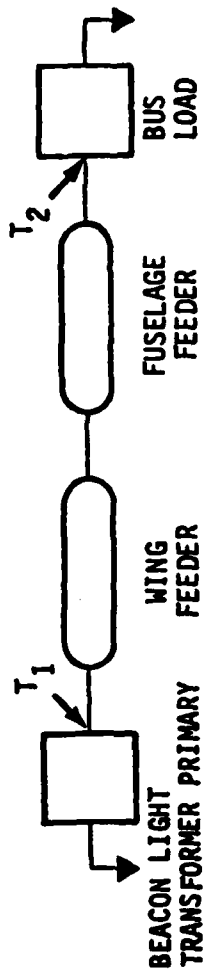
FIGURE 38   Cargo Beacon Light To AC Bus One Line Diagram
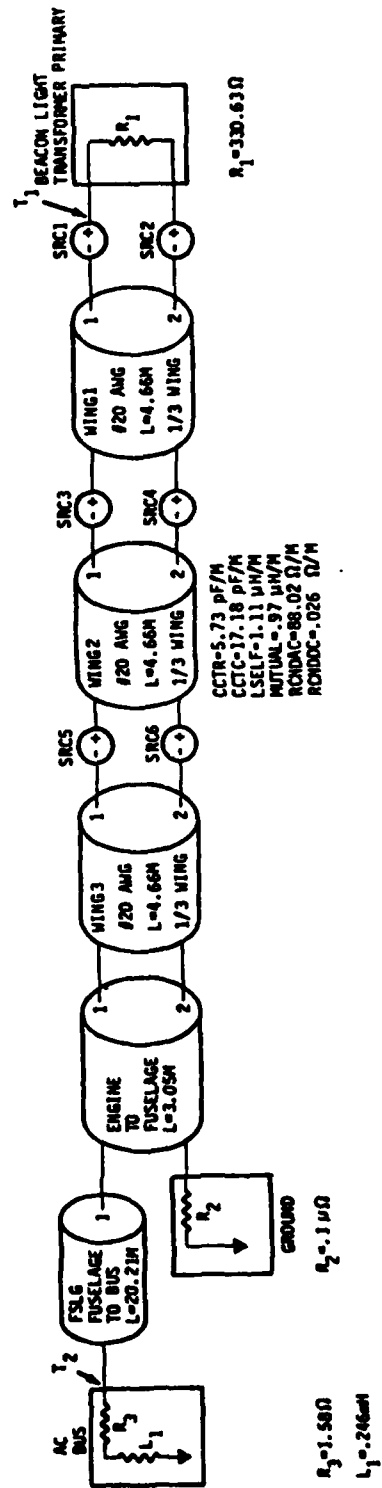
FIGURE 39   Cargo Beacon Light to AC Bus No. 2 Equivalent Circuit

97

TABLE 20 PEAK TRANSIENTS BEACON LIGHT

TEST CASE	TEST POINT/ NAME	TRANSIENT DURATION	POSITIVE AMPLITUDE	NEGATIVE AMPLITUDE	DC OFFSET
			(MODERATE)		
BL MOD	T1/VLIGHT	1u Sec.	18.0 KV	0.0 KV	+5.25 KV
BL MOD	T1/ILIGHT	2u Sec.	1.1 mA	-1.4 mA	-0.45 mA
BL MOD	T2/VBUS	2u Sec.	0.6 KV	-0.62 KV	-80.0 V
BL MOD	T2/IBUS	2u Sec.	0.26 A	-0.52 A	-.05 A
			(SEVERE)		
BL SEV	T1/VLIGHT	4u Sec.	81.0 KV	0.0 KV	+21.0 KV
BL SEV	T1/ILIGHT	4u Sec.	4.6 mA	-7.8 mA	-2.4 mA
BL SEV	T2/VBUS	1u Sec.	2.2 KV	-2.8 KV	-0.4 KV
BL SEV	T2/IBUS	3u Sec.	0.8 A	-2.6 A	-0.25 A

TABLE 21 PEAK TRANSIENTS WINDOW HEATER

TEST CASE	TEST POINT NAME	TRANSIENT DURATION	POSITIVE AMPLITUDE	NEGATIVE AMPLITUDE	DC OFFSET
			(MODERATE)		
WH MOD	T1/VCONLNA	>50u Sec.	48.0 V	-37.0 V	+1.0 V
WH MOD	T1/ICONLAI	10u Sec.	15.0 A	-2.4 A	-0.6 A
WH MOD	T2/VCONLNB	>50u Sec.	170.0 V	-35.0 V	-10.0 V
WH MOD	T3/ICONLAO	10u Sec.	2.1 A	-0.5 A	+0.1 A
WH MOD	T4/VBUSLNA	>50u Sec.	45.0 V	-34.0 V	+3.0 V
WH MOD	T4/IBUSLA	>50u Sec.	0.7 A	-0.7 A	0.0 A
WH MOD	T5/VBUSLNB	>50u Sec.	185.0 V	-30.0 V	-17.5 V
WH MOD	T5/IBUSLB	>50u Sec.	0.7 A	-0.7 A	0.0 A
			(SEVERE)		
WH SEV	T1/VCONLNA	>50u Sec.	420.0 V	-330.0 V	+20.0 V
WH SEV	T1/ICONLAI	>50u Sec.	74.0 A	-11.0 A	-2.0 A
WH SEV	T2/VCONLNB	>50u Sec.	865.0 V	-340.0 V	-60.0 V
WH SEV	T3/ICONLAO	>50u Sec.	11.0 A	0.0 A	+0.4 A
WH SEV	T4/VBUSLNA	>50u Sec.	400.0 V	-340.0 V	+20.0 V
WH SEV	T4/IBUSLA	>50u Sec.	7.8 A	-6.8 A	0.0 A
WH SEV	T5/VBUSLNB	>50u Sec.	920.0 V	-320.0 V	-80.0 V
WH SEV	T5/IBUSLB	>50u Sec.	7.4 A	-6.4 A	0.2 A
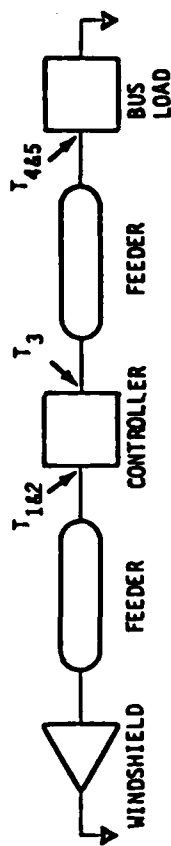
Figure 40 Cargo Windshield Heater One Line Diagram
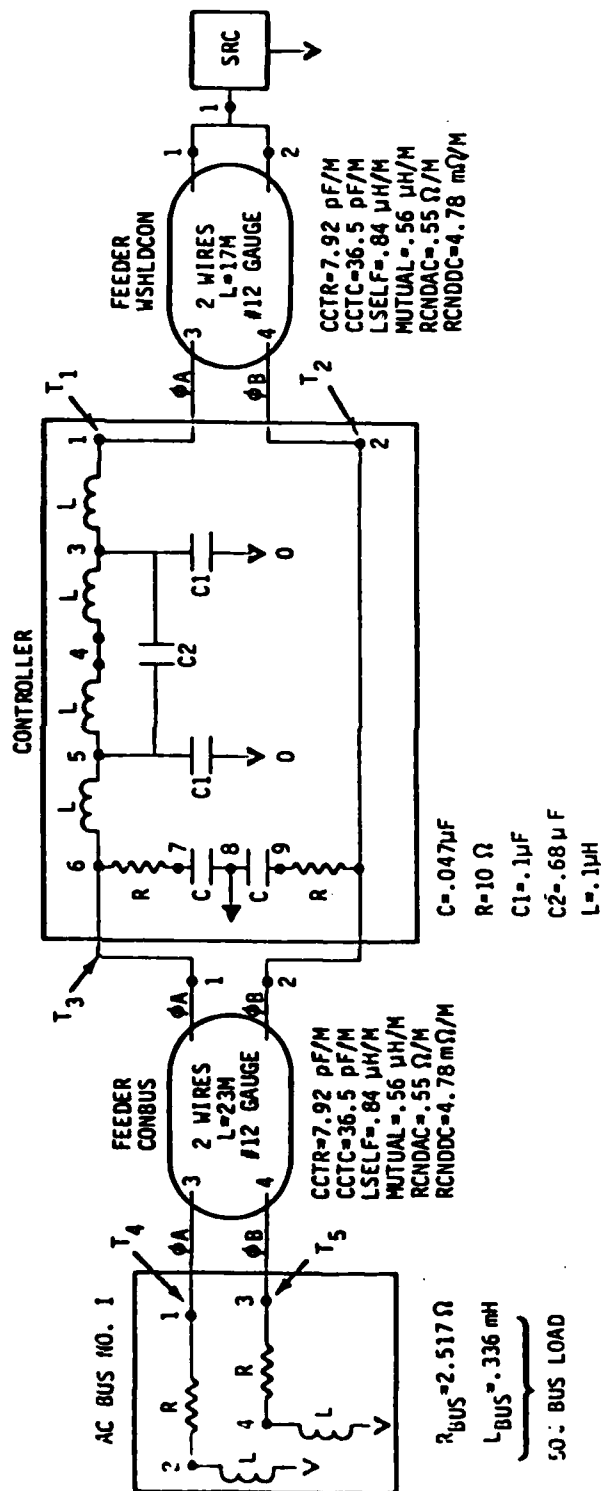
Figure 41 Cargo Windshield Heater to Controller to Bus Equivalent Circuit

99

capacitance, resistance, and inductance for each circuit element and the 50% loaded bus are noted on the equivalent circuit.

(1) CARGO AIRPLANE

Using the circuit described in Section III.1.d, the pair of twelve gauge power feeders were excited with a simulated moderate and then severe lightning transient. Test points for phase to ground voltage and line current were taken at five locations: phase A and B controller inputs (T1, T2), phase A controller output (T3), and phase A and B bus inputs (T4, T5). The lightning source Fortran subroutine equations and definitions are given in Section II.4.d and Table 11, respectively. Table 21, PEAK TRANSIENTS WINDOW HEATER, lists both moderate and severe transients.

e. UPPER SURFACE BLOWING ACTUATORS

One upper surface blowing actuator was modelled in series with an interface unit and AC and DC buses. A strike to the wing was assumed to generate a lightning transient traveling down the wing producing magnetic coupling on the 20 gauge power wiring located along the rear spar. The one line diagram is shown on Figure 42. The impedance values for each circuit element and a 50% loaded bus are listed on the modelled equivalent circuit diagram, Figure 43.

(1) CARGO AIRPLANE

Using the circuit described in Section III.1.e, a bundle of ten number twenty gauge power wires 3.66 meters long were excited by the magnetic field of a moderate and then a severe lightning strike. This excited wire bundle was connected on one end to the AC and DC loads and to an unexcited bundle on the other end. From the interface unit, one number twelve gauge wire fed each respective bus as in shown in Figure 43. Test points for phase to ground voltage and line current were sampled at six locations: input to the AC and DC loads (T1 and T2), input of one AC and DC wire to the interface unit, (T3 and T4), and input to the AC and DC buses (T5 and T6). The lightning source Fortran subroutine equations and definitions are given in Section II.4.a and Table 8, respectively. Table 22, PEAK TRANSIENTS UPPER SURFACE BLOWING ACTUATOR, lists both moderate and severe transients.
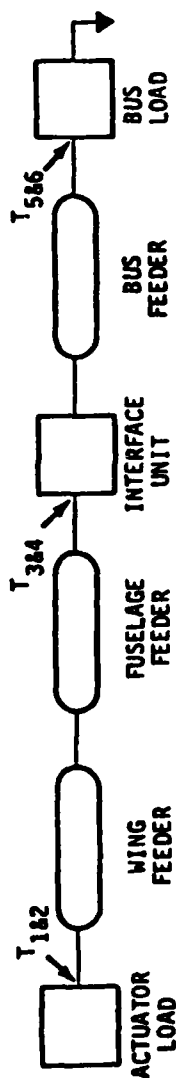
Figure 42 Cargo Upper Surface Blowing AC Actuator to IFU to Bus Block Diagram
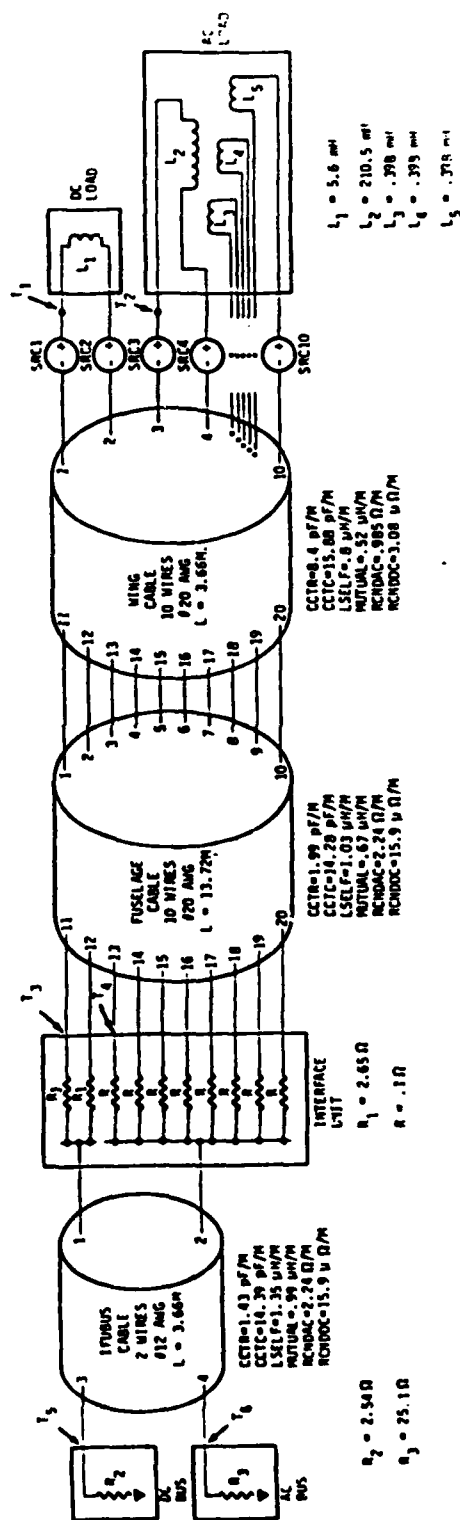
Figure 43 Cargo Upper Surface Blowing Actuator to IFU to Bus Equivalent Circuit

TABLE 22   PEAK TRANSIENTS UPPER SURFACE BLOWING ACTUATOR

TEST CASE	TEST POINT/ NAME	TRANSIENT DURATION	POSITIVE AMPLITUDE	NEGATIVE AMPLITUDE
		(MODERATE)		
USB MOD	T1/VDCLOAD	2u Sec.	18.8 KV	0.0 V
USB MOD	T1/IDCLOAD	>10u Sec.	0.42 uA	-0.25 uA
USB MOD	T2/VACLOAD	2u Sec.	18.8 KV	0.0 V
USB MOD	T2/IACLOAD	>10u Sec.	0.5 nA	0.8 nA
USB MOD	T3/VIFUDC	>10u Sec.	20.0 mV	-40.0 mV
USB MOD	T3/IIFUDC	>10u Sec.	12.0 uA	-160.0 uA
USB MOD	T4/VIFUAC	>10u Sec.	8.0 mV	-50.0 mV
USB MOD	T4/IIFUAC	>10u Sec.	0.16 mA	-0.02 mA
USB MOD	T5/VDCBUS	>10u Sec.	20.0 mV	-40.0 mV
USB MOD	T5/IDCBUS	>10u Sec.	16.0 uA	-24.0 uA
USB MOD	T6/VACBUS	>10u Sec.	8.0 mV	-50.0 mV
USB MOD	T6/IACBUS	>10u Sec.	0.0 uA	-68.0 uA
		(SEVERE)		
USB SEV	T1/VDCLOAD	4u Sec.	82.5 KV	0.0 V
USB SEV	T1/IDCLOAD	>10u Sec.	1.0 uA	-1.4 uA
USB SEV	T2/VACLOAD	4u Sec.	82.5 KV	0.0 V
USB SEV	T2/IACLOAD	>10u Sec.	3.5 nA	-5.4 nA
USB SEV	T3/VIFUDC	>10u Sec.	0.15 A	-0.3 A
USB SEV	T3/IIFUDC	>10u Sec.	70.0 uA	-92.0 uA
USB SEV	T4/VIFUAC	>10u Sec.	0.0 V	-0.34 V
USB SEV	T4/IIFUAC	>3m Sec.	0.77 mA	-0.1 mA
USB SEV	T5/VDCBUS	>10u Sec.	0.15 V	-0.29 V
USB SEV	T5/IDCBUS	>10u Sec.	0.13 mA	-0.19 mA
USB SEV	T6/VACBUS	>10u Sec.	0.0 V	-0.34 V
USB SEV	T6/IACBUS	>10u Sec.	0.0 A	-690.0 uA

2. COMPARISON OF THREAT LEVELS WITH EXISITNG STANDARDS

The threat levels defined in Task 1 and produced in Task 2 exceed the
transient withstanding requirements of the present military equipment
specifications. The summation of applicable specifications for lightning
transients on power systems is shown on Table 23. MIL-STD-704 and RTCA
document DO-160 specify that equipment attached to the power system be capable
of with standing a 600 volt transient test. The purpose of the test is to
ensure that the electrical equipment will not be damaged by switching
transients. MIL-E-6051D has a power system requirement which limits voltage
transients to 50 percent of the nominal line voltage for the AC system and
+50 and -150 percent of nominal line voltage for the DC system. By
specifications, electrical equipment is tested for 600 volts open cirucit and
is not required to withstand larger transients.

3. ALTERNATE WIRING METHODS

a. FIBER OPTICS

In areas of high vulnerability to lightning induced EMI, fiber optic
transmission may be an attractive alternative to conventional wiring. The
fiber optic signal transmission lines are electrically nonconductive and are
not subject to electromagnetic coupling of lightning-caused or any other
transients. Besides EMI/EMP immunity, the primary benefits of using fiber
optics will be weight savings, increased bandwidth and eliminaiton of ground
problems. Fiber optic systems are well suited to either point-to-point links
or data bus systems and can handle digital data transmisison or analog signal
transmission. The implementation of fiber optics will depend upon the
benifits of fiber optics compared to some of the disadvantages which include
interconnect problems, lack of standards, and lack of reliability data.
Subsequent data on fiber optics was extracted from Reference 5.

Table 24 describes the weight and bandwidth advantages of fiber optics. As
shown, the weight savings is dependent upon the type of standard electrical
cable to which it is being compared. Compared to a twisted pair (22 gauge),
fiber optic cables offer approximately 22% savings in weight. For

TABLE 23 APPLICABLE SPECIFICATIONS

PARAMETER	MIL-STD-704B	MIL-STD-704C	MIL-E-6051D	DO-160
AC VOLTAGE SPIKE	+600 v. peak $\overline{1}$ usec rise t. test<500 usec		$\pm$50% of nominal volts test<50 usec	+600 v. peak $\overline{2}$ usec rise t. test
DC VOLTAGE SPIKE	same as AC		+50%, -150% of nominal volts test<50 usec	
AC VOLTAGE SURGE	180 v. rms >500 usec	180 v. rms >50 usec		
DC VOLTAGE SURGE	50 v >500 usec	50 v >50 usec		

TABLE 24 COMPARISON OF FIBER OPTIC AND ELECTRICAL CABLES

CABLE TYPE	WEIGHT	BANDWIDTH (at 4 DB/Km Loss)	COST
Optical (single strand) (graded index glass)	22.8 Kg/Km	1 GHz	$0.25 to $1.00/ft
Twisted Wire Pair (22 gauge)	28.8 Kg/Km	150 KHz	$0.40 to $0.50/ft
Coaxial (RG-58/u)	43.5 Kg/Km	180 KHz	

TABLE 25 PRIMARY COMPONENT SELECTION

TYPICAL APPLICATION   PRIMARY COMPONENT SELECTION

TYPE	SPEED	LENGTH	SOURCE	DETECTOR	FIBER	COMMENTS
POINT TO POINT	<50MHZ	<100M	LED	PIN	PCS	LOWEST IN COST AND CAPABILITY
POINT TO POINT	>50MHz	<100M	ILD	PIN	PCS	ILD REQUIRED FOR SPEED
DATA BUS	>50MHz	<100M	ILD	PIN	PCS	ILD REQUIRED FOR POWER NEEDS COUPLER DEVELOPMENT
POINT TO POINT	>50MHz	>100M	ILD	APD	GLASS ON GLASS	LONG LINE COMMUNICATIONS

coaxial cable (higher data rate information), the savings is over 90%. Table 24 also addresses bandwidth, again as compared to a twisted pair and coaxial cable. At a standard loss of 4db/KM, the fiber optic cable (single strand graded index glass fiber) can operate up to 1 GHz. By comparison, both twisted pair and coaxial cables can operate only below 1 MHz. In this case, there are over ten orders of magnitude increase in bandwidth of a fiber optic cable as compared to a twisted pair or coaxial cable.

(1) System Components

The primary components of various types of fiber optic links are summarized in Table 25. Low speed systems can be driven by light emitting diodes (LEDs) and detected by P-doped/intrinsic/N-doped (PIN) diodes. High speed applications will require the high frequency characteristics of injection laser diodes (ILDs) and avalanche photodiodes (APDs). All of the major fiber optic system components are discussed below.

(2) Sources

There are two types of fiber optics sources, ILD's and LED's. A summary of each is presented in Table 26.

There are two basic types of LED's - edge emitters and surface (Burrus) emitters. Of the two, the Burrus diode is more widely used due to its generally better performance. It is also a more expensive device (as much as a factor of 100 times more expensive, depending on the quality). As the top of the Burrus diode is etched away to expose the active area, the devices normally comes pigtailed. Until recently, these devices were not hermetically sealed. One company now claims to have developed a hermetic pigtail Burrus diode.

Injection laser diodes (ILDs) are threshold devices. After a certain value of drive current, the output efficiency will dramatically increase. The point at which this increase occurs (the lasing threshold) varies from device to device even from the same manufacturer. Manufacturers normally supply a curve of output vs. drive current for each diode. ILDs are high priced devices. The

106

TABLE 26   INJECTION LASER AND LIGHT EMITTING DIODE ANALYSIS

COMPONENT: INJECTION LASER DIODES (ILD, DOUBLE HETEROSTRUCTURE GAALAS)	
RELIABILITY:	1%/1000 HOURS
STANDARDS (MILITARY/INDUSTRY):	1982 LARGE VARIETY OF DEVICES, NEW TECHNOLOGY
APPLICATIONS:	HIGH DATA RATE TRANSMISSION, HIGH EMI, EMP AREAS
FAILURE MODES AND MECHANISMS:	INFANT MOTALITY (FIRST 100-200 HOURS - CRYSTAL DEFECT RELATED). FACET DAMAGE (ELECTRICAL OVERSTRESS, CURRENT SPIKES - HIGH OPTICAL POWER DESTROYS FACETS). BULK DEGRADATION (GRADUAL MIGRATION OF DOPANTS INTO ACTIVE AREA, GRADUAL FACET EROSION - LIMIT OF DEVICE LIFE).
LIMITATIONS:	DEVICE IS TEMPERATURE SENSITIVE. SHOULD BE MAINTAINED AT 25°C OR LESS FOR MAXIMUM LIFETIME AND OUTPUT POWER. SENSITIVE TO ELECTRICAL OVERSTRESS, MUST BE PROTECTED FROM ANY CURRENT SURGES (EVEN OF LESS THAN 1NS).
COMPONENT: LIGHT EMITTING DIODES (LED, SURFACE EMITTER (BURRUS), EDGE EMITTER GAALAS)	
RELIABILITY:	1%1000 HRS
STANDARDS (MILITARY/INDUSTRY):	1981 CURRENTLY BEING GENERATED
APPLICATIONS:	LOW TO MODERATE (<50MHz) DATA RATE TRANSMISSION. LIMITED TO MODERATE LENGTHS (2Km OR LESS) TRANSMISSION. HIGH EMI, EMP AREAS. ANALOG APPLICATIONS.
FAILURE MODES AND MECHANISMS:	INFANT MORTALITY (FIRST 100-200 HOURS-CRYSTAL DEFECT RELATED). BULK DEGRADITION (GRADUAL MIGRATION OF DOPANTS INTO ACTIVE AREA COMMON TO ALL IC'S).
LIMITATIONS:	CURRENT DEVICES LIMITED TO <100MHz OPERATION. WIDE SPECTRAL WIDTH CAUSES DISPERSION PROBLEMS IN LONG LINKS.

reasons given for high price are the high development costs that need to be recovered, the complex structure, the high demand, and the low yields of the devices. One of the reasons for the low yields is that the structures are extremely complex but they are being standardized into 14-pin DIP package.

(3) Connectors

Table 27 is a summary of data on connectors. Fiber optic connectors available today cover a very broad range from simple single contact fiber bundle or plastic fiber types to multicontact types capable of handling bundles, single fibers, and conventional wires in the same shell. Parameters of primary importance to connector performance include fiber alignment, protection, cable strain relief, size, and cost.

Fiber alignment is the prime consideration in the determination of connector transmission characteristics. Alignment is nomally broken down into lateral, axial, and angular modes, as shown in Figure 44. With the telecommunications fibers used today, with core diameters of 50 to 65 microns (2 to 2-1/2 mils), a few tenths of a mil (10% core diameter) lateral misalignment will cause greater than 1/2 a db loss. A 1° angular misalignment will cause 1/3 of a db loss, and a 10% of core diameter end separation will cause a 1/4 db loss. The above losses are also dependent upon fiber numerical aperture (NA). The losses are approximately correct for NA's of about .3 and will be higher for higher NAs, lower for lower NAs. The above misalignment allowances represent typical values and show that extreme precision is required in connector design, manufacture, and assembly to assure low connector losses. Use of large core fibers (100 to 200) can ease the tolerance problem and cut connector costs but a larger core size increases the radiation cross section of the fiber. This is a tradeoff to be considered. It should also be noted that the above losses do not include the fiber/fiber interface losses that are common to the fibers themselves. These include fresnel loss, core diameter variation loss, end surface irregularity loss, and NA variation loss. These losses generally contribute 0.2 to 0.3 db to the overall connector loss. Alignment methods used in multimode single fiber cable connectors vary from manufacturer to manufacturer. The major concern being to hold the lateral alignment and end spacing. Some of the more popular methods include placing

TABLE **27** CONNECTOR ANALYSIS

COMPONENT: CONNECTORS (SINGLE TERMINATION, MULTITERMINATION)	
RELIABILITY:	NO DATA
STANDARDS (MILITARY/INDUSTRY):	1981 CURRENTLY BEING GENERATED
APPLICATIONS:	CONNECTIONS BETWEEN FIBER OPTIC COMPONENTS AND OPTICAL FIBERS.
FAILURES MODES AND MECHANISMS:	CONTAMINATES (SERIOUSLY IMPAIRS COUPLING EFFICIENCY) ADHESIVES FAILURE (BOND BETWEEN FIBER AND CONNECTOR FAILS UNDER ENVIRONMENTAL STRAIN).
LIMITATIONS:	DEVICES NOT DEVELOPED TO MIL/SPACE LEVELS DUE TO LACK OF MARKET AND LARGE EXPENSE. REQUIREMENTS SPECIFIC TO FIBER OPTIC CONNECTORS NEED TO BE DEFINED.

TABLE **28** CABLE AND FIBER ANALYSIS

COMPONENT: CABLE	
RELIABILITY:	NO DATA
STANDARDS (MILITARY/INDUSTRY):	1981 (CURRENTLY BEING GENERATED)
APPLICATIONS:	PROTECTION OF OPTICAL FIBER FROM HOSTILE CONDITIONS.
FAILURE MODES AND MECHANISMS:	BREAKAGE, KINKING, OUT GASSING (PHYSICAL DAMAGE TO FIBER)
LIMITATIONS:	CABLES ABLE TO MEET SPECIFIC MIL/SPACE REQUIREMENTS BUT NOT ALL REQUIREMENTS CONCURRENTLY. REQUIREMENTS SPECIFICALLY OF FIBER OPTIC CABLES NEED TO BE DEFINED.
COMPONENT: OPTICAL FIBER	
RELIABILITY:	NO DATA
STANDARDS (MILITARY/INDUSTRY):	1981 (CURRENTLY IN DEVELOPMENT)
APPLICATIONS:	LOW TO HIGH DATA RATE TRANSMISSION. SUITABLE FOR AREAS CLOSED TO ELECTRICAL WIRING. HIGH EMI, EMP AREAS. LOW BER.
FAILURE MODES AND MECHANISMS:	BREAKAGE OF FIBER.
LIMITATIONS:	TEMPERATURE EXTREMES. SOME FIBER TYPES MORE RADIATION RESISTANT THAN OTHERS. RESISTANT TO ADHESIVES USE.

LATERAL MISALIGNMENT

AXIAL MISALIGNMENT

ANGULAR MISALIGNMENT
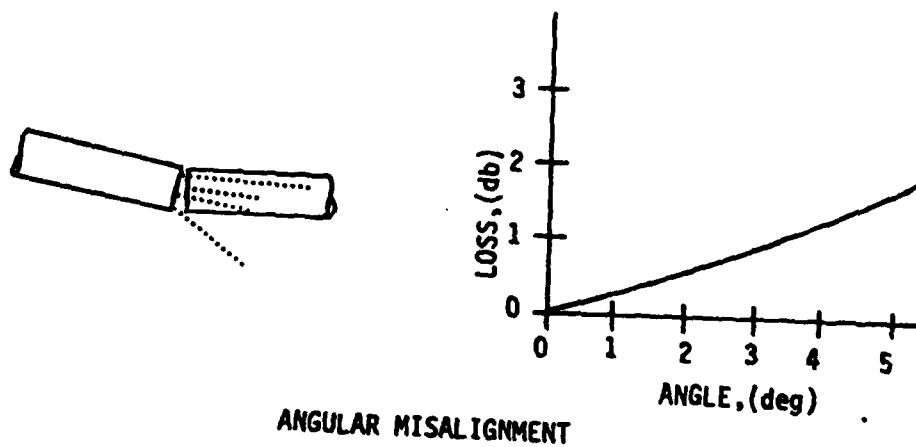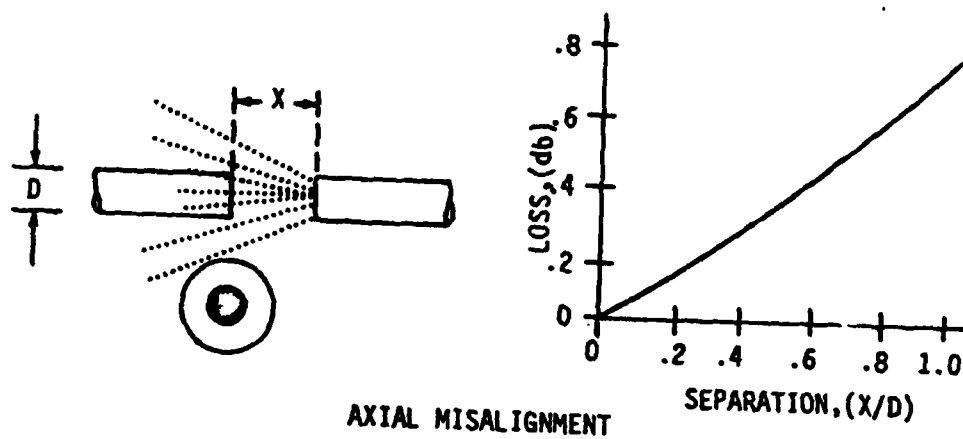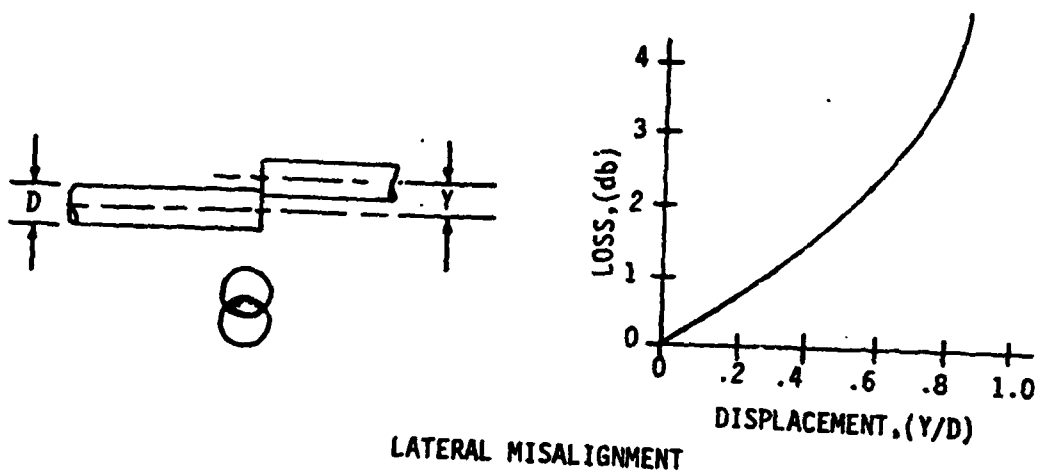
FIGURE 44   MISALIGNMENT LOSS

the fiber in the space between three or four precision rods or spheres, constraining the fibers to a vee groove, use of a precision hole drilled in the termination, and use of a lens to focus the beam from separated fibers. Figure 45 shows examples. Fiber positioning in the alignment mechanism is done primarily with an epoxy adhesive. Because of temperature cycling and moisture problems encountered in the use of expoxies by several manufacturers, alternate methods are being studied and implemented for fiber retention. These include crimping of the fiber using a soft metal ring and use of end pressure to hold fibers in place.

Strain relief of the fiber and cable is of prime importance but is often over-looked in connector design, especially in multicontact connectors. Not only must the fibers be supported axially to prevent tension fracture but laterally as well to prevent shear. The connector cable interface is particularly prone to damage because of the ability to bend the cable at right angles to the connector at this point. Use of cable stiffeners or a heat shrinkable outer sheath at this point can eliminate this problem.

The terminating portion of the connector on at least one half of the connecting pair must have some provision for movement to allow the mating of the two terminations to the tolerances required. This movement must be such that it is restrained after mating and the mated position is not affected by outside stress.

The connector must protect the fiber mating surfaces from contamination both in the mated and unmated condition and, therefore, should be of the hermetic type and should be provided with a form of dust cover or cap.

Connector cost at present is quite high due to low volume production and high engineering and fabrications costs because of the tight tolerances required. Two solutions to this problem are standardization leading to higher volume production and a decrease in tolerance requirements made possible by usage of larger core fibers.
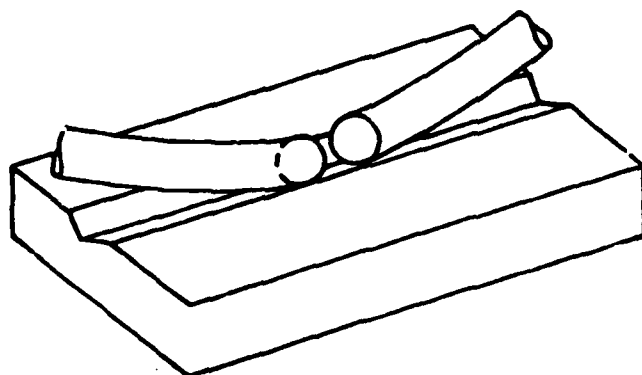
VEE GROOVE
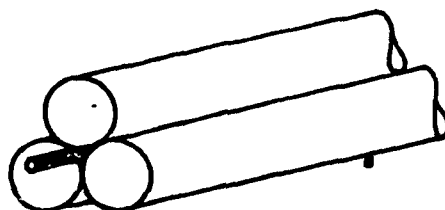
ROD RETENTION
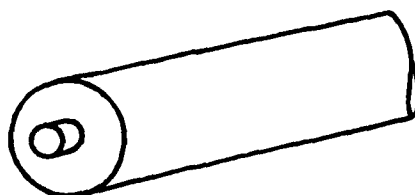
PRECISION CONCENTRIC HOLE

FIGURE 45   FIBER ALIGNMENT METHODS

112

(4) Fibers/Cables

A summary of information on fibers and cables is given in Tables 28. Examples
of cable construction are shown in Figure 46.

Plastic clad silica fiber (PCS) is naturally more radiation resistant than
other fiber types. Larger core diameters are possible with PCS, as compared
to glass on glass, due to the more flexible nature of the plastic cladding. A
larger core makes for increased coupling at the source (LED, ILD) and for
lower connector losses. See Figure 46 for fiber types. PCS does have several
problems: it is sensitive to moisture, the attenuation dramatically increases
at low temperature, and terminations are difficult due to the soft nature of
the plastic cladding. Moisture and low temperature sensitivity are material
related problems. Moisture would be absorbed into the cladding, changing its
properties and increasing fiber attenuation. Cold temperature is a problem in
that the index of refraction of the plastic cladding would change at low
temperatures. The change in the index of refraction would affect the
numerical aperture of the fiber, causing it to become smaller. This limits
most PCS fiber to operating in temperatures higher than -20°C.

The core of the fiber, being harder than the cladding, tends to migrate in and
out at the end of the termination under various fiber load conditions. This
is also a problem during polishing of the termination. Under polishing, the
core would be compressed into the cladding so that when polishing was
completed, the core tended to extrude beyond the end of the connector. This
made it very susceptible to damage and repeated connections would often
destroy the polished end, causing an increase in connector loss. Suitable
adhesives which could grip the plastic cladding and the metal connector are
not available and the fiber end could change its position relative to the
connector under handling or installation. The use of the replaceable cladding
at the fiber end as well as the modified connectors have solved these problems.

(5) Detectors

A summary of detector data analysis is found on Table 29. This technology
appears to be the most highly developed area of fiber optics. The detector

FIBER

JACKET

JACKET

STRENGTH MEMBERS

INNER JACKET

FIBER

JACKET

STRENGTH MEMBERS

INNER JACKET

FIBER

46

100mm GLASS CORE

140mm GLASS CLADDING

GLASS ON GLASS

200mm GLASS CORE

300mm PLASTIC CLADDING

PLASTIC CLAD SILICA

300mm PLASTIC CORE

400mm PLASTIC CLADDING
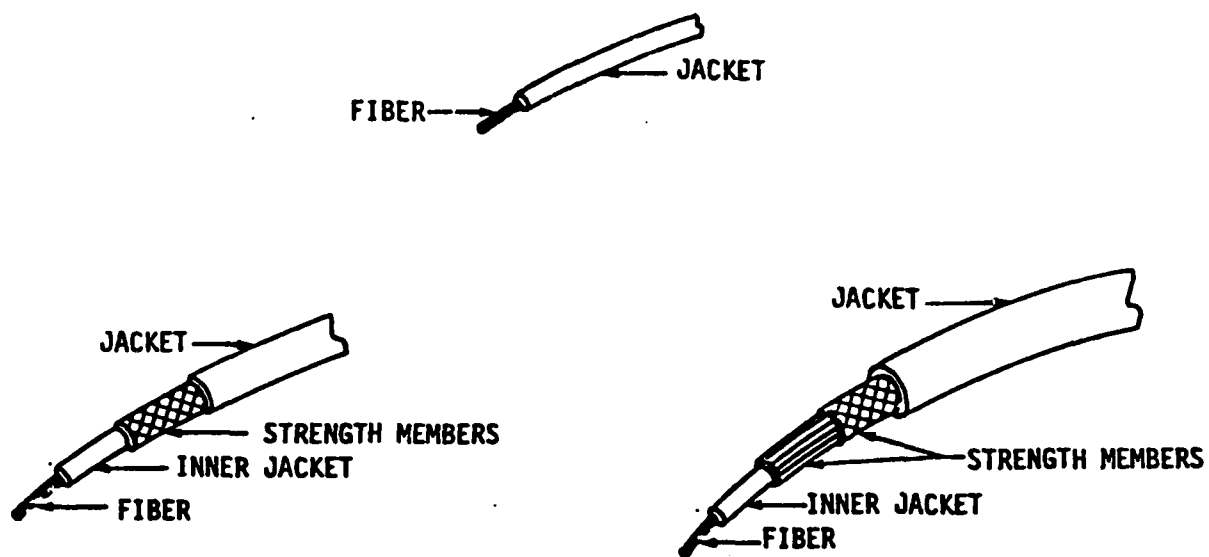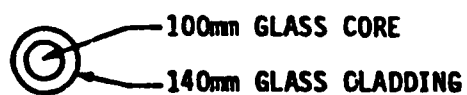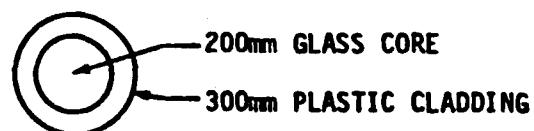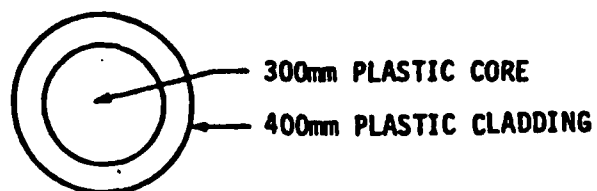
PLASTIC CLAD PLASTIC

FIGURE 47   Cable Construction

114

TABLE **29** DETECTOR ANALYSIS

COMPONENT: DETECTORS	
RELIABILITY:	.1%1000 HRS
STANDARDS (MILITARY/INDUSTRY):	1981 (CURRENTLY BEING GENERATED)
APPLICATIONS:	ALL FIBER OPTIC LINKS
FAILURE MODES AND MECHANISMS:	ELECTRICAL OVERSTRESS. OPTICAL OVERSTRESS (EXTREMELY HIGH LEVELS NEEDED, UNLIKELY IN A FIBER OPTIC LINK)
LIMITAIONS:	PACKAGING IS NOT CURRENTLY OPTIMAL. APD'S GAIN TEMPERATURE AND VOLTAGE DEPENDENT. SILICON DETECTORS GOOD OUT TO 850 TO 900NM WAVELENGTHS

TABLE **30** MODULE ANALYSIS

COMPONENT: MODULES	
RELIABILITY:	2%1000 HRS
STANDARDS (MILITARY/INDUSTRY):	1981 (CURRENTLY BEING GENERATED)
FAILURE MODES AND MECHANISMS:	SUSCEPTIBLE TO FAILURES COMMON TO SOURCES, DETECTORS, IC'S, AND CONNECTORS
LIMITATIONS:	LOW DATA RATES (<10MHz). ENVIRONMENTAL LIMITATIONS (NONHERMETIC, TEMPERATURE RANGE)

TABLE **31** COUPLER ANALYSIS

COMPONENT: COUPLERS	
RELIABILITY:	NO DATA
STANDARDS (MILITARY/INDUSTRY):	1981 (BEING GENERATED)
APPLICATIONS:	DATA BUS REQUIREMENTS FOR USE IN FIBER OPTIC COMMUNICATION SYSTEMS
FAILURE MODES AND MECHANISMS:	INSUFFICIENT DATA
LIMITATIONS:	INPUT LOSSES ARE TOO HIGH. DYNAMIC RANGE OF OUTPUT TOO LARGE. DEVICES ARE BULKY AND FRAGILE.

chips are very durable and should last as long as other silicon diodes.

In order to work at peak speed, detector diodes need to be reverse biased. For example, a certain PIN (P-Doped/Intrinsic/N-Doped) diode has a rise and fall time of 300 ns under zero bias conditions. The application of 20V of reverse bias will reduce the rise and fall time down to only 1 ns. Diodes which possess this fast a response time and are sensitive to light in the frequency range of interest (800 nm to 950 nm) will, of necessity, cost more due to their more complex structures.

PIN diodes consist of three regions: a P and an N region separated by what is know as the intrinsic (I) region. The lifetime of the minority carriers depends on the purity and perfection of the silicon crystrals used. Impurities and imperfections will cause lower collection efficiencies, increased leakage current, higher noise levels, and shorter lifetimes. The conclusion is that performance directly relates to reliability. The silicon PIN photodiodes currently available have been developed to a high degree. Detection is possible down to the levels where thermal noise is the limiting factor.

Avalanche photodiodes (APDs) are also rather well developed. A more complex structure and generally more expensive than PIN diodes, the APDs have two big advantages that may compensate for the added costs. APDs are faster and more sensitive than PIN diodes. APDs have internal gain when strongly reverse biased. The internal gain allows an increase in the dynamic range of the system of 100 db or more. This could be of major importance in designing a data bus system where the high loss of the multiport coupler precludes the use of a PIN diode. Reverse biases of 200 to 400V are common. The high reverse bias also creates a stronger electric field in the diode which reduces the response time. (APDs have been used for detection well into the gigahertz region.) The gain of APDs is temperature dependent, so if used in an environment of temperature fluctuations, a compensation circuit is necessary.

The relationship between performance and reliability appears to be true also for APDs. The same factors (crystal perfection and low impurity levels) which limit the lifetime of the diodes are also largely responsible for noise and leakage.

In contrast to the high degree of development of the photodiode chip is the poor packaging typically used. The chips are normally mounted in a modified transistor/diode package (such as a TO-18). While this allows a hermetic seal, it greatly increases the coupling losses incurred when terminating a fiber. The active area needs to remain small to keep the junction capacitance low. This allows the diode to be used in high speed electronic circuits.

The solution used to date has been to reduce the separation between the end of the fiber and the active area. This has been accomplished by pigtailing a fiber or other optical waveguide directly to the chip. This is done at the expense of losing the hermetic seal. Lenses are also used to increase the coupling. Use of lenses requires a high degree of mounting accuracy. Although it can be done, it is rather expensive.

A better soulution being used/studied by some companies is the use of an integral optical waveguide. This waveguide can be quite large compared to the incoming fiber size. The active areas of chips are often in the 500 m diameter size while the core diameter of the military standard short haul fiber is 100 m. An optical waveguide with a core diameter of 300 m could be mounted to the chip surface. The coupling loss between the waveguide and the surface would be low. Also, use of a large core would insure a low loss between the waveguide and incoming fiber as one of the main loss mechanisms of connectors, axial misalignment would be eliminated.

(6) Fiber Optic Transmitter/Receiver Modules

Table 30 contains a summary of the transmitter/receiver modules data analysis. There is a large variety of fiber optic modules on the market. Most are designed for the commercial market although a few companies claim their modules will meet military specifications with the exception of the LED. One set of modules was designed under an Air Force contract.

The function of the modules is to be the interface between the electronics and the optical fiber. A typical transmitter module will contain an LED and the associated electronics necessary to drive it. The receiver module will be comprised of a photodiode and the electrical circuitry needed to translate the

117

optical signal into an electrical signal. Usually, all that is necessary to operate the module is a supply voltage and an input (or output for the receiver) of the signal.

One major problem with the modules is their packaging. They incorporate epoxy seals, especially around the input/output connectors. This normally limits operating temperatures to the 0° to 70°C range and does not provide true hermetic seals. One company reported being able to produce a military version incorporating a hermetically sealed and screened LED with high reliability integrated circuits.

(7) Couplers

A summary of the analysis on the coupler data is on Table 31. Couplers are a necessary part for use in data buses. A main disadvantage of fiber optics compared to conventional electrical wiring is the difficulty in splitting up the signal. At present, almost all fiber optic links are point-to-point systems, one output to one input. To increase the flexibility and utility of fiber optics, the ability to transmit one output into several inputs (or vice versa) will be necessary.

The usual multiport (star) coupler is normally a series of fibers stacked into a small array and butt joined into a mixing rod. The opposite end of the mixing rod either terminates in a similar array of fibers (in a transmissive coupler) or a highly reflective surface (in a reflective coupler). Figure 48 shows an example of each type.

Another kind of coupler used for small number terminations (normally two in and two out) employs fused fibers. Two fibers are fused together by heating them. Surface tension forms the fused end into a circular shape. The fused end is then cut and/or polished and joined to another similarly formed fiber pair.

4. LIGHTNING HARDNESS OF CONVENTIONAL AND ADVANCED EQUIPMENT

With the advent of the composite aircraft, protecting the airvehicle

OPTICAL FIBERS
STACKED IN ARRAY

MIXING ROD

OUTPUT

INPUT
FIBER

OUTPUT

OUTPUT

OPTICAL FIBER ARRAY
INPUT

MIXING ROD

OPTICAL FIBER ARRAY
OUTPUT

TRANSMISSIVE COUPLER

OUTPUT
FIBER
INPUT
FIBER
OUTPUT
FIBER

ANY FIBER IS EITHER
INPUT OR OUTPUT

MIXING ROD

REFLECTIVE
COATING

REFLECTIVE COUPLER
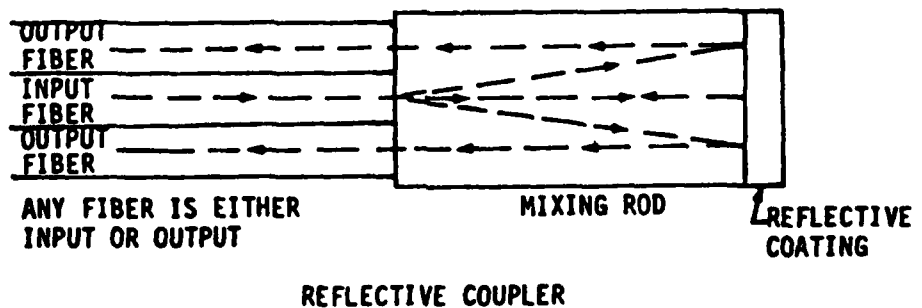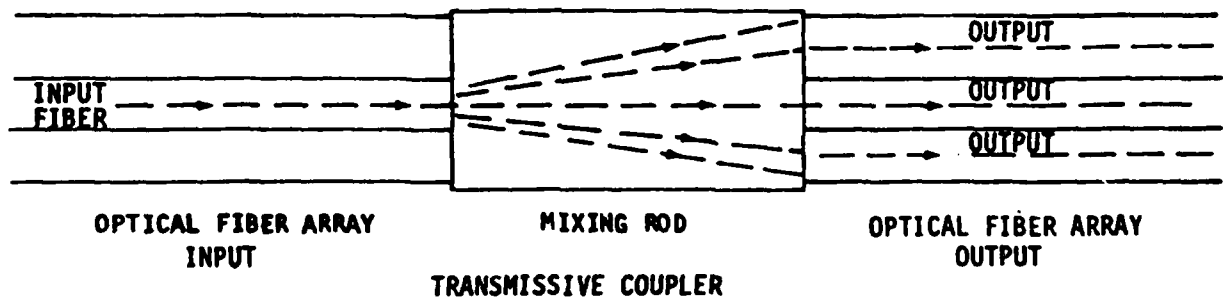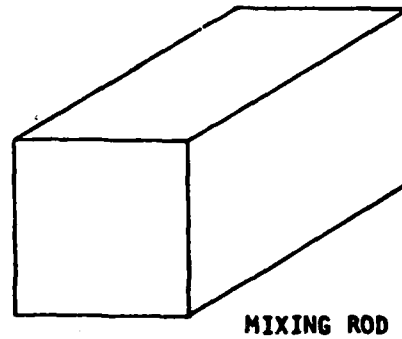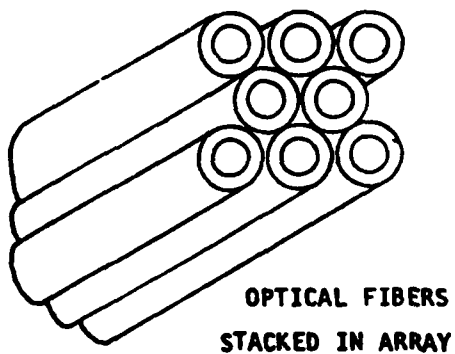
FIGURE 48   MULTI-PORT COUPLER STRUCTURE

-119-

electronic/electrical equipment from lightning transients will become a primary concern in the overall airplane design. No longer will lightning protection be limited to the "leftovers" and not given much thought in the matter of equipment protection. The design engineer will have an input prioritizing the location of the electrical/electronic equipment within the aircraft airframe. Wire routing will be one of the first items to be designed into the airplane as more inherent airframe shielding will be utilized. Section III.4.b highlights the rules governing wire routing. After maximizing the inherent airframe shielding for equipment location and wire routing, the design engineer will be better prepared for judicious usage of shielding and other add on protection devices for the most flight critical equipment.

a. EQUIPMENT DAMAGE

The increasing use of digital flight control systems and integrated circuits is increasing the threat of lightning damage. For example, a typical discrete audio transistor failure to a level of 1M rectangular pulse is in the range of 100 watts to 1 kilowatt. A typical integrated circuit failure level ranges from 5 watts to 100 watts. As the integration scale gets larger and circuit speeds increase, the susceptibility is expected to get worse.

Protection is required for those circuits where damage is predicted by the circuit analysis. The form of protection will vary from passive devices such as resitors and filters to active limiting devices. To determine if any components will fail under a given circuit drive, the voltages and currents associated with vulnerable components must be determined, and the results compared to available component data. This data is usually in terms of a rectangular pulse damage power curve covering a wide range of pulse widths. Thus, instantaneous component power must also be computed.

Usually the most vulnerable circuit components in a good design are the semiconductors. It has been demonstrated that semiconductor junctions are usually most vulnerable to damage from reverse-bias currents, although forward-bias currents are also frequently considered during susceptibility studies. Another consideration is the observation that a transistor base-emitter junction is more vulnerable than the base-collector junction. In

the case of integrated circuits, damage is most likely to occur at the input port. Thus, in evaluating circuit susceptibility to damage, attention is usually focused on diodes, transister base-emitter junctions, and integrated input ports.

Using this criteria, a typical voltage regulator for a conventional generator, Figure 49 was analyzed. This schematic contains semiconductor devices which have been already discussed to be vulnerable to reverse-bias damage. With respect to the diodes and normal conduction, if a lightning transient propagates in the reverse direction, the peak inverse rating may be exceeded and the P-N junction will be destroyed.

In examination of a typical generator control unit (GCU) schematic, it is found there will be damage done to the GCU by coupled lightning transients in the kilo-volt range entering the voltage sensing input terminals. Several diodes will become reverse biased with respect to the lightning transient. The transient will have sufficient potential to destroy the P-N junction of the diodes by surpassing the peak inverse voltage rating. Electrolytic capacitors and transistors downstream may also be critically damaged. The application of Kilo-volt transients in this hand analysis was substantiated by the results of the computer analysis of the VSCF circuit. (See Table 13)

b. WIRING ROUTING

The primary reason for optimizing wire routing is to reduce the amount of electromagnetic flux coupled onto the conductors. Wiring should be located as close as possible to the ground plane or structural frame. Route exposed wiring (e.g., wires underneath a leading edge of a poorly conducting material) close to the metal struture (e.g., aluminum front spar). The amount of flux that is coupled to a wire is proportional with the distance separating the two conducting mediums. Wiring should be located away from apertures (e.g., windows) and regions where the radius of curvature of the airplane frame or outer skin is the smallest. In particular, do not route wiring across obvious slots (e.g., access doors). Magnetic fields are most concentrated at protruding structural framework points and tend to diverge inward producing a weaker field intensity in the corners. Inherent shielding is provided if the

LEGEND
A – Aφ PMG
B – Bφ PMG
C – Cφ PMG
D – Neutral
E – T1 POR voltage
F – T2 POR voltage
G – T3 POR voltage
H – Field +
I – Field –
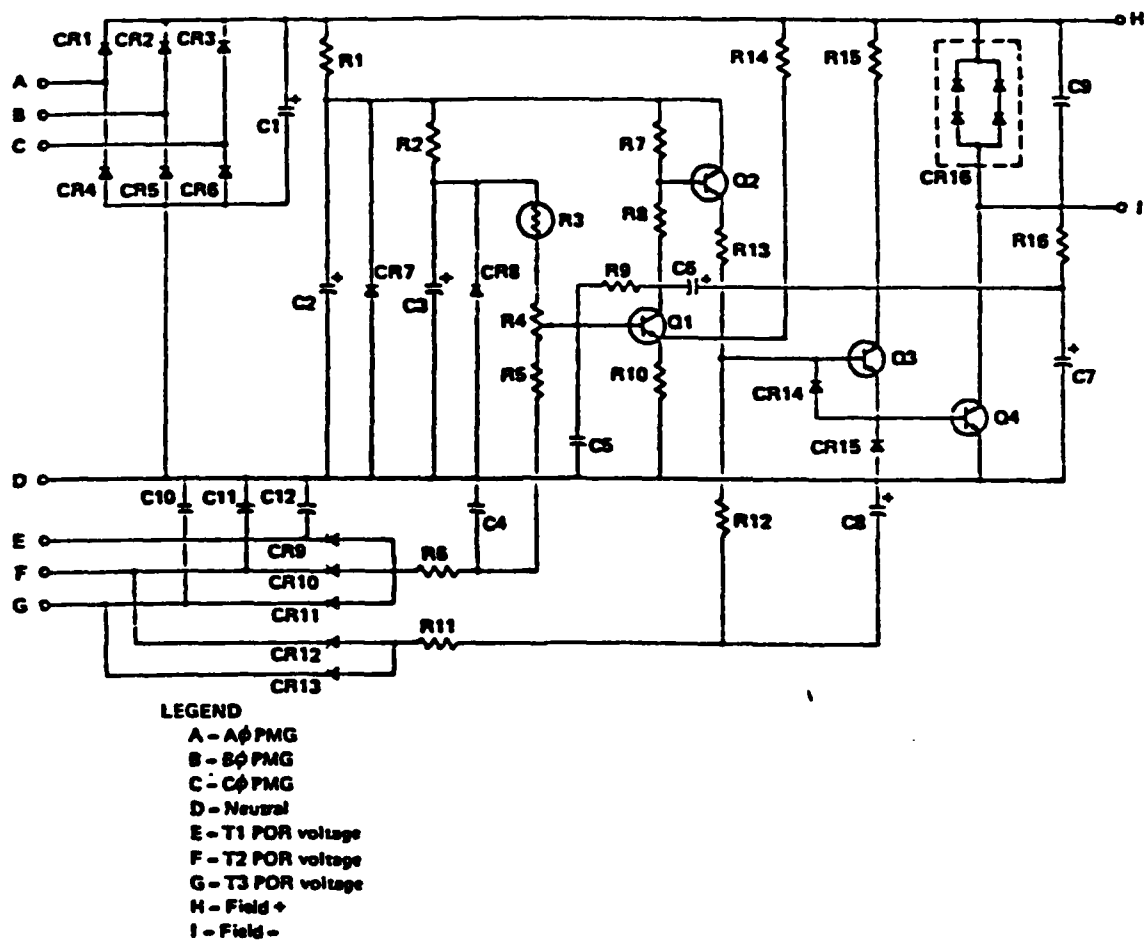
Figure 49 Typical Voltage Regulator for a Conventional Generator

122

cable can be routed in a channel, and better yet inside an enclosed channel. Avoid using stuctural return for exposed power wiring. Figure 50 shows the deviation in magnetic flux linkage due to metallic obstruction with respect to conductor position (Reference 6).

c. EQUIPMENT LOCATION

On the basis of the circuits analyzed under Task 1, the primary threat to equipment is the conducted threat delivered to the equipment by:

a. Exposed intercounecting wiring, or

b. Intercounecting wiring attached to an exposed element (e.g., windshield heater circuit).

The only potential threat which depends upon the fields in the vicinity of the equipment is E-field coupling. I.e., nearby electric fields may induce a voltage upon the wiring terminating in a poorly-grounded case. In order of priority then, the rules for equipment placement are:

1. Locate equipment to minimize exposure of interconnecting wiring.
2. Locate equipment in areas which are shielded from electric fields induced by lightning. Note that, if the case is well grounded to structure, the E-field coupling problem is minimized.

5. IMPACT OF CHANGING EQUIPMENT SPECIFICATIONS TO WITHSTAND LIGHTNING TRANSIENTS

At the present time, there are no power system requirements governing the suppression of lightning induced transients in the kilovolt range. For the case where the generator and frequency converter are located out on the wing kilovolt transients are superimposed on the power bus. If new specifications are imposed requiring the equipment to withstand the lightning induced transients presently observed, filtering or shielding of individual equipment would produce additional weight and cost problems in the overall airplane design. However, by increasing the transient suppression requirement in
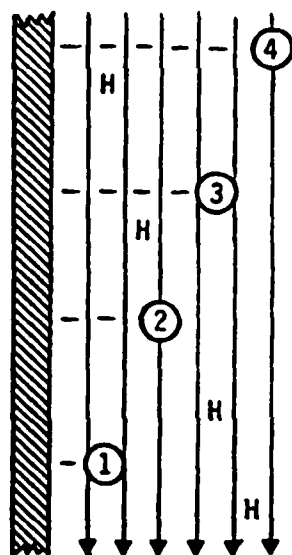
(a) Conductors over a plane   (b) Conductors near an angle
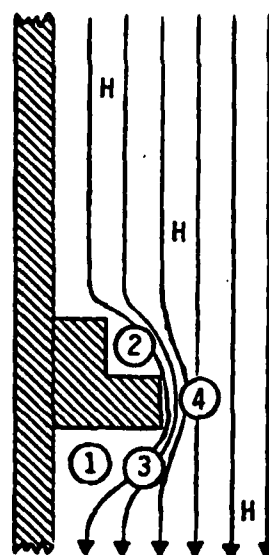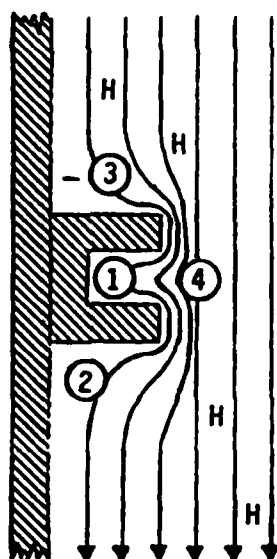
(c) Conductors near a channel   .(d) Conductors near a box
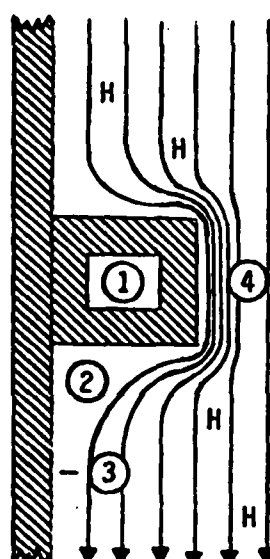
FIGURE 50 Magnetic Flux Linkage Versus Conductor Position

In each case pictured: Conductor 1 - lowest flux linkage: best
                           Conductor 2 - intermediate flux linkage: better
                           Conductor 3 - intermediate flux linkage: good
                           Conductor 4 - highest flux linkage: worst

124

individual equipment from the present military specification of 600 volts to 6000 volts, the loss in EM protection from the usage of graphite composite materials would be less critical. A more viable solution may be to either prevent the transient from being coupled on to the power feeders or to suppress the transient so it does not appear at the main power buses. Preventing the transient from appearing on the buses allows the use of equipment designed to the existing power quality standards. Methods to limit the lightning induced transients to levels below existing power quality standards are examined in Section IV for the various airplane types.

SECTION IV

ADD-ON PROTECTION FOR INDUCED TRANSIENTS

1. ANALYSIS OF ADD-ON PROTECTION

To the design engineer, whose job is to prevent, minimize, or eliminate the effect of lightning transients that may cause permanent equipment damage, this section of the report will be most beneficial. It is more productive to design electrical/electronic equipment to withstand transients on input and output leads prior to manufacturing than it is to retrofit and provide protection to an existing system. Trade-offs must be made between the cost of providing equipment capable of withstanding lightning transients and the cost of shielding equipment and interconnecting wiring. The designer should take advantage of the inherent shielding provided by the aircraft structure and avoid placing equipment and wiring in locations that will be exposed to the electromagnetic fields generated by lightning strikes.

a. WIRE SHIELDING

As was demonstrated in the analysis efforts of this contract, an unshielded conductor, exposed to the magnetic field of a lightning current traveling from the wingtip to fuselage will have high voltage transients induced onto the power feeders or adjacent signal wires. Shielding against magnetic fields requires the shield to be grounded at both ends in order to carry a circulating current that will cancel the magnetic fields which produce common mode voltages.

Of the different types of shields, the solid shield inherently provides better shielding than does a braided shield, while a spiral-wrapped shield is less effective than a braided shield.

Conduits may provide electromagnetic shielding, however they are used more for mechanical protection than for electrical protection of conductors. Conduits for mechanical protection are physically mounted in clamps that use rubber gaskets to prevent mechanical vibration and wear, and only if the conduit is

126

electrically connected to the framework of the airplane at both ends will it be able to carry current and provide shielding for the conductors within.

The typical low frequency shield because it is ordinarily grounded at only one point, is usually not adequate to provide shielding for the high frequency lightning transients. Both sets of requirements can be met by supplying two separate shields, one for each type of interference.

The method of grounding the shield can have a great impact, an order of magnitude or more, on its effectiveness in protecting against lightning generated transients. The best method is the circumferential or 360° connection to the back shell of the connector. The connector itself should have a low dc resistance with respect to its mating panel connector. For a good 360° connection between the shield connector and the mating panel, paint and other lacquers should be stripped down to metal.

Frequently, pigtails are used in grounding shields but are inferior to the circumferential ground. The pigtails force the transient current to become concentrated at the pigtail enhancing the magnetic coupling to the feeders or conductors inside. If pigtails are used, they should be kept as short as possible and terminate on the outside of the equipment case. Grounding of pigtails to the inside of the equipment case is less effective and should be avoided. Never terminate a shield to a signal ground bus.

(1) SHIELDING VSCF GENERATOR AND CONVERTER POWER FEEDERS

After examining the circuit described in Section III.1.a(1), (the baseline VSCF generator and converter located out on an all aluminum wing with 12 meters of excited feeder running behind a fiberglass leading edge toward the fuselage), and finding the coupled lightning transients at the power bus to exceed the acceptable voltage and current levels, the effect of shielding the feeders was examined. Two types of shielding were incorporated into the model. The first case included a braided shield with 6 inch pigtails at each end of the shield. The second case incorporated circumferential terminations at the ends of the braided shield. Section II.4.e describes the subroutine for the two cases. The only difference in the two models is the resistance

and inductance of the shield terminations. For comparison shown in Table 32, VSCF/1 PEAK TRANSIENTS WITH SHIELDING PROTECTION, are the severe transient levels recorded at the generator/converter output terminals and the 50% bus load input terminals for the baseline case, 12 MF, the pigtail shielding case, 12MPT, and the circumferential case, 12MCG. It should be noted that, compared to the unprotected case, two orders of magnitude transient suppression is obtained with the use of the circumferential grounded shield and one order of magnitude suppression is obtained with the pigtail grounded shield. For the circumferential case, the resultant voltage and current levels are acceptable. However, the bus/load voltage in the pigtail case is unacceptable.

b. TRANZORBS, VARISTORS, AND ZENER DIODES

All types of overvoltage devices inherently operate by reflecting a portion of the transient energy back toward the source and by conducting the rest into another branch. Until exposed to an over voltage condition, these devices will maintain the operating voltage of the system. Then, according to their nonlinear voltage--current relationships, these devices will short the overvoltage and conduct the excess current to ground. When the transient subsides, device conduction turns off, and the system returns to its normal operating state. Resetting circuit breakers is not required when the voltage returns to its normal valve.

A TransZorb^{TM} is a silicon PN junction device designed for suppression of high voltage transients associated with power disturbances, switching, and induced lightning effects. The TransZorb is characterized by a 1×10^{-12} second response time and a low series resistance.

A varistor is a two-electrode semiconductor device with a voltage-dependent nonlinear resistance that drops markedly as the applied voltage is increased. The metal oxide varistor is characterized by a 50 nanosecond response time.

Zener diodes are two-layer polarized devices that when foward biased respond as an ordinary rectifier diode. If a voltage applied in the reverse bias direction exceeds the device's breakdown voltage, the device reacts in an avalanche fashion with respect to its current-voltage characteristics.

128

TABLE **32** VSCF/1 PEAK TRANSIENTS WITH SHIELDING

Test Case	Test Point	Test Point Name	Transient Duration	Positive Amplitude	Negative Amplitude
12MF	T1	VCON	1. mS	27. V	-30. V
12MF	T1	ICON	1. mS	180. A	-120. A
12MF	T2	VLOAD	8. uS	65. KV	-40. KV
12MF	T2	ILOAD	.15 mS	289. A	0. A
12MPT	T1	VCON	1. mS	18.5 V	-21.5 V
12MPT	T1	ICON	1. mS	155. A	-80. A
12MPT	T2	VLOAD	.5 mS	5.4 KV	-3.3 V
12MPT	T2	ILOAD	1. mS	132. A	-34. A
12MCC	T1	VCON	1. mS	14.5 V	-17. V
12MCC	T1	ICON	1. mS	122.5 A	-65. A
12MCC	T2	VLOAD	.4 mS	295. V	-30. V
12MCC	T2	ILOAD	1. mS	104. A	-26. A

TABLE **34** VSCF/1 PEAK TRANSIENTS WITH TRANSZORBS PROTECTION

TEST CASE	TEST POINT/ NAME	TRANSIENT DURATION	POSITIVE AMPLITUDE	NEGATIVE AMPLITUDE	DC OFFSET
12MF	T1/VCON	1.0 ms	27.0 V	-30.0 V	+0.5 V
12MF	T1/ICON	1.0 ms	180.0 A	-120.0 A	+4.0 A
12MF	T2/VLOAD	8.0 us	65.0 KV	-40.0 KV	0.0 V
12MF	T2/ILOAD	0.15 ms	289.0 A	0.0 A	0.0 A
12MFT	T1/VCON	0.5 ms	105.0 V	-145.0 V	-10.0 V
12MFT	T1/ICON	0.5 ms	660.0 A	-360.0 A	+40.0 A
12MFT	T2/VLOAD	0.5 ms	285.0 V	-50.0 V	+25.0 V
12MFT	T2/ILOAD	0.6 ms	82.0 A	-18.0 A	+10.0 A

TABLE   VSCF/1 PEAK TRANSIENTS 3 MIL FOIL FIBERGLASS LEADING EDGE

TEST CASE	TEST POINT/ NAME	TRANSIENT DURATION	POSITIVE AMPLITUDE	NEGATIVE AMPLITUDE	DC OFFSET
12M3MF	T1/VCON	1.0 mSec	0.6 V	-1.3 V	0.0
12M3MF	T1/ICON	1.0 mSec	12.0 A	-2.0 A	0.0
12M3MF	T2/VLOAD	1.0 mSec	11.2 V	-1.0 V	+2.4
12M3MF	T2/ILOAD	1.0 mSec	8.5 A	-2.0 A	0.0

Table 33, COMPARISON OF PROTECTION DEVICES, lists some of the advantages and disadvantages of the above mentioned devices and others.

(1) HAND CALCULATION DESIGN OF LIGHTNING PROTECTION USING TRANSZORBS

The following steps give the designer hand calculations for estimating the number of TransZorbs required to protect a three phase load. A TransZorb is normally selected according to the reverse "Stand Off Voltage" (V_r) which should be equal to or greater than the DC or continuous peak operating voltage level.

STEP (1) Approximate the short-circuit current at the protection point as an exponential having peak value I_T and half-value falltime of t_d.

To protect the circuit from both positive and negative transient spikes, two TransZorbs must be placed back to back in series, as is shown in Figure 51. Each forward biased series element contributes negligibly to the total voltage and dissipates very little power.

STEP (2) Choose the maximum allowable voltage transient acceptable in the system or the reverse biased device voltage, V_d. In order to determine the number of devices, n, required to meet the power specification, refer to the manufacturers data sheet for the necessary electrical parameters to satisfy equation (3).

$$n = \frac{I_T \, (V_c - Vb)}{I_{pp} \, (V_d - Vb)} \qquad (3)$$

In selecting a number of devices, n, and satisfying the data sheet parameters in equation (4), the resultant reverse biased device voltage, V_d, can be computed.

$$V_d = Vb + \left(\frac{I_T}{n}\right) \; \left(\frac{V_c - Vb}{I_{pp}}\right) \qquad (4)$$

130

TABLE **33** , COMPARISON OF PROTECTION DEVICES

DEVICE	ADVANTAGES	DISADVANTAGES
Transzorb	1. Large surface area for good energy handling capability (compared with Zener diode) 2. Restores to initial state, no follow on power 3. Tight voltage control 4. Fast response 5. Small size, easily mounted	1. May fail under normal operation if line voltage frequently exceeds rated voltage 2. Requires recovery time after firing 3. Limited power-handling capability 4. Low energy absorbing capability 5. Large capacitance
Metal Oxide Varistor	1. Restores to initial state, no follow on power 2. Energy absorbed through out device volume 3. Fast response/low impulse ratio 4. Small size, easily mounted 5. Self extinguishing 6. High ratio of energy absorbed to energy reflected	1. Low impedance and high capacitance 2. Low energy absorbing 3. Limited power handling capability 4. Operating voltage proportional to material thickness 5. Requires recovery time after firing
Zener Diode	1. Restores to initial state no follow on power, self-extinguishing 2. Low firing voltage and tight voltage control 3. Low dynamic impedance when conducting, low capacitance 4. Absorbs energy in the device 5. Fast Response 6. Small size, easily mounted	1. Are not bilateral 2. High junction capacitance 3. Low energy absorbing capability 4. Limited power handling capability 5. Absorbs energy in junction surface 6. May fail under normal operation if line voltage frequently exceeds rated voltage 7. Requires recovery time
Spark Gap	1. High current, large power handling capability 2. High impedance, low capacitance 3. Bilateral operation 4. No recovery time required 5. Simple and reliable	1. High turn on voltage 2. Does not extinguish follow current, may draw follow on power after turn on 3. Absorbs little power
Gas Discharge Tube	1. Low capacitance 2. Absorbs energy 1: the device 3. High current and power capability 4. Fails short to indicate need to replacement	1. Slow response time 2. Variable breakdown voltage 3. May age with leakage of gas 4. May draw follow on power after turn on

131
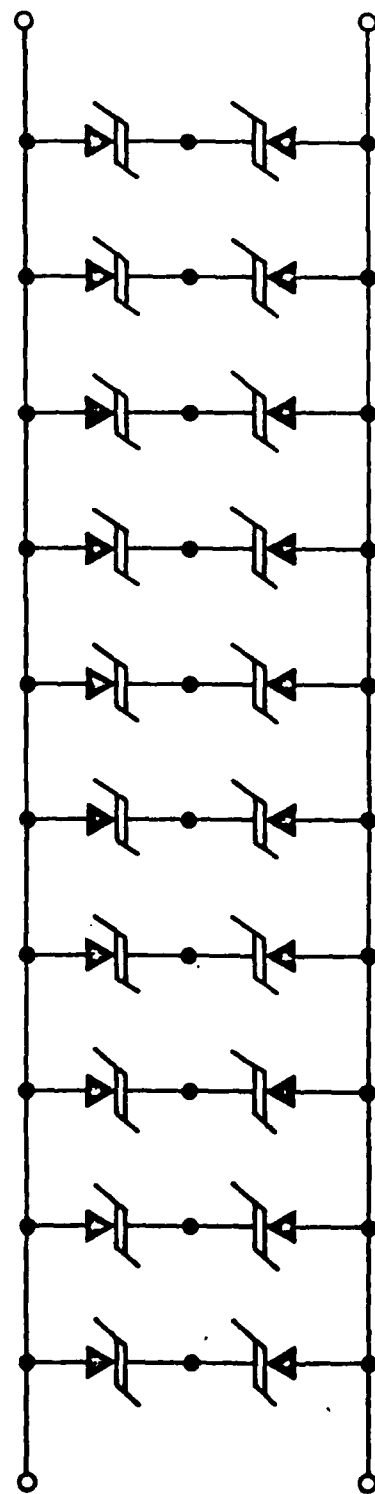
20 DEVICES, DEVICE TYPE 15KP280A

FIGURE 51 TRANSZORB SUPPRESSOR ASSEMBLY USED ON EACH OF THREE PHASES

V_d = reverse biased device voltage

V_c = maximum clamping voltage @ Ipp (1m Sec)

I_{pp} = maximum peak pulse current

Vb = breakdown voltage

I_T = approximate short circuit current

n = number of TransZorbs

STEP (3) Compute the current, Id, and power, Pd, for each device per equations (5) and (6) respectively. Calculate the safety margin, SM, as is shown in equation (7). P_p, the peak pulse power is obtained from the peak pulse power versus pulse time, t_d, wave form shown on Figure 52. If the device current, power, or safety margin values are unsatisfactory, iterate on the device type or device number for the particular application.

$$I_d = \frac{I_T}{n} \tag{5}$$

$$P_d = V_d I_d \tag{6}$$

$$SM = 10 \log_{10} \left(\frac{P_p}{P_d}\right) \tag{7}$$

(2) COMPUTER AIDED DESIGN OF LIGHTNING PROTECTION USING TRANSZORBS

STEP (1) From the computer short-circuit current and open-circuit voltage at the protection point, synthesize a Norton equivalent circuit.

STEP (2) Use the 2-terminal damage model to simulate the TransZorb protective array. Connect this model to the Norton equivalent circuit, along with models for other system loads at this point.

STEP (3) Using CIRCUS-2, run the overall model. Plot the desired waveforms, including V_{cl}. The safety margin is given by equation (8).

$$SM = 10 \log_{10} \frac{1}{V_{cl} \text{ (peak)}} \tag{8}$$

133

GENERAL SEMICONDUCTOR INDUSTRIES, INC.

TRANSZORB
TRANSIENT VOLTAGE
SUPPRESSORS
15KP17
THRU
15KP280A

1
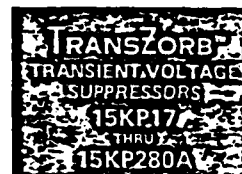
DESCRIPTION

. . . a series of high power, medium voltage TransZorbs, Transient Voltage Suppressors, designed for the protection of Precision Industrial Electronic Equipment. These devices are rated for a peak pulse power of 15,000 watts for 1 millisecond.

TransZorbs have been evaluated for susceptibility to neutron and gamma radiation. Neutron flux irradiation of 1.4×10^{13} neutrons/cm and cumulative gamma dosage of 2×10^7 rad(Si) have been applied to the TransZorb without causing appreciable parameter changes.

TransZorbs are Silicon PN Junction devices designed for absorbtion of high voltage transients associated with power disturbances, switching, and induced lightning effects. This series is available from 17 volts through 280 volts. Special voltages are available from the factory.

- Designed for 15,000 watts
- Easy mounting to printed circuit board
- Available in ranges from 17 to 280 volts

Case 24
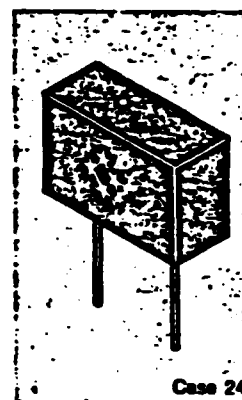
MAXIMUM RATINGS

- 15,000 watts of Peak Pulse Power dissipation at 25°C
- $t_{clamping}$ (0 volts to BV min): Less than 1×10^{-12}
- Operating and Storage temperature: −55°C to +150°C
- Steady State power dissipation: 7.0 watts @ T_A = 25°C
- Repetition rate (duty cycle): .05%

MECHANICAL CHARACTERISTICS

- Molded (Plastic) Case
- Weight: 13 grams (approximate)
- Positive Terminal marked with dot
- Body marked with Logo ✧ and type number

Pulse Wave Form........................ Figure 2, Page 1-3
Power-Temperature Derating Curve........ Figure 3, Page 1-3
Capacitor Discharge Test Circuit.......... Figure 4, Page 1-4
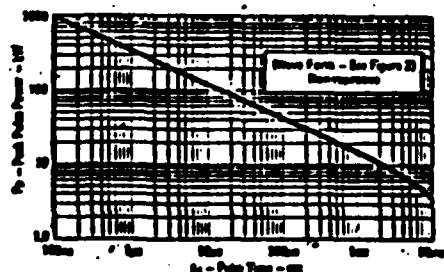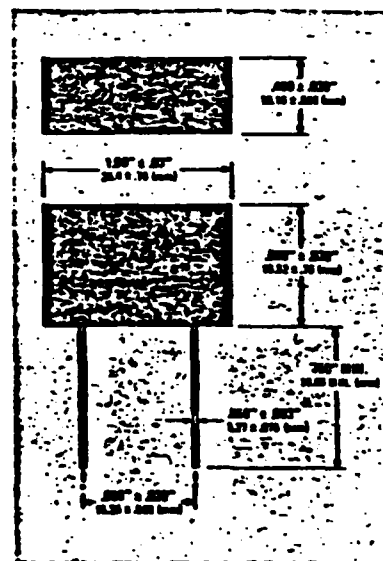
Peak Pulse Power vs Pulse Time

FIGURE 52   TRANSZORB DATA SHEET
- 134

1-10

STEP (4) If the TransZorb array voltage response is low enough and the safety margin is high enough, the design is adequate. If SM is much larger than that calculated by hand, it may be possible to use fewer or lower-power devices to provide the required protection.

c. VSCF GENERATOR/CONVERTER POWER FEEDERS WITH TRANZORBS

Transzorbs were examined as an alternative to shielding for add on protection in the VSCF generator/converter system described in Section III.1.a(1) and shown in Figures 23 to 25. The philosophy incorporated within the model development, applied add on protection to suppress the transient before the transient became superimposed on the power bus. The type of Transzorb used was a series of high power medium voltage transient voltage suppressors. These devices are rated for a peak pulse power of 15,000 watts for 1 millisecond. Table 34, VSCF/1 PEAK TRANSIENTS WITH TRANSZORB PROTECTION, compares the results of the unprotected case with the Transzorb protection case. The design procedure for examining this and similar protective devices is described in Section IV.1.c(1).

(1) COMPUTER AIDED DESIGN EXAMPLE: VSCF GEN/CONV WING AC BUS FUSELAGE

STEP (1) System waveform approximations; see Figure 53 through 56.

<u>Open-circuit voltage</u>

$$v(t) = Ae^{-\alpha t}\sin 2\pi ft \ u(t)$$

$$f \approx \frac{5 \text{ cycles}}{1.85 \times 10^{-6} \text{ sec}} = 2.7 \text{ MHz}$$

$$n = \# \text{ cycles to } \frac{1}{e} \text{ point} \approx 9.5 \text{ cycles}$$

$$\alpha = \frac{f}{n} = \frac{2.7 \times 10^6}{9.5} = 2.84 \times 10^5$$

$$A = 80 \text{ kV}$$
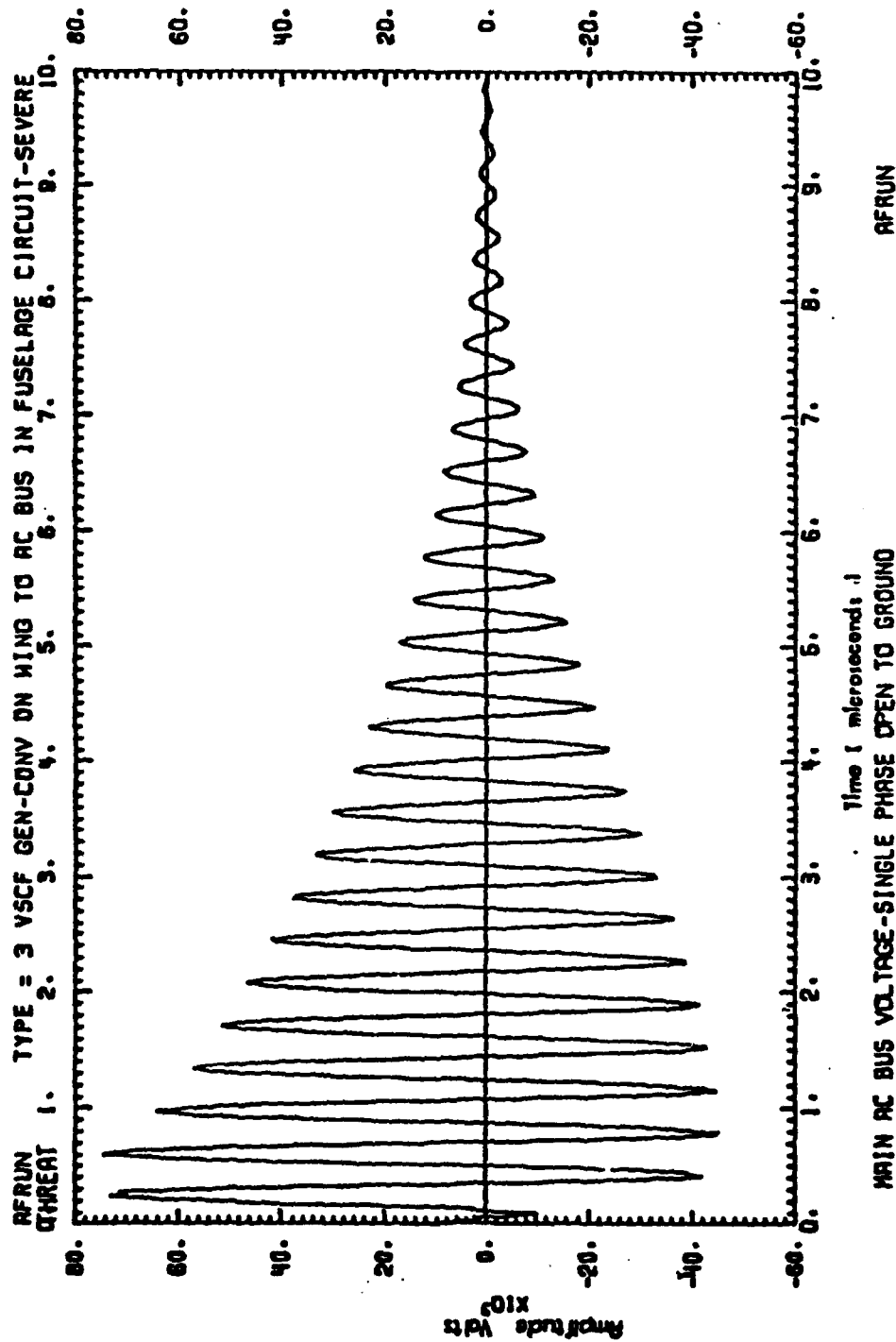
MAIN AC BUS VOLTAGE-SINGLE PHASE OPEN TO GROUND
BUS OPEN CIRCUIT

FIGURE 53   OPEN CIRCUIT VOLTAGE

136

FIGURE 54   SHORT CIRCUIT CURRENT, TIME SCALE #1

137
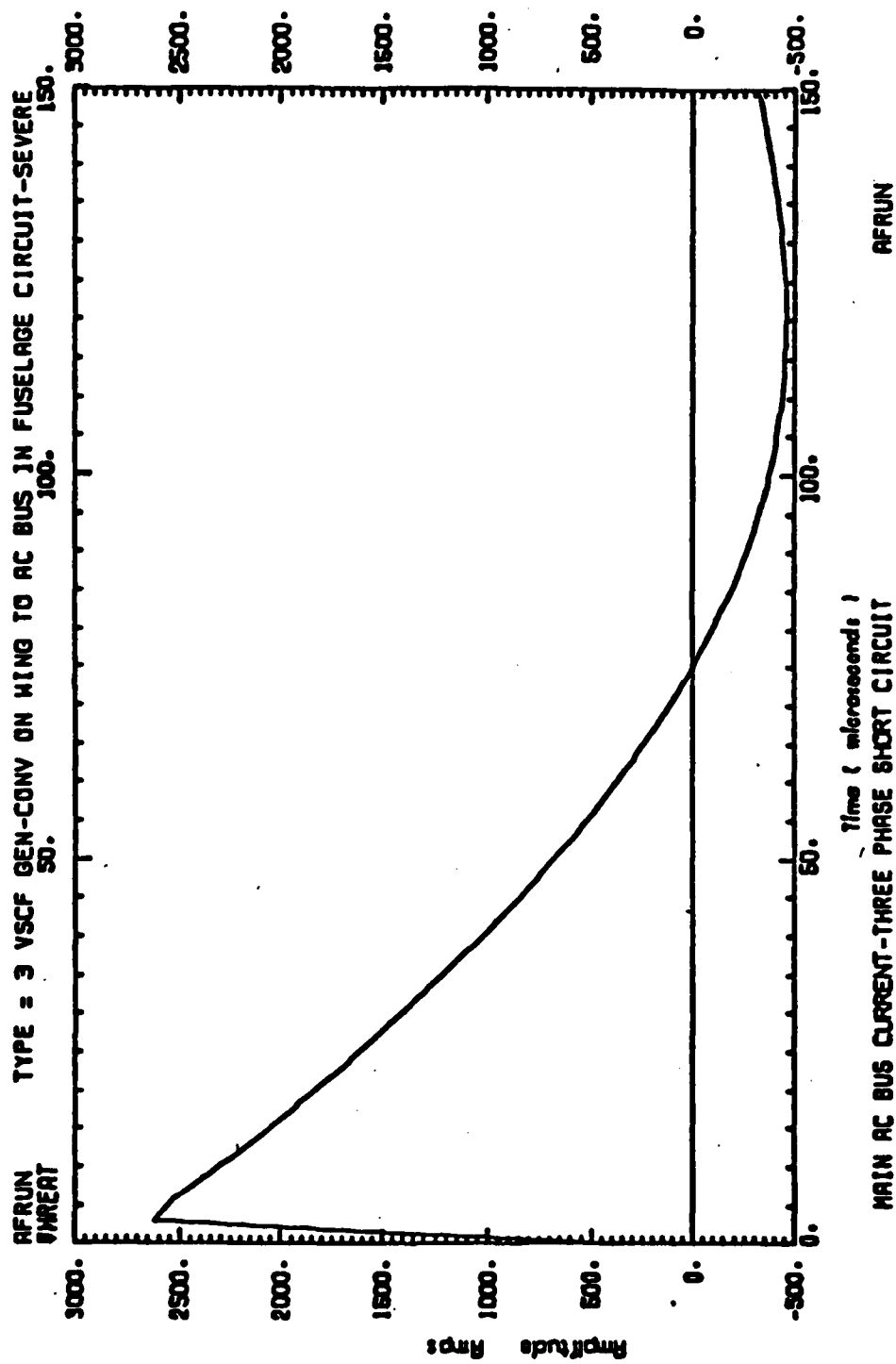
FIGURE 55 SHORT CIRCUIT CURRENT, TIME SCALE #2

138
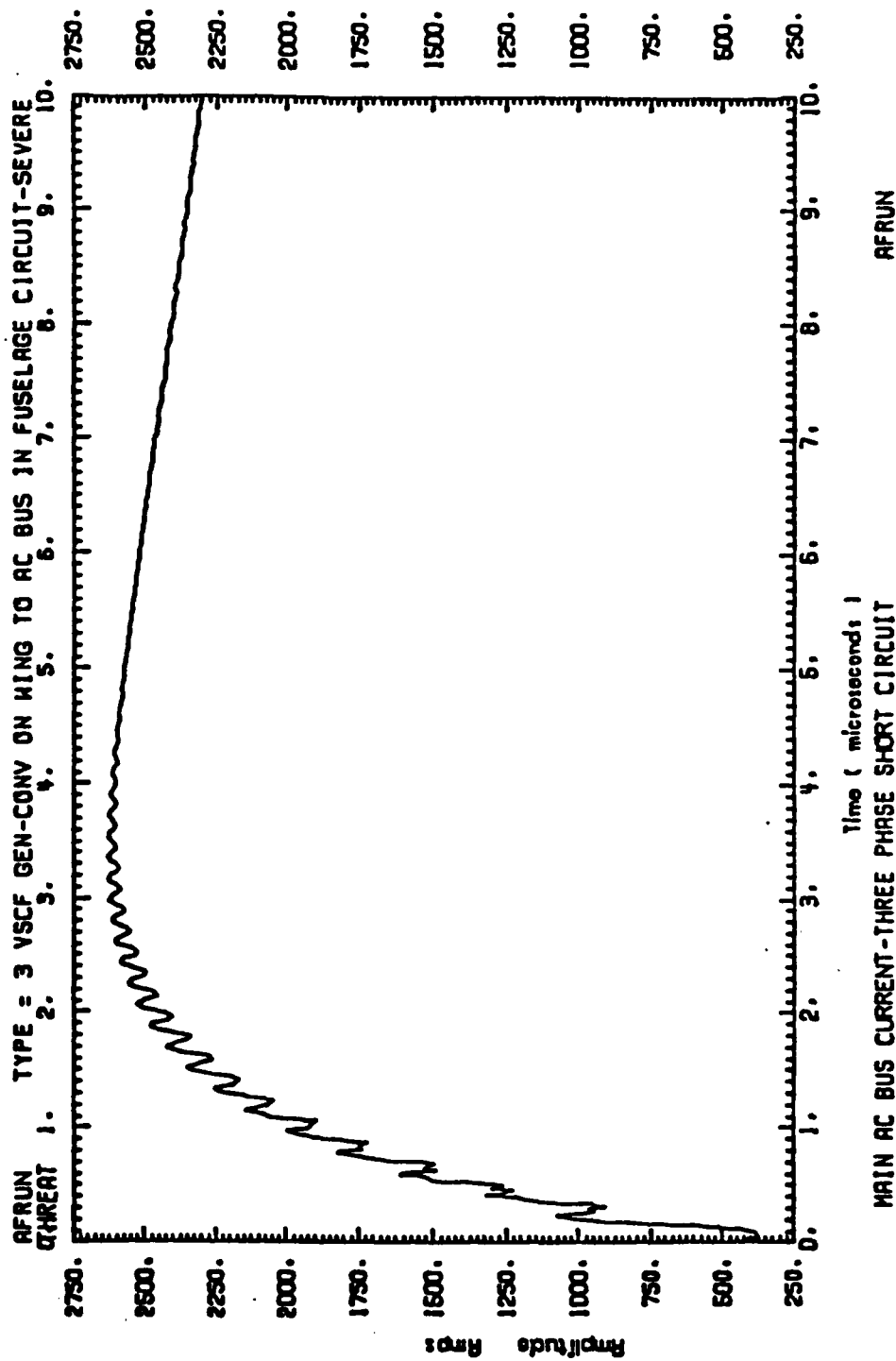
MAIN AC BUS CURRENT-THREE PHASE SHORT CIRCUIT   FIGURE 56   SHORT CIRCUIT CURRENT, TIME SCALE #3

139

Short-circuit current

$$i(t) = I_T \, e^{-t/T} \, u(t)$$

$$I_T \quad = 2600 \text{ amperes}$$

$$T \quad = 37 \text{ microseconds}$$

STEP (2) Choose device and configuration.

The device used here was the 15KP280A discussed in data sheets shown in Figure 52 and Table 35. The suppressor array consisted of ten sets of back-to-back devices, as illustrated in Figure 51, protecting each of the three phases at the power bus. Using the equations defined in Section IV.1.b(1), the following computations are made.

$$P_p = 60 \text{ kW}$$

$$V_d = 330 + \left(\frac{2600}{30}\right) \left(\frac{452-330}{33}\right) \qquad = 650 \text{ volts}$$

$$I_d = \frac{2600}{30} = 86.7 \text{ amperes}$$

$$P_d = (650)(86.7) = 56.4 \text{ kW}$$

$$SM = 10 \log_{10} \left(\frac{60}{56.4}\right) = 0.3 \text{ dB}$$

STEP (3) Norton equivalent circuit.

The Norton equivalent circuit should have the parallel RLC form illustrated in Figure 57. Values for L and C are determined by the equations shown. The value for R is found by running the Norton circuit and adjusting (L and C must follow) to obtain the correct peak voltage.

TABLE 35   TRANSZORB DATA SHEET

ELECTRICAL CHARACTERISTICS @ 25°C

| GENERAL SEMICONDUCTOR PART NUMBER	REVERSE STAND-OFF VOLTAGE (Note 1) V_R VOLTS	BREAKDOWN VOLTAGE BV VOLTS	@ I_T mA	MAXIMUM CLAMPING VOLTAGE @ I_{PP} (1 mSEC) V_C VOLTS	MAXIMUM REVERSE LEAKAGE @ V_R I_R μA	MAXIMUM PEAK PULSE CURRENT (Fig. 2) I_{PP} A	MAXIMUM VOLTAGE TEMPERATURE VARIATION OF BV mV/°C
15KP17	17	18.9 - 23.1	50	32.3	5000	464	19
15KP17A	17	18.9 - 20.9	50	29.3	5000	512	17
15KP18	18	20.0 - 24.4	50	34.2	5000	439	20
15KP18A	18	20.0 - 22.1	50	30.9	5000	485	18
15KP20	20	22.2 - 37.1	20	37.9	1500	396	24
15KP20A	20	22.2 - 24.5	20	34.3	1500	437	21
15KP22	22	24.4 - 29.8	10	41.1	500	365	27
15KP22A	22	24.4 - 26.9	10	37.1	500	404	24
15KP24	24	26.7 - 32.6	5	45.0	150	333	30
15KP24A	24	26.7 - 29.5	5	40.7	150	369	27
15KP26	26	28.9 - 35.3	5	48.7	50	308	32
15KP26A	26	28.9 - 31.9	5	44.0	50	341	29
15KP28	28	31.1 - 38.0	5	52.4	25	286	35
15KP28A	28	31.1 - 34.4	5	47.5	25	316	31
15KP30	30	33.3 - 40.7	5	56.2	15	267	27
15KP30A	30	33.3 - 36.9	5	50.7	15	296	34
15KP33	33	36.7 - 44.9	5	60.6	10	248	42
15KP33A	33	36.7 - 40.6	5	54.5	10	274	38
15KP36	36	40.0 - 48.9	5	66.0	10	227	46
15KP36A	36	40.0 - 44.2	5	59.7	10	251	41
15KP40	40	44.4 - 54.3	5	72.5	10	206	51
15KP40A	40	44.4 - 49.1	5	65.5	10	228	46
15KP43	43	47.8 - 58.4	5	77.1	10	195	55
15KP43A	43	47.8 - 52.8	5	69.7	10	215	50
15KP45	45	50.0 - 61.1	5	80.7	10	186	57
15KP45A	45	50.0 - 55.3	5	73.0	10	205	52
15KP48	48	53.3 - 65.1	5	85.9	10	175	62
15KP48A	48	53.3 - 58.9	5	77.7	10	183	56
15KP51	51	56.7 - 69.3	5	91.5	10	164	66
15KP51A	51	56.7 - 62.7	5	82.9	10	181	60
15KP54	54	60.0 - 73.3	5	96.5	10	155	70
15KP54A	54	60.0 - 66.3	5	87.5	10	171	63
15KP58	58	64.4 - 78.7	5	104.0	10	144	76
15KP58A	58	64.4 - 71.2	5	94.0	10	160	68
15KP60	60	66.7 - 81.5	5	107.0	10	140	78
15KP60A	60	66.7 - 73.7	5	97.3	10	154	71
15KP64	64	71.1 - 86.9	5	115	10	130	84
15KP64A	64	71.1 - 78.6	5	104	10	144	76
15KP70	70	77.8 - 95.1	5	126	10	119	92
15KP70A	70	77.8 - 86.0	5	114	10	132	83
15KP75	75	83.3 - 102.0	5	135	10	111	100
15KP75A	75	83.3 - 92.1	5	122	10	123	89
15KP78	78	86.7 - 106.0	5	140	10	107	104
15KP78A	78	86.7 - 95.8	5	126	10	119	93
15KP85	85	94.4 - 115	5	152	10	99	113
15KP85A	85	94.4 - 104	5	137	10	109	102
15KP90	90	100.0 - 122	5	160	10	94	120
15KP90A	90	100.0 - 111	5	146	10	103	109
15KP100	100	111 - 136	5	179	10	84	134
15KP100A	100	111 - 123	5	162	10	83	121
15KP110	110	122 - 149	5	196	10	77	147
15KP110A	110	122 - 135	5	178	10	84	133
15KP120	120	133 - 163	5	214	10	70	161
15KP120A	120	133 - 147	5	193	10	78	145
15KP130	130	144 - 176	5	231	10	65	174
15KP130A	130	144 - 159	5	209	10	72	157
15KP150	150	167 - 204	5	268	10	56	202
15KP150A	150	167 - 185	5	243	10	62	183
15KP160	160	178 - 218	5	287	10	52	216
15KP160A	160	178 - 197	5	258	10	58	195
15KP170	170	189 - 231	5	304	10	49	229
15KP170A	170	189 - 209	5	275	10	55	207
15KP180	180	200 - 244	5	321	10	47	242
15KP180A	180	200 - 221	5	291	10	52	219
15KP200	200	222 - 271	5	356	10	42	269
15KP200A	200	222 - 245	5	322	10	47	243
15KP220	220	245 - 299	5	393	10	38	297
15KP220A	220	245 - 271	5	356	10	42	269
15KP240	240	267 - 326	5	428	10	35	324
15KP240A	240	267 - 295	5	388	10	39	293
15KP250	250	278 - 340	5	464	10	32	352
15KP250A	250	278 - 319	5	419	10	36	317
15KP280	280	311 - 380	5	500	10	30	378
15KP280A	280	311 - 344	5	452	10	33	342

V_F at 100 amps peak, 8.3 msec sine wave equals 3.5 volts maximum

Note 1: A TransZorb is normally selected according to the reverse "Stand Off Voltage" (V_R) which should be equal to or greater than the DC or continuous peak operating voltage level.

1-20

141
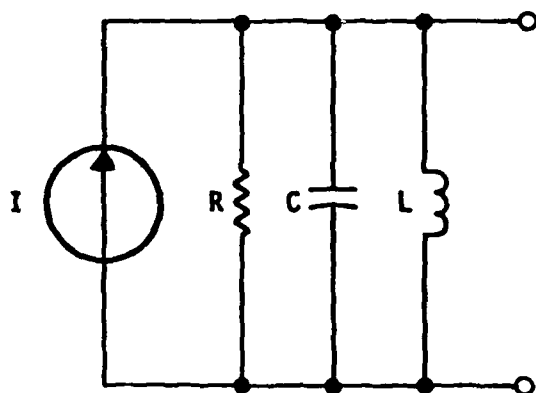
$$f = \frac{1}{2\pi\sqrt{LC}}$$

$$\alpha = \frac{1}{2RC}$$

$$\approx \frac{f}{\#\ \text{CYCLES TO}\ \frac{1}{e}\ \text{POINT}}$$

R=8.0 KΩ
C=0.22 nF
L=16.0 µH

FIGURE 57 NORTON EQUIVALENT CIRCUIT

The CIRCUS-2 short-circuit current and computed open-circuit voltage for this example are shown in Figures 58 and 59, respectively.

STEP (4) Computer analysis results.

A 2-terminal damage model representing the suppressor assembly was connected to the Norton equivalent circuit described above. Plots of the resulting computed suppressor voltage and V_{C1} (representing normalized temperature rise) are shown in Figures 60 and 61.

We get:

$$V_d \quad 633 \text{ volts}$$

$$SM = 10 \, \log_{10}\left(\frac{1}{0.42}\right) \quad = 3.8 \text{ dB}$$

d. FILTERS

In using filters for lightning transient suppression, we must view the protective device behavior in terms of its ability to "reflect" incident transient energy "waves" away from the protected equipment. This concept is illustrated in Figure 62.

An "ideal" protective device would divide the transient voltage and totally reflect the incident energy wave, allowing none of it to reach the protected equipment. At the same time it should not affect normal operational signals. Real-world suppressors do allow transient energy to reach the protected equipment, and do have some effect on normal operational signals. In many cases the normal/transient performance requirements are actually conflicting. It is then the job of the system designer to choose devices providing a realistic compromise in normal/transient performance.

Incident transient waves can be reflected by either very low impedance (negative reflection coefficient) or very high impedance (positive reflection coefficient) terminations. In power systems low transient impedances are
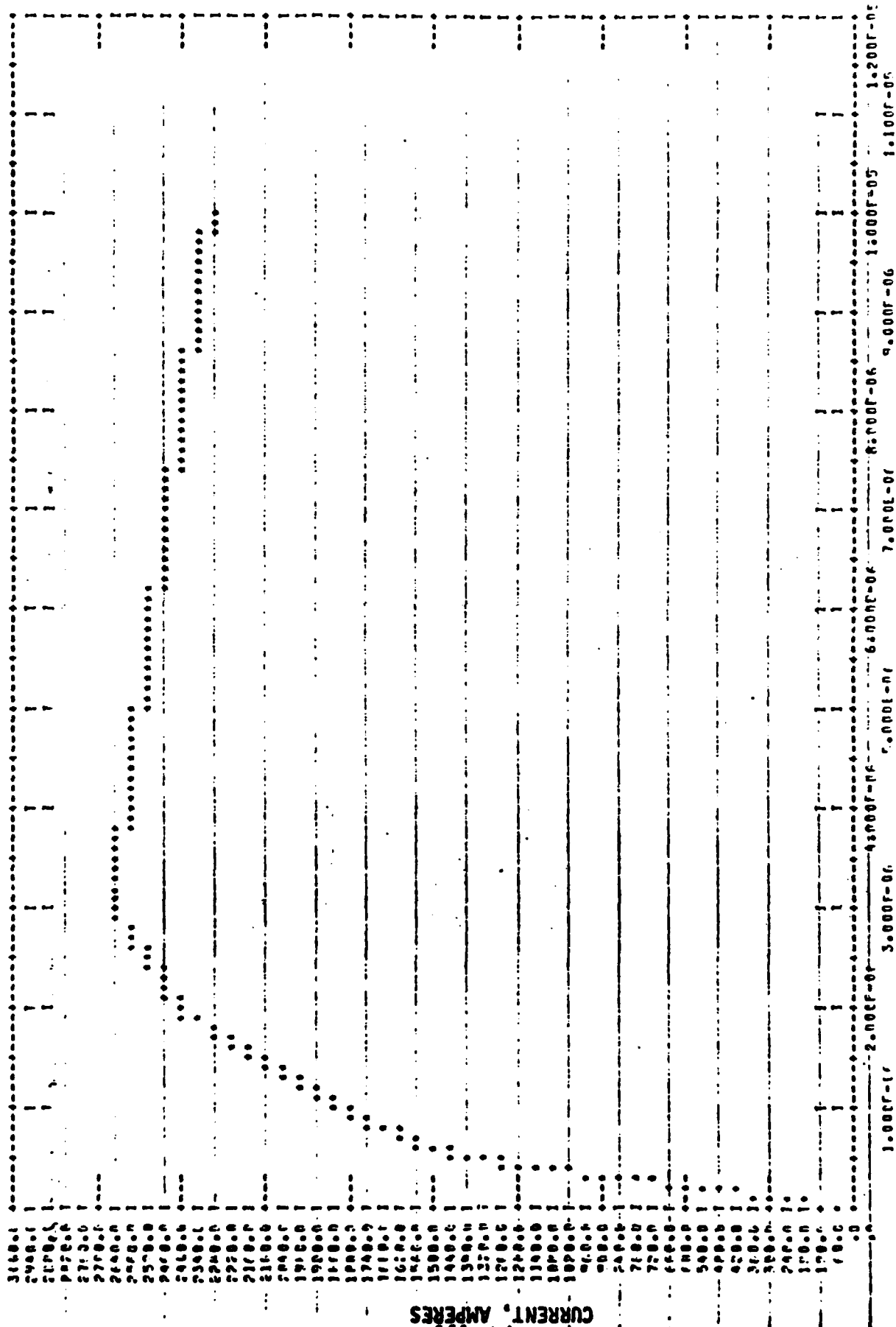
TIME, SECONDS

Figure 58 Short Circuit Current, Tabular Function Used in Circus-2 Runs

CURRENT, AMPERES

MAY 16, 1980
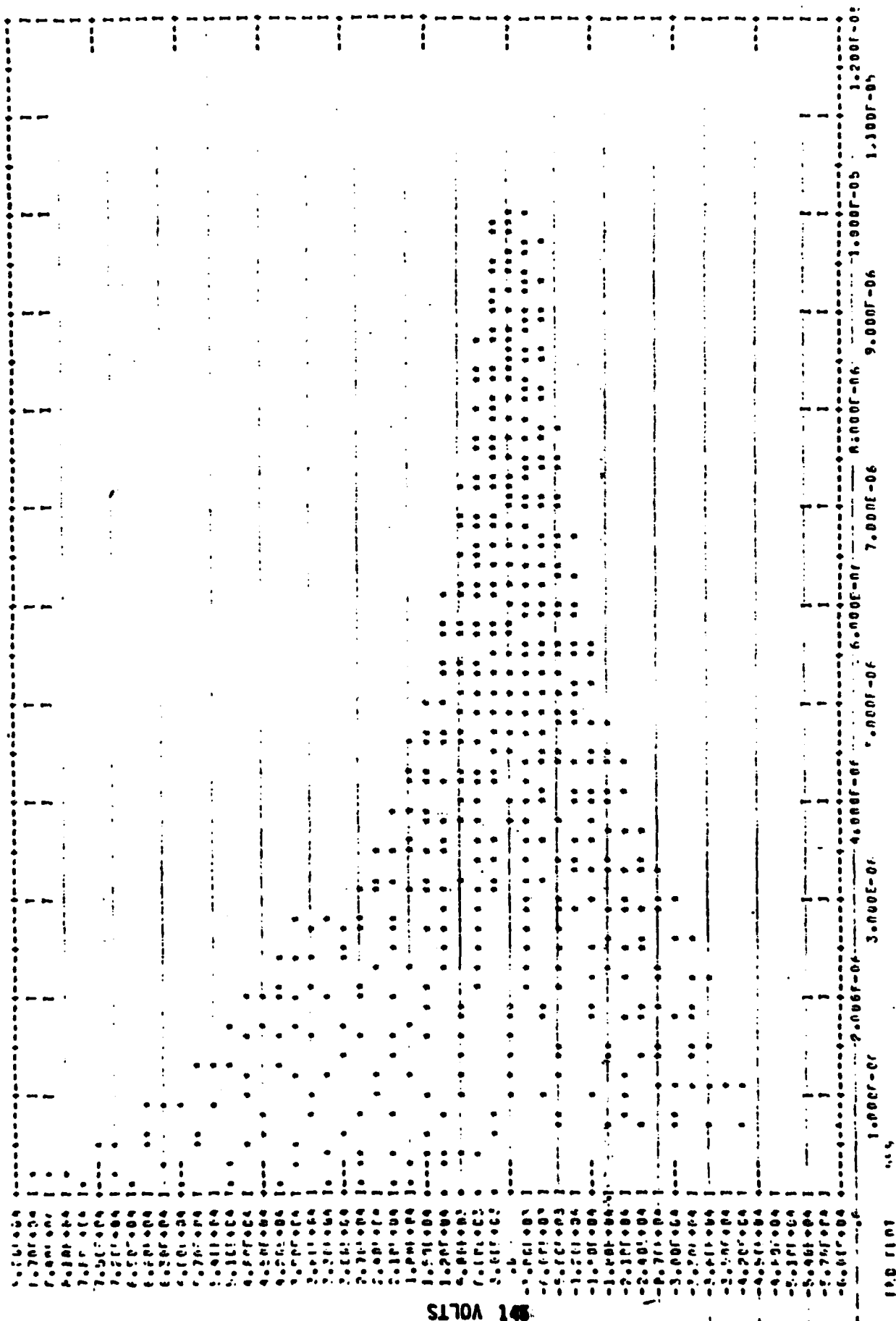
TIME, SECONDS

Figure 59 Computed Open Circuit Voltage For Norton Equivalent Circuit

TIME, SECONDS
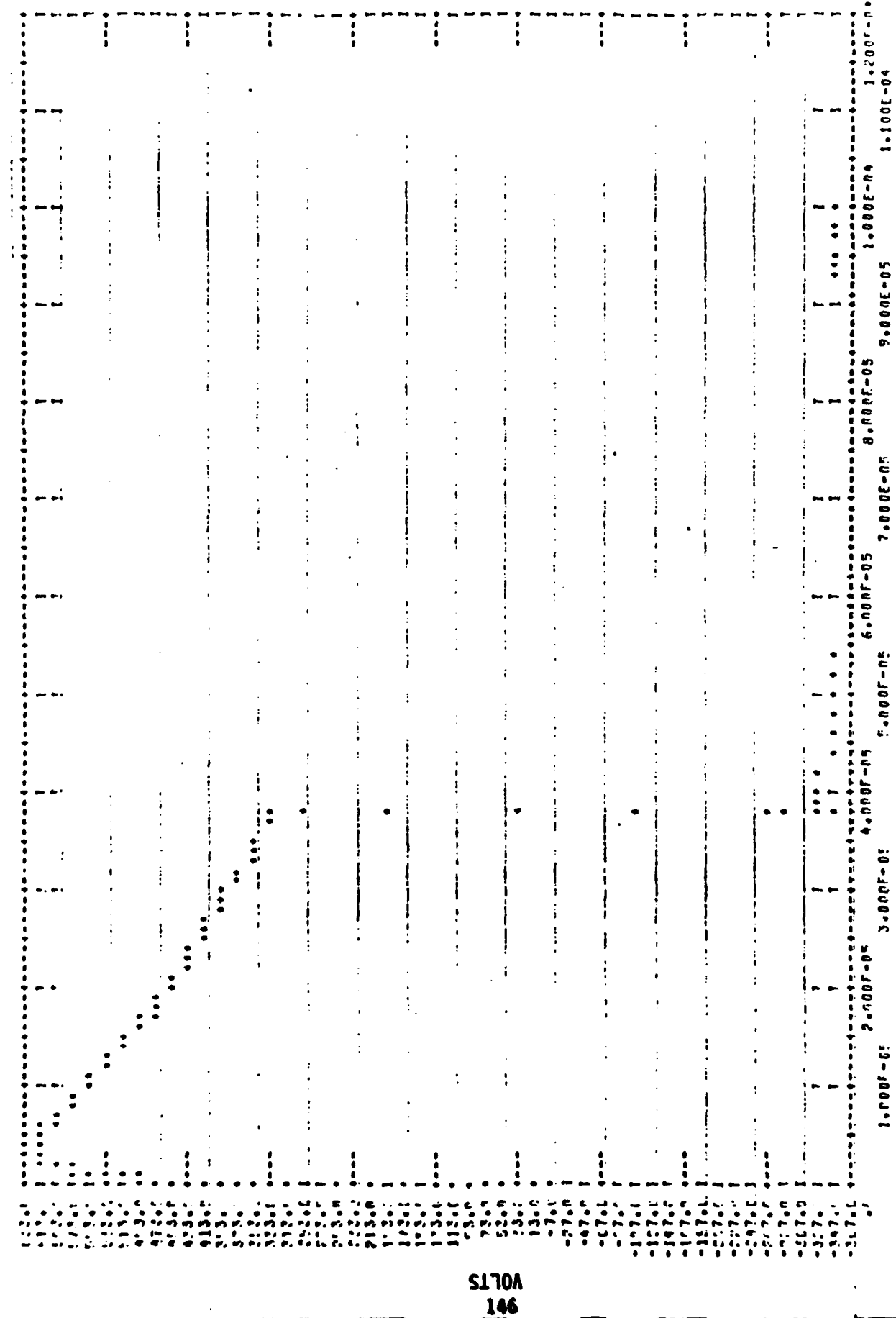
Figure 60 Computed Suppressor Assembly Voltage

VOLTS
146
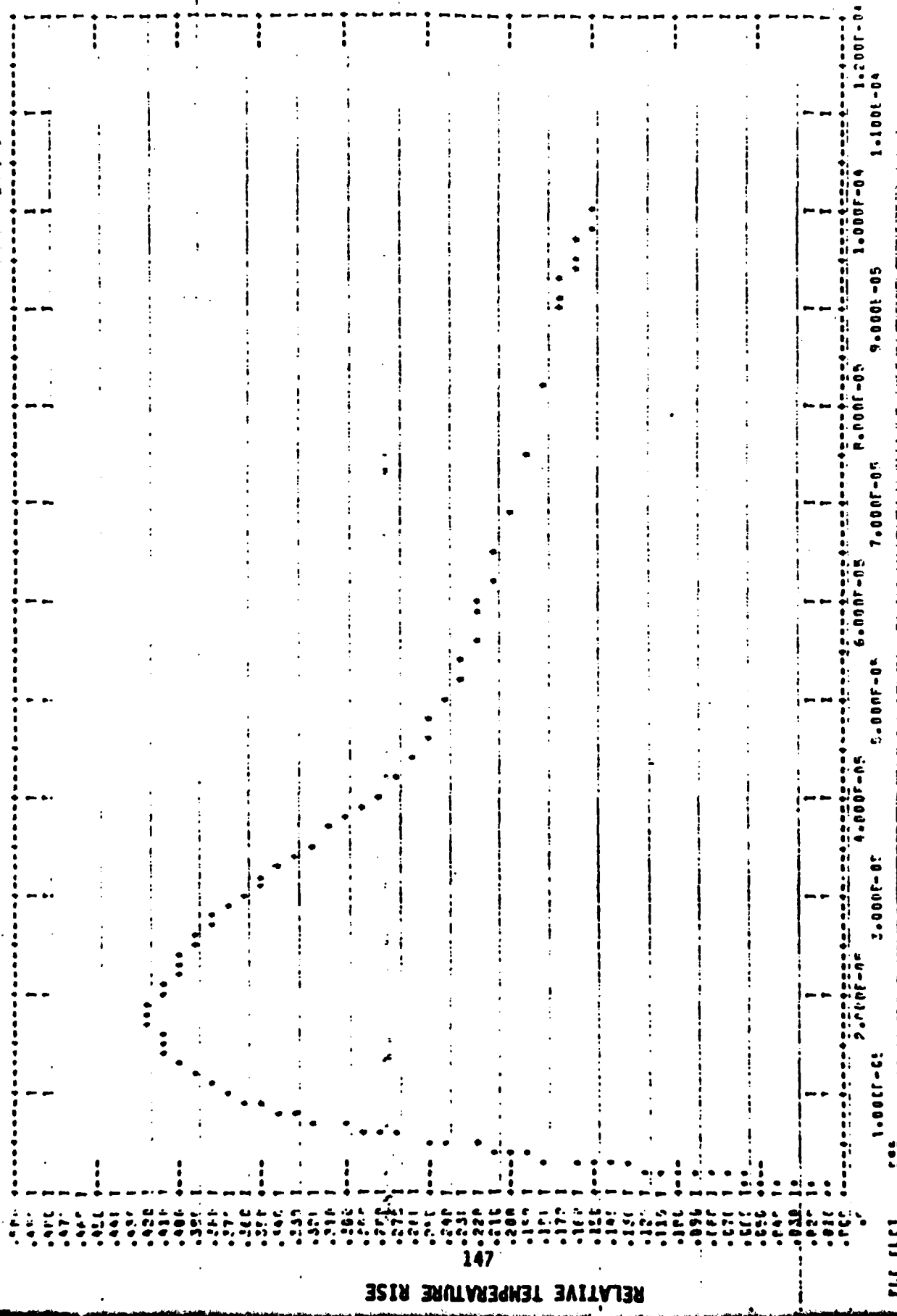
Figure 67 Computed Normalized Temperature Rise In Suppressor Assembly

TIME, SECONDS

RELATIVE TEMPERATURE RISE

147
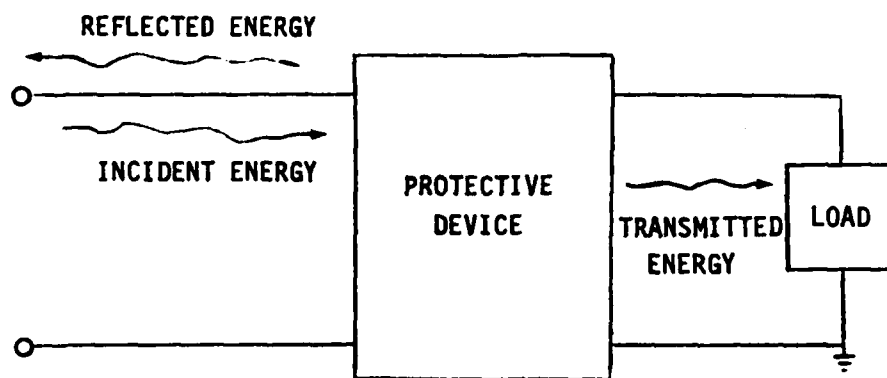
FIGURE 62   Reflective Protection Device Concept
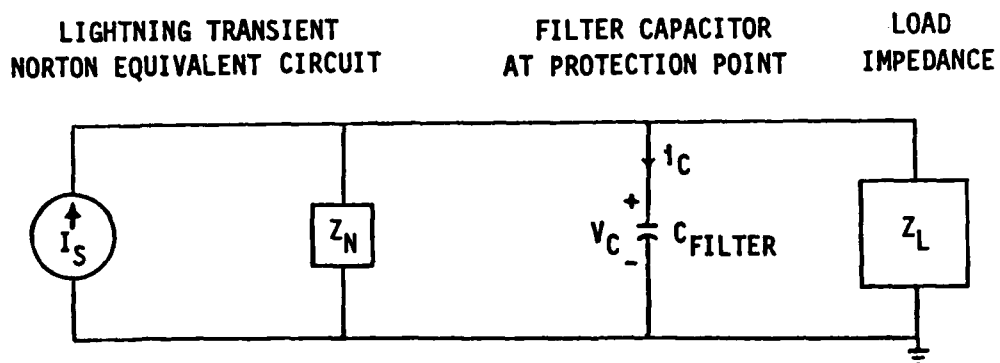
FIGURE 63   Power System Transient Model With Filter Capacitor

obtained using capacitors or solid-state devices (such as diodes or
TransZorbs). High transient impedance devices must also provide load
isolation from the input terminals, and are normally obtained using LC filters.

A major drawback of high transient impedance protection schemes is that high
voltages can exist in the immediate neighborhood of the protective device.
This would likely result in arcing in wiring or connectors. The resulting
large power system follow through current would trip the circuit breaker. A
low transient impedance device would tend to keep these voltages low, thus
avoiding the arcing problem.

All these protective schemes exploit differences between the lightning induced
transients and the normal power signals: (1) level differences (nonlinear
protective devices, such as TransZorbs), (2) spectral differences (linear
devices, such as capacitor or LC filters), or (3) level and spectral
differences (combinations of TransZorbs and capacitor or LC filters).

(1) FILTER DESIGN CONCEPTS

Consider the simplified power system transient model illustrated in Figure
63. Included are a Norton equivalent network representation of the lightning
transient source, a capacitor filter connected to the protection point, and a
load impedance.

If the Norton and load impedances are desirably high compared to the transient
impedance of the capacitor then most of the short-circuit current (I_S) will
flow through the capacitor. For an ideal capacitor

$$v_c(t) = \frac{1}{C} \int i_c(t)dt \qquad (9)$$

If the short-circuit current at the protection point has the form

$$I_S(t) = I_0 \exp(-t/\tau)u(t), \qquad (10)$$

then $\qquad v_c(t) = \frac{I_0\tau}{C} \left[1-\exp(-t/\tau)\right]u(t) \qquad (11)$

is the transient induced component of the capacitor voltage (superimposed on the normal voltage).

Equations (9) through (11) are valid until a level is reached at which device breakdown occurs. At the onset of breakdown, the voltage drops and the current increases suddenly. The result of such a breakdown is to reduce the capacitor's leakage resistance and subsequent breakdown level by creating tracking paths in the insulation material or encapsulation (Reference 7). Capacitance change or device fracture may also occur. The short-pulse voltage level at which breakdown occurs will usually be several times greater than the d.c. voltage rating (typically four to six times for microsecond pulses).

If the Norton and load impedances are very high at low frequencies, the capacitor will discharge very slowly, and the voltage across the capacitor will decay according to the time constant. Low impedances (for low frequencies) would discharge the capacitor rapidly. The discharge rate determines the overvoltage factor at which the capacitor can be operated. For devices having unknown characteristics or for unknown discharge rates, it may be wise to conservatively design so that the direct current voltage rating is not exceeded.

In addition to transient performance, a designer must consider normal system operational performance. Capacitor reactance is defined as:

$$X_c = \frac{1}{2\pi f_{PWR} C} \tag{12}$$

where C is the capacitance value and f_{PWR} is the power system frequency of operation (60Hz, 400Hz, etc.). There will normally be a maximum allowable capacitor "leakage" current (dictated by safety, power factor, or capacitor reliability considerations), which will in turn define an upper limit on the capacitance value:

$$C = \frac{I_{MAX}}{2\pi f_{PWR} V_{PWR}} \tag{13}$$

where I_{MAX} is the maximum allowed power current and V_{PWR} is the power line

voltage. The peak transient voltage is then approximated as:

$$V_{Peak} = \frac{2\pi f_{PWR} V_{PWR} I_o \tau}{I_{MAX}} \qquad (14)$$

where τ is the time constant rate of decay and I_o is the current at zero time.

(2) DESIGNING LIGHTNING PROTECTION USING CAPACITOR FILTERS

The design (through use of quick hand calculation methods) of lightning transient suppressors using capacitor filters can be outlined as follows:

Step (1.) Approximate the short-circuit current at the protection point as an exponential having peak value I_o and e-field fall time of τ.

Step (2.) Choose a candidate series/parallel capacitor configuration.

Step (3.) Compute the resulting capacitor peak voltage, power frequency current, and safety margin:

$$V_p = 1.4 \ V_{PWR} + \frac{I_o}{C} \qquad (15)$$

$$I_{PWR} = 2 \ f_{PWR} C V_{PWR} \qquad (16)$$

$$SM = 20 \ \log_{10} \frac{V_{DAMAGE}}{V_p} \qquad (17)$$

Here V_{DAMAGE} will normally be one to six times the direct current rating. For microsecond voltage pulses an overvoltage factor of three is often used. For devices of unknown characteristics, or voltage pulses of unknown length, a factor of one may be called for to ensure a safe design.

Step (4.) Iterate, as necesary, on device type/value until an acceptable compromise between capacitor peak voltage, safety margin, and power

frequency current is achieved (or until it is determined that an acceptable design using capacitors is not possible).

e. SURGE ARRESTORS

Surge protective devices are used primarily to protect electrical/electronic equipment for physical damage due to transients on the incoming wires and secondarily to limit interference by reflection, suppression, and absorption. Semiconductor devices such as PNPN devices and bipolar transistors are also termed surge arrestors. For example, one lightning protection device consists of a series combination of back to back silicon controlled rectifiers (SCR's) in parallel with a capacitor and shunt resistor.

f. CONDUCTIVE COATINGS FOR EMI SHIELDING

The shielding effectiveness of composites for magnetic (H) fields has been measured by Strawe and Piszker (Reference 8). Composite·material systems and coating materials were selected for evaluation based upon their potential use and shielding quality. Evaluation was accomplished by a flat-plate magnetic field shielding effectiveness (MSE) test. Flat-plate MSE test data were used to rank the materials, since the MSE is a good indication of relative shielding quality. Joining concepts that are in current use in composites technology were evaluated. Others were developed specifically to improve the shielding quality of composite joints and to provide good electrical joints between coating materials. Twelve inch square flat-plate samples were tested using various graphite laminates, foils, screens, and coated graphites. The two charts shown in Figure 64 display typical test results of the tested samples plotting the response of the magnetic field versus frequency.

An important factor which limits the effectiveness of add-on conductive coatings is the degree of electrical contact, across the frequency range of interest, between the perimeter of the conductive coating and underlying metal structure. The admittance of the joint between the conductive coating and metal structure is obtained by testing sample joints, using techniques described in Reference 8. The potential impact of poorly designed joints is analyzed in Reference 1, for the lightning threat. When the joint admittance
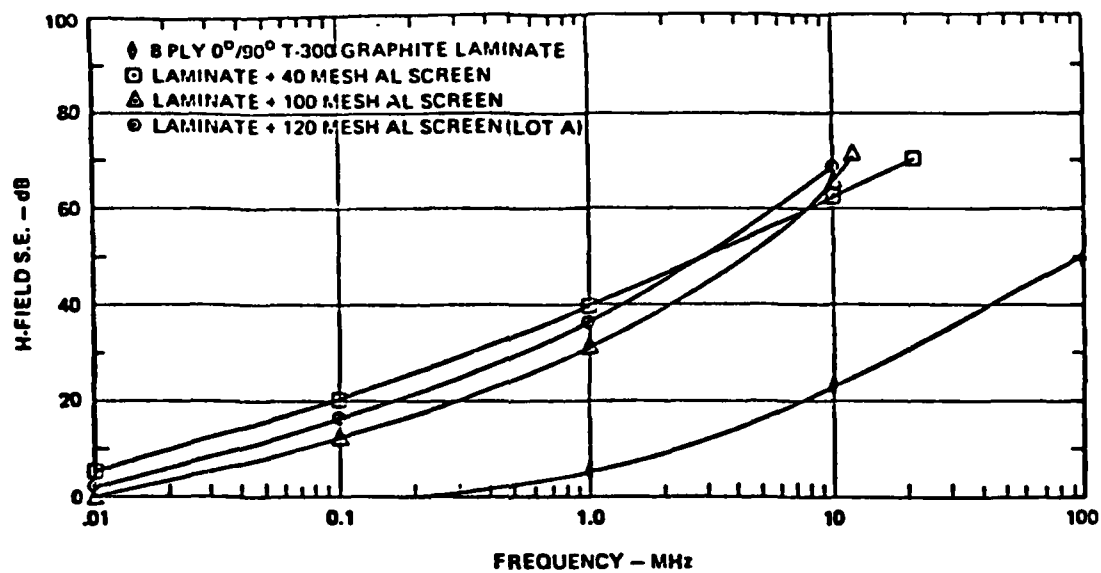
(a)
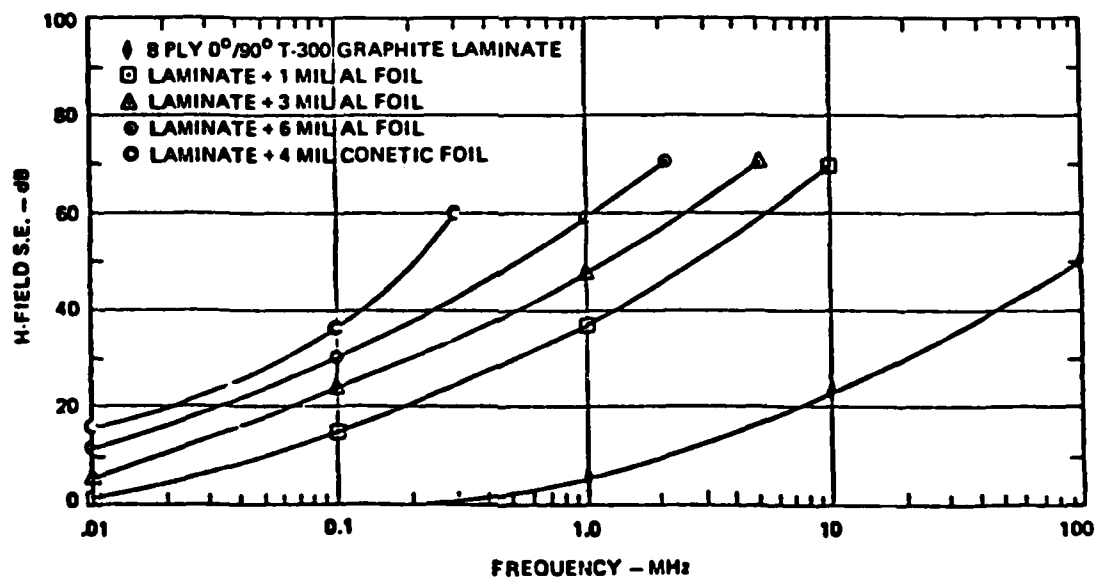
(b)

Figure 64   Measured H-Field S.E. of Coated 8 Ply Graphite Laminates

is known, one may estimate induced transients on internal wiring by the techniques described in Appendix C.

2. ADD-ON COATING PROTECTION FOR DIRECT ATTACHED LIGHTNING

The use of nonmetallic composite materials for airplane construction is increasing because of the weight and cost benefits. Presently, composite materials are primarily being used on wing tips and empennage tips or where structural loads are small. Access doors, fairings, and wire bundle jackets are also being fabricated from the composite materials.

Available advanced composite structure lightning protection coatings and possible sources for the various materials are listed on the following pages. The order in which the protection coatings are listed does not reflect any specific preference or rating. However, the first three were determined to provide the best aircraft lightning protection coating, as detailed in Reference 9. Weights and a ranking of manufacturing difficulty are given in Table 36 for the various protection coatings.

a. **Aluminum Metal Spray Protective Coating, 4.0-6.9 mil Thickness, 0.036 lb/ft^2 (Nominal Weight**

This coating provides good lightning protection for Zone 1 and 2 (see Section II.1.a) conditions. It can be applied to simple or complex shaped parts either in a cocure operation or secondarily applied to cured composite surfaces. This coating requires specialized application equipment and trained personnel to obtain a good uniform coating.

Materials	Possible Source
Pure Aluminum Wire 1/8-in. diameter, Per AMS 4180B	Metco, Inc. 307 East Fourth Street Cincinnati, OH 45202
Sealer Resin FR-40 Hardener 5413C	Fiber Resin Corporation 170 Providencia Ave. Burbank, CA 91503

TABLE 36 SUMMARY TABLE OF PROTECTION COATING

PROTECTION SYSTEM	WEIGHT, LB/FT^2		MANUFACTURING RANKING ①
	WITH ADHESIVE	WITHOUT ADHESIVE	
Aluminum metal flame spray, 4-6.9 mil, 100% coverage	0.036	–	9
Aluminum metal flame spray, 4-6.9 mil, 50% coverage	0.018	–	8
120 x 120 Aluminum wire screen, 100% coverage	0.140	0.070	6
200 x 200 Aluminum wire screen, 100% coverage	0.080	0.050	7
Aluminum foil, 2 mil, 100% coverage	0.060	0.030	2
Aluminum foil, 2 mil, 50% coverage	0.030	0.015	3
Aluminum Foil Tape, 2 Mil Adhesively Backed, 100% Coverage	0.034	–	2
Aluminum Foil Tape, 2 Mil Adhesively Backed, 50% Coverage	0.017	–	3
Aluminum foil, 3 mil, 100% coverage	0.075	0.045	4
Aluminum foil, 3 mil, 50% coverage	0.038	0.022	5
Aluminum Foil Tape, 3 Mil, Adhesively Backed, 100% Coverage	0.050	–	2
Aluminum Foil Tape, 3 Mil, Adhesively Backed, 50% Coverage	0.025	–	3
Kapton film, 2 mil, + 2 mil foil strips	0.044	0.014	1

① 9 = Easiest to apply and repair
1 = Most difficult to apply and repair

155

```
Potting Compound                    Fiber Resin Corporation
FR 8840                             170 Providencia Ave.
Parts A and B                       Burbank, CA  91503
```

b. <u>Aluminum Metal Flame Spray Strips (50% Coverage), 4.0-6.9 mil Thickness,</u>
   <u>0.018 lb/ft^2 (Nominal Weight)</u>

This coating is used in Zone 2 applications to protect large composite surface
areas. The metal strips are typically 3 inches wide with 3 inch spacing.
Comments from Section IV.2.a are applicable here.

c. <u>Aluminum Wire Screen (120 x 120) Protective Coating, 0.14 lb/ft^2</u>
   <u>(Nominal Weight with Adhesive)</u>

This coating provides good lightning protection in Zone 1 and Zone 2
conditions. Good quality application restricts this system to simple contour
shaped parts. Screen width is limited to 36 inches, which complicates
application because of screen splicing requirements for large surface areas.

```
      Materials                         Possible Sources
   120 x 120 Wire Screen,             Cal-Metex Corporation
   0.004-in. diameter                 509 Hindry Avenue
 . 1100 Aluminum wire                 Inglewood, CA  90301
   36-in. width rolls


   Adhesive AF-143 or                 3M Company
   AF-147 or equivalent               3M Center
   0.05-0.08 lb/ft², 18 in            St. Paul, MN  55101
   wide.  Sold in 3-roll              (612) 733-1110
   minimum order, 36 yds
   per roll.
```

d. <u>Aluminum Wire Screen (200 x 200) Protective Costing, 0.08 lb/ft^2</u>
   <u>(Nominal Weight with Adhesive)</u>

This protection coating can provide limited protection in Zone 2 conditions.
Limitations discussed in Section IV.2.c also apply to this system.

Materials	Possible Sources
200 x 200 Aluminum Wire Screen, 0.0021-in. diameter 1100 wire, 36-in. width. Sold by the roll	Cal-Metex Corporation 509 Hindry Avenue Inglewood, PA 90301
Adhesive AF-143 or AF-147 or equivalent, 0.05-0.08 lb/ft^2 18-in. width. Sold in 3-roll minimum order, 36 yards per roll.	3M Company 3M Center St. Paul, MN 55101 (612) 733-1110

e. <u>Aluminum Foil (2 mil) Cocured Protective Coating, 0.060 lb/ft^2 (Nominal Weight with Adhesive)</u>

Aluminum foil (2 mil) offers limited protection in Zone 1 and Zone 2 applications. Good quality surface finish is difficult to obtain except for simple flat surfaces. Foil width is limited to 36 inches, which forces noncontinuous splice areas on large surfaces.

Materials	Possible Sources
Aluminum Foil (2 mil)	Any major aluminum manufacturer
Adhesive AF-143 or AF-147 or equivalent 0.03 lb/ft^2 18-in. width. Sold in 3-roll minimum order, 36 yards per roll.	3M Company 3M Center St. Paul, MN 55101 (612) 733-1110

f. <u>Aluminum Foil (2-mil, Adhesive Backed) Secondarily Applied Protective Coating, 0.034 lb/ft^2 (Nominal Weight)</u>

This coat is best applied to the cured composite structure surface. It conforms reasonably well to complex shapes. It offers limited protection in Zone 1 and Zone 2 applications. The 3-in. width limitation requires close attention to splices for continuous coverage.

Materials	Possible Source
Scotch Aluminum Foil No. 431 Linerless, Tape, 2 mil, acrylic adhesive backed, 3-in. width sold by the case, 12 rolls 60 yds each roll.	3M Company 3M Center St. Paul, MN 55101 (612) 733-1110

g. <u>Aluminum Foil (3-mil) Cocured Protective Coating, 0.075 lb/ft^2 (Nominal Weight with Adhesive)</u>

Aluminum foil (3-mil) offers adequate protection in Zone 1 and Zone 2 application. Manufacturing comments and materials information are as listed in Section IV.2.e.

h. <u>Aluminum Foil (3-mil, Adhesive Backed) Secondarily Applied Protective Coating 0.050 lb/ft^2 (Nominal Weight)</u>

This coat offers adequate protection in Zone 1 and Zone 2 applications. Other comments as to manufacturing complexity are found in Section IV.2.g.

Materials	Possible Source
Scotch Aluminum Foil No. 425, linerless tape, 3-mil, acrylic adhesive backed, 3-in. width sold by the case, 12 roll 60 yds each roll.	3M Company 3M Center St. Paul, MN 55101 (612) 773-1110

i. <u>Aluminum Foil Tape Strips (3-mil, Adhesively Backed), 3-in. width with 3-in. spacing, Protection Coating 0.025 lb/ft^2 (Nominal Weight)</u>

This coat is best applied to the cured composite structure surface. It is intended for Zone 2 swept-stroke conditions only. Comments as to manufacturing complexity and materials are found in Sections IV.2.g and IV.2.h.

j. Kapton Film (2-mil) Plus Aluminum Foil Strips (2-mil, Adhesive Backed)
   Protective Coating, 0.044 lb/ft^2 (Nominal Weight with Adhesive)

This coat is the most complex to incorporate (cocured) into the composite surface and is the most difficult to repair. Kapton film is limited to simple contour or flat surfaces, and must be overlap spliced for areas greater than 36 inches wide.

Materials	Possible Sources
Kapton Film, 2-mil, 36-in. width sold by the pound	Fralock 15441 Carbillo Rd. Van Nuys, CA 91406 (213) 873-6665
Scotch Aluminum Foil No. 431 linerless tape, 2-mil, acrylic adhesive backed, 3-in. width sold by the case, 12 rolls 120 yards.	3M Company 3M Center St. Paul, MN 55101 (612) 773-1110
Adhesive AF-143 or equivalent. 0.05 lb/ft^2 18-in. width. Sold in 3-roll minimum order, 36 Yards per roll.	3M Company 3M Center St. Paul, MN 55101 (612) 733-1110

BLANK PAGE

SECTION V

DESIGN GUIDE SUMMARY

The design guide (Reference 14) for the protection of the electrical system
from EM hazards provides the system design engineer with a means of selecting
the appropriate hardening techniques for his design. This is accomplished by
establishing electrical system lightning hardening criteria for typical
advanced and conventional aircraft.

The lightning threat levels established for the electrical system are then
used to assess the system's ability to withstand the lightning strike. If
hardening is necessary, the hardening criteria are applied to the system and
the appropriate hardening techniques are selected. Rationale are given for
the selection made and alternatives are also suggested.

1. DESIGN GUIDE DESCRIPTION

The des'gr guide is based upon a typical electrical power system design
process as shown in Table 37. From this design process, the sections of the
guide were developed to provide a systematic approach for the design engineer.

The design process begins with an assessment of the lightning threat in
Section II. This section provides the equations for threat estimation and the
rationale used in the derivation of these equations.

Section III of the design guide develops techniques for inherent hardening.
Methods of wire routing, bonding and grounding, and typical design procedures
that can be utilized to provide a maximum amount of lightning protection
inherently.

An assessment of inherent hardening on typical aircraft configurations is
given in Section IV of the design guide. A summary of the data generated from
this assessment is included in Table 1. From the examination of the power
circuits, protection is required from the severe lightning threat for most
circuits.

DEVELOP PRELIMINARY DESIGN
OF TYPICAL SINGLE-CHANNEL
ADVANCED ELECTRICAL SYSTEM
 • POWER SYSTEM CONFIGURATION
 • DISTRIBUTION SYSTEM
 • TYPICAL UTILIZATION SUBSYSTEMS

ESTABLISH HARDENING REQUIREMENTS
 • DEFINE THREAT LEVELS
 • EVALUATE INHERENT HARDNESS
   OF SYSTEMS NOT AIRCRAFT-
   DEPENDENT

METALLIC AIRCRAFT

COMPOSITE AIRCRAFT

ESTABLISH EFFECTIVENESS
OF INHERENT HARDNESS
 • NORMAL DESIGN
   TECHNIQUES
 • ALTERNATIVE DESIGN
   TECHNIQUES

ESTABLISH EFFECTIVENESS
OF INHERENT HARDNESS
 • NORMAL DESIGN
   TECHNIQUES
 • ALTERNATIVE DESIGN
   TECHNIQUES

 • ASSESS NEED FOR ADD-ON
   PROTECTION
 • SELECT APPROPRIATE
   ADD-ON TECHNIQUES

 • ASSESS NEED FOR ADD-ON
   PROTECTION
 • SELECT APPROPRIATE
   ADD-ON TECHNIQUES

EVALUATE BY ANALYSIS
SYSTEM HARDNESS VERSUS
THREAT LEVELS

EVALUATE BY ANALYSIS
SYSTEM HARDNESS VERSUS
THREAT LEVELS

COMPLETE DESIGN OF
DEMONSTRATION SYSTEM
PROTECTION

COMPLETE DESIGN OF
DEMONSTRATION SYSTEM
PROTECTION

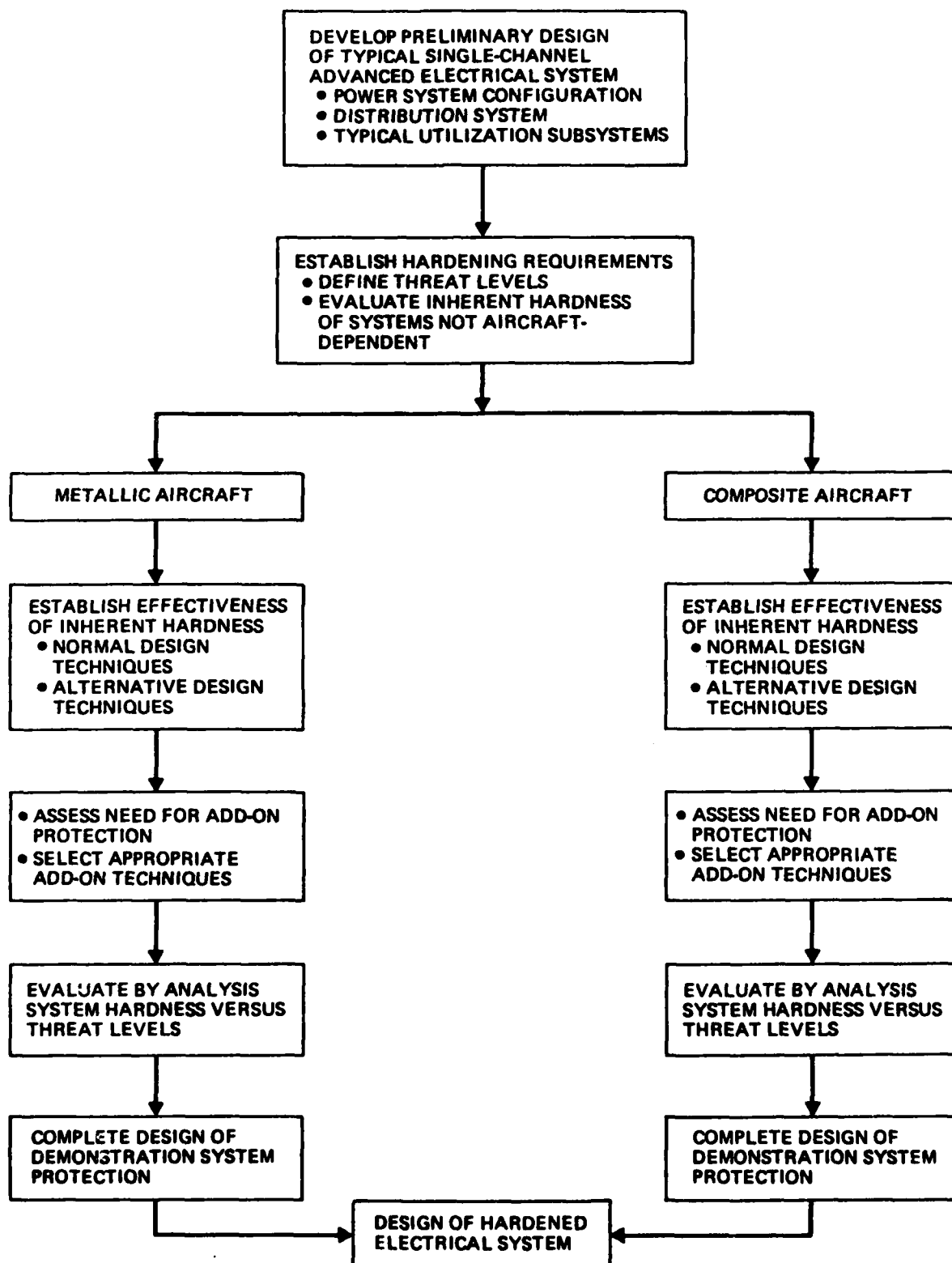DESIGN OF HARDENED
ELECTRICAL SYSTEM

Figure 37 Electrical System Protection Design Process

162

Specifications which govern the operation and design of electrical power
systems are given in Section V. Those portions of the specification which
cover lightning transients are compared.

Section VI of the design guide details the available types of add-on
protection available. These protection devices are assessed as to their
applicability in the system design. Procedures are also specified which aid
the design engineer to select the appropriate protection scheme for his
design. Included is an assessment of shielding, nonlinear surge suppressors,
linear filters and a comparison of several skin materials and coatings.

The add-on protection techniques are evaluated in typical electrical system
circuit configurations in Section VII. Procedures are detailed which enable
the design engineer to calculate the effectiveness of each type of protection
scheme. Overall system protection concepts are also discussed.

Section VIII of the design guide provides a procedure for designing a
lightning hardened electrical system. The design includes references to the
appropriate sections of the design guide and the rationale for the selection
made.

2. PROTECTION CRITERIA

To design a lightning tolerant electrical system as shown in Table 37, the
following hardening criteria must be followed.

   o Identify the lightning threat.

   o Assess the system for inherent hardness.

   o Define all potential hazard areas.

   o Select add-on protection.

   o Evaluate the system for lightning survivability.

As an example of an electrical system design, which utilizes the procedures of the design guide the following illustration is given.

The cargo aircraft (shown in Figure 65) has an electrical system with the basic configuration shown in Figure 66. From this information the lightning threat for this aircraft and its impact on the electrical system components must be determined.

Assuming that the severe threat lightning stroke must be protected against, peak currents of 200 K Amps can be expected in possibly 3 or 4 successive strokes. These lightning strikes are assumed to be by direct attachment creating the much larger surface currents. This assumption seems appropriate with the all weather aircraft scenarios being specified.

The lightning strike zones shown in Figure 67 illustrate the concept of zoning according to the probable magnitude of the strike.

o   Zone 1 (direct stroke attachment) includes wingtips, all projections such as engine nacelles, and the tail group.

o   Zone 2 (swept stroke attachment) includes all exposed fuselage and nacelle surfaces.

o   Zone 3 (low probability of any attachment) includes all areas not covered by Zone 1 and Zone 2.

The equations for threat estimates are based upon the four types of coupling mechanisms listed below:

o   EXPOSED CONDUCTORS - conductors directly exposed to the lightning fields (e.g., windshield heater, front and rear spar wiring).

o   APERTURES - non-conductive portions of airplane exterior. Some examples are the cockpit canopy, windows, and fiberglass access doors.
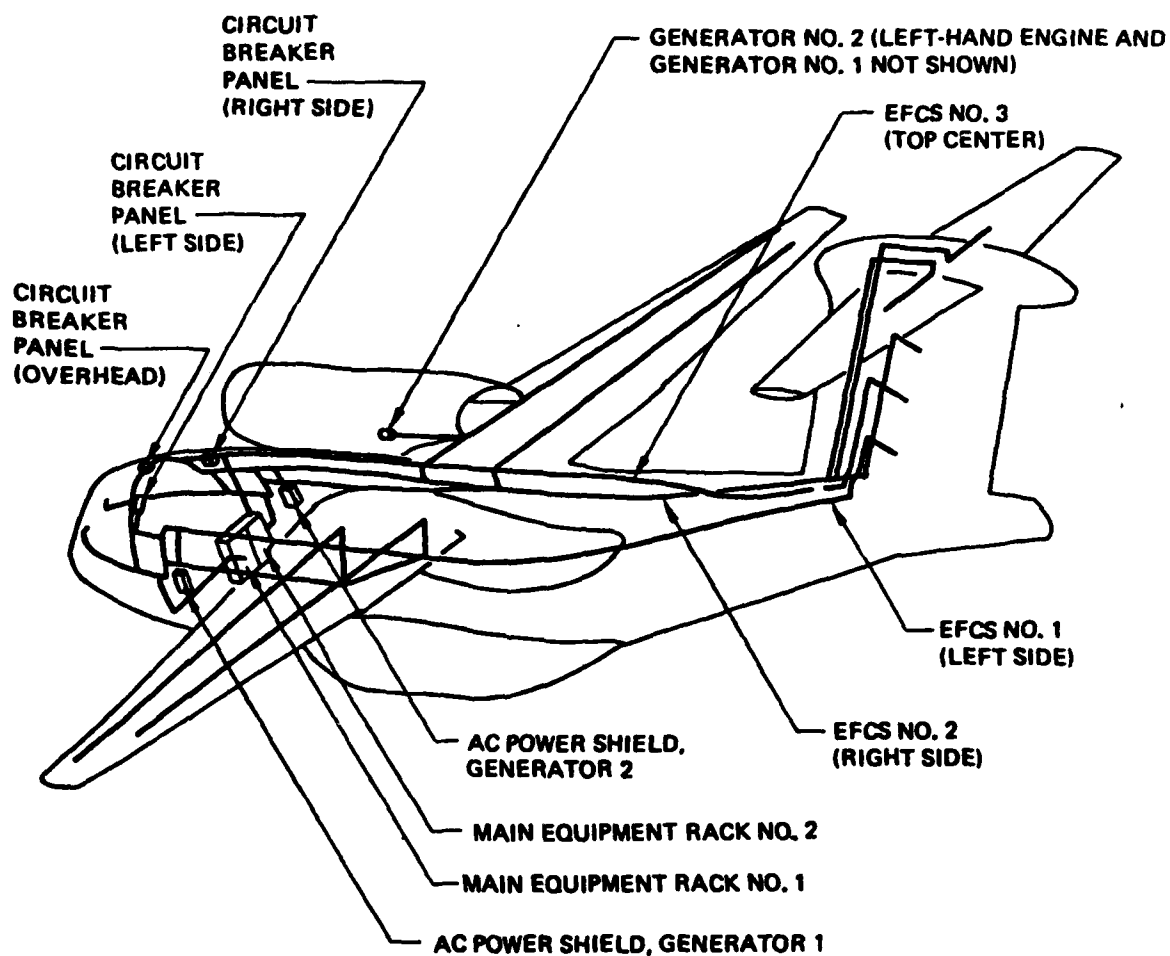
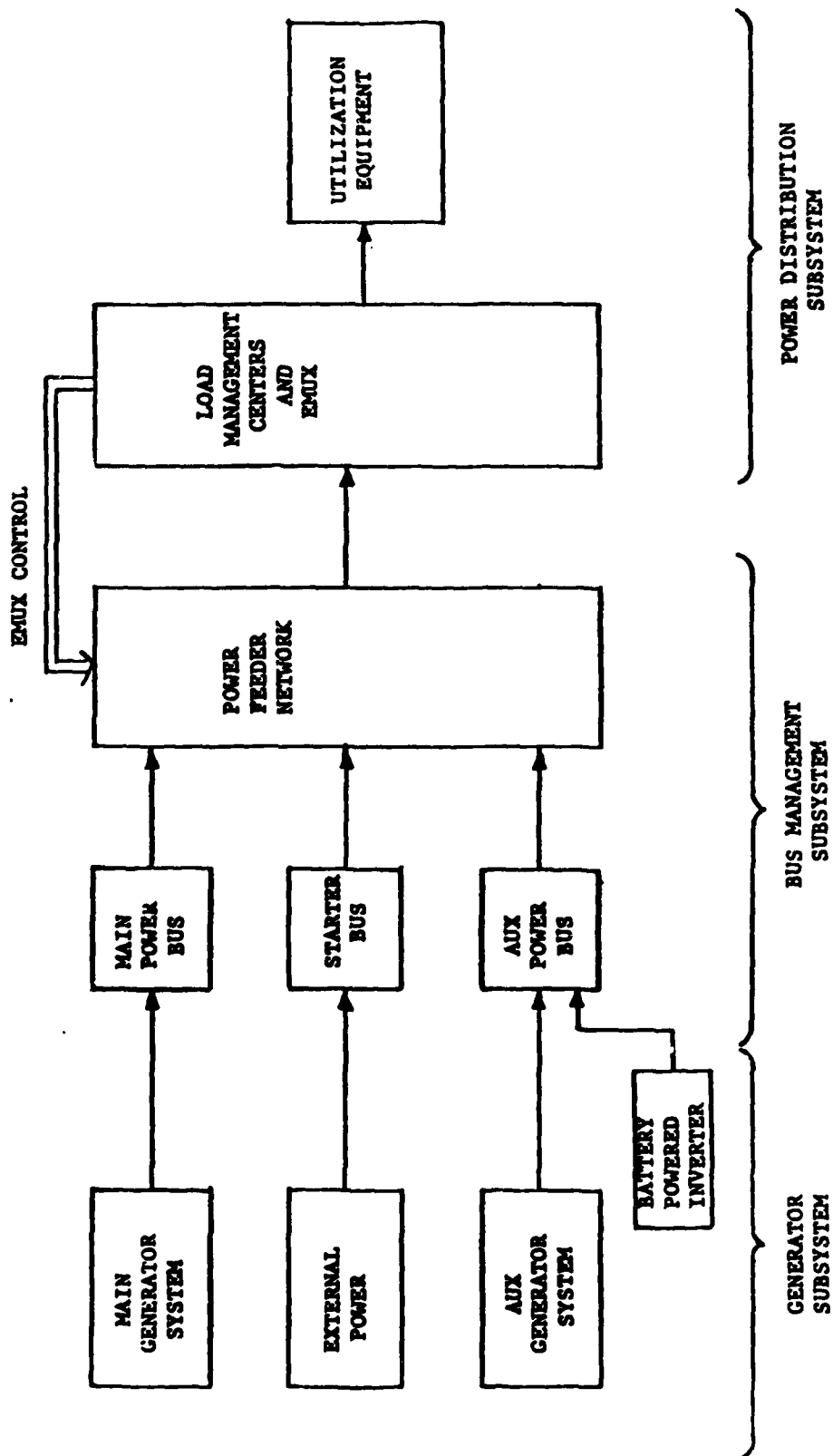Figure 65 *Inherent Hardness From Circuit Redundancy and Separation of Circuits*
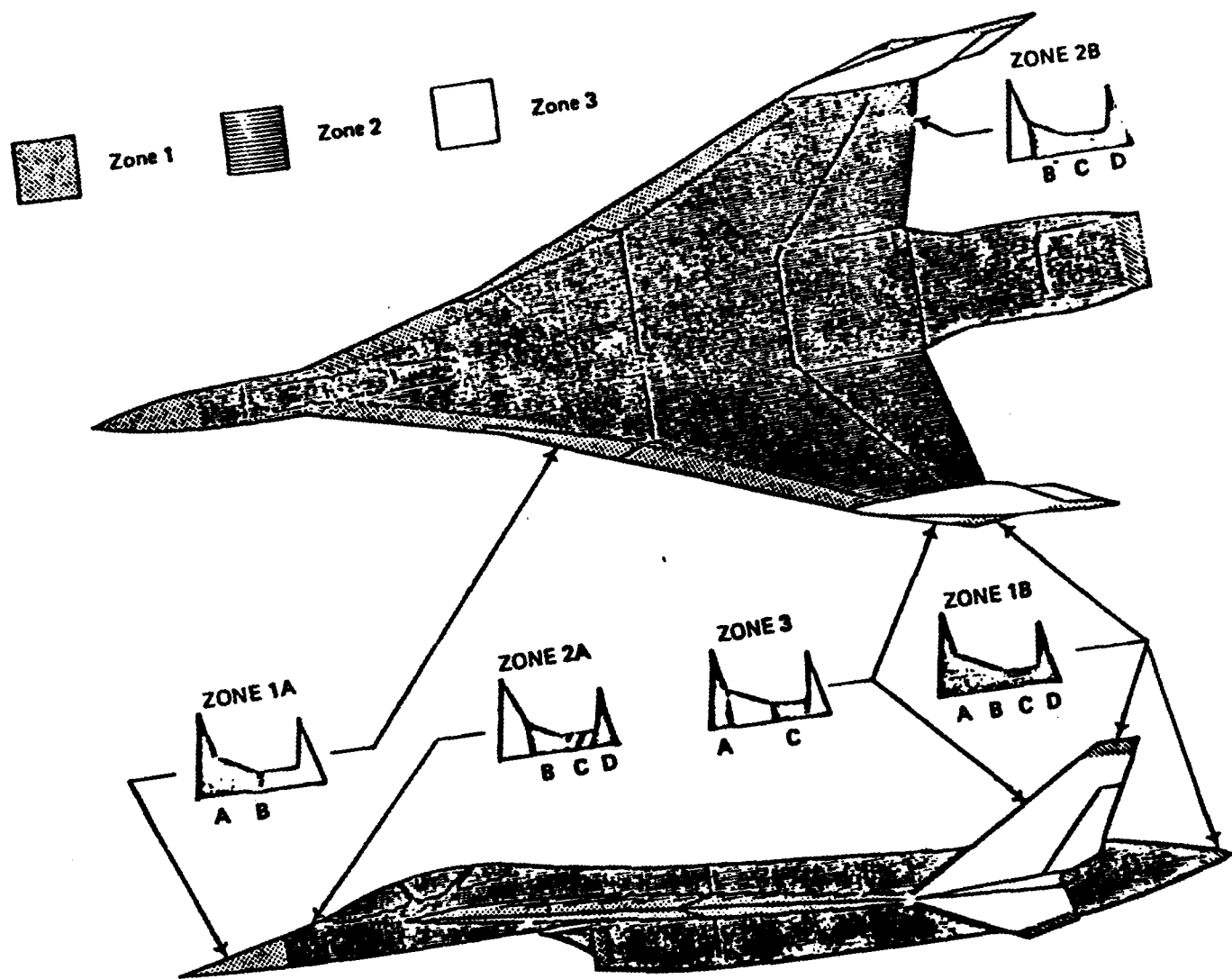
Figure 66 Block Diagram - Single Channel Electrical System

FIGURE 67   AIRCRAFT LIGHTNING STRIKE ZONES

167

o JOINTS - electrical discontinuities in aircraft exterior; e.g., the narrow gap between a metallic access door and underlaying airframe or the interface between two graphite epoxy panels.

o DIFFUSION - low-frequency penetration of fields into the interior of metallic or graphite-epoxy fuselage, wings; etc.
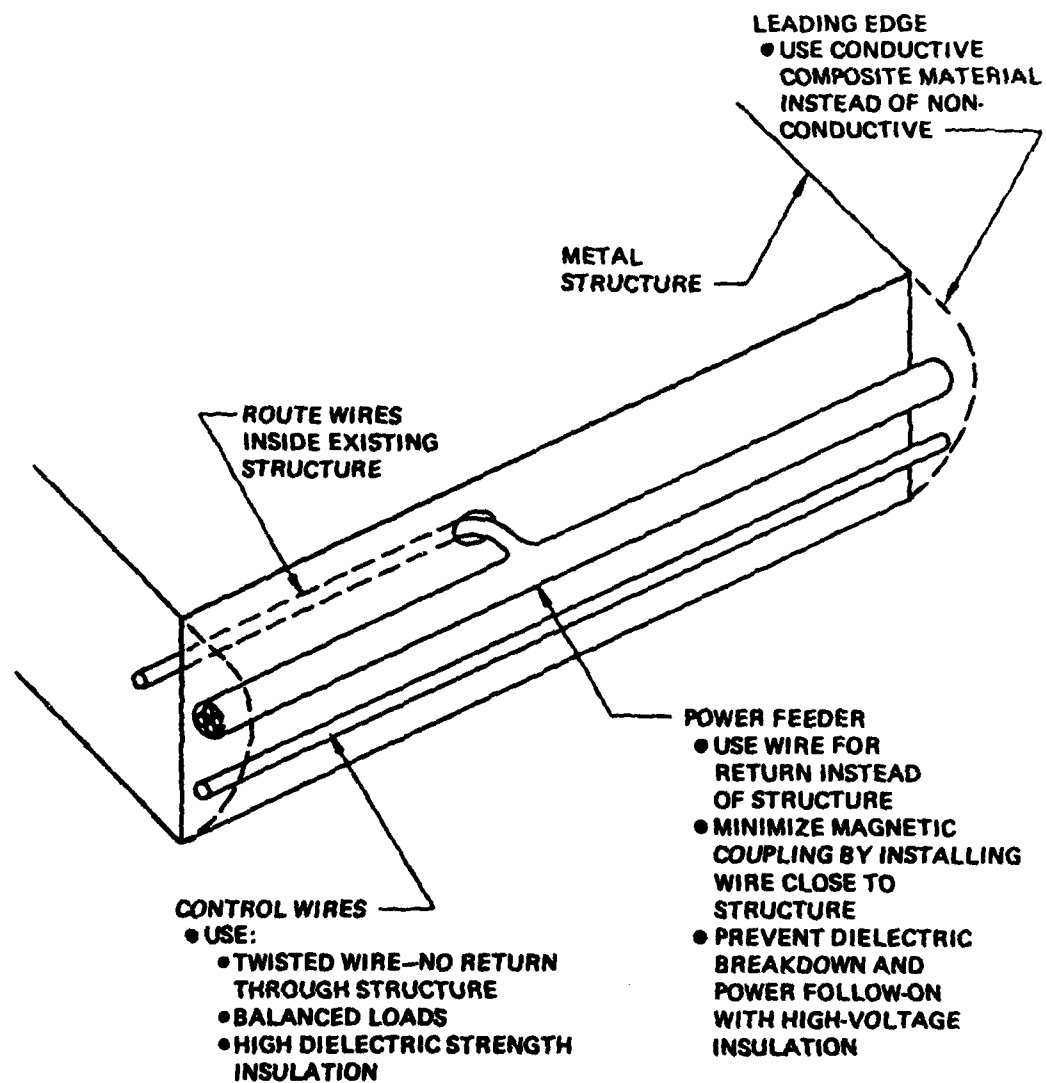
The equations are of the form shown in Figure 68. These are used to determine the open circuit voltages and short circuit currents that would be expected on the system.

Once the threat has been determined and the basic system configuration is known, an assessment of the inherent hardness of the system can be accomplished.

For metallic structured aircraft, the skin provides enough protection in most cases. However, for exposed cables (in the engine nacelle area for example), the lightning threat will be a problem. Apertures caused by non-conductive metal surfaces must be identified as area of potential problems. All wire routing in these areas should be designed carefully (Figure 69). For composite structured aircraft, or aircraft that use composite or fiberglass materials in any part of the structure, the inherent shielding provided by the skin is not available. Where metal structure is available cables should be routed near these spars or structures. Close attention must be paid to bonding and grounding for maximum conduction of the lightning currents.

The inherent hardness assessment of the system design provides the necessary information to define the potential hazard areas. Typical problem areas are exposed electrical cables in the engine nacelle, cabling near the radomes, navigation lights, windshield heaters and cabling routed in the leading edges of the wings behind non-conductive materials. The analysis in Section III provided the data of Table 38 which assesses the cabling routed in the wing leading edge constructed of several different types of materials. The lightning threat requires additional attenuation in most cases.

Several types of suppression devices and suppression techniques are outlined in the design guide.

LEADING EDGE
● USE CONDUCTIVE
COMPOSITE MATERIAL
INSTEAD OF NON-
CONDUCTIVE

METAL
STRUCTURE

ROUTE WIRES
INSIDE EXISTING
STRUCTURE

POWER FEEDER
● USE WIRE FOR
RETURN INSTEAD
OF STRUCTURE
● MINIMIZE MAGNETIC
COUPLING BY INSTALLING
WIRE CLOSE TO
STRUCTURE
● PREVENT DIELECTRIC
BREAKDOWN AND
POWER FOLLOW-ON
WITH HIGH-VOLTAGE
INSULATION

CONTROL WIRES
● USE:
  ● TWISTED WIRE—NO RETURN
    THROUGH STRUCTURE
  ● BALANCED LOADS
  ● HIGH DIELECTRIC STRENGTH
    INSULATION

Figure 68 Inherent Hardness—Normal Design

169

EQUATIONS FOR THREAT ESTIMATION
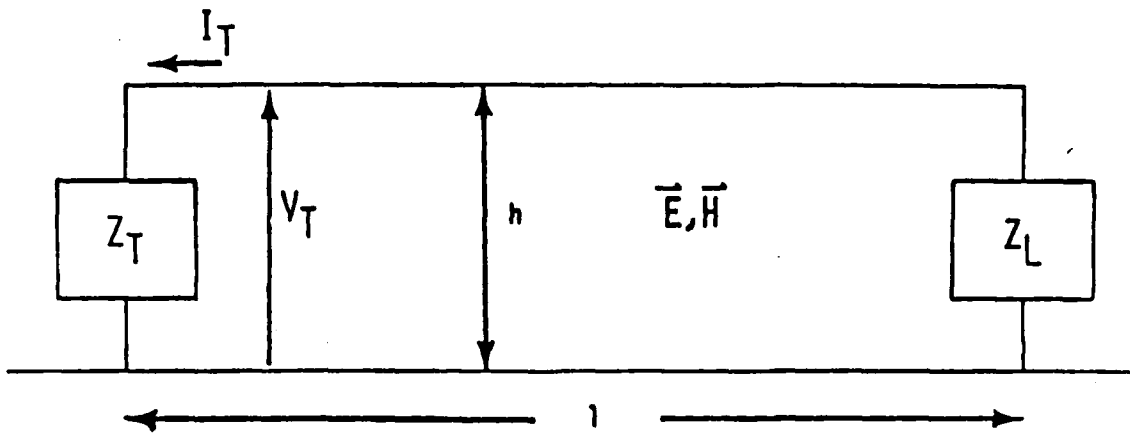
APPROACH: OBTAIN I_{SC}, V_{OC} AT Z_T FOR $Z_L = 0,00$. CONSIDERED FOUR TYPES OF EXCITATION

1. DIRECTLY EXPOSED WIRE
2. INDUCTIVE SLOT
3. RESISTIVE JOINT
4. DIFFUSION

Figure 69   Protection of AEPS From EM Hazards Model

170

TABLE 38 SEVERE LIGHTNING STRIKE TRANSIENTS SUMMARY DATA

TEST CONDITIONS	VOLTAGE PEAK	TRANSIENT DURATION	CURRENT PEAK	TRANSIENT DURATION
An all aluminum wing with fiberglass leading edge, 22 meters from the power bus				
Bus Open Circuit	75 KV	7 mS		
Bus Short Circuit			2.65 KA	0.7 mS
50% Loaded Bus	65 KV	8 mS	289 A	0.15 mS
100% Loaded Bus	58 KV	8 uS	550 A	0.6 mS
An all aluminum wing with a graphite epoxy leading edge, 22 meters from the power bus				
50% Loaded Bus, 35 Plies	410 V	1 mS	305 A	1 mS
50% Loaded Bus, 45 Plies	320 V	1 mS	235 A	1 mS
50% Loaded Bus, 50 Plies, L.E. is 2 ft ahead of feeder	285 V	1 mS	215 A	1 mS
50% Loaded Bus, 50 Plies, L.E. is 1 ft ahead of feeder	570 V	1 mS	420 A	1 mS
50% Loaded Bus, 50 Plies, L.E. is 1/2 ft ahead of feeder	1.14 KV	1 mS	840 A	1 mS

Some types of shielding discussed that seem to be the most favorable alternatives are the foil materials when composite structure is used, cable shielding when cables are directly exposed to the threat, and diverter straps in areas such as around the radome.

A major concern with power and signal shielding is the proper design of signal terminations. Figure 70 displays some advantages of circumferential grounding versus pigtail grounding. When composite materials are used with foil coating, bonding and grounding techniques must be carefully utilized to take advantage of the foil material. See Figures 71 and 72 for some possible bonding techniques for composite material at the joints.

Some typical types of surge suppressors are transzorbs, varistors, zener diodes, hybrid devices and spark gaps. Tables 39 and 40 display some of the characteristics that these devices exhibit. Some typical performance characteristics are shown in Table 41.

The appropriate add-on protection for each area of concern can now be selected. For the case where the cabling is routed behind a fiberglass wing leading edge, a voltage surge of nearly 65 KV must be attenuated. From the analysis of Section III, two orders of magnitude of attentuation can be seen by incorporating 3-mil foil into the leading edge. Table 42 displays the effectiveness of using 3-mil foil, transzorbs, or cable shielding (with pigtail grounding and circumferential grounding). Although all of these techniques provide a similar amount of protection (except for the pigtail grounded shielding case), from a weight and cost perspective the 3-mil foil shows the major advantage, with transzorbs being a consideration for some applications.

This summary is intended to provide the reader with a general idea of the contents of the design guide and its intended function. The design guide details a system design with lightning protection and will hopefully provide some insight into the problems associated with lightning strikes and their impact on advanced electrical systems.

(a) INTENSE MAGNETIC FIELD
AROUND PIGTAIL CAUSES
HIGH SELF-INDUCTANCE

(b) MAGNETIC FIELD ENTIRELY
EXTERNAL TO REGION
OCCUPIED BY SIGNAL CONDUCTORS
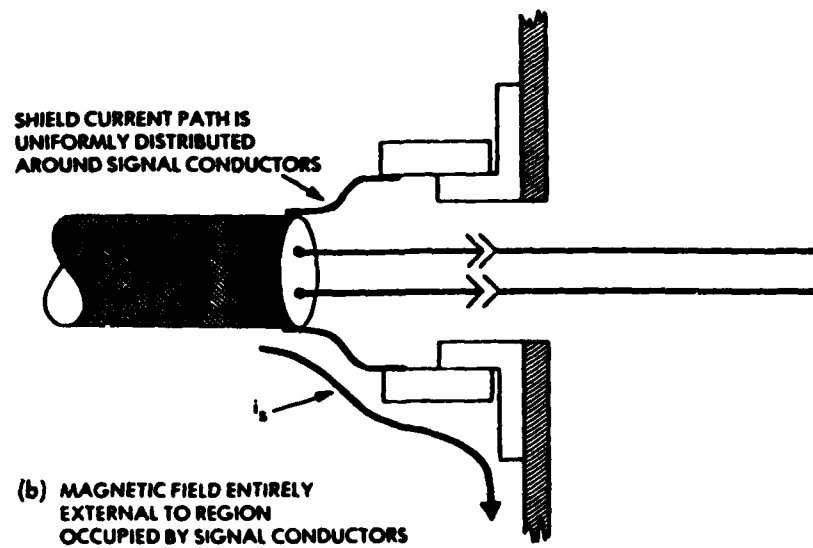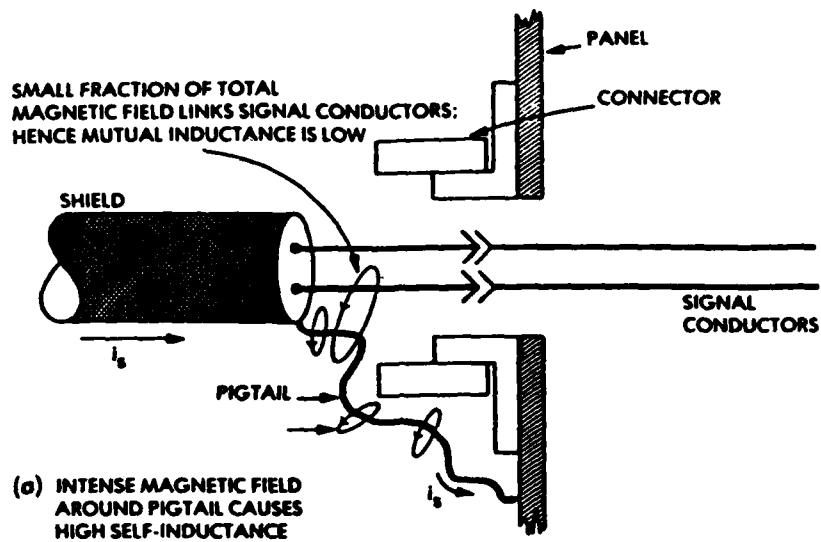
Figure 78   Magnetic Fields Around Shielding Terminations

173

1.0

1.1

1.25

4.5

5.0

3.6

4.0

2.8

3.2

1.4

2.5

2.2

2.0

1.8

1.6

MICROCOPY RESOLUTION TEST CHART

NATIONAL BUREAU OF STANDARDS 1963 A

GRAPHITE PLIES

FILLER PLUG FOR
POSITIVE PRESSURE
ON THE SCREEN

ADHESIVE BOND
DOUBLER FOR
EXTRA STRENGTH

ADHESIVE BOND (CURED AT
90 PSI) OR USE MECHANICAL
FASTENERS
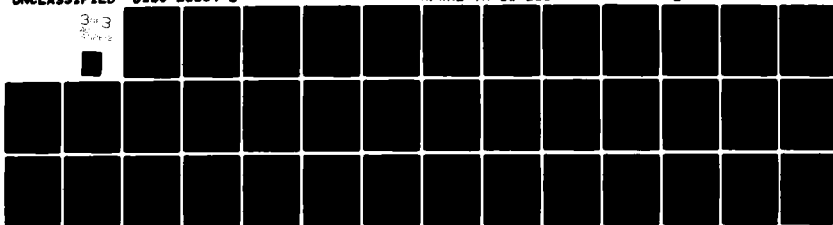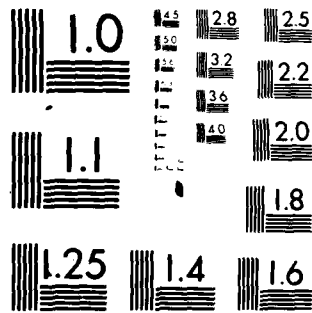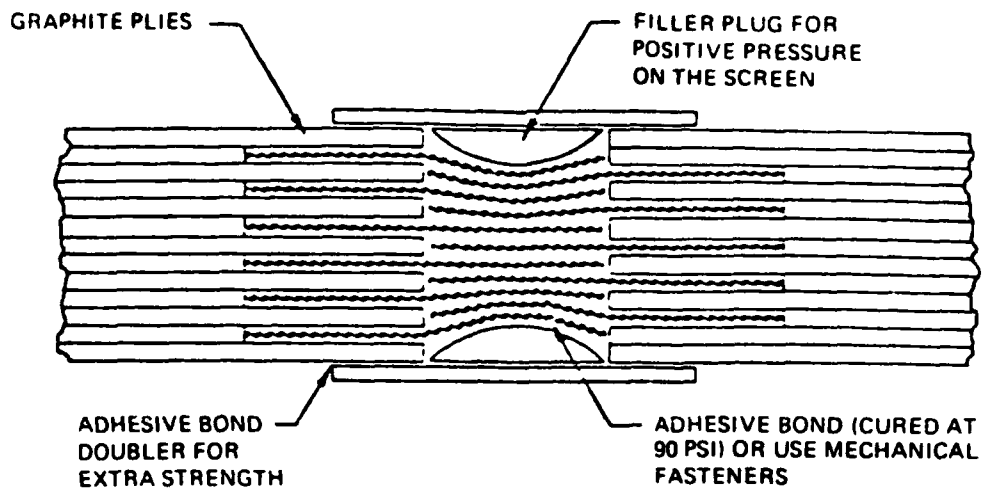
Multiple Screen Interleaved Lap Joint

GRAPHITE PLIES
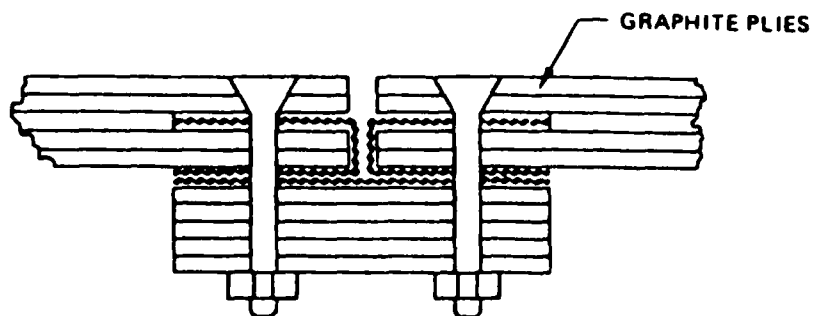
Figure 71   Folded Single Center Screen Mechanically
Fastened Lap Joint

174

ISOLATED FASTENER CONCEPT
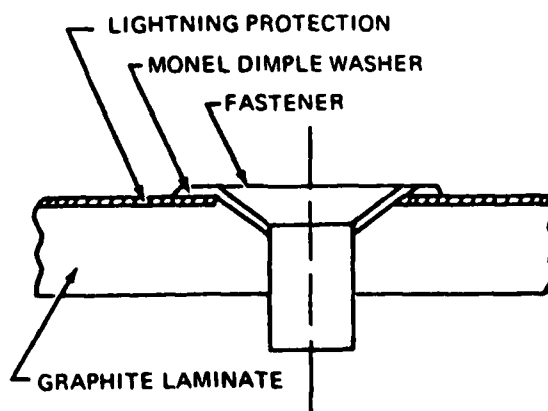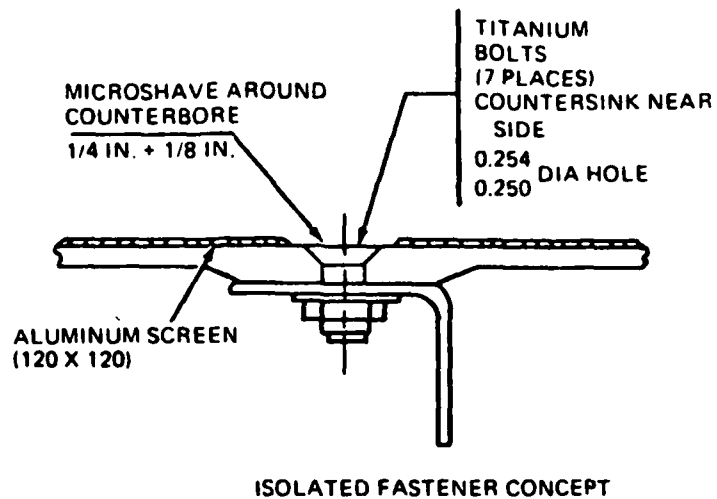
GROUNDING DETAILS

Figure 72 Isolated and Grounded Fastener Concept

175

TABLE 39 TYPICAL SUPPRESSOR CHARACTERISTICS

PARAMETER	GAS DISCHARGE TUBE	SPARK GAPS	VARISTOR DEVICES	ZENER DIODES	TRANSZORBS™
Typical Surge Current Capability (Amps)	40,000	10,000	1000-25K	To 500	30-500
Response Time (Sec)		10^{-8}	10^{-8}	10^{-9}	10^{-12}
Capacitance (farad)	10^{-12}	10^{-12}	10^{-12}	10^{-10}	10^{-9}
AC Voltage Range (Volts)		90 and higher	40-1000	2-300	17-280
Failure Mode	Short	Short	Short	Short	Short
Activated State	Short Circuit	Short Circuit	Clamped	Clamped	Clamped

TABLE 40 PROTECTION LEVEL VERSUS COST

TYPE DEVICE	THREAT LEVEL	PROTECTION LEVEL	PROTECTION LEVEL WITH AN EMI FILTER	UNIT COST (50M QUANTITY)
Spark Cap				
Signalite CG2-350ALT	5 K Volts	810 Volts	400 Volts	$.75
Varistors				
GE-MOV-V220MA2A	5 K Volts	1250 Volts	600 Volts	.22
GE-MOV-V130LA10A	5 K Volts	690 Volts	430 Volts	.38
Transorbs				
General Semi-Conductor - 1.5 KE200C	5 K Volts	320 Volts	195 Volts	1.55
Capacitor Suppressors				
Sprague Film .5 F 600 VDC 160P6TM-P50	5 K Volts	300 Volts	--	.22
GE Film 61F .1 F 100 VDC	5 K Volts	840 Volts	--	.08

TABLE 41 PROTECTION CONCEPT PERFORMANCE CHARACTERISTICS

CONCEPT	NOMINAL PERFORMANCE	VARIABILITY	RELIABILITY	COST
ENCLOSURES				
PERMANENT SEAMS	55 dB	± 25 dB	-20 dB	$(8-12) \times C_M$
ACCESS SEAMS	45 dB	± 15 dB	-20 dB	$(24-28) \times C_M$
SMALL APERTURES	54 dB	± 36 dB	-20 dB	$(24-28) \times C_M$
PENETRATIONS	68 DB	± 22 dB	-20 dB	$(24-28) \times C_M$
NONCONDUCTING SKIN	23 dB	± 17 dB	Unknown	$(24-28) \times C_M$
CONDUCTING SKIN	90 dB	± 10 dB		$(24-28) \times C_M$
INTERCONNECT				
CABLE SHIELDS	70 dB	± 30 dB	-20 dB	$(24-28) \times C_M$
CABLE CONNECTORS	72 dB	± 28 dB	-20 dB	$(24-28) \times C_M$
FIBER OPTIC LINKS	>100 dB	small	$> 5 \times 10^3$ hours	$(8-12) \times C_M$
TERMINAL				
FILTERS	35 dB	± 30 dB	$10^5 - 10^6$ hours	$(24-28) \times C_M$
TPDs	30 dB	± 16 dB	$10^4 - 10^6$ hours	$(24-28) \times C_M$
ELECTRO-OPTIC ISOLATORS	23 dB	± 13 dB	$\geq 5 \times 10^3$ hours	$(8-12) \times C_M$

NOTE: C_M = COST OF MATERIALS

TABLE 42 ADD-ON PROTECTION SUMMARY

SHIELDING PROTECTION

Test Case	Test Point	Test Point Name	Transient Duration	Positive Amplitude	Negative Amplitude
12MF	T1	VCON	1. mS	27. V	-30. V
12MF	T1	ICON	1. mS	180. A	-120. A
12MF	T2	VLOAD	8. uS	65. KV	-40. KV
12MF	T2	ILOAD	.15 mS	289. A	0. A
12MPT	T1	VCON	1. mS	18.5 V	-21.5 V
12MPT	T1	ICON	1. mS	155. A	-80. A
12MPT	T2	VLOAD	.5 mS	5.4 KV	-3.3 V
12MPT	T2	ILOAD	1. mS	132. A	-34. A
12MCG	T1	VCON	1. mS	14.5 V	-17. V
12MCG	T1	ICON	1. mS	122.5 A	-65. A
12MCG	T2	VLOAD	.4 mS	295. V	-30. V
12MCG	T2	ILOAD	1. mS	104. A	-26. A

TRANSZORBS PROTECTION

TEST CASE	TEST POINT/ NAME	TRANSIENT DURATION	POSITIVE AMPLITUDE
12MFT	T1/VCON	0.5 ms	105.0 V
12MFT	T1/ICON	0.5 ms	660.0 A
12MFT	T2/VLOAD	0.5 ms	285.0 V
12MFT	T2/ILOAD	0.6 ms	82.0 A

3 MIL FOIL ON FIBERGLASS PROTECTION

TEST CASE	TEST POINT/ NAME	TRANSIENT DURATION	POSITIVE AMPLITUDE
12M3MF	T1/VCON	1.0 mSec	0.6 V
12M3MF	T1/ICON	1.0 mSec	12.0 A
12M3MF	T2/VLOAD	1.0 mSec	11.2 V
12M3MF	T2/ILOAD	1.0 mSec	8.5 A

SECTION VI

RELIABILITY/MAINTAINABILITY

1. RELIABILITY AND MAINTAINABILITY FOR PROTECTION HARDWARE

Reliability is a problem at all levels of complex system design, from materials to operating systems. Reliability engineering is concerned with the time degradation of materials, equipment design and system analysis (Reference 15).

This section of the design guide looks at some of the lightning protection system components that may affect the reliability of the electrical system. The reliability of the overall electrical system must be reassessed at the time of design.

Predictions of electronic component reliability are given in MIL-HDBK-217C, "Reliability Prediction of Electronic Equipment". From the handbook reliability of electronic surge suppressor devices can be predicted. The part failure rate models in the handbook include the effects of part electrical stress, thermal stress, operating environment, quality level and complexity. Each type of suppressor using electronic components (zener diodes, capacitors, inductors, transistors, etc.) can be assessed as a series system for part failure rate calculations.

The following paragraphs provide reliability analysis data for varistor and transzorb type suppressors. Shielding reliability data is well documented in Mil-Std Handbooks and not included here. Reliability data from graphite/epoxied materials with mil-foil applications is presently being studied under various military programs. Further studies must be done to assess the reliability and maintainability problems of these advance composite materials.

a. TransZorbs[TM] (Based on the data generated by General Semiconductor Inc.)

The reliability of the TransZorb[TM] was studied extensively under NASA Contract
Nos. NAS8-30811 and NAS8-31547 in which more than 12,500,000 test pulses were
generated. Twelve hundred devices were used in the tests with 50 units per
test group. Test pulse magnitudes for two voltage types, 33V, and 190V, were
applied in increments of 25% from and up through 150% of the maximum peak
current rating of the TransZorb[TM]. The Mean Number of Peak Pulses Before
Failure (MP^{2}Bf) is used as a more accurate measure of reliability for a
transient suppressor than Mean Time Before Failure (MTBF). Figure 73
represents the reliability curves in terms of percent of maximum rated peak
pulse current versus the number of peak pulses before failure.

b. Varistors (Based on the GE-MOV[TM] varistor data)

The majority of the applications for the varistor are as transient suppressors
on the ac line. The varistor is connected across ac line voltage and biased
with a constant amplitude sinusoidal voltage. If the varistor current
increases with time, the power dissipation will also increase, with the
ultimate possibility of thermal runaway and varistor failure. Because of this
possibility, an extensive series of statistically designed tests have been
performed to determine the reliability of the GE-MCV[TM] varistor under ac bias
combined with temperature stress. This test series contained over one million
device hours of operation at temperatures up to 145°C. The average duration
of testing ranges from 7000 hours at low stress to 495 hours at high stress.
The results of this test have shown the GE-MOV[TM] varistor to be an excellent
fit to the Arrhenius model, i.e., the expected life is logarithmically realted
to the inverse of the absolute temperature (MTBF = $e^{C + K/T}$). The definition
of failure is a shift 'n V_{NOM} exceeding $\pm$ 10%. Although the GE-MOV[TM] varistor
is still functioning normally after this magnitude of shift, devices at the
lower extreme of V_{NOM} tolerance will being to dissipate more power. As
previously explained, this could ultimately lead to failure. This choice of
failure definition, in combination with the lower stresses found in
applications, should provide life estimates adequate for most design
requirements. Figure 74 illustrates the arrhenius model plot for the line
voltage and the low voltage GE-MOV[TM] varistor.

181

MEAN PEAK PULSE BEFORE FAILURE VS PERCENT OF
RATED PEAK PULSE CURRENT FOR 33V TRANSZORB™
(1N5645A)
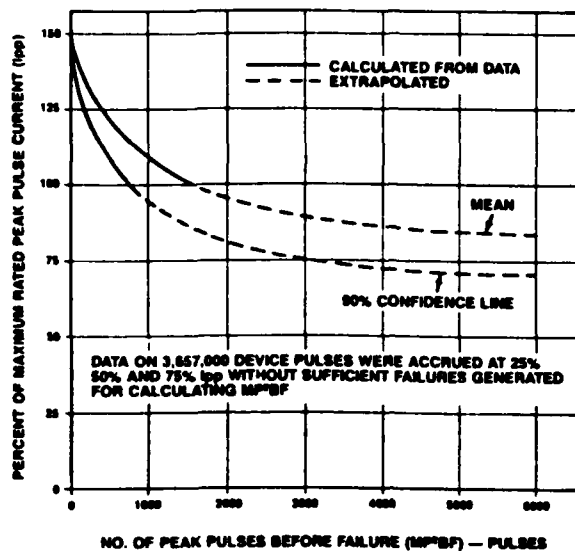
MEAN PEAK PULSE BEFORE FAILURE VS PERCENT OF
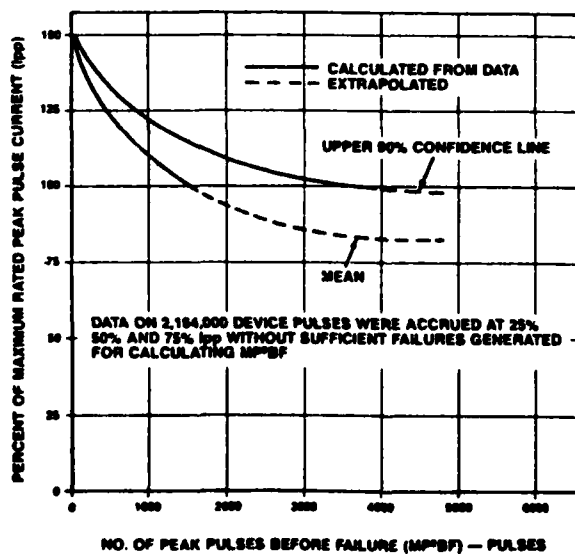RATED PEAK PULSE CURRENT FOR 190V TRANSZORB™
(1N5665)
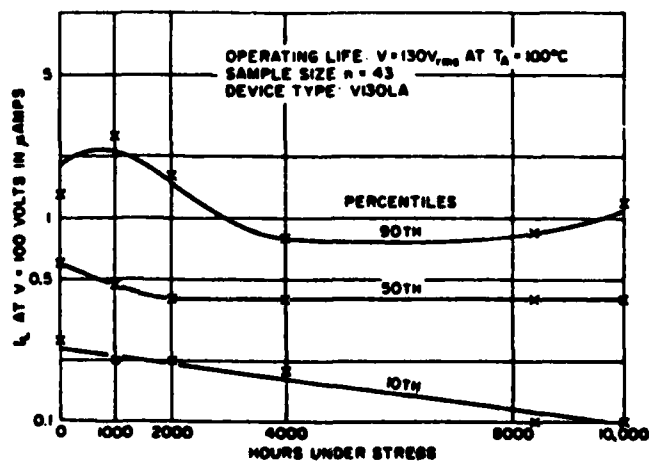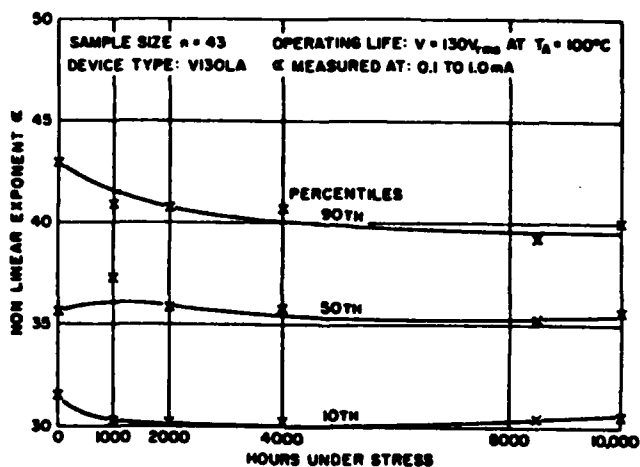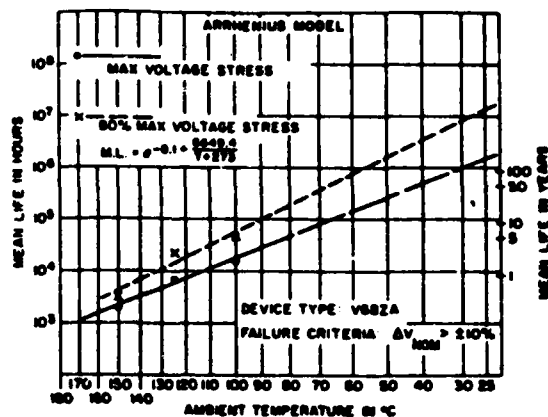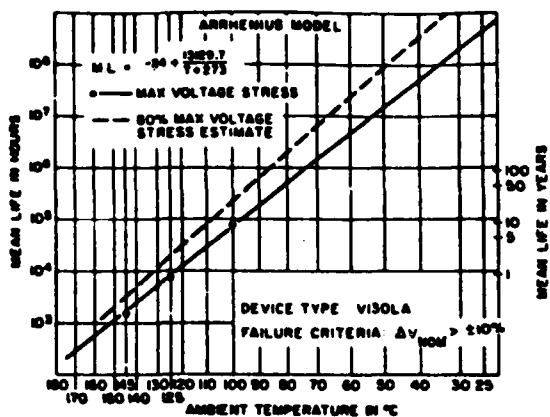
Figure 73 TransZorb^{TM} MTBF Curves

182

Figure 74 Varistor Mean Life Curves

183

This type of statistical model allows a prediction of the reliability level that can be expected at normal operating temperatures. The usual ambients are well below the temperature levels chosen for accelerated testing. For example, a V130LA10 operating at 130V ac in a 55°C environment has a mean life, from Figure 74, of about 10,000,000 hours (= 1140 years!). Using the equation gives a more precise estimate of 9,142,824 hours (1045 years). Note that at lower bias voltage even longer mean life is expected. Although the V130LA and V68ZA type devices are specifically described, the results are representative for all GE-MOV^{TM} varistors. Additional evidence of the conservative ratings of the GE-MOV^{TM} varistor is the absence of systematic or repeated field failures in over seven years of product use. As far as is known, all field failures of the GE-MOV^{TM} varistor to date have been caused by misapplication or by exceeding the transient energy capability of the varistor.

It is noted the mean life curves have a steep slope. This indicates a high activation energy. As operating temperature is dropped, the mean life increases rapidly. Also, as the voltage stress is lowered, life will increase as well. The maximum stress curve represents the worst-case condition of a model at its lowest voltage limit operated at the maximum allowable rating. In usual practice, the median of a population of devices will operate closer to the 80% voltage stress curve.

For some applications the circuit designer requires other stability information to assess the effects of time on circuit performance. Figure 74 also illustrates the stability of additional GE-MOV^{TM} varistor parameters when operated at maximum rated voltage and 100°C for 10,000 hours (= 1.15 years). The graphs indicate upper decile medium and lower decile response, furnishing useful design information on the stability of V_{NOM}, idle power drain, and non-linear exponent.

2. SAFETY

Throughout the design guide safety concerns are stressed as fundamental design concerns. All lightning protection schemes are based upon the safety and therefore survivability of the airplane and personnel within. These concerns are paramount for the all-weather mission capabilities of advanced military

aircraft. Specifically protection criteria developed for aircraft include:

a) Safety of flight
b) Mission success
c) Maintenance economics - Repair costs vs protection costs

To this end several design steps can be taken which increase the probability that system failures can be avoided. One of the most important initial design efforts is to assure that the major entry points are mechanically strong enough to withstand the lightning magnetic forces. Additionally, all wiring entry points should have protection devices that can handle the residual currents which bypass the primary protection of aircraft lightning arrestors or shunt conduction protection. These design considerations are essential in the all composite structural areas where the inherent protection of the metal airframe is not available (Reference 16).

3. DESIGN TO COST

Consideration was given to a specific design-to-cost effort in the design guide. All decisions relative to protecting the electrical system from lightning strike contained basic design-to-cost criteria.

Primary criteria (Reference 17) for providing a cost effective lightning protection design scheme include the following (which are described in detail throughout the design guide):

a. Determine the Lightning Strike Zones

Determine the aircraft surfaces, or zones, where lightning strike attachment to the aircraft is probable, and the portions of the airframe through which lightning currents must flow between these attachment points.

b. Establish the Lightning Environment

Establish the component(s) of the total lightning flash current to be expected in each lightning strike zone. These are the currents that must be protected against.

185

c. Identify Vulnerable Systems or Components

Identify systems and components that might be vulnerable to interference or
damage from either the direct effects (physical damage) or indirect effects
(electromagnetic coupling) produced by lightning.

d. Establish Protection Criteria

Determine the systems and/or components that need to be protected, and those
that need not to be protected, based upon importance to safety-of-flight,
mission reliability or maintenance factors. Establish lightning protection
pass-fail criteria for those items to be protected.

e. Design Lightning Protection

Design lightning protection measures for each of the systems and/or components
in need of protection.

f. Verify Protection Adequacy by Test

Verify the adequacy of the protection designs by laboratory qualification
tests simulating the lightning environments established in step b using the
pass-fail criteria of step d.

Decisions relative to short versus long term production and production values
are also critical in a development program. Tooling costs, mask charges and
assembly techniques can be absorbed on a larger production program. Further
studies would concern production hardware and installation techniques and
their impact.

SECTION VII

CONCLUSIONS AND RECOMMENDATIONS

1. THREAT ASSESSMENT

The circuits analyzed in Section II were based upon data obtained from
existing aircraft. The transmission line models for the wire bundles were in
general multi-conductor, to include differential mode effects. These complex
computer models were used to provide accurate calculations of the threat
waveforms, but are not appropriate for aircraft design purposes.

For preliminary assessment of the lightning threat in the design phase of an
aircraft, the following program is recommended (also see Reference 14):

o   The threat waveforms on selected wire bundles are estimated, using the
    equations of Section II.2.

o   The common mode threat obtained from step 1. is then compared with the
    inherent hardness of the exposed equipment. If the equipment hardness is
    not known, a threat waveform must be applied to the equipment, as
    described in Section II.3.

o   If the equipment hardness is insufficient to survive the lightning threat,
    then additional protection must be added. This may take the form of
    shielding or circuit protection (see Section IV).

o   If shielding is used in step 3. then the threat must be re-calculated.

o   If circuit protection is used in step 3., then the threat must be compared
    with the capacity of the protection devices, as described in Section IV.

These preliminary estimates do not include the additional shielding provided
by nearby conductors (e.g., hydraulic lines, heating ducts) in the vicinity of
the exposed wire. In order to determine that the finished protection design
for lightning induced transients is both adequate and cost-effective,

187

low-level electromagnetic tests on a prototype aircraft are required, in order to quantify this additional shielding.

2. INHERENT HARDNESS OF NORMAL DESIGN

The following three VSCF configurations were examined, (a) Generator and converter located out on the wing, (b) Generator located out on the wing with the converter in the fuselage, and (c) Generator located out on the wing without the converter. On an all aluminum wing with twelve meters of excited feeders behind a fiberglass leading edge and a 50% loaded bus, a wingtip strike produced these respective positive amplitude voltage and current transients (65.KV/289.A, 6.5mV/.11mA, 58.KV/280.A) on the power bus. This comparison shows the value of the converter in circuit (b) as an inherent transient suppressor which allows an insignificant transient level to reach the power bus. For the other two circuits, add on protection will be required.

In a detailed examination of the VSCF worst case (Baseline Generator and Converter on Wing), two orders of magnitude improvement in transient suppression at the bus load was gained by replacing the fiberglass leading edge with a graphite epoxy leading edge. A third order of magnitude improvement over the fiberglass leading edge was made by adding a layer of 3 mil foil to the fiberglass. Positive amplitude voltage and current transients for the baseline fiberglass, graphite epoxy, and 3 mil foil on fiberglass leading edges are 65.KV/289.A, 410.CV/305.0A, 11.2V/8.5A, respectively. The amount of suppression obtained with respect to the three leading edge material types shows that if a fiberglass leading edge is incorporated, transient suppression protection will be required. When a graphite epoxy or derivative (i.e., graphite laminate, etc.) leading edge is incorporated, additional protection may not be required. If 3 mil foil is incorporated with the fiberglass on the leading edge, additional transient protection will not be required. This conculsion agrees with the fact that with the present day metallic leading edge, no problems have been encountered with coupled transients damaging equipments tied to the power bus.

Changing the length of the excited feeder in the fiberglass leading edge case for both a half and full loaded bus, indicated that the current and voltage

transients increase linearly with feeder length. See Figures 26 and 27.
Similar conclusions can be drawn with the substitution of the graphite epoxy
and 3 mil foil on fiberglass leading edges, namely, that with an increase in
exposed feeder length, the magnitude of the coupled transient increases.

Further examination of the graphite epoxy leading edge showed the coupled
transient to become smaller as the thickness of the graphite epoxy material
increased. When the distance separating the graphite epoxy leading edge and
the wire bundle increased, the transient coupled onto the leading edge power
feeders decreased. See Figures 28 and 29.

In examination of the power feeder circuit of the F15 with respect to an all
aluminum and then a graphite/epoxy fuselage, the aperture coupled transients
from the aluminum fuselage are larger than the diffusion coupled transients of
the graphite/epoxy fuselage. Figures 36 and 37 plot the negative amplitude
voltage and current peaks monitored at the generator terminals and main bus,
respectively, for a varying length of excited feeder for the diffusion coupled
transients. As the two material types of F15 airplane were analysed with
different coupling mechanisms for their respective skin material, no direct
comparison or conclusions can be drawn. However, if wire bundles are routed
across access doors (aperture coupling) as was analysed in the aluminum
fuselage case, protection will be required. For the diffusion coupling with
the graphite epoxy fuselage case, transient protection will be required only
if the length of the exposed feeder exceeds a certain length.

Fiber optic systems are well suited to either point-to-point links or data bus
systems and can handle digital data transmission or analog signal
transmission. Besides EMI/EMP immunity, the primary benefits of using fiber
optics will be weight savings, increased bandwidth, and elimination of ground
problems.

In developing lightning hardness for conventional and advanced equipment, wire
routing should be one of the first items designed into an airplane for maximum
utilization of the inherent airframe shielding. Equipment should be located
to minimize the exposure of interconnecting wiring. Also, equipment should be
located in the areas of the airplane which have the lowest penetration of

electric fields and should be well grounded to structure to suppress E-field coupling.

3. ADD-ON PROTECTION FOR INDUCED TRANSIENTS

In examining add on protection techniques for the all aluminum wing, shielding was added to the baseline 12 meter feeder behind the fiberglass leading edge. For the VSCF generator and converter on wing circuit, both pigtail and circumferential connections were used on the shields. The pigtail shield effectively suppressed the transient one order of magnitude from the unprotected case while the circumferential grounded shield reduced the transient by two orders of magnitude. The positive amplitude voltage and current peaks for the unprotected, pigtail shield, and circumferentially grounded shield cases are 65.0 KV/289.0 A, 5.4 KV/132.0 A, 295.0 V/104.0 A. These results show that even with the addition of pigtail terminated shielding, additional transient protection will be required. Circumferentially grounded shields should provide sufficiant protection for leading edge wire bundles, especially when the airframe inherent shielding is taken into consideration. Of the different types of shields, the solid shield inherently provides better shielding than does a braided shield, while a braided shield is more effective than a spiral-wrapped shield.

All types of overvoltage devices, tranzorbs, varistors, zener diodes, etc., inherently operate by reflecting a portion of the transient energy back toward the source and by conducting the rest into another branch. Using transzorbs at the bus in the baseline VSCF circuit reduced the transient from the unprotected fiberglass leading edge case two orders of magnitude from 65.0 KV/289.0 A to 285.0 V/82.0 A. As an alternate to shielding the wire bundles, add on protection of transzorbs is a very promising alternative for providing the necessary protection of the power bus from induced transients. A hand calculation design procedure and a computer aided design procedure for sizing transzorbs for lightning protection is documented in Section IV. Designing lightning protection using capacitor filters is also documented in Section IV.

Uncoated graphite composites and composites coated with foil, screen, or flame

spray must be electrically joined to neighboring structure, so as to form
closed conducting shells, if they are to contribute to the shielding of the
interior. Screens and foils can be incorporated within, or on the surface of,
composites during fabrication without impacting the processing of the
material (Reference 8).

4. THE DESIGN GUIDE

Reference 14, "The Protection of Electrical Systems from EM Hazards - Design
Guide" was written based on the work accomplished in Phase I (Sections II-IV)
and the Phase II Trade Study (Section V). The design guide is summarized in
Section V. The design guide details electrical system protection alternatives
and provides the design engineer with sufficient data to make an appropriate
selection for his application. Examples of how to use the design guide are
included.

5. RECOMMENDATIONS

The recommended approach to lightning design is outlined in Section V (and the
Design Guide Reference 14). Hand calculations for threat definition, using
the equations of Section II.2, should be used instead of elaborate computer
programs. When the threat for a given LRU (line replaceable unit) is defined,
the equipment hardness should be verified by test.

Direct attachment of the lightning strike to power system wiring must be
prevented by incorporation of protective coatings. (See Section IV.2) on
surfaces which satisfy the following criteria:

1. The surface is non-metallic
2. Power wires are underneath
3. The surface is in an attachment zone (See Section II)

The TransZorb^{TM} appears to be the most suitable voltage suppression device for
lightning protection. We recommend a balanced protection approach for wiring
directly exposed to lightning induced fields. The balanced protection will be
a combination of:

1. Control of wire routing
2. Wire/area shielding
3. Voltage suppression devices   191

REFERENCES

1. R.Force, et al. "Investigation of Effects of Electromagnetic Energy on
   Advanced Composite Aircraft Structures and their Associated
   Avionic/Electrical Equipment," The Boeing Company, D180-20186-4 September
   1977.

2. R.H. Golde, Editor, "Physics of Lightning," Volume 1, 1977.

3. N. Cianos and E.T. Pierce, "A Ground-Lightning Environment for Engineering
   Usage," Stanford Research Institute Technical Report 1, SRI Project 1834,
   August 1972.

4. H.G. Carlson and R.N. Wright, "VSCF Aircraft Electrical Power," General
   Electric Company Aircraft Equipment Division, Binghamton, New York.

5. S.P. Sauve, et.al. "Study of Fiber Optics Standardization, Reliability,
   and Application," Prepared for NASA, Boeing Aerospace Company, January
   1980.

6. J.A. Plumer, "Protection of Aircraft Avionics from Lightning Indirect
   Efforts," Advanced Group for Aerospace Research and Development (AGARD),
   AGARD Lecture Series #110, Atmospheric Electricity-Aircraft Interaction,
   SRI International, Menlo Park, CA, June 24-25, 1980.

7. C. Case and J. Miletta, "Capacitor Failure Due to High-Level Electrical
   Transients", Harry Diamond Laboratories Technical Memorandum HDL-TM-75-25,
   December 1975.

8. D.Strawe and L. Piszker, "Interaction of Advanced Composites with
   Electromagnetic Pulse (EMP) Environment," AFWL-TR-75-141, The Boeing
   Company, September, 1975.

9. S.D. Schneider, et. al., Vulnerability/Survivability of Composite
   Structures-Lightning Strike," AFFDL-TR-77-127, Volume 1, The Boeing
   Company, February, 1978.

10. SAE Committee AE4L, "Lightning Test Waveforms and Techniques for Aerospace Vehicles and Hardware," Currently MIL-STD-1757, June 20, 1978.

11. Presto Digital Computer Code Users Guide, DNA 3898F-1, Prepared for: Defense Nuclear Agency, Washington DC, Under Contract: DNA001-77-C-0138., May 1977.

12. SAE Committee AE4L, "Test Waveforms and Techniques for Assessing the Effects of Lightning-Induced Transients," to be published.

13. "Lightning Protection of Aircraft," F.A. Fisher and J.A. Plumer, NASA Publication 1008 (1977).

14. D. L. Sommer, et. al., "Protection of Electrical Systems from Hazards - Design Guide," AFWAL-TR-81-2118, January 1982.

15. "Reliability Prediction of Electronic Equipment," MIL-HDBK-2170, 1979.

16. O. M. Clark, "Long-Term Pulse Life and Design Criteria for TransZorb[TM] Transient Voltage Suppressors."

17. J. C. Hey, Editor, "Transient voltage Suppression Manual," General Electric, 1978.

APPENDIX A

EQUATIONS FOR LIGHTNING THREAT ESTIMATION

Consider a wire or wire bundle exposed to lightning fields. These fields may
either be the exterior fields on the aircraft surface (e.g., front or rear
spar) or may be interior fields due to coupling through apertures, joints or
poorly conducting material. For purposes of estimating the common mode
threat, we need only consider the single conductor case. Given the common
mode threat, one may then define a simulation test as described in Section
II.2.b. The differential mode transients are determined primarily by the
configuration of the wire bundle and the terminating loads. The wire bundle
and terminating loads will be adequately simulated in a properly defined test.
Hence, a common mode test is a good simulation of the actual threat.

Figure A depicts the electromagnetic problem, i.e., a wire bundle of length l
and height h above the ground plane, with exposure to lightning-induced
electromagnetic fields. The Norton equivalent circuit is shown in Figure B.
We are interested in the transient current or voltage waveforms seen at the
terminating load, Z_T. The quantities in Figure B are defined as follows:

$$Z_{IN} = \frac{Z_C (Z_C \sinh \gamma L + Z_L \cosh \gamma L)}{(Z_C \cosh \gamma L + Z_L \sinh \gamma L)}$$

Z_C = Characteristic impedance of wire or wire bundle (common mode)

Z_L = Load at "far end" of wire

$$\gamma = \sqrt{Y_1 Z_1} = \sqrt{j w C_1 (j w L_1 + R_1)}$$

$L_1 = Z_C/\beta_{rel} V$ = inductance/length

$C_1 = 1/Z_C \beta_{rel} V$ = capacitance/length

$V = 3 \times 10^8$ m/sec

β_{rel} = relative velocity for wire or wire bundle (common mode)
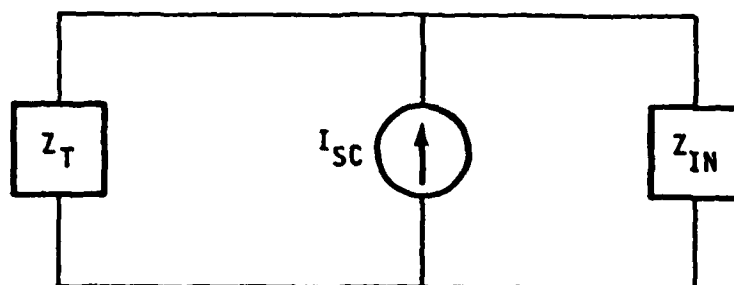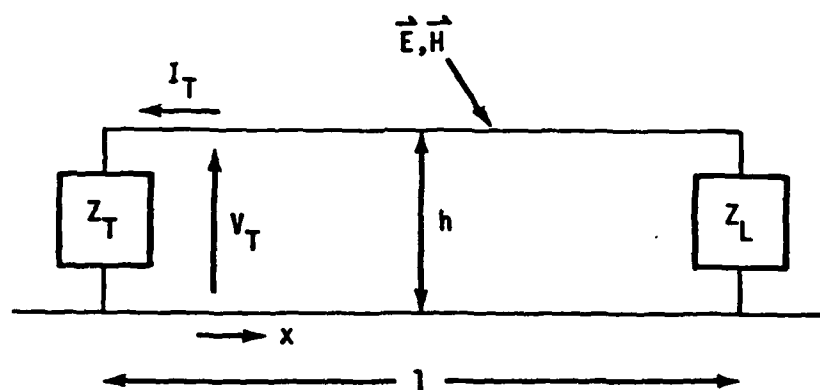
R_1 = resistance/length

194

FIGURE B

FIGURE A

$$I_{SC} = -jw\mu \int h H_t \, G \, dx - \int h \, E_n \frac{\partial G}{\partial x} \, dx$$

$h(x)$ = height of wire above ground plane

$H_t(x)$ = component of tangential magnetic field perpendicular to wire at x

$E_n(x)$ = component of electric field normal to ground plane at x

$$G(x) = \frac{1}{Z_C} \cdot \frac{Z_C \cosh \gamma(1-x) + Z_L \sinh \gamma(1-x)}{Z_C \sinh \gamma 1 + Z_L \cosh \gamma 1}$$

$$\frac{\partial G}{\partial x} = \frac{-\gamma}{Z_C} \cdot \frac{Z_C \sinh \gamma(1-x) + Z_L \cosh \gamma(1-x)}{Z_C \sinh \gamma 1 + Z_L \cosh \gamma 1}$$

For purposes of simplicity, let us restrict our considerations to the following cases:

CASE 1: $Z_L = 0$ V_{OC}, I_{SC} at Z_T

CASE 2: $Z_L = \infty$ V_{OC}, I_{SC} at Z_T

and further, consider the following coupling mechanisms for exposure of the wire:

(1) directly exposed wire
(2) slot
(3) resistive joint
(4) diffusion

Approach: The lightning spectrum is represented by a double exponential. The end result of the following analysis will be a collection of formulas for V_{OC}, I_{SC} for the two cases and for mechanisms which have the form

$$(V, I) = KL \quad (\dot{I}_L + \alpha * \text{ (damped sinusoid)})$$

or

$$= K_R \quad (I_L + \beta * \text{ (damped sinusoid)})$$

196

Where I_L is the lightning current waveform and the damped sinusoid is determined by the quarter-wave or half-wave resonance of the wire or wire bundle (common mode). In obtaining these expressions, we will make the assumptions listed in Table A. These assumptions are justified on the basis of providing a <u>reasonable</u> worst-case estimate of the lightning threat.

Table A - Assumptions for Derivation of Equations

1. Airframe resonances are negligible in comparison to wire bundle reasonances.

2. The first wire bundle resonance is well above ($\sim 10x$ or more) the upper turning frequency of the double-exponential fit to the lightning spectrum ($\sim .5$ MHZ). Note that 5 MHZ corresponds to a length of 54 meters for a quarter wave (lowest possible frequency) resonance of a wire with a relative propogation velocity of .9 times the speed of light. For wire bundles much longer than 54 m, say 100 m, then the assumption may be questionable. Of course, most aircraft wire bundles are shorter than 100 m.

3. The contribution of the sources distributed along the wire will be assumed to add in phase to the V_{oc}, I_{sc} at the termination.

4. Only the first resonance of the wire bundle (common mode) will be considered. The analysis could be extended to include higher order modes, but there is not sufficient knowledge of the high frequency content of the lightning specturm to warrant it.

Derivation of Equations

Suppose we have the following spectra:

197

$$S_1(w) = jw \, I_L(w) \, F(w)/\cosh \Upsilon l$$
$$S_2(w) = jw \, I_L(w) F(w)/Z_C \sinh \Upsilon l$$
$$S_3(w) = I_L(w) \, F(w)/\cosh \Upsilon l$$
$$S_4(w) = I_L(w) \, F(w)/Z_C \sinh \Upsilon l$$

with the following conditions:

(a) $I_L = I_0 \left(\dfrac{1}{\alpha+jw} - \dfrac{1}{\beta+jw} \right)$, $\alpha \ll \beta \ll W_{res}$,

where W_{res} is the first resonance for cosh, sinh.

(b) $F(w) \Big|_{w = -j\beta} \doteq F(o)$ follows if $F = F(\Upsilon l)$ and $\dfrac{\beta L}{C} \ll 1$

note that $\beta \sim \pi \times 10^6$, so $\dfrac{\beta l}{C} = \dfrac{\pi \times 10^6 \, lm}{3 \times 10^8} = \left(\dfrac{\pi}{3}\right) \times 10^{-2} \, lm,$ $\quad lm$ = wire length in meters

Then one may show that:

(A-1) $\quad S_1(t) = F(o) \, \dot{I}_L(t) - \dfrac{4}{\pi} \, \overset{\circ}{I}_{pk} \, e^{-W_0 t/2Q} \, (A \cos_{Rt} - B \sin)$

(A-2) $\quad S_2(t) = \dfrac{F(o)}{L_W} \, I_L(t) + \dfrac{2}{\pi} \, \dot{I}_{pk} \, e^{-W_0 t/2Q} \, (A \sin + B \cos)/Z_C$

(A-3) $\quad S_3(t) = F(o) I_L(t) - \dfrac{4}{\pi} \dfrac{\dot{I}_{pk}}{W_0} \, e^{-W_0 t/2Q} \, (A \sin + B \cos)$

(A-4) $\quad S_4(t) = \dfrac{F(o)}{L_W} Q_L(t) - \dfrac{2}{\pi} \dfrac{\dot{I}_{pk}}{W_0} \, e^{-W_0 t/2Q} \, (A \cos - B \sin)/Z_C$

$A = \operatorname{Re} F(W_+)$, $B = \operatorname{Im} F(W_+)$, $\cos = (W_R t)$, $\sin (W_R t)$,

$W_+ = W_R + JW_0/2Q$, $W_R = W_0 \sqrt{1 - (1/2Q)^2}$, $Q = W_0(L_1/R_1)$

$W_0 = \pi \beta_{rel} \, v/2l$ for S_1 and S_3, $W_0 = \pi \beta_{rel} \, v/l$ for S_2 and S_4

Now consider the four coupling mechanisms:

1. Directly Exposed Wire:

$$I_{sc} = jw\mu \int_h H_t G \, dx + \int_h E_n \frac{\partial G}{\partial x} \, dx$$

a. $Z_T = 0$ $\quad G = \cosh \gamma (1-x)/Z_c \sinh \gamma 1$

$$\frac{\partial G}{\partial x} = -\gamma \sinh \gamma (1-x)/Z_c \sinh \gamma 1$$

$$V_{oc} = jw \, I_L \, F(w)/\cosh \gamma 1$$

$$I_{sc} = jw \, I_L \, F(w)/Z_c \sinh \gamma 1, \text{ where}$$

$$F(w) = \mu \int_h (H_t/I_L) \cosh \gamma (1-x) \, dx - \frac{\mu}{\beta_{rel}} \int_h (E_n/Z_0 \, H_t)(H_t/I_L) \sinh \gamma (1-x) \, dx$$

define $F_c(w_+) = F(w)\Big|_{\cosh \gamma 1 = 0}$, $F_s(w_+) = F(w)\Big|_{\sinh \gamma 1 = 0}$, then

(A-5) $\quad F_c(w_+) = \mu \int_h (H_t/I_L) \sin kx \, dx - j \frac{\mu}{\beta_{rel}} \int_h (Z_s/Z_0)(H_t/I_L) \cos kx \, dx$

(A-6) $\quad F_s(w_+) = \mu \int_h (H_t/I_L) \cos kx \, dx + \frac{j\mu}{\beta_{rel}} \int_h (Z_s/Z_0)(H_t/I_L) \sin kx \, dx$

$F(o) = \mu \int_h h(x) dx/C(x)$, where

$Z_s(x) = E_n(x)/H_t(x)$, β_{rel} = relative velocity for wire bundle

$C(x)$ = effective circumference at x

$H_t(x)/I_L = (I_A(x)/I_L)/C(x)$

$I_A(x)$ = lightning current in airframe at x.

If we neglect airframe resonances, it may be shown that:

$Z_s \longrightarrow Z_L/Z_A$, $I_A/I_L \longrightarrow 1$

Z_L = characteristic impedance of lightning channel

Z_A = characteristic impedance of airframe

Now $|\cos kx| < 1$ and $|\sin kx| < 1$, so upper limits for the integrals appearing in equations A-5 and A-6 are:

$$|Re \, F_c| < F(o) \qquad\qquad |Re \, F_s| < F(o)$$
$$|Im \, F_c| < \frac{1}{\beta_{rel}} \frac{Z_L}{Z_A} F(o) \qquad |Im \, F_s| < \frac{1}{\beta_{rel}} \frac{Z_L}{Z_A} F(o)$$

This is the third assumption of Table A. This gives the results for $Z_T = 0$:

$$V_{oc}(t) = F(o) \, \dot{I}_L(t) + \frac{4}{\pi} \dot{I}_{pk} \, e^{-w_0 t/2Q}(A \cos w_R t - B \sin w_R t),$$

where $w_0 = 2\pi fo$, $\qquad\qquad\qquad\qquad w_R = w_0 \sqrt{1-(\frac{1}{2Q})^2}$

$$F(o) = \mu \int h \, dx/C(x), \quad f_o = \text{quarter wave resonant frequency}$$
exposure

$$|A| < F(o) \qquad\qquad |B| < \frac{1}{\beta_{rel}} \frac{Z_L}{Z_A} F(o)$$

$$I_{sc}(t) = \frac{F(o)}{L_w} I_L(t) + \frac{2}{\pi} \dot{I}_{pk} e^{-w_o t/2Q}(A \sin + B \cos)/Z_c, \quad w_o = 2\pi f_o,$$

f_o = half-wave resonance where, from A-6, $|A| < F(o)$ and $|B| < \frac{1}{\beta_{rel}} \frac{Z_L}{Z_A} F(o)$

For determining equipment susceptibility, the three waveforms should be added incoherently, using the upper limits for A and B .

$$\text{b.} \quad Z_T = \infty \qquad G = (\sinh \Upsilon(1-x)/Z_c)/\cosh \Upsilon 1$$
$$\partial G/\partial x = (-\Upsilon/Z_c) \cosh \Upsilon(1-x)/\cosh \Upsilon 1$$
$$I_{sc} = jw \, I_L \, (F(w)/Z_c)/\cosh \Upsilon 1$$
$$V_{oc} = jw \, I_L \, (Z_c F(w))/Z_c \sinh \Upsilon 1$$

$$F(w) = \mu \int h \, (H_t/I_L) \sinh \Upsilon(1-x) \, dx - \frac{\mu}{\beta_{rel}} \int h \, (Z_s/Z_0) \, (H_t/I_L) \cosh \Upsilon(1-x) \, dx$$

$$F_c(w_+) = j\mu \int h \, (H_t/I_L) \cos kx \, dx + \frac{\mu}{\beta_{rel}} \int h \, (Z_s/Z_0) \, H_t/I_L \sin kx \, dx$$

$$F_s(w_+) = j\mu \int h \, (H_t/I_L) \sin kx \, dx - \frac{\mu}{\beta_{rel}} \int h \, (Z_s/Z_0) \, H_t/I_L \cos kx \, dx$$

as before, this gives:

(A-7) $\quad |A| < \frac{1}{\beta_{rel}} \frac{Z_L}{Z_A} F(o); \qquad |B| < F(o)$

$$F(o) = \mu \int h \, dx/C(x) \text{ for } F_c(w_+), F_s(w_+).$$

so $I_{sc} = \frac{F(o)}{Z_c} I_L - \frac{4}{\pi} \frac{\dot{I}_{pk}}{Z_c} e^{-w_o t/2Q}(A \cos w_R t - B \sin w_R t)$

$w_o = 2\pi f_o$, f_o = quarter wave resonance

$V_{oc} = \frac{Z_c F(o)}{L_w} I_L + \frac{2}{\pi} \dot{I}_{pk} e^{-w_o t/2Q}(A \sin w_R t + B \cos w_R t)$

200

$w_0 = 2\pi f_0$, $f_0 =$ half-wave resonance

A , B limited by A-7,

2. Slot: (See Appendix C)

$I_{sc} = K \, V_{slot} \, G$, $V_{slot} = jw \, L_{slot} \, I_A$

$I_A =$ lightning current in airframe at slot

K, L_{slot} defined in Appendix C

$G =$ Green's function defined in Figure B

a. $Z_T = 0$ $G = \cosh\gamma(1-x)/Z_c \sinh\gamma 1$

$V_{oc} = jw \, I_L \, F(w)/\cosh\gamma 1$

$I_{sc} = jw \, I_L \, F(w)/Z_c \sinh\gamma 1$

$F(w) = K \, L_{slot} \, (I_A/I_L) \cosh\gamma(1-x)$

$F(o) = K \, L_{slot}$

$F_c(w_+) = K \, L_{slot} \, (I_A/I_L) \sin kx$

$F_s(w_+) = K \, L_{slot} \, (I_A/I_L) \cos kx$

Therefore, B=0, $|A| < K \, L_{slot}$ (ignoring airframe resonance), so that

$\lambda/4$ resonance: $V_{oc} = K \, L_{slot} \, \dot{I}_L - \dfrac{4}{\pi} \, \dot{I}_{pk} \, e^{-w_0 t/2Q_A} \cos w_R t$

$\lambda/2$ resonance: $I_{sc} = K \, \dfrac{L_{slot}}{L_w} \, I_L + \dfrac{2}{\pi} \, \dot{I}_{pk} \, \dfrac{e^{-w_0 t/2Q_A}}{Z_c} \sin w_R t$

b. $Z_T = \infty$

$G = \sinh\gamma(1-x)/Z_c \cosh\gamma 1$

$I_{sc} = jw \, I_L \, (F(w)/Z_c)/\cosh\gamma 1$

$V_{oc} = jw \, I_L \, Z_c \, F(w)/Z_c \sinh\gamma 1$

$F(w) = K \, L_{slot} \, (I_A/I_L) \sinh\gamma(1-x) \xrightarrow{w \to o} \dfrac{jw(1-x) \, K \, L_{slot}}{\beta_{rel} C}$

$I_{sc} \xrightarrow{w \to o} (jw)^2 \, C_w \, K \, L_{slot} \, (1 - \dfrac{x}{1}) \, I_L$

$V_{oc} \xrightarrow{w \to o} jw \, K \, L_{slot} \, (1 - \dfrac{x}{1}) \, I_L$

$F_c(w_+) = j \, K \, L_{slot} \, (I_A/I_L) \cos kx$

$F_s(w_+) = -j \, K \, L_{slot} \, (I_A/I_L) \sin kx$

Therefore, A =0, $|B| < K \, L_{slot}$ (ignoring airframe resonance), so that

$\lambda/4$ resonance $I_{sc}(t) = K L_{slot} (1 - \frac{x}{1}) C_w \ddot{I}_L + \frac{4}{\pi} \dot{I}_{pk} B \bar{e}^{w_0 t/2Q} \sin w_R t / Z_c$

$\lambda/2$ resonance $V_{oc}(t) = K L_{slot} (1 - \frac{x}{1}) \dot{I}_L + \frac{2}{\pi} \dot{I}_{pk} B e^{-w_0 t/2Q} \cos W_R t$

3. Resistive joint

$I_{sc} = K V_J G$, $V_J = R_J I_A$, K defined in Appendix C
$R_J = W_1/(Y_J C)$, where Y_J = joint admittance/length
C = effective circumference of airframe at joint

a. $Z_T = 0$

$V_{oc} = I_L F(w)/\cosh Y 1$
$I_{sc} = I_L F(w)/Z_c \sinh Y 1$
$F(w) = K R_J (I_A/I_L) \cosh Y (1-x)$, $F(o) = K R_J$
$F_c(w_+) = K R_J (I_A/I_L) \sin kx$
$F_s(w_+) = K R_J (I_A/I_L) \cos kx$
Therefore, B=0, $|A| < K R_J$ (ignoring airframe resonances), so that

$\lambda/4$ resonance: $V_{oc} = K R_J I_L - \frac{4}{\pi w_0} \dot{I}_{pk} A e^{-w_0 t/2Q} \sin w_R t$

$\lambda/2$ resonance: $I_{sc} = \frac{K R_J}{L_w} Q_L(t) - \frac{2}{\pi w_0} \dot{I}_{pk} \frac{A}{Z_c} e^{-w_0 t/2Q} \cos w_R t$

b. $Z_T = \infty$

$I_{sc} = I_L (F(w)/Z_c)/\cosh Y 1$
$V_{oc} = I_L Z_c F(w)/Z_c \sinh Y 1$
$F(w) = K R_J (I_A/I_L) \sinh Y (1-x) \xrightarrow[w \to 0]{} \frac{jw (1-x) K R_J}{\beta_{rel} C}$
$I_{sc} \xrightarrow[w \to 0]{} jw C_w K R_J (1 - \frac{x}{1}) \dot{I}_L$
$V_{oc} \xrightarrow[w \to 0]{} K R_J (1 - \frac{x}{1}) I_L$

202

$$F_c(w_+) = j K R_J (I_A/I_L) \cos kx$$
$$F_s(w_+) = j K R_J (I_A/I_L) \sin kx$$

Therefore, $A=0$, $|B| < KR_J$ (ignoring airframe resonances), so that

$\lambda/4$ resonance: $\quad I_{sc} = K R_J (1- \frac{x}{1}) C_w \dot{I}_L -\dfrac{4 \dot{I}_{pk}}{\pi w_0} \dfrac{B}{Z_c} e^{-w_0 t/2Q} \cos w_R t$

$\lambda/2$ resonance: $\quad V_{oc} = K R_J I_L (1- x/1) + \dfrac{2 \dot{I}_{pk}}{\pi w_0} B e^{-w_0 t/2Q} \sin w_R t$

4. Diffusion: $(E_n = o)$

$$I_{sc} = \int E_i \; G \; dx \quad \text{exposed area}$$

E_i = interior E-field due to diffusion through a conductive material

E_i/J_s = transfer impedance for material

a. $Z_T = 0$

$V_{oc} = I_L F(w)/\cosh \gamma 1$

$I_{sc} = I_L F(w)/Z_c \sin \gamma 1$

$F(w) = -\int (E_i/J_s)(J_s/I_A)(I_A/I_L) \cosh \gamma (1-x) \, dx$

E_i/J_s = constant along path = $Z_m (w)$

$J_s/I_A = 1/C(x)$, so that assuming the material thickness is small compared to a skin depth at the upper turning frequency of the lightning spectrum, we have:

$F(o) = Z_M(o) \int dx/C(x)$

$F_c(w_+) = Z_M(w_0) \int (I_A/I_L) \sin kx \, dx/C(x)$

$F_s(w_+) = Z_M(w_0) \int (I_A/I_L) \cos kx \, dx/C(x)$

Now $Z_M (w_0)$ is in general complex. Hence, the approximations used in cases 1-3 for the real and imaginary parts of $F(w_+)$ yield:

$F_c(w_+) = A + jB, |A| < |Re (Z_M(w_0))| \int dx/C(x), |B| < |Im (Z_M(W_0))| \int dx/C(x)$

and likewise for $F_s(w_+)$. Therefore,

$\lambda/4$ resonance: $V_{oc} = F(o) I_L - \dfrac{4 \dot{I}_{pk}}{\pi w_0} e^{-w_0 t/2Q}(A \sin w_R t + B \cos w_R t)$

203

$\lambda/2$ resonance: $I_{sc} = \dfrac{F(o)}{L_w} Q_L - \dfrac{2}{\pi} \dfrac{\dot{I}_{pk}}{w_o} e^{-w_o t/2Q}(A \cos - B \sin)/Z_c$

b. $Z_T = \infty$

$$I_{sc} = I_L \ (F(w)/Z_c)/\cosh \Upsilon 1$$
$$V_{oc} = I_L \ (Z_c F(w))/Z_c \ \sinh \Upsilon 1$$
$$F(w) = Z_M(w) \int (I_A/I_L) \ \sinh \Upsilon (1-x) \ dx/C(x)$$

Assuming the material is thin compared to a skin depth at the upper turning frequency of the lightning spectrum, the low-frequency components are:

$$I_{sc} = (Z_M(o) \ C_w \int (1-x/1) \ dx/C(x)) \ \dot{I}_L$$
$$V_{oc} = (Z_M(o) \int (1-x/1) \ dx/C(x)) \ I_L$$
$$F_c(w_+) = j \ Z_M(w_+) \int (I_A/I_L) \ \cos kx \ dx/C(x)$$
$$F_s(w_+) = - j \ Z_M(w_+) \int (I_A/I_L) \ \sin kx \ dx/C(x)$$

As for the $Z_T = 0$ case, have $F = A + jB$, and

(A-8) $\quad |A| < |Im \ Z_M(w_o)| \int dx/C(x) \ |B| < |Re \ (Z_M(w_o))| \int dx/C(x)$
this gives:

$\lambda/4$ resonance: $I_{sc} = Z_M(o)KC_w \dot{I}_L - \dfrac{4}{\pi} \dfrac{\dot{I}_{pk}}{w_o} e^{-w_o t/2Q}(A \sin w_R t + B \cos w_R t)$

$\lambda/2$ resonance: $V_{oc} = Z_M(o) \ K \ I_L - \dfrac{2}{\pi} \dfrac{I_{pk}}{w_o} e^{-w_o t/2Q} A \cos w_R t + B \sin w_R t$,

where $K = \int (1-x/1) \ dx/C(x)$, C_w = total capacitance of bundle, and A and B are bounded above as indicated in A-8.

204

CAPACITIVE COUPLING TO WINDSHIELD HEATER ELEMENT

The windshield heater element is equivalent to a flush-mounted disc antenna. The geometry is indicated below:
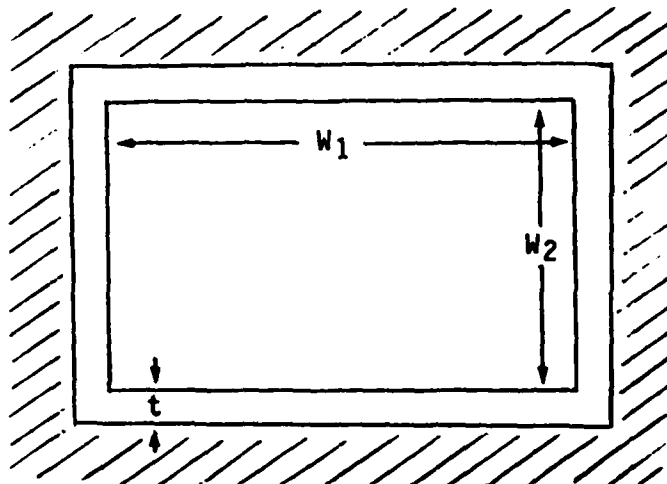
Geometry for Windshield Heater Element

The conductive element couples capacitively to the normal electric fields on the aircraft exterior. The circuit wires attach to the element via bus bars at the top and bottom. Hence, the source model is given by:
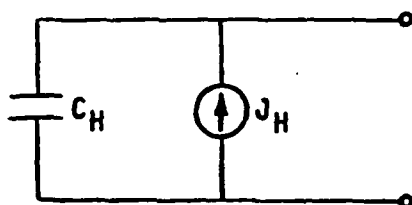
, where

$$C_H = \left[1.58 + \ln \left(^a/t\right)\right] \epsilon_0 a$$

$$a = \sqrt{\frac{W_1 W_2}{\pi}}$$

$$J_H = \left(jw\epsilon_0\right)(A)E_n, \quad A = \pi t a / \ln \left(1 + \, ^t/a\right) \cong \pi a^2 = \text{AREA of element}$$

$E_n =$ normal electric field on aircraft exterior at
location of windshield (obtained from transmission
model for aircraft - lightning column interaction)

APPENDIX C

MAGNETIC COUPLING THROUGH CARGO DOOR SLOT

This problem breaks into two parts. First, one must compute the voltage across the center of the slot. Second, one must obtain the interior magnetic fields induced by this slot voltage.

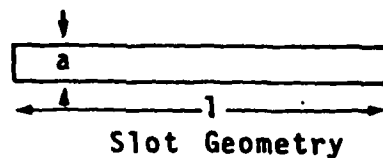The slot is complementary to an electric dipole. The equations for the slot are as follows:

$$V_{Slot} = (Z_{Slot})I_{sc}, \quad I_{sc} = l_{eff} \times J_{sc}$$

J_{sc} = Current density across shorted aperture

$$l_{eff} = \int_0^1 V(x)dx \, / V_{mid}$$

V_{Slot} = Voltage across center of slot

$V(x)$ = Voltage distribution on slot

Slot Geometry

$$Z_{Slot} = Z_0^2 / 4 Z_{dipole} \qquad Z_0 = 120\pi \text{ ohms}$$

$$Z_{dipole} = R + jwL + \frac{1}{JwC}$$

$R = 73$ ohms

$$L = (1 \, \mu o / \pi) K$$

$$C = (1 \, \epsilon o / \pi)/K$$

$$K = \frac{1}{\pi} \left[\ln\left(\frac{2 \, 1}{a}\right) - 1 \right] \left/ \left[1 + \frac{\ln 2}{\ln\left(\frac{2 \, 1}{a}\right) - 1} \right] \right.$$

This expression is a good approximation through first slot resonance. For example, for a 1 meter slot, first slot resonance occurs at 150 MHz. For frequencies well below resonance, have:

206

$$Z_{slot} = Z_0^2/4 \times \left(\frac{1}{jwc}\right) = jw\left(Z_0^2 C/4\right) = jwL_{slot}$$

Thus, in the low frequency limit, the slot is inductive. The voltage across the slot center in the low frequency limit is:

$$V_{oc} = jwL_{slot} \times l_{eff} \times J_{sc}$$

$$L_{slot} = (120\pi)^2 C/4, \quad C = (\epsilon_o l/\pi K)$$

$$K = \text{Same as above}$$

$$l_{eff} = \frac{1}{2} l$$

The voltage at the slot center, V_{oc}, determines the voltage induced on internal wiring in the slot vicinity. There are two cases. For both cases, we assume the wire is perpendicular to the slot, for maximum coupling.

a) Wire directly over slot:

$$V_{wire} = \left(1 - \frac{2x}{l}\right) V_{slot}, \quad x = \text{distance of wire from slot center}$$
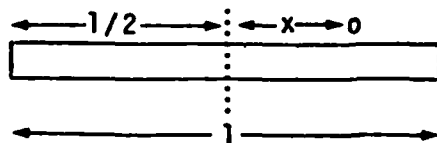
b) Wire to side of slot:

$$V_{wire} = (R)(V_{slot}) \quad , \text{ where}$$

$$R = \left(\frac{2h}{l\pi}\right)(\ln)\left[\frac{\sin^2\left(\frac{l/2 + d}{2a}\right)}{\sin\left(\frac{d}{2a}\right)\sin\left(\frac{l + d}{2a}\right)}\right]$$

207
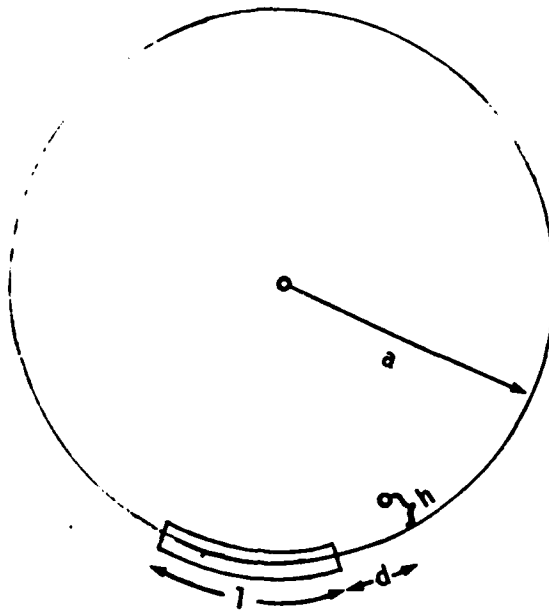
The coupling coefficient, R, falls off with increasing d, and is a minimum for a wire location directly opposite the slot.

2. Application of Equations to a Resistive Joint

$V_J = J_S/Y_J$, where

V_J = voltage across joint

J_S = surface current density across joint

Y_J = joint admittance

The voltage induced in a wire located as shown in the above figure is given by:
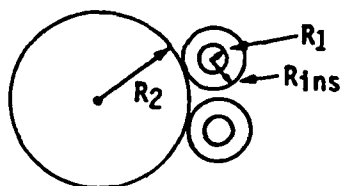
a) wire directly over slot: $V_{wire} = V_J$

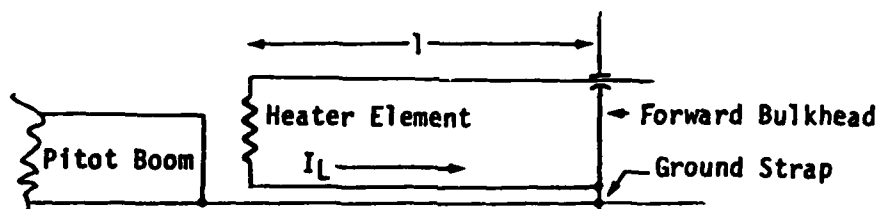b) wire a distance d to the side: $V_{wire} = RV_J$

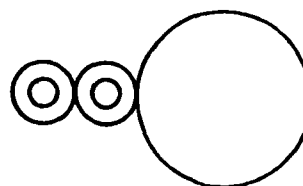$$R = \frac{h}{2\pi a}\left[\cot (d/2a) - \cot (1+d/2a)\right]$$

CAPACITIVE AND INDUCTIVE COUPLING OF PITOT HEATER WIRES TO GROUND STRAP

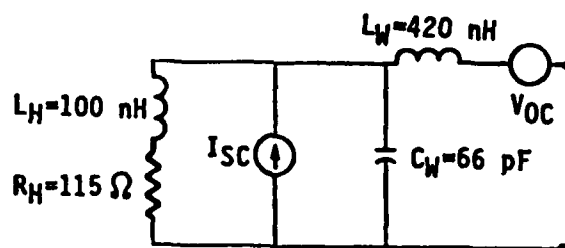The geometry for the pitot heater wires is indicated below:

Minimum Magnetic Coupling

Maximum Magnetic Coupling

The circuit model is:

L_H, R_H = inductance and resistance of heater element

L_w, C_w = inductance and capacitance of ungrounded heater wire

I_{sc} = Electric field coupling source

V_{oc} = Magnetic field coupling source

$$I_{sc} = (jwC_M) \ (R_2) \ (F_s/\epsilon_0) \ \ln \left(1 + \frac{R_{ins}}{R_2}\right)$$

209

C_m = mutual capacitance between heater wire and ground strap

$$C_m = 2\pi \varepsilon l / \cosh^{-1}\left[\frac{S^2 - R_1^2 - R_2^2}{2R_1 R_2}\right]$$

$$S = R_{ins} + R_2$$

F_s = surface charge density on ground strap

$= \lambda/2\pi R_2$, λ = change/unit length in ground strap

$$V_{oc} = (jw\mu_0)\left(\frac{2 R_2 R_{ins}}{R_2 + 2 R_{ins}}\right)(l_{eff})\ (J_s)$$

l_{eff} = length over which wires lay in maximum magnetic coupling configuration

J_s = surface current density on ground strap ($= I /2\pi R_2$)

ε = dielectric constant of wire insulation

$C_w = C_{12} + \dfrac{C_M}{2}$, C_{12} = mutual capacitance between heater wires

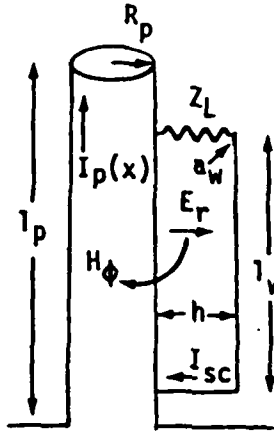$$= 2\pi \varepsilon l / \cosh^{-1}\left[\frac{S_1^2 - 2R_1^2}{2 R_1^2}\right]$$

$L_w = \dfrac{(\mu_0 \varepsilon l^2)}{C_w}$, $S_1 = 2\ Rins$

F_s and, J_s are obtained from the transmission model for the aircraft-lightning column interaction.

ANALYSIS OF WIRE AGAINST POST

Geometry for Wire Against Post

Consider the excitation of a wire routed alongside a metal post (e.g., landing gear strut) attached to the airframe. Lightning currents flowing on the airframe in the vicinity of the post induce surface fields along the post which in turn induce transients on the wire. The short circuit current at the end of the wire is given by:

(1) $$I_{sc} = -j\omega\mu h \int_0^{lw} H_\phi(x)\, G dx - h \int_0^{lw} E_r(x)\, \frac{\partial G}{\partial x}\, dx$$

Z_{cw} = characteristic impedance for wire

$$\Upsilon = j\omega \sqrt{\mathcal{E}_w}\,/C,\quad C = 3\times10^8 m/sec$$

$\mathcal{E}_w$ = relative dielectric constant for wire insulation

$$G(x) = \frac{1}{Z_{cw}}\, \frac{Z_{cw}\cosh\Upsilon(lw-x) + Z_L \sinh\Upsilon(lw-x)}{Z_L \cosh\Upsilon lw + Z_{cw}\sinh\Upsilon lw}$$

$$Z_{cw} = \frac{Z_o}{\sqrt{\mathcal{E}_w}}\, \ln(2h/a_w),\quad a_w = \text{radius of wire}$$

Near the surface of the post, the lightning induced fields are given by:

211

(2) $\quad H_\phi(x) = {}^-I_p(x) /2\pi R_p$, $\quad E_r(x) = -\dfrac{1}{jw\mathcal{E}_0}\dfrac{\partial I_p/\partial x}{2\pi R_p}$

inserting (2) into (1) and integrating by parts gives:

(3) $\quad I_{sc} = \left(\dfrac{h}{2\pi R_p}\right)\displaystyle\int_0^{1w}\left(-\dfrac{1}{jw\mathcal{E}_0}\right)\ \left(\cancel{K_0^2 I_p} + \dfrac{\partial I_p}{\partial x^2}\right)\ Gdx + \left(\dfrac{h}{2\pi R_p}\right)\left(\dfrac{1}{jw\mathcal{E}_0}\right)\ G\ \left.\dfrac{\partial I_p}{\partial x}\right|_0^{1w}$.

where the first term cancels, since I_p is a solution of the wave equation.
The current in the post is given, through the first post resonance (75 MHz for
a 1 meter post) by:

(4)
  a. $\quad I_p(x) = (I_0^p)\ \dfrac{\sin k\,(1_p - x)}{\sin k\,1_p}$

  b. $\quad I_0^{P} = (Y_p)\,(h_{eff})\,(E_n^0)$

  c. $\quad Y_p = Z_p^{-1};\quad Zp = R + jwL_p + {}^1/jwC_p$

  d. $\quad R = 73\ \text{ohms}$

  e. $\quad L_p = ({}^{21}p/\pi c)\left(Z_0^p\right)$

  f. $\quad C_p = ({}^{21}p/\pi c)/\ Z_0^p$

  g. $\quad C = 3 \times 10^8\ \text{m/sec}$

  h. $\quad Z_0^p = 60\ (\ln\,({}^{21}p/R_p)\ -1)$

  i. $\quad h_{eff} = 1p/2$

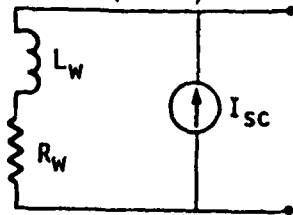 j. $\quad E_n^0 = \text{lightning induced electric field at post location}$

inserting (4)a. into (3) and using the expression for G(x) gives the general
expression:

(5) $\quad I_{sc} = \left(\dfrac{h}{2\pi R_p}\right)\ \left(\dfrac{Z_0}{Z_{cw}}\right)\left(I_0^p\right)\left(\dfrac{\tan\,(k1_w\sqrt{\mathcal{E}_w})}{\tan\,(k1_p)}\right)\left(\dfrac{Z_L + jZ_{cw}\ \tan\,(k1_p)}{Z_L + jZcw\,\tan\,(k1w\sqrt{\mathcal{E}_w})}\right)$

This equation may be put into a fortran subroutine to calculate induced transients for arbitrary wire loads, Z_L.

When $Z_L = 0$: $\quad I_{sc} = \left(\dfrac{h}{2\pi R_p}\right) \left(\dfrac{Z_0}{Z_{cw}}\right)(I_0^p)$
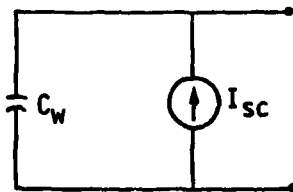
The model is:

$$L_W \quad R_W \quad I_{sc}$$

When $Z_L = $ infinity: $I_{sc} = \left(\dfrac{h}{2\pi R_p}\right) \left(\dfrac{Z_0}{Z_{cw}}\right) (I_0^p) \left(\dfrac{\tan(kl_w\sqrt{\varepsilon_w})}{\tan(kl_p)}\right)$

The low frequency limit: $I_{sc} = \left(\dfrac{h}{2\pi R_p}\right) \left(\dfrac{Z_0}{Z_{cw}}\right)(I_0^p)\left(\dfrac{l_w}{l_p}\sqrt{\varepsilon_w}\right)$

The model is: $\quad C_w \quad I_{sc}$

213

APPENDIX F

CALCULATION OF VOLTAGE DROP IN METALLIC STRUCTURE
DUE TO THE LIGHTNING LOW FREQUENCY CONTINUING CURRENT

The potentially damaging low frequency currents through circuits which use the airframe for ground return is the so-called "IR drop". (See Ref. 12, pages 263-266). The magnitude of this threat may be obtained by the equations

$$V_{oc} = (R_a) (I_{cl})$$
$$I_{sc} = (R_a/(R_a + R_t + R_w)) I_{cl}$$

where V_{oc}, I_{sc} are the open circuit voltage and short circuit current seen at the end of a circuit with a terminating impedance R_t.

R_a = airframe resistance along circuit length
R_w = wire resistance
I_{cl} = continuing current

Ref. 10, page 8 gives a value for I_{cl} of 800 amps for 0.25 seconds. For a typical airframe resistance of 2.5 milliohms,

$$V_{oc} = (2.5 \times 10^{-3})(800)(L_w/L_a) < 20 \text{ volts}$$
$$L_w = \text{wire length}$$
$$L_a = \text{airplane length}$$

For $R_a + R_w << R_t$, $I_{sc} = (R_a/R_w)I_{cl}$. Both the voltage and current waveforms have a time duration of 0.25 seconds. These considerations only apply to metallic structure. For graphite-epoxy, the current peak component is the severe threat and was so treated in the threat definition.

214